Supply Function Equilibrium Analysis for Electricity Markets

Prepared by

Andreas G. Petoussis

A Thesis submitted for partial fulfilment of the requirements for the degree of Doctor of Philosophy

University of Warwick, School of Engineering

March 2009

Abstract

The research presented in this Thesis investigates the strategic behaviour of generating firms in bid-based electricity pool markets and the effects of control methods and network features on the electricity market outcome by utilising the AC network model to represent the electric grid. A market equilibrium algorithm has been implemented to represent the bi-level market problem for social welfare maximization from the system operator and utility assets optimisation from the strategic market participants, based on the primal-dual interior point method. The strategic interactions in the market are modelled using supply function equilibrium theory and the optimum strategies are determined by parameterization of the marginal cost functions of the generating units. The AC power network model explicitly represents the active and reactive power flows and various network components and control functions. The market analysis examines the relation between market power and AC networks, while the different parameterization methods for the supply function bids are also investigated.

The first part of the market analysis focuses on the effects of particular characteristics of the AC network on the interactions between the strategic generating firms, which directly affect the electricity market outcome. In particular, the examined topics include the impact of transformer tap-ratio control, reactive power control, different locations for a new entry's generating unit in the system, and introduction of photovoltaic solar power production in the pool market by considering its dependency on the applied solar irradiance. The observations on the numerical results have shown that their impact on the market is significant and the employment of AC network representation is required for reliable market outcome predictions and for a better understanding of the strategic behaviour as it depends on the topology of the system.

The analysis that examines the supply function parameterizations has shown that the resulting market solutions from the different parameterization methods can be very similar or differ substantially, depending on the presence and level of network congestion and on the size and complexity of the examined system. Furthermore, the convergence performance of the implemented market algorithm has been examined and proven to exhibit superior computational efficiency, being able to provide market solutions for large complex AC systems with multiple asymmetric firms, providing the opportunity for applications on practical electricity markets.

Table of contents:

List of Figures:

List of Tables:

List of Acronyms and Abbreviations:

CP	-	Complementarity Problem
CSF	-	Conjectured Supply Function
EPCC	-	Equilibrium Program with Complementarity Constraints
EPEC	-	Equilibrium Program with Equilibrium Constraints
EPIA	-	European Photovoltaic Industry Association
EU	-	European Union
HHI	-	Herfindalh-Hirschman Index
ISO	-	Independent System Operator
KKT	-	Karush-Kuhn-Tucker
LCP	-	Linear Complementarity Problem
MPCC	-	Mathematical Program with Complementarity Constraints
MPEC	-	Mathematical Program with Equilibrium Constraints
MWh	-	MW-hour
NCP	-	Nonlinear Complementarity Problem
NLP	-	Non-Linear Programming
OPF	-	Optimal Power Flow
PC	-	Perfect Competition
p.u.	-	per-unit
PV	-	Photovoltaic
RES	-	Renewable Energy Sources
SFE	-	Supply Function Equilibrium

Acknowledgements:

I would like to thank my academic supervisor Dr. Xiao-Ping Zhang and express my gratitude for his continuous support and guidance throughout my PhD studies. His valuable supervision and encouragement over my postgraduate and also undergraduate studies have given me the opportunity to expand my field of knowledge and broaden my academic horizons.

My sincere thanks to my second supervisor Prof. Keith Godfrey for his constant help and support during my time in the University of Warwick. His helpful comments and discussions on my work are much appreciated.

My deepest gratitude is expressed to my family for their continuous encouragement, emotional support and patience over the 7 years of my studies at the University of Warwick. In particular, I would like to thank my brother Savvas for always being there for me.

Financial support from the UK Engineering and Physical Sciences Research Council (EPSRC) doctoral training grant and from the Division of Electrical and Electronic Engineering of the University of Warwick is gratefully acknowledged.

Declaration:

Parts of the work presented in this Thesis have been published or submitted for publication to scientific journals and conferences:

1. S. G. Petoussis, X.-P. Zhang, A. G. Petoussis and K. R. Godfrey, "The impact of reactive power on the electricity market equilibrium," Panel session paper, *Proc. IEEE PES Power System Conference & Exposition (PSCE)*, Atlanta, Georgia, USA, pp. 96-102, Nov. 2006.

2. A. G. Petoussis, S. G. Petoussis, X.-P. Zhang and K. R. Godfrey, "Market equilibrium in congested transmission networks with transformer tap-ratio control," *Proc. IEEE PES Power Tech Conference*, Lausanne, Switzerland, pp. 949-954, July 2007.

3. S. G. Petoussis, A. G. Petoussis, X. P. Zhang and K. R. Godfrey, "Impact of the transformer tap-ratio control on the electricity market equilibrium," *IEEE Trans. Power Syst.*, vol. 23, no. 1, pp. 65-75, Feb. 2008.

4. A. G. Petoussis, S. G. Petoussis, X. P. Zhang and K. R. Godfrey, "New entries in the electricity market: choosing the best location for a new generating unit," Panel session paper, *Proc. IEEE on Electric Utility Deregulation and Restructuring and Power Technologies (DRPT) 3rd International Conference*, Nanjing, China, pp. 61-65, April 2008.

5. S. G. Petoussis, A. G. Petoussis, G. E. Georghiou, X. P. Zhang and K. R. Godfrey, "Grid-connected photovoltaic power plants: the effect on the electricity market equilibrium," *Proc. IEEE on Electric Utility Deregulation and Restructuring and Power Technologies (DRPT) 3rd International Conference*, Nanjing, China, pp. 457-462, April 2008.

6. A. G. Petoussis, X. P. Zhang, S. G. Petoussis and K. R. Godfrey, "Electricity market equilibrium of nonlinear power systems with reactive power control," submitted to *Electric Power Systems Research*, Dec. 2007.

7. A. G. Petoussis, S. G. Petoussis, X. P. Zhang, G. E. Georghiou, M. Patsalides, G. Makrides and K. R. Godfrey, "Electricity market modelling with photovoltaic active and reactive power generation," accepted for presentation at the *IFAC Symposium on Power Plants and Power Systems Control (PP&PSC)*, Tampere, Finland, July 2009.

8. A. G. Petoussis, X. P. Zhang, S. G. Petoussis and K. R. Godfrey, "Parameterization of supply functions in AC electricity market equilibrium models," submitted to *IEEE Trans. Power Syst.*, Nov. 2008, under revision.

Chapter 1:
Introduction to the electricity markets

1.1 Introduction

In recent years electricity market reform has taken place all over the World, with the objective of replacing the existing monopolistic structure by a more competitive one giving the opportunity to new participants to enter the electric power trading sector. However, the electricity market has been proven to have a tendency to oligopolistic behaviour due to a number of factors, such as the entry barriers caused by the unique nature and operational complexities of the electrical power systems, the potential market power of the participating generating firms related to locational and other characteristics of the electrical grid, and the distinctive requirements for the transmission and distribution of electrical power. The resultant deregulated market structure and the establishment of independent generating firms in a liberalised environment have brought forward the development of economic tools for the investigation and analysis of the function of electricity markets. Among the variety of the different methods proposed, the concept of market equilibrium analysis has received considerable attention, since it is an appropriate tool for exploring the oligopolistic strategic behaviour that characterises the restructured electricity sector being able to provide meaningful predictions for the market outcome.

The research on the subject has contributed to the literature in several ways by the proposition of employing different economic approaches for the determination of the electricity market equilibrium. The equilibrium models proposed differ in the representation of the market competition and structure in terms of firms' behaviour, market regulation, interactions between the market participants and practicality of model assumptions. The supply function equilibrium model has been found to match the requirements for representing the features of the electricity market and has been proven to exhibit certain

advantages over the choice of the other relevant methods. In addition to the diversity of the applicable economic principles, various numerical methods have been suggested for the implementation of appropriate algorithms for computing the electricity market solution. The evolution in the area of mathematical programming has provided the ability of improving the computational performance and precision of the proposed numerical methods, enabling more advanced and comprehensive investigations.

The work presented in this Thesis proposes an electricity market equilibrium model based on supply function theory applied to bid-based pool markets, for the investigation of market power and the interactions between the strategic generating firms. The analysis explores topics that have not be addressed well in the literature, including investigations of the impact of control methods and network constraints on the market equilibrium related to the nonlinearities of AC systems, the effects of new generating units of conventional nature and grid-connected photovoltaic sources, and the different methods in which a profit-maximising supply function strategy can be constructed by parameterizing the marginal cost of generation. The numerical algorithm for the market solution is implemented based on primal-dual interior point optimisation, which has been proven to be very efficient.

The remainder of this chapter provides a comprehensive introduction on the electricity markets and the deregulation process towards the liberalised environment, followed by Chapter 2 that presents an extensive review on the concept of market equilibrium and in particular the supply function equilibrium. Chapter 3 provides information about the numerical method employed and outlines the mathematical formulation for the proposed electricity market algorithm. Chapters 4 and 5 present numerical results and discussions on the impact of transformer tap-ratio and reactive power control on the electricity market equilibrium. Chapters 6 and 7 illustrate how the introduction of new generating units and photovoltaic sources in the system affects the existing market conditions. Chapter 8 investigates the different parameterization methods that the generating firms utilise to construct their strategic supply function offers. Chapter 9 analyses the convergence characteristics of the implemented algorithm

and concluding remarks are provided in Chapter 10. Further details on the structure of the Thesis are given in the last section of this chapter.

1.2 History and evolution of electricity markets

The electricity industry has existed for more than 130 years, in which time major changes in structure and regulations have occurred. Alterations due to continuous technical and economic developments have been experienced, resulting in an overall transformation of the electricity sector.

In the very beginning, the infancy of the electricity industry was dictated by privately owned companies, experiencing brutal competition and high inefficiencies. The transmission grid development was very limited and almost no regulation existed. Initially in the USA, Thomas Edison has offered a replacement to gas lighting using DC technology, around 1878, charging by the number of light bulbs installed on the site. In the following years, suppliers that were also providing the electricity infrastructure were taking advantage of areas of dense load, such as cities and industrial sites. For example, between 1887 and 1893 there were 24 power companies within the city of Chicago, with overlapping lines and enormous costs, subject to fierce competition [1].

Following the innovative example of the Westinghouse Company, which introduced high-voltage transmission and AC technology in the USA in 1886, the Southern California Edison integrated a full-service utility, operating a 10kV 28-miles transmission line, in 1892. A few years later in 1898, the president of the National Electric Light Association, Samuel Insull, which had already switched his support to the AC technology, attempted to eliminate the problems associated with inefficiencies due to brutal competition. Insull acquired a monopoly over all central-station production in Chicago, explaining why the electricity business was a natural monopoly that should be regulated at state level, with all charges based on costs plus a reasonable profit. The aforementioned measures led to the introduction of regulatory laws in the USA, establishing the first state utility commissions, around 1907 [1].

In the following years, the states in many countries tried to guide the electricity industry, regarding electrical power as an everyday necessity, instead of a luxury commodity. Further developments on the transmission grid had been observed, but there was a lack of interconnection between individual networks and also inadequate network control. This resulted in uncertain supply and large losses during the transmission of electrical power [2]. After World War II, it has been addressed that in many countries, mainly in Europe and Latin America, the electricity industry was integrated into a single nationalised company, for strategic reasons. Such state ownerships led to new problems, since some governments were unable to invest in generation to cover the high-pace demand growth [3]. Meanwhile, economic concepts were employed in the electricity sector in order to deal with the negative economic behaviour. The increasing economics of scale prevailed and the transmission and distribution grids were nearing completion. Eventually, almost all governments in Europe considered the electricity sector as a natural monopoly and small producers were merged into single nation-wide monopolies, placed under public ownership to prevent oligopolistic behaviour; France initiated this in 1946, while Italy, in 1962, was the last one. In many countries new entries into the electricity sector were forbidden by law, with the exception of Spain that had no entry barrier laws and some local competition also existed [2]. During the following years, it was well accepted that the electricity industry is principally of a monopolistic nature [4].

In the USA, the established privatised monopoly was regulated by an independent regulatory commission until the early 1970s, during which the first doubts about the efficiency of the regulated monopoly utility emerged. Earlier studies had already showed that a private monopoly subject to a “fair rate of return” regulation gives incentives to overinvest in capital assets [5]. In the meantime, the oil crisis of 1973 raised the price of the main input fuel of electrical power. While efforts in replacing oil with coal for the electricity production and investments to nuclear programs had been attempted, a critical discovery was made: independent generators can operate without destroying the stability of the system [2]. The conclusion was that other structures than the vertically integrated monopoly could exist. The impending result was that the USA adopted a new regulatory policy in 1978, requiring the utilities to buy

electricity from “qualified facilities”, such as cogenerators and small power producers [6]. However, improvements in transmission, which were done mainly for reliability purposes, were responsible for removing the natural monopoly character of the wholesale market, rather than changes in generation technology. Development in high voltage networks over long distances made possible the trading of electricity from producers located away from the consumers [1].

The pioneer in introducing some competition in the electricity market was Chile in 1982, by allowing large consumers to choose their suppliers and negotiate the prices. This was followed by the establishment of market mechanisms for the determination of generators’ dispatch and the wholesale price of electricity, permitting competition between generators. In 1990, the England and Wales market established the pool market mechanism for the first time in the history of the electricity power sector, by privatising the electricity supply industry [7,8]. The following year Norway also adopted a competitive electricity pool scheme creating the Nord Pool, which was afterwards extended to include Sweden in 1996, Finland in 1998 and Denmark in 1999 [9]. The Nord Pool is the only multinational exchange for trading electric power, while it is the first that permitted all end-users to choose their supplier. By that time the European Union (EU) directive on the internal electricity market [10] has allowed large purchasers of electricity to choose their suppliers freely from throughout the EU, introducing full competition amongst generating firms. During the 1990s several other countries, including Argentina, Colombia, Canada and Australia, created regulated pool markets for electrical power, while competition in various forms was introduced in most countries [6]. These actions initiated the era of deregulation and liberalisation of the electricity market.

1.3 Liberalisation and deregulation of the electricity markets

Liberalisation of the electricity market refers to one or more reforms related to the electricity supply industry. These include the corporatisation of previously state-owned utilities, the transfer of electricity industry assets from the state to private organisations (i.e. the privatisation), the deregulation of various aspects

of the industry operations and the introduction of competition. However, besides the unbundling of most branches of the electricity sector in the restructured power systems, the transmission ownership is still considered, in general, as a monopoly element not subject to competition [11].

The electricity markets around the World, following the liberalisation trend during the 1990s, were undergoing major reforms, as the governments were privatising and restructuring the initially monopolistic state-owned, or private state-regulated, electricity utilities. The competitive part of the former utility companies, mainly the electricity generation sector, was separated from the natural monopolies, such as the ownership of the grid for transmission and partly the distribution of electrical power [6]. While many countries associated the liberalisation of the electricity market with direct privatisation of the existing utilities, some of the leading European energy companies, such as EDF in France [12] and Vattenfall (translated as Waterfall) in Sweden [13], remained partially or completely in government ownership. Market forces were gaining control over the electricity business environment as government regulations were withdrawn during the liberalisation process, shifting the decision making from the state to the market and giving choice to the consumers. The main reasons that led to extensive deregulation of the electricity sector were that new technologies reduced the optimal size of generators, mainly due to the development of combined cycle gas turbines, and that the competitive global economy required lower input costs. The existing state-owned utilities were unable to respond to these economic and technological changes as quickly as private owners, while advances in communications made possible the exchange of large information needed for the management of electricity markets [2,3].

In order to guarantee the independent operational control of the transmission grid and facilitate a competitive market for power generation and retail, an independent entity that monitors the market, often referred to as the Independent System Operator (ISO), is required. The ISO must be unbiased and independent of all the individual market participants, such as the transmission owners, generating firms, distribution companies, retailers and end-users, in order to operate the competitive market effectively and ensure the reliability of the power

system. Certain rules must be established by the operator regarding the energy and ancillary services markets, the management of the transmission system, the market risks and the monitoring of the system for the elimination of any sources of market power. Among others, the ISO responsibilities include monitoring of ancillary services auctions if in effect, for example spinning reserve, and congestion management [14].

1.4 From perfect competition to oligopoly

The main objective of deregulation was to achieve efficiency through competition. Competition provides strong minimising incentives for the suppliers in terms of labour savings, efficient maintenance, reduced construction costs for new plants, wiser investment choices and flexibility in new projects, such as distributed generation and renewable energy sources. It also encourages real-time pricing, which is considered to be more accurate [1]. In a monopolistic environment where the electrical power generation, transmission and distribution are bundled, the monopolist can set prices above the cost of production, while competition in a deregulated environment can bring the market price down to marginal cost of generation levels [3]. Although many attempts have been made all over the World to increase the degree of competition in the electricity markets, especially at the wholesale level, perfect competition conditions have not been established [15].

Perfect competition exists if all market participants act as price takers. Each supplier should increase its production up to the point where its marginal cost equals the market price. If a supplier asks for a price higher than the market price or a consumer offers less than the market price, in a market that consists of a large number of small competitors, this action will be ignored and other participants will replace that particular participant’s contribution to the market. Hence, the market price is set by the interactions of sellers and consumers, taken as groups [16].

The requirements for successful perfect competition in the short-run in a deregulated environment are that the market participants act as price takers, the traders have adequate information including the electricity market price to be publicly known, and the costs are well-behaved. Long-run perfect competition conditions include the above, while the production costs should not allow natural monopoly conditions to emerge, and the competitors must be able to freely enter the market with no entry barriers [1].

The lack of each of the aforementioned requirements for the existence of perfect competition will result in oligopolistic conditions, such as the ability of particular participants for exercising market power leading to high prices, or in other forms of economic deficiencies. An oligopolistic market is characterised by a small number of producers of significant size where the action of one has an influence on the overall market, and the prices and payoffs are influenced by the behaviour of the producers. The main reasons for the electricity market to be an oligopoly rather than a perfect competition market are the limited number of producers, the transmission constraints and congestion that isolates consumers from some generators, the transmission losses that discourage consumers from distant producers, and the entry barriers for new competitors, such as the large investment size [17]. Considering these circumstances, which result from the unique nature of the power generation, transmission and distribution, perfect competition is very difficult to be established in the deregulated electricity markets, and therefore the traditional assumptions of a perfect competitive market in the economic sense should be replaced with those of the more realistic oligopolistic approach, as far as the electricity sector is concerned [15].

1.5 Electricity market types: contracts and centralised trading

In an electricity market, physical trading of power may be allowed between buyers and sellers directly, in the form of bilateral contracts. A bilateral contract involves two parties that they trade power quantities at negotiated prices, terms and conditions, with no interference from a third party. Generating firms can directly contract with buyers in wholesale electricity markets and purchase

transmission services from the transmission owner or system operator. If retail competition is allowed, the generating firms can also directly contract with the consumers [3]. All the transactions are announced to the operator to verify if the transmission capacity is sufficient to complete the transaction and maintain the transmission security, but it determines the feasibility of the contract without knowing the prices agreed. This trading approach has the advantage of being extremely flexible, while its disadvantages stem from the high cost of negotiating for the contracts and the risk of creditworthiness of counterparties [14]. Nonetheless, the implementation of bilateral contracts minimises the role of the system operator [1].

Certain contracts require immediate delivery, while the terms and conditions of others may be fixed in advance. A forward contract states the agreed price and defines the location for the delivery of an asset at a specified time in the future, without any payment until the time of delivery. Any differences between the current market price and the contract price at the time of delivery, represents a profit or loss for the contractors [18]. A secondary market may exist, in which producers and consumers buy and sell forward contracts, called future contracts, in order to manage their exposure to fluctuations in the spot price. Other parties apart from generating firms, retailers and consumers may participate, such as speculators who want to buy a future contract hoping of being able to sell it later at a higher price [16].

A different type of electricity market, where centralised trading takes place, is the poolco type market. Instead of agreements between the market participants, the poolco market assumes that the generating firms sell power into a pool, which is supervised by a market or system operator, usually an ISO. In wholesale markets, the distribution companies buy from the pool to sell at retail to small customers, while if retail competition is also allowed, buyers could be individual customers, suppliers or retailers. The operator holds an auction in which each producer bids different prices for different amounts of power for each trading period (the bidding interval), which can be the following day, or the following hour, etc [3]. The sellers compete with each other to supply power to the pool, but not for specific customers, while the buyers compete to buy power from the pool. If a

seller bids too high it may not be able to sell, and if a buyer bids too low it may not be able to purchase [14]. The ISO implements the economic dispatch, usually based on a social welfare maximisation or a costs minimisation scheme, and sets the market clearing price based on the submitted bids, the demand levels and the supply quantities. A standard procedure is that the ISO chooses first the generators with the lowest bids and the customers with the highest offers in order, until the load demand is met. The scheduled producers and customers are represented by the intersection of the supply and demand curves (see Section 2.1). Trading outside the pool, as in a bilateral agreement, may avoid the general management costs created by centralised coordination shared by all market participants, but as the pool market price is publicly known, significant savings result by avoiding the need to discover prices. A poolco market is more efficient than a market based on bilateral contracts because most market participants are scheduled and tracking agreements between pairs of traders is not necessary [3]. Furthermore, a pool market gives incentives to small consumers to have an active part in the electricity market, while, since the pool reduces the scheduling risk, the generating costs will be less [16].

In the case were the market participants are obliged to trade only through a centralised market and bilateral agreements are not allowed, they may choose to enter into contracts for differences in order to reduce their exposure to price risks. In a contract for differences the parties agree on a strike price and an amount of power. Once the trading through the centralised market is complete, if the strike price is higher than the centralised market price, the buyer pays the seller the difference between the two prices times the amount agreed, or if the strike price is lower than the market price, the seller pays the buyer the price difference times the specified amount [16].

A hybrid market that combines various features of the aforementioned market models can exist. A bid-based pool market may open after the bilateral contract market closes, giving the opportunity to the market participants to buy or sell more electricity to meet their requirements if not already concluded in their transactions [15]. Apart from the fact that such a combined market gives the choice to sellers and buyers to participate in both or only one of the two markets,

the most important reason for the simultaneous existence of bilateral trades and pool market is to ensure the reliability of the system. Since the actual demand is never exactly equal to the value forecasted and unpredictable problems may prevent generators to deliver the contracted amount of power, a pool-type market mechanism is used to settle the imbalances between supply and demand at every moment. Such a market for imbalances is often called a spot market, since power is delivered immediately and the buyer pays on the spot. Even if bilateral trading represents the main market mechanism in a wholesale environment, a spot market can be implemented as a balancing mechanism, by pooling all available surplus generation, in a similar manner as in the poolco type market. A spot market for handling the supply-demand imbalances has the advantage of immediacy, but the spot prices tend to change quickly depending on the load demand, and are essentially unpredictable [16].

In addition to energy prices and quantities for selling and buying electrical power, the ISO in a pool type market may require other information associated with the generating units to be provided with the submitted bids by the competing producers. These may include start-up prices, offered capacities, ramp up and down rates or rate limits, minimum and maximum generation levels, minimum up and down times, and regulation band for automatic generation control, depending on the specifications and regulations of the particular market [19]. Note that, in some markets the operators run appropriate competitive processes or establish joint markets for energy and ancillary services, such as spinning reserve, reactive power control, frequency control and black start capability services. Depending on the service procured, bids may be required to be submitted or flat rates may be applied for each service. However, these issues are not discussed here as they are beyond the scope of this Thesis.

1.6 Pricing of electrical energy

Producers and buyers in different electricity markets may receive and pay different prices for the same amount of energy delivered, depending on the pricing scheme employed. When the vertically integrated institution was still in

effect, flat rates were defined annually or monthly, based mainly on expected costs. By the time that electricity deregulation was a close target the spot pricing method has emerged. The spot prices, that were recalculated every hour (or every fixed time interval), were dependent on the variation of generation fuel costs and capacities, the transmission losses and capacities, and the demand patterns. The average spot price was proven to be lower than the corresponding annual flat rate [20].

As far as the deregulated environment is concerned, the most common method to set prices in auction-type electricity markets is the uniform pricing approach. For each bidding interval, all the market participants pay or receive the same system-wide pool price that equals the bid of the last generator scheduled, and there are no transmission price differences. Therefore, a firm can receive profit even by bidding its marginal cost. Such an approach could be particularly appropriate for well connected networks with no congestion problems [3]. Since the choice of setting the uniform price at the last bid accepted is regarded as a process that does not reveal costs, another alternative, which is considered to be more efficient, is to set the uniform market price at the first bid rejected [21].

The pay-as-bid pricing, where each supplier is paid the price quoted, has also been used, but only in very few electricity markets [18]. It has been argued that such a scheme would lower the risk for tacit collusion compared with uniform pricing [22]. However, its adaptation would discourage generators to submit bids that reflect their marginal costs and low-cost generators may be left out of the schedule by bidding high [16]. The analysis in [23] has shown that a change from a uniform price auction market to this discriminatory pricing scheme will result in a trade off between efficiency and prices in a perfect competition environment, while under monopoly conditions there will be a negative effect on the profits and output, as the market power of the generating firms will be strengthen. The oligopolistic approach of [24] demonstrates that for an unconstrained electricity market the optimum market outcome for both pricing mechanisms is the same, but the introduction of network constraints discriminates between the two. In addition, the study in [25] carries out short-run duopoly simulations using both pay-as-bid and uniform pricing electricity market models and concludes that the

expected total revenue under uniform pricing is larger than under pay-as-bid pricing when the firms compete in prices. Then it proves that, under elastic demand, the expected demand served for the pay-as-bid scheme is more and the expected total revenue less than for uniform pricing.

Despite the fact that some markets charge for the electrical energy using a uniform price, the energy prices differ by location because it is cheaper to produce energy in some locations, and transmission is limited [1]. The pricing of electricity is affected by the transmission line capacities and losses, the energy balance constraint, and the power flows, which cannot directly be allocated among transmission lines. For more accurate pricing, the network characteristics should be reflected in the price of electricity at different locations and times. A methodology was developed in [26] for pricing network transmission losses and constraints in real time, which was the foundation for the locational spot pricing analysis.

Pricing methods based on locational prices have become popular in the deregulated electricity markets, following the pricing mechanisms provided by Schweppe et al. in [26] and [20]. The study in [27] has first proposed the application of locational spot pricing in real power systems. The locational spot pricing, also called nodal pricing, assigns a different price at each bus (node) and considers, apart from the generation costs, the cost of transmission losses and the extra generation cost to supply the demand increment if transmission congestion exists. The difference between two nodal prices is the value of the transmission between the two nodes, resulting from the transmission capacity constraints. Note that congestion in a line produces nodal price differences in other noncongested lines as well [3]. The use of such efficient short-run pricing is consistent with economic dispatch and provides an efficient use of the transmission system [27]. The nodal prices allow for an efficient management of congestion, since higher price at a node will decrease demand and resolve congestion, but they are not immune to the consequences of exercising market power [6] (see Section 1.8).

An alternative to nodal pricing is the zonal pricing, in which nodes are grouped into zones bounded by potential constraint interfaces and each zone has a spot price. This method encourages generators to locate within high-priced zones and focuses on relieving flow constraints in the congested interfaces between zones. In such a market, the boundaries must be updated from time to time to accommodate the generation and transmission expansion [3].

1.7 Electricity from renewable energy sources

Apart from the conventional generating units that utilise fossil fuels, such as coal, heavy fuel oil and natural gas, and nuclear generators, investment in other developing technologies for generating electricity is taking place. The EU is currently in the process of promoting the exploitation of the available Renewable Energy Sources (RES) by its Member States for the production of electrical energy. The directive of the European Parliament and Council [28] issued in January 2008 proposes that an overall binding target of a 20% share of RES in energy consumption must be achieved by the Member States by the year 2020. One of the principal aims of this effort is to mitigate the climate change effects by reducing greenhouse gas emissions, such as CO_2. Furthermore, as the increasing dependence on energy imports threatens the EU supply security and implies higher electricity prices, the boosting of investment in energy efficiency, renewable energy and new technologies is expected to exhibit wide-reaching benefits, since RES are largely indigenous. It is anticipated that the broad usage of RES will contribute to growth and jobs in the EU, as they constitute a key element of a sustainable energy future [28].

According to the figures presented in [28] for the individual European countries, the percentage share of energy from RES in final energy consumption in the year 2005 was found to vary from 0% in Member States with isolated electrical networks, such as the island of Malta, up to about 40% in northern European countries where they utilise the largely available hydroelectric energy. The percentage targets for each member state by 2020 have been set to within a range of 10% to 50% depending on the starting point for each state, in order to achieve

an overall 20% share. The primary RES that are expected to be largely exploited in the EU apart from the hydroelectric energy are the solar and wind energies. Other notable RES include geothermal, wave, tidal and biomass. Further details on RES and solar energy are provided in the introductory section of Chapter 7.

1.8 The issue of market power

Market power is the antithesis of competition [29]. Several definitions have been proposed, for example, market power is the ability of one or more market participants to maintain prices profitably above competitive levels for a significant period of time [29]. More generally it is defined as the ability of the market participants to manipulate the market in their own favour [15].

The generating firms may be able to exercise market power due to several reasons. Global market power may exist in the market due to the relative size of the competitors [15]. In a market with a small number of competitors, a producer with a large share can raise the market price by asking for a higher price, or by withholding output that could be produced profitably at the market price [1]. In addition, especially in electricity markets, entry barriers prevent new competitors to enter the market, acting as a source of market power. The entry barriers may be created by existing market participants, e.g. by predatory pricing where the product is available in very low prices that will also drive other producers out of the market [18], but typically entry barriers exist due to the high investment costs and the cost in obtaining permission to build generation [1]. In the case where the electricity market is still vertically integrated in some degree, vertical market power may be exercised from a single firm that controls domains in the generation, transmission and distribution sectors [3].

Locational or local market power may exist in certain areas in the market due to the geographical nature of the power system and the physical and operational constraints of the transmission network. Transmission congestion may isolate regions from outside competition and transform a reasonably competitive global market into a collection of smaller local markets where the small number of

participants will give rise to market power [16]. Early investigations have shown that transmission costs isolate generators from competition with distant producers [30]. Large firms may increase their production in order to lower some prices, exploiting the network constraints to foreclose competition from others [31]. On the contrary, a firm may reduce its output to congest transmission into its area of dominance, in order to remain the sole local supplier [32]. Similarly, firms can buy physical transmission rights and choose not to use them to enhance their market power by artificially reducing the transmission capacity into their area [16]. Load pockets, such as cities that require more power than that they can import may give rise to the ability of exercising extreme market power during peak hours. In some cases, certain generators may be declared must-run, mainly for the need of reactive power instead of their active production, enhancing their market power [1]. Furthermore, as the level of transmission congestion directly relates to the load, the demand behaviour will affect market power abilities [33], while a slow response of the consumers to lower-price supply options favours market power [34].

1.9 Assessment and mitigation of market power

Any attempt of a player to exercise any form of market power interrupts the proper function of competition. In addition to higher prices, the consequences of market power by the suppliers include higher profits for all firms due to the higher market price, transfer of wealth from consumers to producers and higher economic inefficiency in the form of deadweight welfare loss [1].

Several measures can be applied for the mitigation of market power. In order to eliminate the market power of large producers, regulations for reducing the market shares of dominant suppliers can be applied, and the regulators can encourage more suppliers to enter the market by providing profitable entry in a short period of time. Long-term contracts will reduce the incentives of the firms to exercise market power, since they will be less motivated to participate in the spot market. Demand-side bidding is important for the mitigation of short-term market power, because the lack of real-time price responsiveness exacerbates the

potential for market power during peak-load hours, but this may affect the market efficiency. If the market prices are persistently high, certain market rules, such as price caps or bid caps in bid-based pool markets, can be established in order to limit the prices. Such measures should only be used after careful study of the current economic signals, because it may not be possible to prove that the high prices result from market power abuse [17]. Regarding this, the firms may be restraining prices in order to deter new competitors or to avoid substantial regulatory actions taking place [35].

For the elimination of local market power due to transmission congestion, expansion on the network can take place. However, this is a less popular approach due to the opposition of the market participants, based on the fact that this will affect the overall power flow operation of the system and, consequently, dramatically change the electricity market [17]. The study in [34] argues whether it will be more profitable to provide new transmission capacity by augmenting the existing system, altering the operating procedures or building new lines, or by constructing additional nearby generating capacity. For the case where transmission capacity expansion is not attractive, the incentives to develop distributed generation by implementing smaller scale technologies are highlighted. Furthermore, distributed generation can serve as a price hedging mechanism during peak load periods [36].

The main methods that have been developed to detect the presence of market power in the electricity market can be categorised in the following:

- market concentration analysis
- estimation of pricing behaviour
- oligopoly equilibrium analysis.

The market concentration analysis utilises appropriate indices to assess the market competitiveness. The most widely used index is the Herfindalh-Hirschman Index (HHI), which equals the summation of the percentage of the market share of each supplier squared, to represent the market concentration. Such indices are used only as a rule of thumb and their disadvantages include the lack of supporting theory and ability to explicitly represent the supply and demand elasticity [17,37]. The estimation of pricing behaviour through

simulation analysis is a better approach, in which the market clearing price can be estimated by studying the optimal bidding strategies of the market participants and then be compared with the perfect competition price, or ex-post analysis using historical data can take place to measure the margin between the market price and the marginal cost of generation. A retrospective method that assesses the market price level is the application of the Lerner Index, which is defined as the difference between the actual market price and the marginal cost divided by the market price [17]. However, these methods have the disadvantage that marginal costs and perfect competition prices cannot be easily revealed, while retrospective analysis is only a way of ex-post assessment [15].

The most effective method for evaluating the sources and degree of market power in the electricity market is the oligopolistic equilibrium analysis, in which the equilibrium market prices are calculated. This analysis is based on the modelling of specific markets in terms of operational, physical and market constraints, and the simulation of the strategic behaviour of the generating firms [15]. The main oligopolistic competition types applied in such electricity market models are the Cournot, Bertrand and Supply Function Equilibrium (SFE) competitions, which are discussed in detail in the next chapter. The SFE competition, which is considered as the most appropriate for modelling the electricity market, is the main topic of the research presented in this Thesis.

1.10 Structure of the Thesis

The structure of the remainder of this Thesis is organised as follows:

- ***Chapter 2:***

This chapter commences with the description of basic economic theory related to the concept of market equilibrium, such as the supply-demand equilibrium, the theory on economic surplus, and the Nash equilibrium and non-cooperative games. The available oligopolistic equilibrium models for the investigation of the electricity market are discussed and the advantages of the linear supply function equilibrium model are highlighted. The literature on the latter model is presented,

with discussions on the parameterization methods employed for the strategic bid, the representation of the electrical network and the numerical methods applied.

- ***Chapter 3:***

The proposed work for this Thesis is analytically presented with justifications for the chosen methodology, identifying the major contributions to the literature. The primal-dual interior point method is outlined with a brief review on relevant applications, pointing out its advantages. The mathematical formulation for the implemented equilibrium market model is presented, accounting for the AC network representation and the iterative process of the algorithm.

- ***Chapter 4:***

The contribution of the mathematical formulation of modelling the transformer power flows, losses and tap-ratio control in the electricity market algorithm is described. Numerical results are presented for test cases with and without transformer tap-ratio control to demonstrate its appreciable impact on the electricity market outcome for different operating conditions. The analysis extends to cases with congested transmission networks, illustrating the significance of modelling such control functions in the electricity market equilibrium algorithms.

- ***Chapter 5:***

This chapter investigates the impact of reactive power control on the electricity market equilibrium. The examined control methods include voltage control using different regulation modes, variations of the reactive capabilities of the generating units in terms of reactive power generation and absorption, and load power factor adjustments. The analysis employs a wide range of test systems with networks from 3 to 118 buses, to show the effects on the market outcome of larger power systems.

- ***Chapter 6:***

The choice between different buses in the system for the instalment of new generating units is investigated. The analysis focuses on the impact of the new entrant’s location on the profits and scheduled production of the existing firms,

social welfare and nodal prices. It is shown that the new firm receives profits of substantial difference depending on the location chosen across the network, showing the importance of employing the AC meshed network constrained market model.

- ***Chapter 7:***

The modelling of grid-connected photovoltaic (PV) systems in terms of economic and operational aspects is integrated into the electricity market algorithm, in order to represent a diverse market able to accommodate power generated from conventional sources and RES. The modelling of the PV unit output performance that explicitly represents the solar irradiance-dependent active and reactive PV power components is based on statistical analysis on experimental data recorded in a PV test facility. The importance of modelling the dependency on the solar irradiance and the nonlinear characteristics of PV reactive generation in the market model is highlighted.

- ***Chapter 8:***

The different parameterization methods for obtaining the SFE strategic bids from the generating firms and the interrelation between the corresponding market solutions are investigated. The analysis focuses on the examination of the different market outcomes for the available parameterization methods under different levels of network congestion, showing that the parameterization impact on the market depends on the level of network stress and on the system size. Possible reasons for the convergence problems encountered in large systems for the arbitrary parameterization of linear supply function bids are established.

- ***Chapter 9:***

This chapter examines the convergence characteristics of the proposed market model in terms of CPU time and number of iterations for convergence requirements. It is shown that the implemented algorithm exhibits superior computational performance and robustness, being able to provide market solutions in terms of milliseconds. The convergence for the different SFE parameterization methods is also examined.

- ***Chapter 10:***

The last chapter of the Thesis provides concluding remarks on the main contributions of the presented research and evaluation of the analysis and numerical studies performed. The opportunity for integrating other network components and control functions in the electricity market model for a more precise and versatile market analysis and the possibility for further work on related research topics are discussed.

- ***Appendix***

The Appendix presents a list of the Newton matrix elements that result from modelling the transformer power flows, losses and tap-ratio control in the electricity market algorithm and evaluation of their respective derivative terms.

Chapter 2:
Electricity market equilibrium

2.1 Supply - demand equilibrium

In a competitive electricity market the total cost of generation of each unit is directly related to the supply. The operating cost can be represented by a variable quadratic expression C that depends on the quantity q produced, such that:

$$C = \alpha \cdot q + \frac{1}{2}\beta \cdot q^2 \tag{2.1}$$

where α and β are the generation coefficients that reflect the characteristics of the various forms of costs involved. The corresponding utility function for the consumers, i.e. the consumers' willingness to pay, also termed as the consumers' benefit, depends on the load demand d for each market period. This can be defined as the following quadratic inverse demand function D:

$$D = \gamma \cdot d - \frac{1}{2}\delta \cdot d^2 \tag{2.2}$$

where γ and δ are the load demand cost coefficients.

In a centralised market the bidding process supervisor, such as an ISO, may ask the market participants to reveal the quantities they are willing to buy or sell over a range of prices for a given time period. The supply and demand curves can be used to graphically represent quantities as a function of price. In a perfect competition market for electricity, the marginal cost of generation and the linear inverse demand function can be used as the supply and demand curves. The marginal cost of generation is given by:

$$MC = \frac{\partial C}{\partial q} = \alpha + \beta \cdot q \tag{2.3}$$

and is defined as the change in total cost for a unit change in quantity produced. The linear inverse demand function, given by:

$$MD = \frac{\partial D}{\partial d} = \gamma - \delta \cdot d \tag{2.4}$$

shows the change in willingness of the consumers to pay for a unit change in the load demand. Figure 1 shows a typical supply-demand relationship. If the buyers and the sellers are both satisfied with the market outcome, the supply and demand curves intersect at the market equilibrium point (q^*, p^*). At this point, where *MC* equals *MD*, there is no shortage or excess of supply. The supply curve has a positive slope because as the price becomes higher the firms are more willing and able to produce power, and the demand curve has a negative slope since the willingness of the customers to pay is restrained at higher prices.

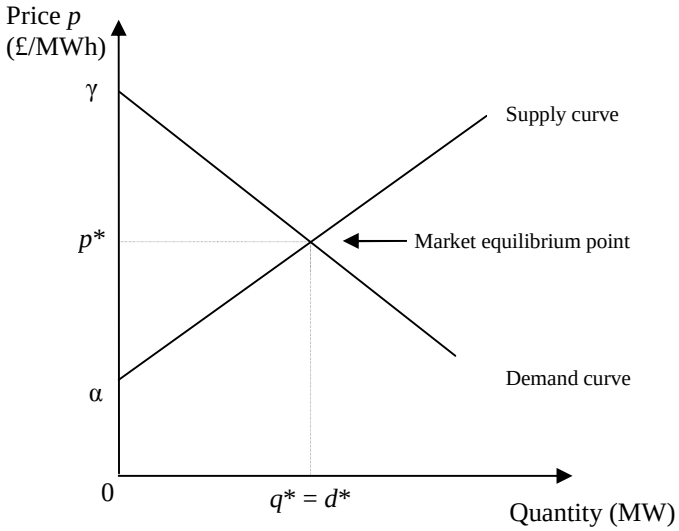

Figure 1: Supply-demand equilibrium.

2.2 The concept of economic surplus

A basic tool for classical economic analysis is the theory of economic surplus. The social surplus *SS*, i.e. the surplus to economy, is divided between buyers and sellers as consumers' and producers' surplus. The producers' surplus is the difference between the market price and the marginal cost of production summed over the output that benefits the producer, and the consumers' surplus is the benefit that the consumers have by purchasing at a lower price than that which they were willing to pay [3]. The surpluses are graphically presented in Figure 2, for a market in perfect competition equilibrium. The horizontally shaded triangle is the consumers' surplus *CS* and the vertically shaded triangle is the producers' surplus *PS*. The corresponding mathematical expressions are:

$$CS = \int_0^{d^*} (MD - p^*)dd = \frac{1}{2}(\gamma - p^*)d^* \tag{2.5}$$

$$PS = \int_0^{q^*} (p^* - MC)dq = \frac{1}{2}(p^* - \alpha)q^* \tag{2.6}$$

$$SS = CS + PS = \int_0^{d^*} MD \cdot dd - \int_0^{q^*} MC \cdot dq = \frac{1}{2}(\gamma - \alpha)q^* \tag{2.7}$$

where $p^* = \alpha + \beta \cdot q^* = \gamma - \delta \cdot d^*$ at the perfect competition equilibrium point. The expressions for oligopolistic markets can be worked out using integration.

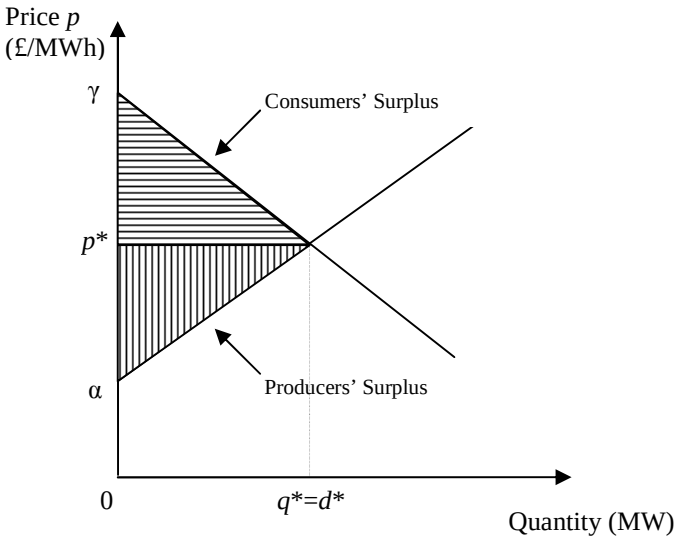

Figure 2: The consumers' and producers' surpluses.

The producers' surplus *PS* corresponds to the sum of the profits of all suppliers, which can be defined as the revenues minus the true generating costs *C*. For a market that employs uniform pricing, the profit is given by:

$$\Pi = p^* q - C = p^* q - \alpha q - \frac{1}{2}\beta q^2 \tag{2.8}.$$

The social surplus *SS* is also termed the social welfare. From (2.7), the social welfare *SW* is given by the consumers' benefit, i.e. the inverse quadratic demand function *D*, minus the true production costs *C*, such as:

$$SW = \sum D - \sum C = \sum [\gamma \cdot d - \frac{1}{2}\delta \cdot d^2] - \sum [\alpha \cdot q + \frac{1}{2}\beta \cdot q^2] \tag{2.9}.$$

The social welfare is at its maximum when a competitive market is allowed to operate freely and the market price equals the perfect competition equilibrium price at the intersection of the supply and demand curves, as shown in Figure 1. If, due to a reduction in the traded amount caused by a price distortion, the

market price is set to a different value, a reduction in the social welfare will occur and the remaining surplus will be redistributed among the consumers and producers depending on the occasion. A price distortion may occur due to several causes; for example it may be of the form of price caps that will benefit the consumers, or of minimum price settings that will be in favour of the producers [16]. However, neither the producers nor the consumers enjoy the lost surplus. This is called the deadweight loss and is a representation of the loss to economy of a market failure. In the case of the oligopolistic market, strategic producers able to exercise market power may attempt to transform more consumers' surplus into profit, and this will result in a deadweight loss [3]. This is discussed further in Section 2.8.

If transmission expenses are included into the market structure, the transmission rights owner claims the cost for the transportation of the product, such as in the case of the electricity market where the market operator or a separate entity collects the transmission congestion rent. For this case, the social welfare consists of the sum of the consumers' and producers' surplus and the transmission congestion rent. If the consumers are paying for the transmission costs, the congestion rent *CR* for different locations *l* can be calculated by the difference between the total consumers' payment and the total producers' income, such that:

$$CR = \sum_{l} (p * d) - \sum_{l} (p * q) \qquad (2.10).$$

In the electricity market modelling in this Thesis it will be assumed that the congestion rent is detained by the ISO.

2.3 Nash equilibrium

Any market environment for which each participant acts independently and no coalitions are present among the players, can be described as a non-cooperative game. John Nash [38] has proved that a finite non-cooperative game always has at least one equilibrium point for which the strategy of each player is optimal against those of its rivals. At that point each player cannot increase its payoff by changing its strategy unilaterally. That profile of strategies for which each

player's strategy is an optimal response to the other players' strategies is defined as a Nash equilibrium. Nash equilibria may be defined by pure strategies or as mixed strategies, in which the players choose from a set of strategies based on associated probabilities. In a bid-based electricity market equilibrium model, a Nash equilibrium results if none of the market participants has an incentive to unilaterally change its bid. The equilibrium point of an electricity market for a given market period can be defined as the set of prices at different nodes, profits of the generating firms, social welfare, power generation output, power distribution in the electrical network and load demand at each node.

Nash equilibria are consistent predictions of the outcome of the game in the sense that if all the market players are able to predict that a particular Nash equilibrium will occur, then no player will have an incentive to change its strategy. This will occur if all the players predict a particular Nash equilibrium point and also predict that their opponents will predict it. A prediction that any fixed non-Nash profile of strategies will occur, implies that at least one player will make a mistake in predicting its rivals' strategies or in optimising its payoff [39].

In many games, such as markets in which the supply curve crosses the demand curve more than once, several Nash equilibria may exist. In this case, the assumption that the outcome of the game will be a Nash equilibrium relies on some process that will lead all the players to the same equilibrium point. Thomas Schelling [40] suggested that the participants in a game can often concert their intentions or expectations with their opponents, if each player knows that the others are trying to do the same. In a situation that provides some clue for coordinating behaviour, each player's expectation of what the others expect him to expect to be expected to do, will lead to a focal point. This Nash equilibrium point is called a focal equilibrium [41] (also sometimes called a Schelling point) and, if its existence is realised, it is preferred by all players. Although games with multiple equilibria may have focal points, game theory lacks a general argument that a Nash outcome will occur [39].

2.4 Oligopolistic electricity market equilibrium models

Several equilibrium models have been proposed for the simulation and investigation of markets that exhibit oligopolistic behaviour, such as the emerging deregulated electricity markets, which vary in terms of competition and market assumptions. Some of the most popular models include the Cournot, Bertrand, and Supply Function competition, while other approaches, such as the Stackelberg competition and the conjectural variations method, have also been used for electricity market analysis. These models are described below.

2.4.1 Cournot competition

The Cournot competition model has been proposed by Augustin Cournot in 1838 [42]. This is an oligopolistic, non-collusive economic model, which assumes that all the firms that participate in the market act strategically and choose the quantities that they are willing to produce simultaneously, which they will then sell at the market clearing price. In Cournot's original model the price mechanism was not specified, but the market clearing price can be thought as being determined by an auctioneer that equates the total supply and demand. Suppliers maximise profits under the assumption that all the other players will keep their output fixed and all the market participants are assumed to have the same information for their rivals' cost functions and the load demand. An equilibrium point for this game can be determined by the condition that all the firms will choose strategies that are best responses to the anticipated actions of their opponents. This will be a Nash equilibrium of the Cournot game and none of the firms will benefit by changing its output quantity, given the output levels of the rival firms [39].

In the early development of the electricity market equilibrium analysis, the Cournot model was considered as the most appropriate one to be applied. Such orientation resulted from the fact that it was an important step beyond monopoly models, being able to assess market power up to a point. However, experience has revealed drawbacks for this approach. The principal shortcoming of the

application of the Cournot model in the electricity markets is that a power generation market is a type of supply-curve competition and not a quantity-based one. Such applications may provide inconsistent or non-realistic estimates for the market outcome, or misinterpret the ability of a firm to exercise market power. Other shortcomings arise from the fact that demand elasticity in the electricity markets is unknown [1]. The Cournot competition model suggests that the strategic generating firms should be able to sustain prices above marginal cost levels with the difference determined by the price elasticity of demand. The Cournot results for the market outcome are very sensitive to this elasticity and the equilibrium prices calculated by Cournot models tend to be higher than the prices observed in practice because the electricity markets have very low elasticity [16]. For instance, the investigation on the England and Wales market in [35] reports that the actual market prices observed were higher than the marginal costs, but not nearly as high as the theoretically calculated prices. Nevertheless, applications of the Cournot model have contributed in the literature in many distinct ways and this method is still used for investigating numerous subject matters concerning the electricity markets. Some notable applications include the following.

The studies in [33,43] have recognised that the shortcomings of applying concentration measures techniques to assess market power abilities are exacerbated in the case of restructured electricity markets and proposed a Cournot oligopolistic model that considered transmission constraints. The model was applied on the California electricity market and the geographic extent of the restructured market was explored, as it was argued that transmission congestion could isolate competition. The analysis shows that the congestion effects depend on the levels of demand and it is also advised that policy makers should take a strong interest in improving the short-run demand price responsiveness in the electricity market in order to limit market power. A subsequent study [37] that simulated future situations in the California market by representing the hydroelectric production in the Cournot model has also shown that the hydroelectric availability affects the extent of market power.

Based on the arguments in [44], the investigations in [45,31] have applied Cournot competition in linearized DC power networks to show the interactions of geographical and electric topology of the network and identify sources of market power other than capacity withholding for raising prices. The representation of network loop flows has illustrated that firms may increase their production in order to block transmission of competitive power supply to increase their profits. The firms may foreclose competition by even producing below marginal costs [46] and this action will affect the nodal prices across the whole network.

The model proposed in [32] shows that transmission constraints affect pure Cournot equilibria, demonstrating that limited transmission capacity may give a producer incentive to restrict its output in order to congest transmission into its area. The analysis in [47] investigates the existence and uniqueness of Cournot equilibria in looped transmission constrained systems and shows that a pure strategy equilibrium may cease to exist when a transmission constraint is introduced, even if the limit is higher than the flow in the unconstrained equilibrium. In addition, the existence and uniqueness of Nash-Cournot equilibria in cooperative games are investigated in [48].

In [49,50], using a DC network Cournot model, it has been shown that generators are able to capture the congestion rents and leave the transmission rights holders uncompensated by adjusting prices accordingly even in the absence of locational market power, resulting in inefficient dispatch and misplaced investment incentives. It has been suggested that strategic consumers may contribute to this inefficiency. This analysis was contradicted in [51], where transmission congestion contracts were introduced in the Cournot model, showing that they may force the firms to sell at marginal cost. A subsequent report [52] classifies the solution of [49,50] as one for a particular type of game that deviates from the definition of non-cooperative games, but it is stated that in Cournot games firms will be able to exercise market power and capture some of the congestion rent. However, the Cournot investigation in [53] shows that an integrated market for transmission and energy, in which the ISO allocates transmission capacities based on optimal operation of a meshed network, reduces market power and

prices compared with a design for separate markets where transmission rights are allocated by auctions.

Following the models proposed in [45,49], other Cournot competition studies have also employed numerical methods to calculate equilibrium solutions for more realistic systems. The model in [54] incorporates generation and transmission constraints to calculate long-term Cournot equilibria for markets in which the generators commit their output to customers through long-term contracts. A more comprehensive numerical model was proposed in [55], where the DC power network representation is implemented. Bilateral and poolco markets are simulated and unique Cournot solutions are computed. An extension of this model that considers forward contracts and accounts for the interactions with pollution emission permits markets was provided in [56], while [57] presented a modification of the DC network Cournot model that includes nonlinear losses, phase shifters and controllable DC lines. A more advanced Cournot analysis that considers nonsmooth demand functions, price caps and joint constraints incorporated in the producers' optimisation problem, such as bounds on the proportion of transmission capacity allocated to each producer, is provided in [58].

A two-settlement market model with DC network representation has been proposed in [59]. The market is characterised by a two-period game, for which a forward market is first operated and a spot market is settled in the second period. Firms' strategic behaviour and social welfare maximisation are assumed for both markets and network uncertainties are modelled in the spot market. The system capacities are unknown when firms enter forward contracts and Cournot equilibrium is calculated for the spot market subject to stochastic fluctuations. The model was modified in [60] to include price caps for both the forward and spot markets, showing that this results in reduced forward contracting. A review on such models can be found in [61] and a case study on a 24-bus system was presented in [62], where it was observed that the strategic firms have incentives for forward contracting. A developed version of the two-settlement market model was proposed in [63], where alternative solution methods that aim to facilitate

Cournot simulations of realistic electricity markets with probabilistic demand and system contingencies are provided.

The report in [64] compares Cournot results for case studies carried out using oligopolistic models from three different research groups and declares that structural and behavioural assumptions affect the equilibrium results. A Cournot game of incomplete information was presented in [65] and equilibria were calculated for different estimation models of the rivals' production costs, to show how the accuracy of such predictions affects the market outcome. Additionally, a computationally efficient algorithm for the calculation of Cournot equilibria with comparisons of test cases for different market concentration and demand elasticity is provided in [66].

The report in [67] calls to attention that reactive power and voltage related issues are commonly neglected in Cournot oligopolistic models. The authors proposed that a DC approximation does not capture properly the features of the electrical network, providing an example in which Cournot players identify the potential for market power due to voltage constraints and reactive power in the system. Then, they presented a Cournot model that employs AC network representation and considers both active and reactive power quantities as strategic variables in [68,69], showing the significant impact of reactive power on the market outcome. Comparisons of Cournot outcomes under DC and AC assumptions are presented in [70].

2.4.2 Bertrand competition

A review that criticised Cournot's theories on oligopolistic competition was published by Joseph Bertrand in 1883 [71]. His argument was that an equilibrium based on quantity decisions was not a true equilibrium because if a supplier was offering the product at a lower price could attract all buyers. In the Bertrand model, prices are considered to be the strategic decision variables, instead of quantities. The non-collusive firms compete by setting their prices simultaneously and letting the market decide how much each firm will sell, under the assumption that all firms can produce as much output as required to meet

demand. Since there are no output restrictions and the buyers will choose the cheapest price, a firm can capture the entire market by setting its price slightly less than those of the other firms, if the product is homogeneous (as in the case of a general deregulated electricity market). The other firms will anticipate the action of the one with the lowest price offer and in retaliation they will bid slightly lower, so that a sustainable equilibrium will be reached only when the price is reduced to the marginal cost of generation, since lower offers will result in a loss and a firm will choose instead not to produce at all. The market price will be equal or near to the marginal cost of generation of the most efficient firm, since a higher price will be undercut by the offer of a firm with lower costs. Therefore, the competitive price is the best price that firms rationally expect to achieve [16].

The assumption that a single supplier can capture the entire market is not applicable in the case of the electricity market where the generation capacities have strict constraints. In addition, a supplier cannot bid a lower price with the aim of increasing its output, since the marginal cost of generation is increasing as the output increases [17]. Also, it has been addressed in the literature that in the presence of transmission costs and generation or transmission constraints, prices can drift above the marginal cost and may fluctuate continually eliminating the possibility for pure strategy equilibria. Consequently the only equilibrium is a mixed strategy (probabilistic) one [72]. However, the analysis in [32] pointed out that in a duopoly where a transmission constraint is present the firms' behaviour in choosing price offers will differ from the standard Bertrand outcome. In addition, the discussions in [73] argue that the Bertrand model can give interesting results if used in the context of generation capacity constraints and increasing marginal costs, implying that since no single firm can capture the entire market the resulting market outcome will no longer be competitive and the equilibrium price will be higher than the marginal cost. However, this model still assumes that the price decisions of one's competitors are weakly linked to its own decisions, while it does not resemble the supply-curve type competition that dictates the electricity market.

Oligopolistic models based on Bertrand competition have been occasionally applied to electricity market analysis. Nash-Bertrand equilibria were calculated in [30,74], which consider spatial variations in demand functions and production and transport costs, in order to compare regulated and deregulated electricity markets. The Bertrand prices are assumed to be undercut to a value just less than the second lowest marginal cost of the participating firms and the results have shown prices above the marginal costs. A similar study [75] compares Bertrand results for spatial and mill pricing (i.e. customer buys at the plant and transmission is disregarded), as well as Bertrand and Cournot outcomes, for short- and long-run operations.

A numerical approach for a Bertrand model was presented in [76], in which the market participants submit prices with the quantity that they want to sell and they are ordered by price to meet demand in a pay-as-bid scheme resulting in mixed strategy equilibria. Similar assumptions are considered in [25], where firms compete by submitting prices for their available production and a cap for the bid prices is considered. Comparisons are made for price competition outcomes under uniform and pay-as-bid pricing. Another study that employs unconstrained Bertrand competition and assumes that the market clearing price equals the marginal cost of generation is proposed in [77], in order to compare the mean and variances of electricity prices for different competition types, with the Bertrand solution being the lower benchmark.

2.4.3 Supply function equilibrium

In 1989 a publication by Klemperer and Meyer [78] has proposed a new oligopolistic market model, called Supply Function Equilibrium (SFE). The original model was set as an oligopolistic framework in which the market players are facing uncertain demand. Each firm in this non-cooperative game chooses a strategy based on a supply function that relates the quantity it is willing to sell to its price. This supply-curve bidding allows a firm to adapt better to changing conditions, such as an uncertain environment, than either bidding fixed quantities or in a commitment to fixed prices as in the Cournot and Bertrand settings. The decision variables for the strategic firms are the parameters of their supply

functions that are usually related to production costs, capacity constraints and demand elasticity to price. Klemperer and Meyer calculated the equilibrium solution by solving a differential equation for profit maximisation to find the optimum bids for the firms and allow the supply functions to take any form. This approach will be referred to as the general case SFE. Furthermore, under sufficient conditions they have proved that the linear SFE solution is unique (see subsequent sections). Later studies have utilised different formats of supply functions, while it was proposed that the modelling of supply function bids restricted to linear form exhibits certain advantages, which will be discussed later on. Qualitative examples for general, linear and step-wise supply function bids are shown in Figure 3, (a), (b) and (c) respectively.

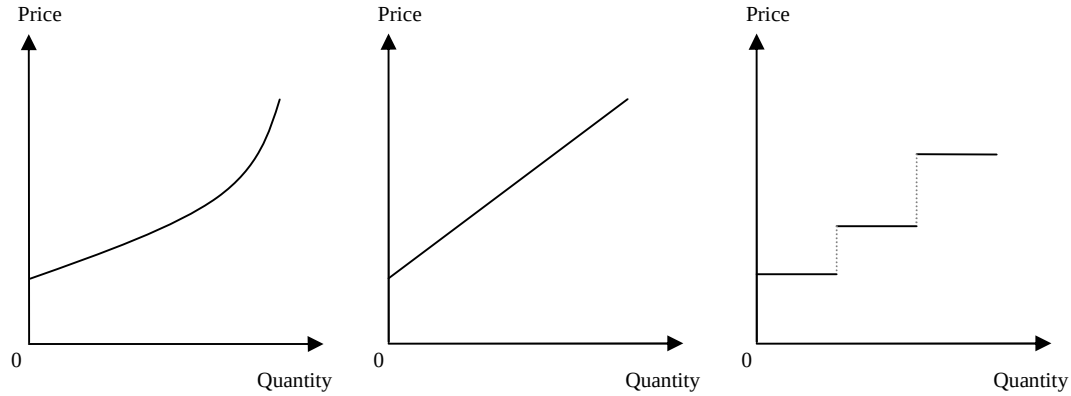

Figure 3: Examples of supply function bids.

At the equilibrium point of the supply function game each player determines its optimum supply-curve bid that maximises its profit based on how the other players will adjust their output to changes in market prices, anticipating their strategies. This type of competition leads to a less profitable outcome for all suppliers compared with Cournot competition. By switching from quantity bids to supply function bidding it is possible to exercise market power in any demand level in the case of uncertain demand, but if all players bid in this manner the majority of the profits will be reduced as competition will be increased [1]. Klemperer and Meyer [78] have shown that price and quantity in any SFE are bounded by the Cournot and Bertrand outcomes. Cournot equilibrium resembles a vertical supply function, being a worst-case scenario, and Bertrand corresponds to a horizontal supply curve. Therefore, they suggested that a Cournot model

could be a better approximation in markets with steep marginal cost curves relative to demand, while markets with flat marginal costs may be approximated by Bertrand competition. However, if supply-curve bidding is allowed, a fixed price or a fixed quantity cannot be an equilibrium strategy if marginal costs are upward sloping, as in the case of the electricity market.

In contrast to the Cournot model, the SFE model offers the possibility of developing insights into the bidding behaviour of the firms and offers the ability of representing the obligation to bid consistently over a time horizon. As electricity markets often require suppliers to offer a price schedule that applies throughout a day rather than a series of quantity bids, the SFE approach is more attractive compared to the Cournot model since it is a more realistic view of electricity markets. Furthermore, the SFE prices are not very sensitive to their dependency on demand as in Cournot competition, and the price predictions will be more reliable [79].

The study in [78] shows that in the absence of uncertainty an enormous multiplicity of equilibria exists, but uncertainty reduces this set dramatically. It is shown that if the range of demand is unbounded then there is a unique symmetric linear SFE for a market with linear demand and identical marginal cost curves. If demand is bounded, as in realistic electricity markets where the load demand cannot be infinite, then a continuum of equilibria exists, ranging from Cournot solutions being the highest prices, to competitive prices. A similar effect to demand uncertainty can be imposed if the market players are required to submit a single bid schedule for a time horizon that accommodates a variety of different demand levels. The main criticism of the SFE models is that they produce multiple equilibrium solutions and therefore they have little predictive value in practical investigations. Fortunately, several studies have determined conditions under which the range of equilibria can be very narrow, or a unique SFE may be established.

Concerning the electricity market, the strategic bid of a generating firm can be interpreted as a function mapping price into a level of active power production, independent of time. Since cost functions for producing electricity are in general

increasing functions of output power and different demand levels that are unknown at the time of bidding require different quantity bids, the supply function equilibrium has been widely considered as the most appropriate model to represent the interactions between strategic generating firms. The first that applied the SFE model in the electricity market were Green and Newbery [8] and Bolle [80] in 1992.

Green and Newbery's innovative model, which opposed the opinion that the 1990 restructuring in the England and Wales market would eventually result in a competitive market, has drawn the attention of many researchers to focus on different approaches that employ the SFE model. Research in the following years varies in market assumptions and representations of suppliers' constraints and electricity networks. Apart from the general SFE model, the most popular approach is the linear SFE model [81], in which the market players parameterize their linear marginal cost function by varying its slope and intercept in order to construct their optimum bids. A detailed literature review on the linear SFE models and their applications, as well as on advances of the general case SFE, follows in the subsequent sections.

2.4.4 Stackelberg and multi-leader-follower games

The Stackelberg model has been proposed by Heinrich von Stackelberg in 1934 [82] to investigate non-cooperative games in which a leader that dominates the market acts strategically and naive followers believe that they cannot affect the market conditions through their decisions. The leader chooses its strategy first, while the followers observe this action and participate in the market sequentially. The leader recognises how the followers' decisions will depend on the market variables and is able to explicitly account for their reactions in its strategy. The original formulation by Stackelberg examined duopolies that take decisions on their quantities, but different strategies with a number of market participants can be modelled in this manner. This single-leader-follower method has been regarded as an oligopolistic application, but due to its hierarchical structure it is a rather monopolistic approach. An extension of the Stackelberg game is the multi-leader-follower game, in which two or more leaders act strategically and compete

with each other. In the case of the electricity pool market, the ISO is considered to be a follower [83]. It may be assumed that the followers compete with each other and with the ISO after the leaders choose strategies, but most commonly perfect competition conditions hold for the followers in most electricity market models.

Stackelberg formulations have sporadically appeared in electricity market studies. A dynamic Stackelberg model that examines the long-run transmission expansion decisions was outlined in [84]. It describes the interactions between a transmission firm that takes decisions on transmission capacity availability (the strategic variable) and two followers that supply and purchase power. Another Stackelberg equilibrium model, in which the leader is a strategic generating firm that acts in a Cournot manner to maximise profit and the followers comprise a competitive fringe, was presented in [85]. The electrical network is represented by AC formulation to account for transmission congestion and reactive power related issues and the numerical results show that the reactive power influences the equilibrium point, while the leader exercises more intense market power in the presence of tighter transmission capacity constraints. A detailed investigation of Stackelberg games in a joint energy and emission permits market with DC network representation was presented in [86]. The leader chooses quantities of output and emission allowances to withhold, while the group of followers consists of price-takers (Bertrand behaviour) and Cournot players that can influence prices. Furthermore, the numerical algorithm of the SFE model in [87], which undertakes two stages in updating the supply function strategies of the firms in order to reach an equilibrium solution, employs a Stackelberg game in the first stage.

The properties and numerical approaches for multi-leader-follower models were explored in [88,83]. Multi-leader-follower games for the electricity market have been proposed by using Cournot and supply function bids. The analysis in [69] provides equilibrium results for leader-follower games where leaders bid in the Cournot manner and present cases for different number of leaders. Also, Stackelberg and 2-leader results were presented in [89] by employing supply

function bids. Other studies that consider markets with strategic firms and price-taking competitive fringes include [33,37,45,79].

2.4.5 Conjectural variations method and conjectured supply functions

The conjectural variations approach is used to estimate the strategic behaviour of market players that maximise their profits while taking into account the reactions of their rivals. This economic concept has been brought into attention by Bowley in 1924 [90]. The first application for electricity market analysis appeared in [91], where the conjectural variations method is used to overcome the shortcomings of Cournot equilibrium related to demand elasticity. Instead of considering the actual rivals' supply bids, the model employs only public past market data to represent the beliefs about the rivals' bidding behaviour. The rivals are supposed to adjust their supply offers in response to price changes and their reactions are modelled by the residual demand, i.e. the remaining demand after subtracting the rivals' supply functions from the market demand curve, which is characterised by its elasticity. The optimal supply decision is then made based on this elasticity, which expresses the market conjecture of each firm. The significance of this parameter is that different levels of competition can be modelled by varying it, being a measure of the firms' perception about their market position, and the numerical results obtained are found to be more realistic than the corresponding Cournot outcome. This method was extended in [92] by defining the conjectural variation of a firm as its belief about the response of its rivals' quantity to a change in its own quantity, by facing its competitors as a single entity. It is proven that conjectural variations solutions for electricity markets are Nash equilibria, showing that a firm does not need to know the rivals' cost functions in order to make optimal decisions, and the strategies of other games, such as Cournot, Stackelberg and perfect competition, are shown to be special cases of conjectural variations strategies. A subsequent study [93] presented a method in which the firms conduct learning in a conjectural variations framework and tune their own responses to rivals' decisions. The main criticism for this method is the static nature of the analysis and the theoretical difficulties involved in empirical estimation of the conjectural variations parameter in the absence of cost data [94].

A model that represents the conjectures of the firms regarding how their rivals will adjust sales in response to price changes by implementing conjectured supply functions in a DC network has been proposed in [94]. This approach is termed as the Conjectured Supply Function (CSF) method and can be viewed as an approximation of the SFE, but the assumed and actual response functions may differ. The CSF approach represents the full range of the different types of strategic interactions that vary in how firms anticipate the rivals' reactions to their decisions concerning either prices or quantities. It has the advantage that the calculation of equilibria can be simplified, but it shares the same limitations as the conjectural variations model. Formulations for bilateral and poolco market models are presented by utilising linear response functions and the CSFs are parameterized by varying either their slope or intercept. The presented results on the England and Wales market show that the equilibrium prices from the CSF model are more consistent with those actually experienced when compared with Cournot results. Another study that employs the CSF method appears in [95], which considers the deviation of the forecasted rivals' reaction from the actual response and introduces financial risk. A multi-period CFS model is presented in [96] for a joint energy and spinning reserve market. CSFs are used for both energy supply and spinning reserve in a DC network framework with intertemporal constraints for ramp up/down rates and maximum output over a time horizon. In addition, a CSF approach that analyses the demand responsiveness to price is presented in [97].

2.4.6 Choosing the most appropriate method for electricity market analysis

All the aforementioned oligopolistic models have contributed in their own way to the electricity market literature in terms of, among others, investigating the issue of market power and the strategic behaviour of the firms and predicting the market outcome. However, considering the pros and cons of each method, the SFE approach has been employed for this Thesis' research because it has been proven to be the more realistic representation for the electricity market. Furthermore, despite the references about SFE's limited potential in realistic applications due to the mathematical complexity involved, this Thesis presents a

versatile novel numerical SFE model able to solve large and complex systems, contributing in a distinct way to the literature as shown in the subsequent chapters. Therefore, the discussions that follow are limited to SFE studies only.

2.5 General SFE models

The SFE model proposed by Bolle [80] considers a pool type market in which there are no restrictions for the producers in choosing the strategies that relate prices and quantities. The model is based on the assumption that there are no supply capacity constraints and different market scenarios in terms of pricing are examined. A continuum of symmetric equilibria results for all the examined games and the equilibrium selection is based on the solution with the highest profit for all players. Recalling the proof from [78] Bolle shows that for the symmetric unique equilibrium with linear demand and marginal cost curves, the market prices decrease as the number of generating firms increases. The prices will eventually converge to marginal cost values in the case where consumers pay spot prices. If constant prices chosen by the auctioneer are to be paid, the monopoly solution, i.e. the joint profit maximisation case, has been found to be an equilibrium and the concluding remarks refer to the unrestricted supply function model as a market that may be governed by tacit collusion.

The aforementioned study did not consider any limitations for the shape of the supply functions. In some cases, such as in the numerical results of Bolle, the SFE may be characterised by a decreasing supply function. Even though the original SFE model by Klemperer and Meyer did not restrict the supply offers from being decreasing functions, a non-decreasing constraint for the supply function bids should be included, since in most realistic electricity markets the participants are not allowed to commit to a decreasing schedule of supply function offers, or decreasing supply functions are explicitly ruled out by design [98].

Green and Newbery [8] have proposed an SFE approach to model the major restructuring in the England and Wales electricity market using the general SFE

model that solves a Klemperer-Meyer differential equation, by simulating a symmetric duopoly to show the interactions of the two dominant firms in the market. Instead of a single supply function bid for one bidding interval, the generating firms submit a whole supply schedule of prices for active power generation. The bidding takes place for the following day (a time horizon of 24 hours) for half-hour intervals. The dispatcher determines the spot price and the required supply quantities assigned to each firm for each interval, by equating supply to demand at each moment. The spot price is set at the bid of the marginal (most expensive) generator. This model takes into account the generation capacity constraints of the suppliers and it is shown that these constraints narrow down the range of possible equilibria. The study extends to a simplified asymmetric capacitated duopoly case and focuses on possible inefficiencies, such as high deadweight losses due to the influence of the dominant firms on the prices, and suggests that they can be avoided by subdividing the duopolistic industry into five equal firms. An extension to this model was proposed in [99], where the impact of the divestitures in the England and Wales market on the prices is analysed, by simulating the market capacity from the asymmetric firms as evenly distributed to symmetric firms, together with a competitive fringe.

The study in [100] has extended the model of [8] to include contracts, contestable entry and variable number of competitors, showing the interactions of contract and spot markets. It shows that the range of possible equilibria can be narrowed down not only by generation capacity constraints, but also by increasing the number of competitors in the market. Furthermore, it proves that the entry threats and contracts can further narrow down the range of equilibria to give a unique equilibrium point without the unrealistic assumption of unbounded demand. This unique equilibrium can be sustained as long as entry is backed by contracts. Market power of the incumbent players is reduced if entry remains contestable and the contract market is reasonably active, while increased competition reduces the prices. Another general SFE model that investigates the impact of contracts on the bidding behaviour of strategic firms in the electricity spot market has been proposed in [101]. This model considers a duopoly where the players submit a smooth non-decreasing supply function. Price caps and generation capacity constraints are considered, and the demand is a nonlinear function of price

subject to a bounded random shock. However, these models consider the firms to be symmetric, which is an unrealistic assumption.

In [102] a numerical approach has been proposed to calculate equilibria in electricity markets with non-decreasing supply function bidding, considering asymmetric generation capacity constraints, firms with asymmetric quadratic cost functions, and price or bid caps. It is argued that it may not be effective to calculate asymmetric SFEs using the Klemperer-Meyer differential equation approach by itself because it produces solutions with supply functions that fail to be non-decreasing, while even when non-decreasing SFEs are produced many of these are unstable. In order to provide a method to calculate non-decreasing stable equilibria, the model iterates in the function space of the allowable supply functions to numerically solve for the solution. The resulting supply function curves at the equilibrium point consist of a large number of successive affine (linear) supply function segments, each constructed by one step of the iterative process. A local search algorithm that identifies the optimum direction for the supply function is used, and it is expected to yield only stable equilibria. Since decreasing supply functions and unstable equilibria are ruled out the range of the equilibrium solutions that are likely to be observed in practice is narrowed. However, this search algorithm does not guarantee to find a global optimum solution because there may be multiple local optima for the direction in the function space. This algorithm was also used in [103] and a similar approach has been proposed in [104] to provide a more computationally efficient algorithm.

The numerical results in [102] and [103] have shown that when price caps are binding the range of stable equilibria is very small, and even when price caps are not binding, this range is also relatively small. It is shown that with moderately tight capacity constraints and price caps, unique equilibria with prices well below Cournot prices will yield. All but one equilibrium are unlikely to be observed in practice, with those that firms offer prices much higher than their marginal costs being the less stable. It is shown under some restrictive assumptions that, with quadratic cost functions (i.e. linear marginal costs), all SFE solutions between the most competitive and the Cournot solutions, except the linear SFE, are unstable. With bid caps, similar SFE bids result, while the profits are higher since the

market price can exceed this cap. The investigation has shown that the SFE prices appear to be well below Cournot prices at all times, strengthening the observations of [8] for markets requiring fixed bids over a time horizon with substantial demand variation, depicting the time horizon coupling effects on limiting the possible resulting equilibria.

The model proposed in [105] has advanced the theory of Klemperer and Meyer by implementing a special case for a market in which symmetric profit-maximising firms submit step-wise supply functions to a pool. The uniform market price is set by the bid price of the marginal unit and generation capacity constraints are considered. The model was applied to data from the Pennsylvania electricity market to produce symmetrical SFEs and the analysis elaborated on the resulting equilibrium prices to show that even with a large number of market participants the market price will still be significantly higher than the perfect competitive price. The prices at equilibrium have been found to be sensitive to the average reliability of the generators, the amount of the reserve capacity in the system and the precision at which the strategic firms are able to predict the demand. Subsequent studies [106,107] have provided the formulation and methodology to implement general SFE games for uniform and pay-as-bid pricing mechanisms, investigating the existence of equilibria and the ability of the players to convergence to a linear equilibrium. The approach in [105] attracted the attention for further investigations, such as the one in [108] where the model was extended to include arbitrary convex cost function instead of piece-wise linear forms. Also, the stochastic model in [77] that predicts the mean and variance of electricity prices over a time horizon employs the aforementioned SFE model and exhibits the advantage of capturing the effect of the entire supply system on the prices, over similar models that employed the Cournot and Bertrand theories.

Another study by Bolle [109] used aggregated step-wise supply and demand functions to explore the effects of strategic demand-side bidding in unconstrained markets. It was noted that depending on the proportion of the strategic demand, such as big customers that can switch on and off their electricity-consuming devices, the market prices may be much higher than marginal costs, or mixed

strategies may result. If the market participants choose to play mixed strategies, then instability in the form of fluctuations of supply and demand should be expected and it may be advantageous for big customers to collude. It concludes that the existence of strategic demand seems to be crucial for the absence of pure strategy equilibria with low prices, and raises the question whether or not demand-side bidding should be allowed in the electricity markets.

A different type of market equilibrium closely related to the SFE model was investigated in [110], based on the Australian electricity market. This study examines a duopoly where the firms choose a set of discrete prices that will be fixed for 24 hours and then each firm chooses quantity bids to offer at each price for each half-hour interval of the day. The actual scheduled quantities are determined based on the system demand during a 5 minute period, in which the cheapest bids are dispatched with a uniform market price. Nash equilibrium is obtained for the quantity setting sub-game, in which the players aim to maximise their expected profit based on probabilistic uncertain demand levels when prices are already known. This study examines the stability and existence of equilibrium for this particular type of market.

2.6 The linear SFE model

In 1996, Green [81] has proposed for the first time an SFE model that deals exclusively with linear supply functions. The model considers asymmetric firms with cost functions that dependent on a single quadratic component, i.e. the marginal costs are linear and normalised to zero at zero output, and the time-dependent demand is a linear function of price with negative slope. The bidding process is similar to that of [8], i.e. the firms submit bids for the next 24 hours etc. The form of the supply function bid that the firms are allowed to submit to the pool is restricted to a linear function that relates price and quantity and passes through the origin with positive slope – the same form as the marginal cost. The firms make decisions on their strategies by varying the slope of the supply function, which is the strategic variable. The pool operator schedules the firms by ranking them in order of increasing bids to ensure that the bids are non-

decreasing in price. The model solves a differential equation for profit maximisation as in previous general SFE models but considers as an equilibrium solution only the unique linear SFE solution. As already mentioned, in the case of unbounded demand and linear marginal costs, the linear solution is the unique one. In the electricity market where the demand is not infinite the linear solution is not unique but is still the most tractable. Green shows that the linear solution is a reasonable approximation for any equilibrium function at low levels of demand, while even if, for higher demand levels there are multiple equilibria, the linear solution still remains an equilibrium. The model has been successfully applied to represent different policies that could increase the competition in the England and Wales electricity spot market.

Even though Green [81] did not emphasise the unique advantages of the linear SFE model, it has become the most popular oligopolistic equilibrium model superseding the Cournot approach to a large extent. A comprehensive development of the linear SFE model and discussions on its advantages and properties have been given in [79]. The main advantage of linear SFE models with linear marginal cost functions over the general form is the ability to handle asymmetric firms for cases with more than two strategic firms. The general SFE model requires the solution of a set of differential equations or iteration in the function space of supply functions, which renders the solution very difficult to find. Therefore, most investigations were confined to consider symmetric firms. The linear SFE can handle asymmetry, as well as multiple strategic firms. Furthermore, apart of Green's remarks, the choice of approximating the market by the linear SFE model can be justified, since [102] shows that for symmetric cases with linear marginal costs and no capacity constraints, all SFEs except the linear SFE are unstable, while based on numerical simulations of asymmetric cases it suggests that the less competitive SFEs than the linear one are also unstable. A different approach for the mathematical proof of existence and uniqueness of the linear SFE is provided in [111].

The linear SFE model in [79] is a generalisation of [81] that includes asymmetric costs, capacity limits, non-zero marginal cost and supply function bid intercepts, a competitive fringe and allowance for piece-wise linear supply function bids. It

simplifies the mathematical complexity of the problem by choosing a slope for the demand function that is independent of time, and since the linear SFE model does not depend on the load duration characteristic but only on the demand function slope, it enables profits to be estimated over a time horizon, such as a year. Also, by using the aggregated demand and price as a function of time, equilibrium prices at any instance in a time horizon can be evaluated. In contrast to Green's model, this investigation suggests that a linear marginal cost function that passes through the origin will overestimate profits compared with a more realistic piece-wise function with non-zero cost at zero output that has the same cost at full production. Therefore, a zero-intercept function is not sufficient being particularly unrealistic if supply is close to the lower limit of the generator and a linear approximation of the marginal cost function must match the piece-wise function at both full and zero output. A very important feature of this investigation is the analytical proof for the uncapacitated case that it is profit incentive for the strategic firms to reveal the true intercepts of their marginal cost functions for equilibrium bidding. Therefore, as in Green's model, the strategic variable is the slope of the supply function, but this stems from the mathematical analysis of varying independently both coefficients of the marginal cost function showing that the strategic players should bid an intercept equal to the true value in order to achieve maximum profit at the equilibrium point. The market model in [79] has successfully simulated the divestitures in the England and Wales electricity market and seems to fit the price behaviour better than the zero-intercept linear SFE model in [81]. An earlier version of this investigation can be found in [112].

2.7 Parameterization of linear supply functions

The models in [81] and [79] have used the slope of the supply function as the parameter that defines their strategy, while they kept the intercept of the supply function fixed to the true value of the linear marginal cost function intercept. This can be interpreted as parameterizing the marginal cost function by adjusting its slope to construct the strategic supply function bid. Such an approach for modelling the SFE bids has been referred in the literature as slope-

parameterization. Four different parameterization methods have been proposed for the linear SFE models, each one considering different strategic variables and restrictions on the choice of the supply function offer. Discussions on the impact of the chosen parameterization method on the resulting SFE can be found in [113], while further elaboration on this takes place in Chapter 8.

By considering a linear marginal cost function as in (2.3) and a supply function bid $SB = \hat{\alpha} + \hat{\beta} \cdot q$ with $\hat{\beta} > 0$, where $\hat{\alpha}$ and $\hat{\beta}$ are the parameterized bid terms that correspond to the true generation coefficients α and β, the different parameterization methods that can be used to construct the linear supply function bid *SB* can be described as:

(i) Intercept-parameterization: the strategic players adjust the intercept α of their marginal cost functions to construct the profit-maximising bid to be submitted to the pool, while keeping constant the slope β. Most models keep the slope fixed at the value of the marginal cost function slope, but a model may assume that the players are allowed to fix the slope at a pre-assigned non-negative value that might be other than the true slope. In this Thesis the intercept-parameterization approach will be referred as α-parameterization.

(ii) Slope-parameterization: the strategic players' behaviour is modelled by varying the slope β of the marginal cost functions while keeping constant the intercept. Again, most models set the intercept equal to the true value of the marginal cost function intercept, but pre-assigned intercepts at other values may be allowed. The slope-parameterization method will be referred as β-parameterization.

(iii) Slope $\propto$ intercept-parameterization: in this parameterization method the strategic players adjust both the slope and intercept in the supply function, but in a fixed linear relationship as the one between the true α and β parameters of the marginal cost function. This can be interpreted as multiplying the marginal cost function by an arbitrary non-negative constant, say k_F, in order to construct the supply function bid, such that $SB = k_F(\alpha + \beta \cdot q)$. The strategy of the players is defined by parameterizing the supply function by adjusting the k_F factor. In this Thesis the k_F term is termed as the bidding parameter and this parameterization method will be referred as k_F-parameterization.

(iv) Slope-intercept-parameterization: this method allows more degrees of freedom for the choice of the strategic supply function by arbitrarily parameterizing both slope α and intercept β independently. This represents the true flexibility in strategies available to bidders in the context of the linear SFE model. It will be indicated as (α, β)-parameterization.

The choice of the parameterization method depends on the purpose of the analysis for which the oligopolistic model is designed. The (α, β)-parameterization is considered as the most realistic of these four since it allows any non-decreasing linear supply function to be implemented as an equilibrium strategy. It illustrates the true potential of the firms to exercise market power, as far as linear SFE is concerned, and is expected to yield superior profits compared with the other parameterization methods, as demonstrated by numerical results in [104] for a 5-firm unconstrained system, and in [113] and [114] for linearized 2-bus and 6-bus DC systems. However, such high profits may be limited and subject to the network and market constraints present as it will be discussed later in Chapter 8. The (α, β)-parameterization method has been employed only by a limited number of studies for two reasons. Firstly, a unique (α, β)-parameterized SFE exists only in rare cases under very restrictive conditions and therefore it will be difficult to perform mathematical analysis for comparison of different market situations as multiple equilibria will most probably be encountered. Such comparisons would be fraught, even though the market outcome predictions are more realistic, because it will not be apparent which equilibrium to select. The second reason is related to the fact that complicated systems that consider the electrical network and multiple players cannot be solved analytically and numerical algorithm approaches are required. As this type of parameterization has multiple SFE solutions, the algorithm employed will have difficulties in converging if the SFE points are not (at least) locally unique, due to oscillations in the convergence process caused by a continuum of equilibria [115,116]. Yet, other reasons related to AC network modelling may also be responsible and further discussions take place in Chapter 8. Other studies that use the (α, β)-parameterization include [117-119,89] that present results for DC or relatively small systems.

The other three parameterization methods have been criticised to be less predictive than the (α, β)-parameterization in describing the market behaviour, since they may provide equilibrium results that can be artifacts of their restrictive assumptions. In [113] it has been shown with a simple example that the SFE solution of the (α, β)-parameterization differs from those of the other three methods and in certain cases even the existence, non-existence or multiplicity of equilibria can be an artifact of the numerical framework. Nevertheless, the α- and β-parameterization methods tend to have locally unique equilibrium points when modelling markets with transmission network representation, and the numerical algorithms employed will converge to comparable equilibrium solutions for different operating conditions in an electricity market. Furthermore, if only intercepts or only slopes are manipulated by fixing the other coefficient to its true value, the resulting local equilibrium point will also be an equilibrium for the (α, β)-parameterization game as well, as long as the strategic variables do not reach any limits specified in the market model [115,116]. Therefore, in either case, the coefficient held constant can be chosen accordingly to result in a (very probably unique) Nash equilibrium that corresponds to the most desirable equilibrium point under (α, β)-parameterization (for further elaboration see Section 2.12). However, congested lines in network constrained models may also lead to multiplicity of local SFEs [120,116]. Note that the investigation in [118] reports through numerical results on a 2-firm market structure that the choice between the α-, β-, or (α, β)-parameterizations does not show appreciable difference in the unconstrained SFE market outcome, while the investigation in [104] for a 5-firm market makes similar observations for the α-, β- and k_F-parameterizations. Nonetheless, it seems that this is not the case if more complicated network constrained systems are considered (as it will be shown later in Chapter 8). However, each of the aforementioned parameterization methods may be used for qualitative comparisons of different market situations and their employment can be justified by the purpose and requirements of the apparent oligopolistic analysis, but the equilibrium results of each parameterization model are expected to differ from each other. Comparisons of the four methods based on numerical results on an unconstrained system were provided in [104], while Chapter 8 in this Thesis extends the analysis on AC network constrained systems.

The slope-parameterization, as already discussed, is closely related to the unconstrained linear SFE model resulting from the Klemperer-Meyer formulation, in which revealing the true intercept in the strategic bid is profit incentive, being an equilibrium condition for supply function bidding over a time horizon [79]. Therefore, since this type of parameterization is naturally related to the original SFE model in [78], it enables the ability to provide an extension to model situations that incorporate network or other constraints. It has been used in [81,111,104,118,113,115,116,124-132], being the most popular parameterization approach.

The intercept-parameterization has been regarded by some studies as more appropriate than the slope-parameterization, because the slopes of the marginal cost functions are usually very shallow and the steep slopes that would result from the strategic behaviour would not be credible. The intercept manipulation approach can be utilised instead, since the steepness of an aggregate bid curve for an entire multi-unit firm can be manipulated by different markups ($\hat{a}$-α) for different generating units [87]. A major advantage of the α-parameterization is that in the case where the SFE approach is intended to be used for market power assessment in the oligopolistic environment, the manipulation of the intercept provides a clear picture of how the strategic firms shift their supply functions up or down, specifying the price at which a generator is willing to start producing [116]. This conception was primarily considered in [121] to assess the extent of market power in the Nordic power market. The intercept-parameterization method has also been employed by the studies of [87,118,115,104,114,24,122,123,116].

The k_F-parameterization method can be regarded as exercising market power by offering optimised supply functions that are scaled versions of the true marginal cost functions. Hence, this model depicts successfully the strategic behaviour in the oligopolistic environment of the electricity market and is eligible for comparisons of different market situations for qualitative purposes, such as the investigation of the impact of network constraints on the equilibrium market outcome and the interactions between the strategic firms. Examples of such studies that employ the k_F-parameterization include [73,133,120]. Furthermore, it

appears to be a convenient way to simplify the SFE model in order to employ easily numerical computation techniques to deal with complicated market structures that involve electricity network representation and large systems. An aspect that can be regarded as a drawback, which can also be shared with the α- and β-parameterization methods if the non-manipulated term is fixed to its true value, is that it cannot predict the focal equilibrium if multiple SFE solutions exist [113]. However, the investigation in [128] has shown that the existence of multiple equilibria should not be expected in large numbers for realistic cases but only for small trivial systems (see Section 2.12). Other investigations that employ the k_F-parameterization appeared in [134-138,104].

2.8 Deadweight loss in SFE oligopolistic markets

As mentioned earlier, any distortion that forces the market prices to move away from the perfect competition price will result in different consumers' and producers' surplus, as well as in deadweight loss. The market prices in any environment in which the players act strategically, as in oligopolistic electricity markets, drift away from the perfect competition values. A graphical example that depicts the qualitative behaviour of the oligopolistic market based on the k_F-parameterization SFE model is given in Figure 4 (PC stands for perfect competition). The graph shows that if the strategic bidder chooses to submit a supply function with a bidding parameter larger than 1.0, which is the most likely case, the equilibrium point will be shifted to a higher price and lower supply.

The social welfare for perfect competition is graphically defined by the area bounded by the marginal cost function, the demand curve and the price axis; this is divided to consumers' and producers' surplus by the horizontal line $p = p^{PC}$. For the SFE case, the strategic producers transform some consumers' surplus into profit, resulting in deadweight loss. The resulting SFE social welfare is the area enclosed by the line $q = q^{SFE}$, the marginal cost function, the demand curve and the price axis, which is smaller than that for perfect competition, divided into consumers' and producers' surplus by the horizontal line $p = p^{SFE}$. It can be seen that the consumers' surplus becomes smaller and the producers' surplus

higher, with a deadweight loss defined by the area enclosed by the marginal cost function, the demand curve and the line $q = q^{SFE}$. Similar observations apply for all the aforementioned parameterization methods of the SFE model.

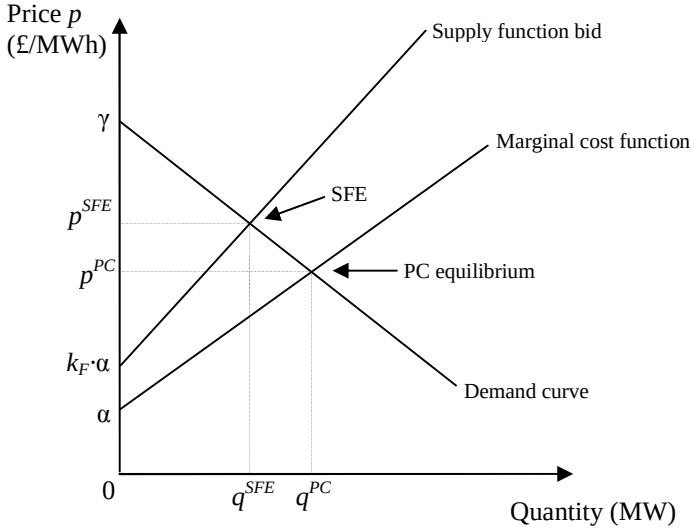

Figure 4: Distortion of social welfare in SFE oligopolistic markets.

In the case where for some reason the k_F term in a submitted bid is less than 1.0, perhaps due to a particular pricing scheme where a firm may expect to sell more output and get profit from increased market prices due to strategic actions from other firms, or due to other exogenous profit factors such as subsidies, it will appear that the social welfare increases due to a deadweight gain as the decrease in producers' surplus will appear to be less than the increase in consumers' surplus [139]. However, even if such uncommon strategies are possible for individual generating units in a multi-unit system, this is impossible for aggregated supply curves in electricity markets.

2.9 Electrical network representation and SFE market modelling

The models that employ the general SFE competition do not consider the electrical network representation as this will introduce mathematical complexities that render inoperative the solution process. For example, Bolle [80] did not consider any physical or operational constraints, while [8,100,105,101-103] consider only the maximum generation capacities of the

firms, but ignore the fundamental power system network theory[1]. This was also the case for early investigations of the linear SFE model [81,124,117,125-127], but as the exploration of the deregulated power markets have shown the relevance of the network constraints to the potential of the firms to exercise market power and change the market outcome as discussed in Chapter 1, network constraints were introduced. The main conclusions on how the constraints affect the market outcome are discussed in this section, while the impact on the nature of the market equilibrium follows in Section 2.12. Note that, in contrast with SFE models that do not represent the electrical network such as [8,81,117,105,102,79], most of the linear SFE models discussed from this point onward consider consistent bids only over a single bidding time interval rather than over a time horizon, for example day-ahead markets. Such single-bidding interval models may predict higher prices and profits, as reported in [102].

The analysis of the linear SFE model with transmission constraints in [73] shows clearly that the outcome of a simple duopoly market is heavily dependent on the presence of transmission constraints, the level of available transmission capacity and also the topology of the network, and a similar approach appears in [131]. The study in [118] has introduced in addition to the transmission constraints the DC model representation for the electrical network. Kirchhoff's current and voltage laws for linearized DC power systems have been incorporated in the numerical formulation of a linear SFE model, in which the market clears based on social welfare maximisation while the ISO takes into account the strategic actions of the producers for profit maximisation[2]. The numerical results of this framework have shown that, due to transmission constraints, dissimilar prices exist at different buses of the system when the transmission lines are congested. The prices, as well as the quantities dispatched by the ISO, depend on the level of the transmission limits. It is also shown that the transmission capacity limits have a distinctive effect on the profits and the surplus for consumers, producers

[1] Other game theoretical applications on the electricity market that use supply function bidding but not SFE had already introduced network representation; for example the study in [140] that analyses the coalition behaviour of firms employed generation and transmission constraints.

[2] Previous studies were usually adopting a market clearing process based on costs minimisation or on the selection of the lowest bid offers first until demand is met. Most of the models mentioned from this point onward consider maximisation of social or system welfare/benefit by the ISO while considering the strategic actions of the market players to optimise their payoffs.

and transmission right holders. It is mentioned that such constraints allow the strategic bidders to bid around the transmission limit restraining the line from being congested and effectively capture the transmission rent that otherwise would be required from the transmission operator, being consistent with the Cournot results in [49]. While this study explores new ways in analysing electricity markets by innovatively introducing the linearized DC network representation, it states that there may be ways of exercising market power that are made possible only by the nonlinearities of the AC transmission systems.

A more comprehensive linear SFE model based on the DC network representation was proposed in [87], where generation capacity limits for the active power and a non-negativity constraint for the load demand have been added in the DC formulation. Other models that include all or some of the aforementioned features of the DC network representation can be found in [119,122,123,128,134-136].

The model in [121], which considers generation and transmission limits, introduces a constraint for the unavailability of installed generation capacity over certain periods due to maintenance, and intertemporal constraints for the hydro-production units, such as annual inflow, inflow storage between successive periods and storage reservoir capacities, in order to simulate imports and exports of power across the Scandinavian countries in the hydro-power supply dominated Nordic market.

The DC model in [114] considers, in addition to the DC formulation, ramp up and down rate constraints for the active power generation to simulate successive bidding time intervals, and constraints for spinning reserve since it simulates a joint energy and spinning reserve spot market with fixed load demand. The strategic firms submit linear spinning reserve function bids, constructing their strategies based on the α- and (α, β)-parameterization method. The results of this model show that the active power and spinning reserve limits have a definite effect on the market prices and firms profits. Different bids are submitted for each period and, when the multi-bidding process is simulated, it is found that the

strategic firms attain greater profits when both transmission and ramp up/down rate constraints are enforced.

The dynamic non-cooperative game in [130], which relies on consistent bidding over a time horizon as in [8,79] to simulate a multi-session market, defines the concept of reference transmission network, i.e. an optimal network upgrade used as benchmark for the approval or rejection of a transmission expansion, from an economic point of view by employing the linear SFE model. Using DC power generation, demand and transmission constraints it shows that the capacity of the transmission network determines the degree at which the strategic players in different locations compete with each other.

The lossless DC model in [115,116], which considers transmission constraints defined by distribution factors based on the network topology and lines susceptances, models in addition demand-side bidding. Strategic consumers bid linear utility functions of the form of (2.4), which may deviate from their actual demand functions by parameterizing the load demand cost coefficients γ and δ in the same fashion as in supply function bidding, with the difference that the demand function bid must be non-increasing. Equilibria are computed using all parameterization techniques, applied in both supply and demand function bidding. The numerical results in [115] have shown that consumers' strategic bidding results in higher consumers' surplus at the expense of high deadweight losses and less scheduled generation. Furthermore, demand-side bidding is found to reduce significantly the congestion rents with the consequence of concealing market signalling for new investment requirements. Therefore, it worsens both short-run and long-run economic efficiency and these observations contradict with earlier studies, such as [37], that make suggestions to policy makers to promote demand-side bidding as a measure of market power mitigation.

The day-ahead market model in [138] considers the reliability of the generating units in the market clearing process. The ISO observes the forced outage probability of the generators from data submitted with the bids, and units with low probabilities are rewarded by being scheduled for more output than others. Therefore, the firms have incentives to improve the reliability of their units by

regular maintenance, which increases costs. This cost should be compared with the benefit secured, in order to take decisions on the bidding strategies and whether or not reliability improvements are required. The model that accounts for consistent linear supply function bids over one day considers DC power flows, transmission constraints, generation capacity limits and inter-temporal constraints for the generators, such as ramp up and down rate constraints, minimum up and down time limits and state transition constraints for switching the units on and off. Terms for the cost of activating the reserve and procuring for reserve replacements due to outages in generation capacity and for the reliability increments are incorporated into the objective functions.

Following the discussions in [141], which raise the suspicion that since reactive power in AC power systems is of localised nature it may have a greater role in the presence of market power than active power, a linear supply function model with an AC network representation has been proposed in [133,120]. The model is based on an individual welfare maximisation algorithm, for which each individual market participant may control several strategically generating units and/or loads to represent both supply- and demand-side bidding. It takes into account the active and reactive power flow equations, the transmission limits for MVA power flows, the reactive losses and the bus voltage limits. Examples on meshed networks show that the strategic players may act in different ways depending on the presence of MVA network constraints in order to exercise market power for their benefit.

Even though the model in [133,120] has taken into account the presence of reactive power and bus voltage limits, apart from the discussions for gaming due to the MVA transmission flows, they received little attention. Another model [137] based on linear SFE theory has implemented the nonlinear AC network representation, which explicitly represents the active and reactive power flows, MVA transmission line constraints, active and reactive power generation limits and losses, and voltage limits. The preliminary results from this study appear to fulfil the speculation in [118] about the connection of the AC nonlinearities and market power abilities. It has been shown that the enforcement of constraints such as the active power generation limits and the transmission MVA limits

influence the market outcome by increasing the nodal prices and altering the active and reactive dispatch, firms' strategies, social welfare and profits. The relevance of the presence of reactive power on the strategic behaviour that alters the market equilibrium is depicted by comparing cases with and without reactive load demand.

Another study that uses the AC network representation appears in [89]. In addition to the abovementioned constraints for AC modelling, the constraints for the active and reactive power generation are modelled as a trapezium domain that spans from positive to negative values of the reactive power generation to approximate the field generation limit and the under-excitation limit of the generating unit, respectively (for the relevant assumptions see [68]). This accounts for the trade-off between active and reactive power generation, being an approximation of the capability curve of electrical power generators. Furthermore, a spinning reserve market is also considered and the relevant constraints are present, in which the strategic firms submit a constant bid for spinning reserve offers rather than a function. The model considers elastic active load demand, but the reactive load demand is uncoupled and constant. The presented results for a monopolist demonstrate that by varying the constant reactive load demand its profit fluctuates and the power distribution in the network changes, since higher values of reactive demand require more reactive power production and the use of higher transmission capacities. The discussion highlights that reactive power flows congest the system to the same extent as active power and the analysis extends to investigate the interrelation between reactive power and bus voltages, and how the strategic producers may exploit the voltage constraints to congest the system for their favour.

The results obtained from the implementation of the nonlinear AC network in the linear SFE models in [133,120,137,89] have effectively demonstrated the superiority of the AC model over the approximate linearized DC representation. It enables the analysis of more realistic systems in order to identify how the features of real-life power systems will allow the strategic players to explore ways to exercise market power and gain profits in the expense of social welfare and rivals' payoffs. Such conclusions will help in identifying and eliminating

such inefficiencies in the oligopolistic environment by the intervention of the ISO and therefore ensure a more competitive and efficient market operation. Other studies that have partially employed AC formulation include [142,132].

Apart from the implementation of the various network constraints discussed, some linear SFE models consider constraints for the strategic variables as well. The model in [87] incorporates maximum and minimum limits for the intercept bid with the minimum value being zero, thus allowing supply function bids being lower than the marginal cost function down to functions that pass from the origin. Similarly, the formulation in [134] confines the strategic variable k_F in the range of 0 to 10 allowing even zero supply function bids. The model in [115,116] sets limits for the intercept bids within the range of 0 to 200, and for the slope bids within 10^{-5} to 6. This is done in order to tolerate for a wider range of strategies, while restricting the supply function bid to be either zero or resemble Cournot strategies (vertical supply functions). However, none of the reported numerical results from these investigations present bid variables that reach the aforementioned limits at the SFE solution. The models in [130] and [122] consider only a lower constraint for the strategic variables, the slope and intercept respectively, being equal to the true value from the marginal cost function to force the bids to be higher than the marginal costs. Other studies that consider constraints for the strategic variables include [135,137,89].

2.10 Contract markets in linear SFE models

The analysis in [117] has extended the preceding investigations on the day-ahead restructured England and Wales electricity market by incorporating a contract market in the SFE model, in which the firms hedge the price of the spot market with forward contract sales. The contract agreements are set as contracts for differences modelled using the conjectural variations approach and the spot market equilibrium is based on the (α, β)-parameterization used by applying the Klemperer-Meyer differential equation method. The equilibrium of the overall market is achieved by optimal quantity and supply function offers in the contract

and spot markets respectively, and the analysis shows that this setting removes much of the short-run incentive for the exercise of market power.

A study that examines a 10-firm generation capacity limited day-ahead spot market where the power traded by contracts is considered in the spot market decisions appeared in [125]. It has been shown that the presence of bilateral contracts causes the strategic supply function bids to move closer to perfect competition offers as the traded amount of power increases, shifting the market closer to perfect competition conditions. Another model [119] examines the linear SFE of DC transmission constrained electricity spot markets using the (α, β)-parameterization, for which particular levels of forward contracts are given and the firms are allowed to own transmission congestion rights to hedge the risk of congestion prices. It is proved that the slope of the strategic bids at equilibrium does not depend on the amount of forward contracts and the transmission congestion rights shares, while the intercept does, and for no contracts is equal to the true value as it was shown in [79]. Numerical results based on the Texas day-ahead electricity market are presented and the conclusions are in agreement with those in [125]. Furthermore, the model in [132] considers optimal bilateral contracting prior to spot market participation in an electrical system with active and reactive generation and voltage constraints, illustrating the impact of active transmission capacity constraints and bilateral contracts on the market outcome.

2.11 Application of metrics in linear SFE models

The SFE analysis has been used in conjunction with the application of appropriate indices to assess and explore the level of competition and the different weight of strategic behaviour in electricity markets, as well as the locational privilege and market power of the competitors, in the presence of network constrains. Such approaches surpass the practicality of using conventional market power indices alone, such as the HHI and Lerner Index, since they correct their shortcomings as oligopolistic analysis that considers the

demand elasticity and network representation is taking place prior to the introduction of the metrics as a prediction of the market outcome.

The analysis in [122] depicts the effects of network constraints when strategic behaviour takes place, by proposing performance and efficiency indices based on price and surplus changes, respectively. It shows that these effects depend on the actual structure of the grid and the type of the generators, while congestion offers additional opportunities for gaming. In addition, [123] explores the advantages of the producers related to their location and the degree of market power abilities provided by the network structure, such as the exploitation of transmission lines. The assessment identifies the most critical lines in the network, prompting for the needed reinforcement.

The study in [136] utilises metrics to assess market power opportunities in electricity markets, showing how demand elasticity affects the market performance and facilitates market power mitigation. The analysis utilises linear inverse demand functions and concerns with the impact of demand-side price responsiveness on the market performance. It is argued that the market effects of an increase in demand elasticity are the same as those of an increase in competition. However, the results may not be favourable for the consumers' surplus and, consequently, the social surplus, but the congestion costs and nodal price differences appear to be reduced. It is concluded that the effects of exercising market power in network constrained markets is more evident with low demand elasticity and therefore real markets should introduce measures to prevent such situations.

2.12 Existence and multiplicity of pure equilibria in linear SFE models

The optimal response curve approach can be used to investigate the strategic reactions of market participants on the strategy of their rivals and the consequent impact on the existence of pure strategy equilibria in the presence of network constraints. This approach is straightforward for analysing models that use the α-,

β- or k_F-parameterizations where only one strategic variable is involved, if the market has only two strategic players, since the optimal response space will be a 2-dimensional graph. The optimal values for the strategic variable of one player are plotted for all the possible values of the strategic variable of the other player, and then this is repeated for the second player. The point or points at which the two reaction curves intersect indicate the pure strategy equilibria for the linear SFE game. If the reaction curves do not intersect no pure equilibrium point exists and the Nash equilibria of the SFE game are confined to mixed strategies.

Numerical algorithmic market simulations of a simple 2-bus system have been performed in [133,120] using the k_F-parameterization SFE model to show the dependency of the existence and multiplicity of pure SFE on the transmission line constraints. The investigation in [133] considers one strategic supplier at each bus, while that in [120] considers one strategic supplier at the first bus and one strategic consumer (load) at the second bus. In both cases, the optimal response curves for the k_F variables of the players are found to intersect at a single point when no transmission line constraint is considered between the buses, indicating one pure strategy SFE for each case. When a transmission limit is induced between the two buses, in [133] there is no intersection due to a discontinuity on the response curve of the supplier at the load bus that eliminates the pure strategy SFE, and in [120] the reaction curves overlap over a range of values indicating a continuum of pure Nash equilibria. In the first case, the nonexistence of pure SFE is owed to the fact that the supplier's profit has two local maxima and there is no preference in bidding either of the corresponding strategic variables. Therefore, any probabilistic combination of choosing either strategy is a mixed Nash SFE. In the second case, the continuum of equilibria indicate the optimum responses of the market participants in order to adjust the power flow to be exactly at the transmission limit and avoid the transmission congestion penalties from the ISO. These simple trivial cases show that the presence of network constraints may eliminate the pure strategy equilibrium or introduce SFE multiplicity.

The study in [73] investigated a 3-bus duopoly with a single load by employing the k_F-parameterization SFE and highlighted the idea that the choice of the

equilibrium strategies determines the output quantities and which lines will be congested. The reaction curve space is separated in two areas, corresponding to congested and uncongested operation of the transmission line and the reaction curves are compared with those for a case with no transmission constraints. For a particular topology of the system it is shown that for a relatively low constraint the equilibrium is in the uncongested area, being the same as in the absence of the transmission limit. For an intermediate constraint level a continuum of equilibria appears on the boundary that separates the two areas, while when the constraint is tightened a single equilibrium point exists in the congested region. It is then shown that for different topologies the equilibrium point for a low level constraint may be moved on the congestion boundary or eliminated, and that nonexistence of SFE may occur if the demand elasticity becomes low enough. This investigation proves that the particular topology of the network, as well as the level of the transmission line limit and demand elasticity, play a major role on the existence and nature of the SFE solution. A discussion of the same system appeared in [131] where the slope parameterization is used, and speculates that in more complicated systems there will be a continuum of equilibria if the binding network constraints induce consistent bidding behaviour from the strategic players around the constraint to eliminate congestion charges, or there will be no pure equilibrium if this behaviour is inconsistent. Furthermore, a comprehensive analysis in [116] based on the intercept parameterization method strengthens the observations of [73] by showing that nonexistence or multiplicity of SFE solutions occur in the presence of transmission constraints, depending on the properties of the particular network arrangement of the examined market.

Unlike other studies that are based on the static analysis of the market equilibrium, the analysis in [129] is concerned with the market evolution under repeated bidding and with the learning behaviour of the market participants, i.e. how the players use the available information to improve their bidding strategies from their acquired knowledge. Recalling the proof from [111] that when all players learn a unique equilibrium under slope-parameterization exists, it is shown for an unconstrained market that each supplier has incentives to learn about its opponents' past submitted bids in order to maximise profit, since its optimum strategy depends on its rivals' strategies.

The investigation in [113] has presented graphically the profits of the suppliers of the 2-bus system in [133] at the SFE point, as a function of the strategic variables using the (α, β)-parameterization. It is shown that there is an enormous (seemingly infinite) number of equilibrium points in the unconstrained case, and some of them are eliminated when the transmission constraint is introduced (those that correspond to flows higher than the line limit). The SFE points that cease to exist are among those that correspond to relatively low values of profits and therefore the binding constraint can support high equilibrium profits. The discussion compares the SFE solutions for the (α, β)-parameterization with the Cournot solution and shows that the profits from bids with slopes that tend to infinity and the corresponding intercepts that move towards large negative values are equal to the Cournot profits. This limiting SFE is a focal equilibrium point because it is mutually beneficial to all players and may be preferred by everyone to all the other equilibria.

Since the optimal response curve method is effective in finding SFE solutions only for duopolies, as markets with more than 3 strategies players cannot be represented graphically, more complex situations have been investigated by applying numerical algorithmic approaches based on the (α, β)-parameterization method. The numerical model in [89] presented results for a monopolist in an AC 3-bus network and shows that it can choose equivalent strategies from within a range of pairs of strategic variables to achieve the same level of maximum profit at the equilibrium point; this is consistent with the results in [120] where the total surplus of the market players along the SFE continuum is the same. A similar observation was made in [104] where an unconstrained market with 5 strategic firms is investigated showing that the submitted strategic variables at an SFE point are not unique. Instead, several equivalent optimum strategies exist and the corresponding profits, market price and output levels at the SFE point are unique and equal to those of the Cournot solution for the single bidding period game. In such cases the slope of the supply function for profit maximisation is required to be a very large positive value and the intercept a very large negative value, being in agreement with the discussion about the focal equilibrium in [113]. However, when a single bid was applied to multiple pricing periods in [104] the bidding variables for the (α, β)-parameterization become unique and the equilibrium

results are close to those of slope-parameterization, as discussed by Baldick in [113].

The investigation in [120] extends to analyse the behaviour of strategic firms in a 9-bus system showing that different local maxima for total profits may occur due to the presence of physical system constraints. The SFE calculated from the numerical algorithm may be attracted by a local maximum and miss the notion that a global SFE would be more desirable in terms of predicting the market behaviour. In order to deal with such complications in multi-unit networks an algorithm has been implemented in [128] to identify all possible multiple SFE points. The algorithm is searching the regions defined by all combinations of system constraints (generation and transmission limits) and identifies the different non-cooperative equilibrium points. It has successfully produced results for a 30- and a 57-bus system showing that even though the existence of multiple equilibria in realistic systems is possible they should not be expected in large numbers.

2.13 Stochastic optimisation with linear supply function bidding

The discussion in the previous section concerns linear SFE models that assume perfect and complete information among competitors, i.e. all players have the same knowledge about their rivals' true cost functions and the system specifications. This represents the assumption that all market participants are long-term players that have learned about their competitors [1]. However, gaming in an electricity market may be characterised by incomplete information depending on the knowledge of the players on their rivals' payoffs and strategies, on the amount of information that other players have on various aspects of the game, and so on, such that players lack full information on the mathematical structure of the game. An incomplete game, also called a Bayesian game, can be transformed into a complete game with imperfect information in which the market participants lack information on other players' benefits in previous stages of the game [143]. A game of imperfect information depends on whether the market participants have complete knowledge of their rivals' strategic actions or

not. Such games have been modelled for the electricity market based on linear supply function theory and solved by employing stochastic optimisation approaches.

The first electricity market model that presented a non-cooperative game with incomplete information using supply function bidding appeared in [124], where players lack information on their rivals' costs in an unconstrained system. The incomplete game is transformed into a complete game with imperfect information and a probability distribution is assigned to the unknown variables. The market players compete by choosing strategies based on expected profit maximisation and the optimal strategies depend on the level of information that they have for their opponents. An extension of this model has been proposed in [135], in which the probability distribution for the unknown information is estimated based on information on fuel contracts and transmission availability.

The investigation in [142] modified the individual welfare maximisation algorithm of [120] to propose a method for calculating Bayesian Nash SFEs in games where asymmetric strategic firms have incomplete information about their rivals' costs. The model considers AC power flow equations with inelastic demand and the unknown cost parameters are represented by probability density functions. Numerical results report Bayesian Nash solutions computed by applying the Monte-Carlo simulation that provides an approximate solution by performing statistical sampling on the probability density functions [144]. It has been shown that the uncertain information makes the players to bid less aggressively and consequently they receive (slightly) less profits.

In the model presented in [126], the market players have imperfect information for their rivals' knowledge and act strategically based on the expectations about how their opponents will bid. It is assumed that from a single player's point of view the coefficients of the supply function bid of each of its rivals obey a normal probability distribution. A stochastic optimisation problem that considers generation capacity limits is solved by two different methods; the first one is based on the Monte Carlo simulation and the second one is an optimisation approach that finds the solution by calculating the mean values of the expected

variables of the market outcome. The Monte Carlo approach was extended in [127] to model strategic demand-side bidding.

Based on the above market assumptions, the same authors have presented a stochastic optimisation model for a joint energy and spinning reserve markets with imperfect information [145], in which the players submit linear functions for both energy supply and spinning reserve. Instead of calculating an approximate solution for the market equilibrium, a solution for the optimal strategy of a single supplier is obtained using a genetic algorithm. Moreover, the model in [146] integrated this method with the optimisation approach from [126] to provide a different method for obtaining optimal strategies for energy supply and spinning reserve. Furthermore, the genetic algorithm approach is expanded to model a day-ahead joint energy and spinning reserve market in [147], where a single supplier is also required to take strategic decisions about its unit commitment status. The benefit maximisation strategy considers start-up costs, permissible starts/stops per day and unit min/max up and down times, and the solution depends on the estimation of the cost functions of its rivals.

Another model that considers incomplete knowledge of rivals' cost functions was presented in [148]. DC network representation was employed and the uncertain load demand is treated as a random variable. An arbitrary probability function is assigned to the opponents' behaviour and the resulting stochastic optimisation problem is solved using the Monte Carlo method and a genetic algorithm in order to calculate the optimum strategy for a single player. Other models that use linear supply function bidding with the same objective can be found in [149,150], where the particle swarm optimisation method is employed.

2.14 Numerical methods for SFE solutions

As already mentioned, early investigations on unconstrained linear SFE models have used the Klemperer-Meyer differential equation method [81,117,79] while others that involve transmission constraints have applied the optimal response curve approach [73,131] to calculate mathematically the equilibrium point for

simple systems, mainly duopolies. Other models, which examine markets that involve larger or more complex (meshed network constrained) systems, require the implementation of appropriate numerical algorithms. This section reviews noteworthy iterative methods that employ DC or AC network constrained systems. First, some necessary terms are introduced:

- Optimal Power Flow (OPF):

The formulation of a constrained nonlinear optimisation problem, which determines the optimal settings for control variables in a power system by optimising an objective function, while satisfying various constraints. This concept was primarily proposed during the 1960s [151,152]. The most common application of the OPF problem is the generation costs minimisation by the system operator to obtain the optimal dispatch, but other optimisation applications, such as transmission loss minimisation for reactive power planning, production scheduling, maintenance scheduling, generation and transmission expansion planning, are applicable. The constraints represent the physical laws governing the electrical network, including AC or DC power flow equations, power generation-demand balance constraints, generation limits, bus voltage limits, transmission limits, reactive power support, load shedding, transformer representation, security and contingencies constraints, and so on [153,154,19]. A review of the literature on the programming methods employed over the years for the solution of the OPF problem was given in [155,156] and a survey on the OPF models proposed can be found in [157].

- Karush-Kuhn-Tucker (KKT) 1^{st} order optimality conditions:

The necessary conditions in an optimisation problem for determining the extreme values of a function *f* that are obtained by setting to zero the first derivative of *f* with respect to all of its independent variables [158].

- Complementarity constraints:

A complementarity constraint restricts two variables to be both either non-negative or non-positive and in either case their product to be zero [159].

In general, the SFE problems that incorporate an ISO are of bi-level nature. In the first level, each firm chooses strategy by taking as input its perceived market conditions to maximise profit, restricted by given bounds on the bid. The second level corresponds to the ISO market clearing process, which is an OPF problem

that takes into account the relevant network constraints and is parameterized by the firms' bids [87]. One of the first algorithmic approaches that solve a system with DC network constraints for calculating Nash SFEs appears in [118]. The iterative process employed is referred to as a diagonalization algorithm and it was previously applied to Cournot models [45,31]. This procedure starts by fixing all supply function bids, say to the marginal cost function, except the bid of the generator under consideration. Given the other generators' fixed strategies, the ISO problem is solved for a series of different parameterized bids and the bid that produces the maximum profit is chosen to be fixed for that generator, and then the procedure is repeated for another generator. This process continues until the strategies of all firms are profit maximising given the strategies of their rivals. When no firm can further improve its profit in this manner, Nash SFE is reached.

The DC model in [87] has employed the same diagonalization approach but it formulates the quadratic parametric problem of the second level as a Linear Complementarity Problem (LCP). A mixed LCP formulation results by introducing the KKT optimality conditions of the ISO's second-level problem into the first-level, regarded as constraints. The resulting constrained optimisation problem for a single firm is a Mathematical Program with Equilibrium Constraints (MPEC), which here is solved using a penalty interior point algorithm. Each firm is solving an MPEC considering fixed strategies for the other firms and the process is repeated for all firms until a satisfactory solution is obtained. This method has been proven able to solve systems with several buses, in which the firms may own more than one generating units. The studies in [130,114,138] extend this approach to multi-period markets.

Another model that uses the diagonalization approach based on a different optimisation method, termed as the individual welfare maximisation algorithm, has been proposed in [133,120]. Nash equilibria are reached by individuals (economic entities) that control one or more generators and/or loads, while maximising their welfare. In doing so, each player solves the ISO's OPF problem based on assumptions about its own and others' strategies and, using the information from the resulting OPF solution, it updates its bid to improve its

welfare by determining a Newton-step. When all players stop modifying their strategies Nash equilibrium is computed. Similar approaches are presented in [135,132] with the implementation of interior point algorithms to solve the OPF problem. As in the case of the diagonalization models above, the resulting Nash SFE points are local equilibrium points, while a global equilibrium cannot be guaranteed[3].

A different approach for calculating Nash SFEs was presented in [134]. It was argued that, since the supply and price terms included in each firm's profit maximisation problem are produced by the ISO's quadratic program and can be expressed as implicit functions of all the firms' strategies, they should satisfy the KKT conditions of the ISO problem. Hence, these are formulated as complementarity conditions and incorporated into each firm's MPEC as constraints. Then, by gathering the KKT conditions of all firm's MPECs, the equilibrium market problem that solves the overall game is faced as an Equilibrium Program with Equilibrium Constraints (EPEC) and is formulated as a mixed Nonlinear Complementarity Problem (NCP). This is then reformulated as a set of nonlinear equations using the nonlinear complementarity Fischer-Burmeister merit function [160] and is solved simultaneously –rather than by re-iterating over each MPEC– to give the SFE solution. A different version of this method is provided in [137] by implementing a primal-dual nonlinear interior point algorithm, in which a logarithmic barrier method is used to reformulate the bi-level market problem into a set of nonlinear algebraic expressions. Both models have been proven applicable for large systems.

The aforementioned EPEC approach presents iterative SFE results without verifying that the equilibrium outcome is indeed a local Nash SFE. Those results are classified as Nash stationary equilibria, since they satisfy the EPEC's first order stationary optimality conditions, i.e. the KKT conditions of the firms' MPECs, being weaker variants of the classical Nash equilibrium concept [115]. However, the following two references show via numerous numerical tests that

[3] Local Nash SFEs are less credible than their global counterparts, but they still have meaning as they may be sufficient for the satisfaction of the players, due to difficulties in identifying a global SFE or due to limitations on their rationality and knowledge [116].

such methods always yield local Nash SFEs. The model in [115] replaced all firms' MPECs, or more precisely MPCCs since the equilibrium conditions are of complementarity form, with their KKT conditions to express the game as an EPEC (or EPCC). This EPCC represents the Nash stationary equilibria, which are then obtained by applying Non-Linear Programming (NLP), in particular the PATH solver [161], to solve the EPCC's stationary (KKT) system. Then, these stationary SFEs are verified to be local Nash equilibria by checking the sufficient second-order conditions for optimality. A more comprehensive EPEC analysis that distinguishes between Nash stationary and local equilibria was provided in [116], where the differences in algorithm convergence and identification of local Nash points for two diagonalization methods and an NLP approach for solving the Complementarity Problem (CP) formulation of the EPCC similar to [115] are compared. The diagonalization process that updates the players' strategies in the MPEC formulation is solved by applying either a standard NLP method or a regularisation iterative method that remodels the MPECs as a better-behaved NLP problem. The latter has also been used in [89]. In both [115] and [116], all the acquired solutions from the complementarity formulation tests were numerically established as local Nash equuilibria, proving the robustness of this methodology. Further discussions about EPEC's properties and formulations are provided in [162].

Chapter 3:
Methodology and implementation of the electricity market SFE algorithm

3.1 The work in this Thesis

The research described in this Thesis is focused on the investigation of the linear SFE methods and the analysis of the impact of various network constraints and operational conditions on the electricity market equilibrium. The implementation of an advanced nonlinear primal-dual interior point algorithm that considers AC network representation is undertaken, and the efficiency and robustness of the algorithmic iterative procedure is investigated and assessed. Numerous numerical tests on several subject matters related to the electrical network operation and the issue of market power in the electricity market are performed, in order to examine particular and general situations that affect the individual market participants and the market as a whole. The observations and conclusions are compared with those from the existing literature and discussions are provided for several issues that have not been addressed well in the literature. The reasons for choosing the particular methodology and the modelling assumptions are given below.

The electricity market equilibrium analysis was chosen over the market concentration analysis with indices and the ex-post estimation of pricing behaviour methods, since it is a much better representation of the interactions between the strategic firms in the oligopolistic environment of the electricity market. As discussed in Section 1.9, the oligopolistic equilibrium analysis is an efficient method for the evaluation of the sources and degree of market power, and hence it can provide a better depiction of the outcome of bid-based electricity pool markets.

The modelling of the market mechanism is based on the SFE theory, which was chosen due to its perceived advantages over the other available equilibrium methods. As discussed in Chapter 2, the market players are able to adapt better to the uncertain environment of the electricity market owing to the unknown load demand, by implementing function bids that relate different supply quantities to different prices rather than discrete quantity or price bids, as in the Cournot and Bertrand competitions. Hence the price predictions from the SFE model are more reliable than the Cournot prices, since they are not very sensitive to demand, and are more realistic than Bertrand prices, which resemble perfect competition behaviour. In addition, the supply function bids, which are increasing in price, reflect the generating costs for power production that are increasing with the quantity produced; such features cannot be represented successfully by applications of the Cournot and Bertrand settings.

In particular, the linear SFE model has been chosen for this investigation over the other SFE forms for several reasons. The study in [81] has shown that the linear SFE solution is a reasonable approximation for the general SFE form at low levels of demand, while it still remains an equilibrium at higher demand levels. The analysis on the California energy market in [163] is in agreement with this by showing that the cumulative supply function bids in a practical market appear to be 2-segment linear curves and modelling with linear bids is reasonably accurate. Furthermore, the study in [102] has shown that, in the absence of capacity constraints, the only stable SFE between the most competitive and the Cournot solution is the linear SFE, if quadratic cost functions (linear marginal costs) are modelled, and hence the only possible to appear in practice. In addition, this model results in considerably reduced mathematical complexity compared with the other available models, being able to handle multiple asymmetric firms with quadratic cost functions [79], while it can offer intelligible interpretations of the resulting market equilibrium solution. Since the above findings support the functionality of the linear SFE model, the study in this Thesis employs this theory with the prospect of further contributing to the literature.

The proposed electricity market model is implemented by considering AC power flow analysis and the representation of various network constraints. As discussed in Chapter 2, the AC model has several advantages over the DC model, since the latter is a linearized version of the nonlinear AC system that stems from the real characteristics and physical properties of practical power systems. Hence, in the context of market equilibrium analysis, the DC representation cannot identify the sources of market power related to the nonlinearities of real-life power systems and electricity markets. In this Thesis, the AC representation is employed in order to account for a more realistic market outcome, since the strategic interactions between the generating firms are directly dependent on the operational constraints and conditions. The market clearing price is determined in terms of nodal prices to represent both the energy price and the short-term transmission costs. The network constraints considered include the active and reactive power flow equations accounting for flows through transmission line and transformer branches, the bus voltage limits, the MVA transmission capacity limits and transmission losses for both transmission line and transformer branches, the transformer tap-ratio control to represent on-load tap-changing transformers, and the active and reactive generation capacity limits. The power load demand is price-responsive and represented by both active and reactive components, which are interrelated by means of the power factor angle. In addition, modelling of grid-connected solar PV systems that accounts for both PV active and reactive generation has been undertaken, considering the effect of the intensity of the applied solar irradiance. The model for the operation of the PV systems is based on real PV output performance data recorded in an experimental PV park. The purpose of the implementation of such a complicated network model, apart of enhancing the accuracy and realism of the market results, is aiming to investigate the effects of the individual network constraints and different system operational conditions on the market equilibrium. Several of these features, such as the transformer representation, the optimisation of the tap-ratios, the price-responsive reactive load demand, and the representation of PV systems in the electricity market equilibrium model, have not been addressed in the literature so far.

The implemented market model accounts only for supply-side bidding, while it considers competitive loads, for the following reasons. The study in [109] discusses that strategic demand-side bidding may result in instability due to the absence of pure strategy equilibria with low prices, or in market prices that are much higher than the marginal costs, being in agreement with [164], which examines a different market structure. Furthermore, the numerical results in [115] have shown that strategic bidding by the consumers lowers the economic efficiency and conceals market signalling of the need for new transmission investment, as already discussed in Chapter 2. Since the strategic demand-side bidding exhibits these adverse effects on the electricity market, it is not considered in this investigation. However, note that the competitive load demand function in this model is price-responsive.

The bi-level problem is formulated in a similar manner as in [134,137], where the 1st order KKT conditions of the lower level (ISO problem) are incorporated into the upper level to give a combined problem for the market equilibrium solution. The associated complementarity constraints of certain KKT condition equations are transformed into nonlinear mathematical expressions using the Fischer-Burmeister merit function in order to avoid possible complications due to ill-conditioning problems. Such modelling techniques are expected to be robust and applicable for large systems and, in addition, the analysis in [116] has shown that the resulting Nash stationary equilibria from such formulations are in fact local Nash equilibria. This finding further enhances the realism of the market model, since local equilibria are possible to be observed in practice.

In order to implement a market algorithm that involves the aforementioned network and market features, a numerical approach that is able to tackle successfully the associated mathematical complexity is required. In the past, formulations using the nonlinear primal-dual interior point method have been used to solve a wide variety of large scale OPF problems, while this method is also applicable to problems of bi-level nature, such as the bid-based electricity pool market equilibrium problem. This method has been chosen for the investigation that takes place in this Thesis, because it can easily handle the nonlinearities of the AC model and the inequality constraints required for the

representation of the network operation. Such iterative processes, based on the primal-dual interior point method, converge within a reasonable number of iterations, which is expected to enhance the computational performance. A comprehensive review of the mathematical theory and the advantages of the primal-dual interior point method is provided in Section 3.2.

The mathematical formulation for the power flow equations, the representation of the losses for the transmission lines and transformer branches, the bus voltages, and the complex power components is derived using rectangular coordinates instead of employing the polar representation. By using this technique, advantages that enhance the computational efficiency of the algorithm arise due to the fact that the resulting objective functions and the constraints of the bi-level market problem will appear in quadratic form. A quadratic function has the desirable properties of constant Hessian (2^{nd} derivatives of the objective function and the power flow equations), Taylor series expansion that terminates at the 2^{nd} order term without truncation error, and easy evaluation of the higher order term. These features allow for an attractive matrix setup and reduce the number of iterations for the convergence of the primal-dual interior point algorithm [165]. Furthermore, no trigonometric functions are incorporated in the primary formulations as in the case of the polar coordinates representation. More information about the rectangular coordinates representation is given in subsequent sections.

***Major contributions of this Thesis*:**

The major contributions of the work presented in this Thesis include the following:

a) Implementation of a nonlinear primal-dual interior point algorithm to solve the bi-level electricity market equilibrium problem based on linear SFE theory and considering advanced AC network modelling.

b) Achievement of superior computational performance of the electricity market algorithm in providing SFE solutions for complicated realistic systems in the presence of binding functional constraints.

c) Modelling of the transformer in the equilibrium market algorithm and investigation of the impact of the transformer tap-ratio control on the electricity market equilibrium.

d) Determination of the impact of reactive power control on the electricity market equilibrium, in terms of voltage control, limitations on the reactive power generation and absorption, and power factor adjustments.

e) Analysis of the effects of a new generating unit's location for a new entry in the electricity market, on the interactions between the strategic firms and the market outcome.

f) Modelling of grid-connected PV generating units in the electricity market algorithm, with representation of the economic and technical aspects based on PV output performance data recorded from an outdoor experimental PV park.

g) Investigation of the effects of introducing PV generation in the electricity market with respect to the applied solar irradiance, and determination of the impact of representing the nonlinear PV reactive power generation in the electricity market model.

h) Implementation of the four different parameterization methods in the linear SFE market model and investigation of the respective market equilibrium solutions.

i) Determination of the interrelation between network congestion and the individual network components, such as the transformer tap-ratio control and the PV generating units, and the different linear SFE parameterization methods.

3.2 The primal-dual interior point method

Even though the interior point method has been studied by Fiacco and McCormick [166] during the 1960s in the context of nonlinear programming, it did not receive widespread attention until 1984 when Karmarkar [167] presented a novel algorithmic procedure for solving linear programming problems. The process of the Karmarkar's algorithm was following a path through the interior

of the problem's constraints directly towards the optimal solution, rather than following a series of points that were on the boundary of the constraints as frequently suggested by other applicable methods. The solution path always remained within the interior of the constraints' boundaries and the current solution was positioned as the centre of the space in order to find a better direction for the next step. The major advantage of this methodology is the highly reduced computational effort of the algorithm convergence. It has been reported that the speed advantage gained for large systems by the reduction of the number of iterations is as much as 50:1 when compared to other methods available at the time [154].

As this approach became very popular, the analysis in [168] has shown the relationship between Karmarkar's algorithm and the Logarithmic Barrier function that was already investigated by Fiacco and McCormick [166]. It was shown that a method based on Fiacco and McCormick's analysis is equivalent to Karmarkar's algorithm for solving linear programming problems. Based on this finding, the study in [169] analyses the crucial building blocks that comprise the methodology for the interior point method. These blocks are the Fiacco-McCormick Logarithmic Barrier method for optimisation with inequality constraints [166], the Lagrange method for optimisation with equality constraints [170], and Newton's method for solving nonlinear equations for unconstrained optimisation [171]. Using these three techniques, the primal-dual interior point method was constructed and applied to solve linear programming problems. It is shown in [169] that the number of required iterations for convergence when using the interior point method is very insensitive to the size of the problem because it increases with the logarithm of the number of variables involved. The primal-dual interior point method has found numerous applications in linear programming, including [172-175]. A simple mathematical illustration of this method follows.

Consider an optimisation problem with the following structure:

$$\textit{Minimise } \{f(x)\} \tag{3.1}$$

subject to:

$$h_n(x) > 0 \tag{3.2}$$

where *f* is the objective function of the problem, *x* is the set of the associated variables, and *h* is the set of the *n* inequality constraints, which can be of linear or nonlinear form.

The first step of the primal-dual interior point method is to transform each inequality constraint from the set $h_n(x)$ into an equality constraint by introducing a nonnegative slack variable s_n. Using the Fiacco-McCormick logarithmic barrier method, the above optimisation problem with inequality constraints is transformed into an equivalent optimisation problem with equality constraints only, such that:

$$Minimise \left\{ f(x) - \mu \sum_n \log(s_n) \right\} \tag{3.3}$$

subject to:

$$h_n(x) - s_n = 0 \tag{3.4}$$

where μ is the barrier parameter, and $s_n > 0$ is the slack variable associated with the inequality constraint *n*. The logarithmic term $\log(s_n)$ forces the solution procedure to begin from a point well within the feasible region bounded by the inequality constraints of the problem, in order to accommodate for a solution path characterised by strictly feasible iterates. Hence, a path along the constraints' boundaries is avoided, resulting in less computational effort. The logarithmic term maintains the objective function well above the value that corresponds to the limits of the constraints when the values of $h_n(x)$ approach zero. The role of the barrier parameter μ is to minimise the logarithmic term introduced in (3.3) as the iterative process progresses, in order for the objective function of the equivalent problem from the Fiacco-McCormick barrier method to equal the objective function of the original optimisation problem at the final solution. The value of μ is minimised as the iterative procedure of the algorithm progresses and it approximately equals zero at the final solution.

The second step for the implementation of the primal-dual interior point method is to transform the optimisation problem with equality constraints (3.3)-(3.4) into

an unconstrained optimisation problem by applying the Lagrange method. The Lagrange function for equalities optimisation for the problem (3.3)-(3.4) can be derived by introducing Lagrange multipliers for each of its equality constraints, such that:

$$L_\mu = f(x) - \mu \sum_n \log(s_n) - \sum_n \pi_n [h_n(x) - s_n] \tag{3.5}$$

where the Lagrange multipliers π_n are the dual variables for the problem. In order to minimise the Lagrange function, the 1st order KKT conditions are required. These can be obtained by differentiating L_μ with respect to all the primal (x and s) and dual variables (π), and setting the corresponding derivatives to zero, as follows:

$$\nabla_x L_\mu = \frac{\partial L_\mu}{\partial x} = \frac{\partial f(x)}{\partial x} - \sum_n \pi_n \frac{\partial h_n(x)}{\partial x} = 0 \tag{3.6}$$

$$\nabla_{s_n} L_\mu = \frac{\partial L_\mu}{\partial s_n} = -\mu \sum_n \frac{\partial \log(s_n)}{\partial s_n} + \sum_n \pi_n = 0 \tag{3.7}$$

$$\nabla_{\pi_n} L_\mu = \frac{\partial L_\mu}{\partial \pi_n} = -\sum_n [h_n(x) - s_n] = 0 \tag{3.8}.$$

The final step of the primal-dual interior point method is to solve the set of the KKT condition equations (3.6)-(3.8) using the Newton's iterative method for unconstrained optimisation. The general mathematical derivation for this method is presented here, based on the guidelines in [176]. Consider a matrix equation that consists of a set of non-linear algebraic equations, such that:

$$\underline{g}(\underline{y}) = \begin{bmatrix} g_1(\underline{y}) \\ g_2(\underline{y}) \\ \vdots \\ \vdots \\ g_N(\underline{y}) \end{bmatrix} = \underline{z} \tag{3.9}$$

where $\underline{y}$ and $\underline{z}$ are N-dimensional vectors, and $\underline{g}(\underline{y})$ is an N-dimensional vector of functions, with $\underline{z}$ given. The vector $\underline{z}$ can be approximated by considering Taylor series expansion about an operating point $\underline{y}_o$. In the case of OPF applications with rectangular coordinates, there are no terms in the expansion

series being higher than the 2nd order, and hence there is no truncation error, as explained in the previous section. Therefore, the Taylor series expansion of $\underline{z}$ is given by:

$$\underline{z} = \underline{g}(\underline{y}_o) + \frac{d\underline{g}}{d\underline{y}}\bigg|_{\underline{y}=\underline{y}_o} \cdot (\underline{y} - \underline{y}_o) \tag{3.10}$$

By solving (3.10) for $\underline{y}$:

$$\underline{y} = \underline{y}_o + \left[\frac{d\underline{g}}{d\underline{y}}\bigg|_{\underline{y}=\underline{y}_o}\right]^{-1} \left[\underline{z} - \underline{g}(\underline{y}_o)\right] \tag{3.11}$$

The differential term in (3.11) is the $N \times N$ square matrix *J*, called the Jacobian matrix of $\underline{g}(\underline{y})$. The Jacobian is composed of the partial derivatives of $\underline{g}(\underline{y})$, such that:

$$J = \begin{bmatrix} \frac{\partial g_1}{\partial y_1} & \cdots & \frac{\partial g_1}{\partial y_N} \\ \vdots & \ddots & \vdots \\ \vdots & \ddots & \vdots \\ \frac{\partial g_N}{\partial y_1} & \cdots & \frac{\partial g_N}{\partial y_N} \end{bmatrix} \tag{3.12}$$

By considering an iterative procedure, the term $\underline{y}_o$ in (3.11) can be replaced by the old value for the variable $\underline{y}^{old}$ and the term $\underline{y}$ by the new value $\underline{y}^{new}$. Therefore, equation (3.11) can be written as:

$$\underline{y}^{new} = \underline{y}^{old} + J^{-1}\left[\underline{z} - \underline{g}(\underline{y}^{old})\right] \tag{3.13}$$

By considering (3.9), the vector mismatch for the iterative process convergence can be defined as:

$$\Delta\underline{z} = \underline{z} - \underline{g}(\underline{y}) \tag{3.14}$$

and the correction vector is defined as:

$$\Delta\underline{y} = \underline{y}^{new} - \underline{y}^{old} \tag{3.15}$$

Therefore, from (3.13)-(3.15):

$$\Delta\underline{y} = J^{-1}\Delta\underline{z} \tag{3.16}$$

Since $\Delta \underline{z}$ is known and J can be computed from $\underline{g}(\underline{y})$, the correction vector $\Delta \underline{y}$ can be calculated. Then, the next approximation of $\underline{y}$ in the iterative procedure is given by:

$$\underline{y}^{new} = \underline{y}^{old} + \Delta \underline{y} \tag{3.17}.$$

In order for the algorithmic procedure to converge to a satisfactory solution for the variables in $\underline{y}$, the process described above is repeated until a specified tolerance for Δz is met.

By considering the original optimisation problem (3.1)-(3.2) and the resulting KKT system (3.6)-(3.8), the vector $\underline{y}$ corresponds to the set of the primal and dual variables of the problem, the functional vectors $\underline{g}_1(\underline{y})$ to $\underline{g}_N(\underline{y})$ are represented by the differential terms ∇L_μ, and the vector $\underline{z}$ is equal to zero[4]. Therefore, the set of equations (3.6)-(3.8) can be linearized and rearranged into a Newton matrix equation of the form $J \cdot \Delta \underline{y} = (0 - \underline{g})$, such that:

$$\begin{bmatrix} \nabla_x \nabla_x L_\mu & \nabla_s \nabla_x L_\mu & \nabla_\pi \nabla_x L_\mu \\ \nabla_x \nabla_s L_\mu & \nabla_s \nabla_s L_\mu & \nabla_\pi \nabla_s L_\mu \\ \nabla_x \nabla_\pi L_\mu & \nabla_s \nabla_\pi L_\mu & \nabla_\pi \nabla_\pi L_\mu \end{bmatrix} \cdot \begin{bmatrix} \Delta x \\ \Delta s \\ \Delta \pi \end{bmatrix} = \begin{bmatrix} -\nabla_x L_\mu \\ -\nabla_s L_\mu \\ -\nabla_\pi L_\mu \end{bmatrix} \tag{3.18}.$$

The direction vector $[\Delta x \ \Delta s \ \Delta \pi]^T$ is called the Newton step and is used to provide a better approximation for the system variables for every successive update, using equation (3.17).

3.3 Applications of the primal-dual interior point method

The first application of the primal-dual interior point method on nonlinear and nonconvex programming problems with nonlinear constraints has taken place in [177], where the optimal reactive dispatch problem was investigated. Numerical results on large power systems with thousands of buses have revealed several

[4] Note that multiple derivatives correspond to a sum of differential terms. For example, the expression $\nabla_y L_\mu = g(\nabla_y^2 A)$, where $y = [a, b]^T$ and A is a differentiable term, represents two equations, such that $\nabla_a L_\mu = g(\nabla_a \nabla_a A + \nabla_a \nabla_b A)$ and $\nabla_b L_\mu = g(\nabla_b \nabla_a A + \nabla_b \nabla_b A)$.

advantages, including the robustness of the algorithm and the effectiveness in dealing with OPF problems that involve ill-conditioned networks. A further development of the nonlinear primal-dual interior point method is provided in [178], where two different versions of the model are provided and compared, one of which incorporated a predictor-corrector scheme according to [174,175]. A similar study that focuses on the implementation issues of the algorithmic procedures is described in [179], where the nonlinear OPF problem is linearized and then successive linear programming is applied.

The applications of the primal-dual interior point method for solving nonlinear OPF problems in [177-179] employed the polar coordinates representation for the active and reactive power flow equations and bus voltages. The model of [165] explains that when nonlinear OPF problems are formulated using rectangular coordinates representation, they have quadratic objective functions and quadratic constraints that allow for ease of matrix setup. These features have the advantages already discussed in the previous section, which improve the computational performance of the algorithm, as demonstrated by the numerical tests performed in [165]. Other studies that used rectangular coordinates with modifications in the mathematical formulation of the interior point problem are provided in [180,199-201].

Numerous publications for solving OPF problems based on the primal-dual interior point method have appeared since. A classification of the major publications and software codes that employ interior point methods is provided in [181]. Primal-dual interior point studies related to the analysis of nonlinear electricity market problems were also undertaken. The model in [182] investigates the decomposition of spot prices for active and reactive power by solving a constrained nonlinear optimisation problem. The OPF model in [183] minimises the generation costs in the presence of constraints for transmission, spinning reserve, load curtailment, and price dependent load. A similar investigation [184] on the OPF dispatch problem that incorporates transformer representation accomplishes reductions in the computational time, while the study in [185] investigates the properties of this algorithm. A modified version of the primal-dual interior point OPF with AC modelling is provided in [186],

where the computational challenges introduced by the deregulation of the electricity market structure related to algorithm convergence and accuracy are discussed. Interior point methods were also applied for electricity market equilibrium solutions. The primal-dual interior point method has been used for the SFE models of [132,137], while a software package based on this method has solved the market equilibrium problem in [135]. Furthermore, another variant of the interior point method, called the penalty interior point algorithm [187], has been used for the implementation of a model that calculates Cournot equilibria [59] and for an SFE model that is based on the MPEC approach [87].

3.4 Introduction to the implemented market equilibrium algorithm

A primal-dual nonlinear interior point algorithm has been implemented for the investigation of bid-based pool markets, based on linear SFE theory. The AC power flow analysis has been employed to represent the electrical network, in order to add realism to the proposed market equilibrium model and provide useful information about the effects of the individual network components on the electricity market equilibrium solution. The following operational aspects of the power system network have been taken into account:

- active and reactive power generation capacity limits,
- active and reactive price-responsive variable load demand,
- bus voltage limits,
- active and reactive power flows and losses for transmission lines and transformer branches,
- transmission line and transformer branches MVA capacity constraints,
- transformer tap-ratio control.

Furthermore, the operational and economic aspects for grid-connected PV systems have been modelled in the equilibrium algorithm, but this will be presented in Chapter 7.

The subsequent sections of this chapter outline the modelling of the individual components for the power system operation, the market considerations for the

implementation of the proposed algorithm, and the features of the primal-dual interior point method required for the function of the algorithmic procedure. The formulation provided in this section corresponds to supply function bids that are modelled using the k_F-parameterization, while the modelling for all the other available parameterization methods will be presented in Chapter 8. The reason for choosing the k_F-parameterization for illustrating the formulation of the market algorithm is that this method is desirable to be employed in the market analysis that takes place in Chapters 4 to 7, since the equilibrium k_F parameters are a relative measure that relates to the marginal cost of generation. By observing the k_F bidding parameters from the market equilibrium numerical results, the strategic behaviour of the generating firms can be easily interpreted without the requirement of referring to the actual generating costs.

3.5 Modelling of the electricity network

For the implementation of the proposed algorithm, rectangular coordinates have been employed for the modelling of voltages, admittances and power components in the electricity network. Guidelines for the derivation of the power flow equations using rectangular coordinates can be found in [188]. The following rectangular coordinates equations are considered in the subsequent formulations:

- $V_i = e_i + jf_i$ represents the voltage at bus i,
- $y_{ij} = g_{ij} + jb_{ij}$ represents the admittance of a transmission branch i-j,
- $S_{ij} = P_{ij} + jQ_{ij}$ represents the complex power flow from bus i to bus j through a transmission branch i-j.

3.5.1 Representation of the transmission line branch

The transmission line branch is modelled by the π-equivalent circuit representation, as shown in Figure 5.

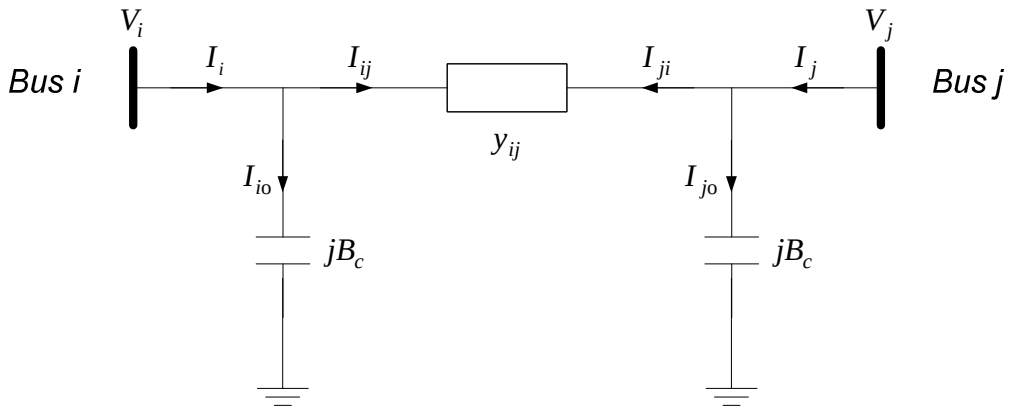

Figure 5: Π-equivalent circuit for modelling the transmission line branch.

The following expressions hold for the currents flowing in the circuit:

$$I_i = I_{ij} + I_{io} \tag{3.19}$$

$$I_{ij} = y_{ij}(V_i - V_j) \tag{3.20}$$

$$I_{io} = jB_cV_i \tag{3.21}$$

where V_i and V_j are the voltages at buses *i* and *j* respectively, and B_c is the shunt susceptance of the transmission line.

Substituting (3.20) and (3.21), into (3.19), and decomposing the voltages and admittances to their real and imaginary parts, gives:

$$I_i = [g_{ij} + j(b_{ij} + B_c)]V_i - (g_{ij} + jb_{ij})V_j \tag{3.22}.$$

Similarly, by considering current I_j, on the other side of the transmission branch:

$$I_j = -(g_{ij} + jb_{ij})V_i + [g_{ij} + j(b_{ij} + B_c)]V_j \tag{3.23}.$$

By rewriting equations (3.22) and (3.23) in matrix form:

$$\begin{bmatrix} I_i \\ I_j \end{bmatrix} = \begin{bmatrix} g_{ij} + j(b_{ij} + B_c) & -(g_{ij} + jb_{ij}) \\ -(g_{ij} + jb_{ij}) & g_{ij} + j(b_{ij} + B_c) \end{bmatrix} \begin{bmatrix} V_i \\ V_j \end{bmatrix} = \begin{bmatrix} Y_{ii} & Y_{ij} \\ Y_{ji} & Y_{jj} \end{bmatrix} \begin{bmatrix} V_i \\ V_j \end{bmatrix} \tag{3.24}$$

where the *Y* elements represent the admittance matrix of the transmission line branch *i-j*.

The complex power flow through the transmission line branch *i-j*, as defined in Figure 5, is given by:

$$S_{ij}^{LINE} = P_{ij}^{LINE} + jQ_{ij}^{LINE} = V_i I_i^* \quad (3.25).$$

By substituting voltage V_i by its rectangular components and multiplying with the conjugate of current I_i through the transmission line branch, the complex power flow is calculated as:

$$\begin{aligned} S_{ij}^{LINE} = {} & e_i\left[g_{ij}e_i - (b_{ij} + B_c) f_i - g_{ij}e_j + b_{ij} f_j\right] - je_i\left[g_{ij} f_i + (b_{ij} + B_c)e_i - b_{ij}e_j - g_{ij} f_j\right] \\ & + f_i\left[g_{ij} f_i + (b_{ij} + B_c)e_i - b_{ij}e_j - g_{ij} f_j\right] + jf_i\left[g_{ij}e_i - (b_{ij} + B_c) f_i - g_{ij}e_j + b_{ij} f_j\right] \end{aligned} \quad (3.26).$$

By decomposing the complex power into the active and reactive power components, the active and reactive power flows through the transmission line branch *i*-*j* are:

$$\begin{aligned} P_{ij}^{LINE} &= e_i\left[g_{ij}e_i - (b_{ij} + B_c) f_i - g_{ij}e_j + b_{ij} f_j\right] + f_i\left[g_{ij} f_i + (b_{ij} + B_c)e_i - b_{ij}e_j - g_{ij} f_j\right] \\ Q_{ij}^{LINE} &= -e_i\left[g_{ij} f_i + (b_{ij} + B_c)e_i - b_{ij}e_j - g_{ij} f_j\right] + f_i\left[g_{ij}e_i - (b_{ij} + B_c) f_i - g_{ij}e_j + b_{ij} f_j\right] \end{aligned} \quad (3.27).$$

The complex power flowing through branch *i*-*j* can also be defined as flowing from bus *j* to bus *i*. By using:

$$S_{ji}^{LINE} = P_{ji}^{LINE} + jQ_{ji}^{LINE} = V_j I_j^* \quad (3.28)$$

and applying similar substitutions as above, the active and reactive power flows from bus *j* to bus *i* are:

$$\begin{aligned} P_{ji}^{LINE} &= e_j\left[g_{ij}e_j - (b_{ij} + B_c) f_j - g_{ij}e_i + b_{ij} f_i\right] + f_j\left[g_{ij} f_j + (b_{ij} + B_c)e_j - b_{ij}e_i - g_{ij} f_i\right] \\ Q_{ji}^{LINE} &= -e_j\left[g_{ij} f_j + (b_{ij} + B_c)e_j - b_{ij}e_i - g_{ij} f_i\right] + f_j\left[g_{ij}e_j - (b_{ij} + B_c) f_j - g_{ij}e_i + b_{ij} f_i\right] \end{aligned} \quad (3.29).$$

3.5.2 Representation of the transformer

The modelling for the transformer considered in this formulation includes modelling of the transformer tap-ratio control, such as in the case of on-load tap-changing transformers, and representation of the admittance elements and transmission losses of the transformer branch. A power transformer with on-load tap-changing mechanism has the ability to regulate the network voltages (see Section 4.1). The physical meaning of the tap-changing mechanism is that it can

adjust the turns ratio between the primary and secondary coils of the transformer. The single-line diagram for the transformer branch is shown in Figure 6. An auxiliary intermediate bus, with apparent voltage $V_i^{/}$, is used to separate the turns ratio mechanism part, from the admittance of the transformer. The admittance element is given by $y_t = g + jb$.

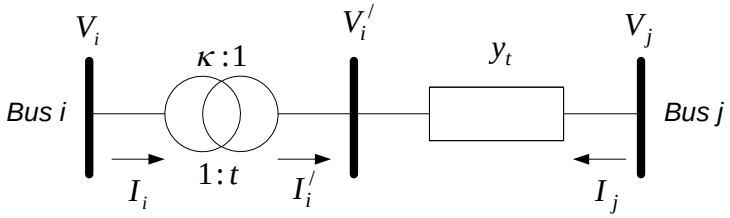

Figure 6: The single-line diagram for the transformer.

For the transformer tap-ratio control located at the *i*-side of the branch, the tap-ratio is defined from the diagram of Figure 6 as:

$$\kappa = \frac{V_i}{V_i^{/}} = \frac{I_i^{/}}{I_i} = \frac{1}{t} \tag{3.30}.$$

The following expressions hold for the currents flowing through the transformer branch:

$$I_i = tI_i^{/} \tag{3.31}$$

$$I_i^{/} = y_t(V_i^{/} - V_j) \tag{3.32}.$$

By substituting (3.32) into (3.31), and the voltage of the intermediate bus with $V_i^{/} = tV_i$, the current flowing in the direction *i* to *j* is given by:

$$I_i = t^2 y_t V_i - t y_t V_j \tag{3.33}.$$

By similar considerations, the current flowing in the direction *j* to *i* is given by:

$$I_j = -t y_t V_i + y_t V_j \tag{3.34}.$$

By rewriting equations (3.33) and (3.34) in matrix form:

$$\begin{bmatrix} I_i \\ I_j \end{bmatrix} = \begin{bmatrix} t^2 y_t & -t y_t \\ -t y_t & y_t \end{bmatrix} \begin{bmatrix} V_i \\ V_j \end{bmatrix} = \begin{bmatrix} Y_{ii} & Y_{ij} \\ Y_{ji} & Y_{jj} \end{bmatrix} \begin{bmatrix} V_i \\ V_j \end{bmatrix} \tag{3.35}$$

where the *Y* elements represent the admittance matrix of the transformer branch *i*-*j*. Note that the transformer branch admittance matrix is dependent on the variable tap-ratio term.

By observing the transformer matrix equation (3.35) and considering simple network analysis [176], the transformer equivalent circuit, for the case where the tap-ratio control is located at the *i*-side of the branch, can be expressed as shown in Figure 7.

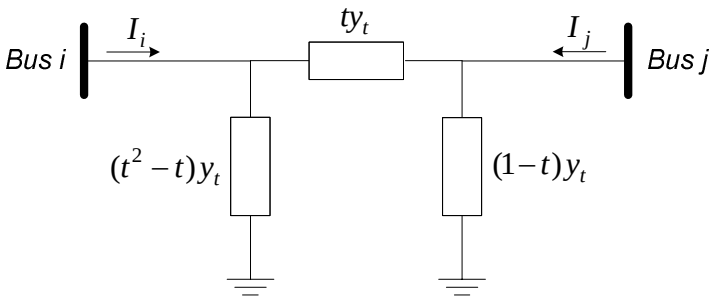

Figure 7: The equivalent circuit for the transformer.

The complex power flow through the transformer branch in the equivalent circuit of Figure 7, from bus *i* to bus *j*, is given by:

$$S_{ij}^{TR} = P_{ij}^{TR} + jQ_{ij}^{TR} = V_i I_i^* \tag{3.36}$$

By substituting voltage V_i by its rectangular components and multiplying with the conjugate of current I_i through the transformer branch, the complex power flow is calculated as:

$$\begin{aligned} S_{ij}^{TR} = {} & e_i\left[t^2(g_{ii}e_i - b_{ii}f_i) - t(g_{ij}e_j - b_{ij}f_j)\right] - je_i\left[t^2(b_{ii}e_i + g_{ii}f_i) - t(b_{ij}e_j + g_{ij}f_j)\right] \\ & + f_i\left[t^2(b_{ii}e_i + g_{ii}f_i) - t(b_{ij}e_j + g_{ij}f_j)\right] + jf_i\left[t^2(g_{ii}e_i - b_{ii}f_i) - t(g_{ij}e_j - b_{ij}f_j)\right] \end{aligned} \tag{3.37}$$

By decomposing the complex power into the active and reactive power components, the active and reactive power flows through the transformer branch in the direction from bus *i* to bus *j*, for tap-ratio control located at *i*-side, are:

$$\begin{aligned} P_{ij}^{TR} &= e_i\left[t^2(g_{ii}e_i - b_{ii}f_i) - t(g_{ij}e_j - b_{ij}f_j)\right] + f_i\left[t^2(b_{ii}e_i + g_{ii}f_i) - t(b_{ij}e_j + g_{ij}f_j)\right] \\ Q_{ij}^{TR} &= -e_i\left[t^2(b_{ii}e_i + g_{ii}f_i) - t(b_{ij}e_j + g_{ij}f_j)\right] + f_i\left[t^2(g_{ii}e_i - b_{ii}f_i) - t(g_{ij}e_j - b_{ij}f_j)\right] \end{aligned} \tag{3.38}$$

By similar considerations, the complex power flow through the transformer branch, from bus *j* to bus *i*, is given by:

$$S_{ji}^{TR} = P_{ji}^{TR} + jQ_{ji}^{TR} = V_j I_j^* \tag{3.39}$$

By substituting voltage V_j by its rectangular components and multiplying with the conjugate of current I_j through the transformer branch, the complex power flow is calculated as:

$$S_{ji}^{TR} = e_j\left[-t(g_{ij}e_i - b_{ij}f_i) + (g_{jj}e_j - b_{jj}f_j)\right] - je_j\left[-t(g_{ij}f_i + b_{ij}e_i) + (b_{jj}e_j + g_{jj}f_j)\right] + f_j\left[-t(g_{ij}f_i + b_{ij}e_i) + (b_{jj}e_j + g_{jj}f_j)\right] + jf_j\left[-t(g_{ij}e_i - b_{ij}f_i) + (g_{jj}e_j - b_{jj}f_j)\right] \quad (3.40).$$

By decomposing the complex power into the active and reactive power components, the active and reactive power flows through the transformer branch in the direction from bus *j* to bus *i*, for tap-ratio control located at *i*-side, are:

$$P_{ji}^{TR} = e_j\left[-t(g_{ij}e_i - b_{ij}f_i) + (g_{jj}e_j - b_{jj}f_j)\right] + f_j\left[-t(g_{ij}f_i + b_{ij}e_i) + (b_{jj}e_j + g_{jj}f_j)\right]$$

$$Q_{ji}^{TR} = -e_j\left[-t(g_{ij}f_i + b_{ij}e_i) + (b_{jj}e_j + g_{jj}f_j)\right] + f_j\left[-t(g_{ij}e_i - b_{ij}f_i) + (g_{jj}e_j - b_{jj}f_j)\right] \quad (3.41).$$

3.5.3 Formulation of the power flow and power mismatch equations

The power flow equations for a particular node in the electrical network represent the power injections from all the branches connected to that node. The complex power injection into bus *i* is given by:

$$S_i = \sum_j S_{ij} = \sum_j S_{ij}^{LINE} + \sum_j S_{ij}^{TR} \quad (3.42)$$

where the summation over *j* represents all the buses that are connected through transmission branches to bus *i*. The expression for S_{ij}^{LINE} is given in (3.26). The term S_{ij}^{TR} have been calculated in (3.37) for the transformer tap-ratio control located at the bus under examination (bus *i*), or in (3.40) for the tap-ratio control located at the other side of the branch connected to the bus under examination (bus *j*). By decomposing the complex power injection into its real and imaginary components, the active and reactive power injections into bus *i* are given by:

$$P_i = \sum_j P_{ij}^{LINE} + \sum_j P_{ij}^{TR} \quad (3.43)$$

$$Q_i = \sum_j Q_{ij}^{LINE} + \sum_j Q_{ij}^{TR} \quad (3.44).$$

The analytical expressions for the active and reactive power injections in rectangular coordinates are shown in equations (3.27) for the transmission line components, and in equations (3.38) for the transformer tap-ratio control located at bus *i*, or in equations (3.41), for the transformer tap-ratio control located at bus *j*, for the transformer branch components.

The power mismatch equations required for the modelling of the power balance constraints in the electricity market algorithm are derived from the energy conservation rule, such that the power generation at a bus must be equal to the sum of the power injection and the power load demand at that bus. The active and reactive power balance equations at bus *i* are:

$$Pg_i = P_i + Pd_i \tag{3.45}$$

$$Qg_i = Q_i + Qd_i \tag{3.46}$$

where *g* denotes the power generation and *d* the load demand. In order for the algorithm to converge by satisfying these two constraints, the power mismatch equations ΔP and ΔQ are defined as:

$$\Delta P_i = Pg_i - P_i - Pd_i = 0 \tag{3.47}$$

$$\Delta Q_i = Qg_i - Q_i - Qd_i = 0 \tag{3.48}.$$

The Δ-terms are required to be approximately equal to zero at the end of the iterative process in order for the algorithm to provide a satisfactory solution.

3.6 Electricity market assumptions and ISO obligations

The proposed algorithm is used to calculate the Nash equilibrium for wholesale bid-based electricity pool markets, by applying linear SFE theory, as discussed above. The market players are considered to be individual strategic firms that are profit-maximisers and no collusion or coalition exists between them, as in a non-cooperative game. For every bidding time interval, each strategic generating firm *F* submits a linear supply function bid for all of its generating units to the ISO, where $F = 1,2...,NF$ is the number of the firm. Each firm chooses strategy by anticipating the profit-maximising actions of its rivals and this holds for all individual firms. For the formulation in this section, the supply function bids are

assumed to be proportional to the marginal cost of generation and therefore the k_F-parameterization method is employed.

The generation cost function of the generating unit of firm *F* at bus *i* is given by:

$$C_{Pg_{F_i}} = \alpha_{F_i} Pg_{F_i} + \frac{1}{2}\beta_{F_i} Pg_{F_i}^2 \tag{3.49}$$

where Pg_{F_i} is the active power generation of unit of firm *F* at bus *i*, α_{F_i} and β_{F_i} are the linear and quadratic generation cost coefficients of that unit, respectively, for $i = 1,2...,NG$, where *NG* is the number of generation buses in the system. The marginal cost of generation $MC_{Pg_{F_i}}$ is given by the first derivative of the generation cost function with respect to its active power generation, such that:

$$MC_{Pg_{F_i}} = \frac{\partial C_{Pg_{F_i}}}{\partial Pg_{F_i}} = \alpha_{F_i} + \beta_{F_i} Pg_{F_i} \tag{3.50}.$$

It is likely that the supply function bids submitted do not represent the actual marginal costs, since the firms will attempt to favour their individual profits by raising the market clearing price at the expense of other players or the consumers; this act may result in deadweight loss and hence in a social welfare lower than that of the perfect competition market [137]. The supply function bid for the generating unit F_i is given by:

$$SB_{F_i} = k_{F_i} MC_{Pg_{F_i}} = k_{F_i}(\alpha_{F_i} + \beta_{F_i} Pg_{F_i}) \tag{3.51}$$

where k_{F_i} is the bidding parameter for this unit, considered to be the strategic variable for the firms as in [120,134]. The components $(k_{F_i}\alpha_{F_i})$ and $(k_{F_i}\beta_{F_i})$ are the intercept and the gradient of the linear supply function bid, respectively. It is assumed that the market participants are long-term players and have learned about their rivals' generating cost functions, such as in a complete information game. However, the ISO does not know the true generation cost function for the market participants, as will be discussed later. The decision of the strategic firms for the choice of the bid depends on the perception that a firm has about the rival firms' behaviour. If it is assumed that the bidding strategies for all the firms are responses to the other players' profit-maximising strategic actions, the resulting market solution will describe a Nash equilibrium state.

The consumers' benefit function at each load bus is given by:

$$D_{Pd_i} = \gamma_i Pd_i - \frac{1}{2}\delta_i Pd_i^2 \tag{3.52}$$

where Pd_i is the active load demand at bus *i*, and γ_i and δ_i are the linear and quadratic load cost coefficients at that bus, respectively, for $i = 1,2...,NL$, where *NL* is the number of the system buses that have load demand. Therefore, the linear inverse load demand function given by the first derivative of (3.52) with respect to the active load demand is:

$$MD_{Pd_i} = \gamma_i - \delta_i Pd_i \tag{3.53}.$$

Strategic demand-side bidding is not considered.

The primary objective of the ISO is to maximise the social welfare for the consumers, for each time interval. Once the firms submit the supply function bids for their generating units and the bidding process is closed, the ISO clears the market by balancing the power supply and demand and determines the market clearing price, while maximising the social welfare. During this process, the ISO adjusts the power levels across the network to those most favourable for the social welfare by determining the transformer tap-ratio settings and the voltage levels at each bus, while abiding by the network and supply-demand balance constraints. While doing so, the strategic actions of the generating firms, i.e. the submitted bids, are taken into account.

After the ISO balances the market, the market clearing price is obtained in terms of nodal prices for the active power supplied to the system, for one time interval. By repeating this process, the nodal prices are continuously readjusted over each time interval, depending on the amount of the energy delivered. The pool operator pays the firms according to the nodal prices at the buses where their generating units are connected, for the active power supplied to the pool. It is assumed that the generators produce an amount of active power equal to that of the ISO schedule, which is entirely sold to the power pool. For the scope of this research it is assumed that the reactive power provision does not account for any profit since the wholesale market model is only for active power, but it is

mandatory that the firms provide the required reactive power generation or absorption to support the voltage levels determined by the ISO.

The end-users (loads) pay the pool according to the nodal prices at their buses for the active power provided. This payment includes both the price of the energy supplied and the short-term transmission costs. The difference of the nodal prices at the different buses of the system corresponds to the energy transmission expenses from the generation site to the consumption point. These expenses include the costs for the network congestion and for the power losses in the transmission lines and transformer branches. The congestion cost is the cost of achieving system security by redispatching the power in the network in a different way to that of the economic dispatch in order to confine the power flows within the allowable transmission limits by shifting power generation from one unit to another that may correspond to higher generation costs, resulting in transmission congestion in the network. The cost of the power losses in the system depends on the physical characteristics of the transmission lines and transformers, but it is predictable and not as high as the congestion cost. The level of nodal prices depends on the properties of the constrained network, as the physical laws take precedence over the market laws. According to equation (2.10), the sum of the product of the nodal price and the power delivered at each load bus minus the sum of the product of the nodal price and the power supplied at each generation bus is the congestion rent and merchandising surplus collected by the transmission rights owner, which is assumed to be the ISO.

A depiction of the ISO process is shown in the block diagram of Figure 8.

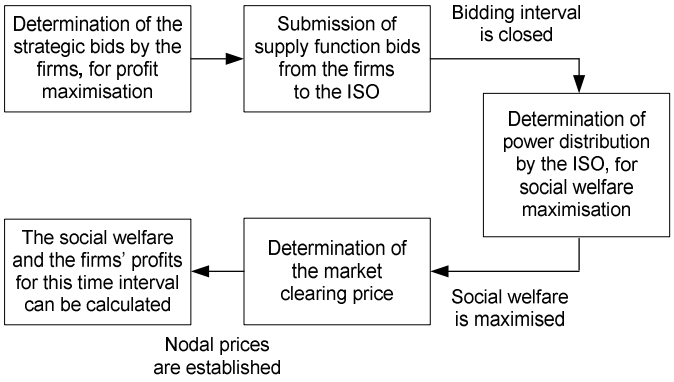

Figure 8: The ISO market process for one time interval.

3.7 The optimisation problem of the ISO

The formulation for the optimisation problem of the ISO considers the objective of social welfare maximisation, while it is subject to the AC network operational constraints. Since the ISO receives only the strategic bids from the firms and does not know the actual generating costs, the objective function Π_{ISO} that is going to be maximised is represented by the quasi social welfare function that depends on the strategic bids of the market players. This is defined as the consumers' benefit minus the generating costs reflected by the submitted bids. Therefore, the ISO optimisation problem is defined as:

$$Maximise \left\{ \Pi_{ISO}(x) = \sum_{i=1}^{NL} (\gamma_i Pd_i - \frac{1}{2}\delta_i Pd_i^2) - \sum_{i=1}^{NG} k_{F_i} (\alpha_{F_i} Pg_{F_i} + \frac{1}{2}\beta_{F_i} Pg_{F_i}^2) \right\} \quad (3.54)$$

subject to:

$$\Delta P_i = Pg_{F_i} - Pd_i - P_i(e, f, t) = 0 \quad (3.55)$$

$$\Delta Q_i = Qg_{F_i} - Qd_i - Q_i(e, f, t) = 0 \quad (3.56)$$

$$P_{ij}^2 + Q_{ij}^2 \le S_{ij}^2 \quad (3.57)$$

$$Pg_{F_i}^{\min} \le Pg_{F_i} \le Pg_{F_i}^{\max} \quad (3.58)$$

$$Qg_{F_i}^{\min} \le Qg_{F_i} \le Qg_{F_i}^{\max} \quad (3.59)$$

$$V_i^{\min} \le e_i^2 + f_i^2 \le V_i^{\max} \quad (3.60)$$

$$t^{\min} \le t_i \le t^{\max} \quad (3.61)$$

$$Pd_i \ge 0 \quad (3.62)$$

where $x = [e_i, f_i, Pg_{F_i}, Qg_{F_i}, t_i]$ for $i = 1,2,...,N$ is the system variables vector, the subscript '*i*' stands for the relevant bus for each case, ΔP_i and ΔQ_i are the active and reactive power mismatches, Pg_{F_i} and Qg_{F_i} are the active and reactive power generations (or reactive power absorption) by a unit of firm *F* at bus *i*, Pd_i and Qd_i are the active and reactive power load demands, P_i and Q_i are the active and reactive power injections, P_{ij} and Q_{ij} are the power flows through transmission line or transformer branch *i-j* in the direction *i* to *j* with maximum transmission limit S_{ij} formulated in rectangular coordinates, e_i and f_i are the real and imaginary components of the bus voltage in rectangular coordinates, $V^{\min}$ and $V^{\max}$ are the minimum and maximum voltage magnitude

limits squared, and t_i is the transformer tap-ratio for tap-ratio control located at bus *i*-side of the transformer branch *i*-*j*. The reactive load demand is set to:

$$Qd_i = Pd_i \tan\theta_i \tag{3.63}$$

where θ_i is the load angle of bus *i*, assumed to be constant for each bus over one time interval. Since the active load demand is variable and responds to changes in the market price, the reactive load demand is also price-responsive.

3.8 The optimisation problem of the generating firms

The aim of a utility maximiser participating in the game is to achieve the highest profit possible. Therefore, the primary objective of each of the strategic firms in the electricity market is to maximise the profits of their individual generating units, given by the sales income minus the true generating costs. The optimisation problem for the generating firms is given by:

$$Maximise \left\{ \Pi_F(x) = \sum_{i=1}^{NG} (\lambda p_i Pg_{F_i} - \alpha_{F_i} Pg_{F_i} - \frac{1}{2}\beta_{F_i} Pg_{F_i}^2) \right\} \tag{3.64}$$

subject to:

$$k_{F_i}^{\min} \le k_{F_i} \le k_{F_i}^{\max} \tag{3.65}$$

where Π_F is the firm's profit, $k_{F_i}^{\min}$ and $k_{F_i}^{\max}$ are the lower and upper limits for the bidding parameter, and λp_i represents the nodal price at bus *i* [182]. Note that the inequality constraint for the submitted bid may be different from the one shown in (3.65), depending on the choice of the parameterization method for the linear supply function bid. This will be elaborated in Chapter 8 where the formulations for the different parameterization methods are provided.

3.9 The solution for the SFE market problem

In order to solve the SFE problem and obtain the Nash equilibrium point for the electricity market, all the constraints and the optimisation of the objectives from the ISO and the generating firms' problems must be satisfied. To do so, each firm should recognise the best bidding strategy for profit maximisation, by taking into account that all the other firms will behave in a similar manner, and the ISO

should clear the market while maximising the social welfare by considering the strategic bids from the firms. In order to represent this, the original bi-level optimisation problem will be transformed into a single combined problem that satisfies both optimisation objectives and constraints. The implemented primal-dual interior point algorithm will solve iteratively the resulting combined optimisation problem and converge to the SFE point for the electricity market. This market equilibrium solution can be characterised by the equilibrium set of variables, which consists of the nodal prices, the firm's bidding factors and profits, the social welfare, the voltages across the system, the transformer tap-ratio settings and the power distribution in the network.

3.9.1 Reformulation of the ISO optimisation problem

The first step for the reformulation of the bi-level SFE problem is to transform the ISO maximisation problem with equality and inequality constraints, into an equivalent minimisation problem with equality constraints only. This is done by introducing the slack variables *sl* and *su* for the lower and upper bounds of the inequality constraints, respectively, with the application of the Fiacco-McCormick Logarithmic Barrier method. By grouping the inequalities (3.57)-(3.61) into the following inequality vector:

$$h_n^{\min} \le h_n(x) \le h_n^{\max} \tag{3.66}$$

the equivalent minimisation problem for the ISO is:

$$Minimise \left\{ -\Pi_{ISO}(x) - \mu \sum_n \ln(sl_n) - \mu \sum_n \ln(su_n) \right\} \tag{3.67}$$

subject to:

$$\Delta P_i = 0 \tag{3.68}$$

$$\Delta Q_i = 0 \tag{3.69}$$

$$h_n(x) - sl_n - h_n^{\min} = 0 \tag{3.70}$$

$$h_n(x) + su_n - h_n^{\max} = 0 \tag{3.71}$$

where $\mu > 0$ is the barrier parameter, *n* is the number of inequality constraints of the ISO problem, and $sl_n > 0$ and $su_n > 0$ are the slack variables for the *n* inequality constraints. The inequality for the active load demand (3.62) is not

included in (3.66) because it will be incorporated in the formulation in a later stage as an equivalent complementarity condition.

By employing the Lagrange method for optimisation with equalities the Lagrange function $L_{1\mu}$ for the problem given in (3.67)-(3.71) can be obtained as:

$$\begin{aligned} L_{1\mu} = & -\Pi_{ISO}(x) - \mu\sum_{n}\ln(sl_n) - \mu\sum_{n}\ln(su_n) \\ & - \sum_{i=1}^{N}\lambda p_i \Delta P_i - \sum_{i=1}^{N}\lambda q_i \Delta Q_i \\ & - \sum_{n}\pi l_n[h_n(x) - sl_n - h_n^{\min}] \\ & - \sum_{n}\pi u_n[h_n(x) + su_n - h_n^{\max}] \end{aligned} \tag{3.72}$$

where λp_i, λq_i, $\pi l_n > 0$ and $\pi u_n < 0$ are the Lagrange multipliers (dual variables) for the equality constraints (3.68)-(3.71) respectively, and *N* is the number of total buses in the system.

The optimal solution for the above problem satisfies the 1st order KKT conditions of (3.72), which can be obtained by differentiating the Lagrange function $L_{1\mu}$ with respect to all the primal and dual variables. The set of the KKT condition equations for (3.72), which represent the ISO optimisation problem, are as follows:

$$\nabla_x L_{1\mu} = -\nabla_x \Pi_{ISO} - \sum_{i=1}^{N}\nabla_x \Delta P_i \lambda p_i - \sum_{i=1}^{N}\nabla_x \Delta Q_i \lambda q_i - \nabla_x h_n \pi l_n - \nabla_x h_n \pi u_n = 0 \tag{3.73}$$

$$\nabla_{\lambda p_i} L_{1\mu} = -\Delta P_i = 0 \tag{3.74}$$

$$\nabla_{\lambda q_i} L_{1\mu} = -\Delta Q_i = 0 \tag{3.75}$$

$$\nabla_{\pi l_n} L_{1\mu} = -(h_n - sl_n - h_n^{\min}) = 0 \tag{3.76}$$

$$\nabla_{\pi u_n} L_{1\mu} = -(h_n + su_n - h_n^{\max}) = 0 \tag{3.77}$$

$$\nabla_{sl_n} L_{1\mu} = \mu - sl_n \pi l_n = 0 \tag{3.78}$$

$$\nabla_{su_n} L_{1\mu} = \mu + su_n \pi u_n = 0 \tag{3.79}$$

$$\nabla_{Pd_i} L_{1\mu} = -\nabla_{Pd_i} \Pi_{ISO} - \sum_{i=1}^{N}\nabla_{Pd_i} \Delta P_i \lambda p_i - \sum_{i=1}^{N}\nabla_{Pd_i} \Delta Q_i \lambda q_i = 0 \tag{3.80}.$$

The KKT condition equation (3.80) that corresponds to the active load demand *Pd* is treated separately from the other conditions, in order to be transformed into a nonlinear complementarity function. This function will represent the KKT condition for *Pd* and, in addition, the non-negativity constraint (3.62). The analysis is shown in the next section.

3.9.2 Introduction of the complementarity constraint

The nonlinear complementarity method, based on the Fischer-Burmeister merit function [160], can easily handle complicated complementarity conditions for optimality. The complementarity conditions must satisfy the following property:

$$\Psi(a,b) = 0 \Leftrightarrow a \geq 0, b \geq 0, ab = 0 \tag{3.81}$$

where Ψ is the Nonlinear Complementarity Problem (NCP) function that relates the complementarity parameters *a* and *b*. This property states that the NCP function Ψ is equivalent to the complementarity constraint associated with *a* and *b*, and vice versa. The NCP function in this analysis is represented by the Fischer-Burmeister merit function, as in [189], given by:

$$\Psi(a,b) = a + b - \sqrt{a^2 + b^2} \tag{3.82}.$$

By evaluating the derivatives in the KKT condition equation for the active load demand (3.80) and then multiplying by Pd_i, since the expression is equal to zero, the following equation can be obtained:

$$Pd_i(-\gamma_i + \delta_i Pd_i + \lambda p_i + \lambda q_i \tan\theta_i) = 0 \tag{3.83}.$$

Since the properties,

$$Pd_i \geq 0 \tag{3.84}$$

$$(-\gamma_i + \delta_i Pd_i + \lambda p_i + \lambda q_i \tan\theta_i) \geq 0 \tag{3.85}$$

hold, by setting $a = Pd_i$ and $b = (-\gamma_i + \delta_i Pd_i + \lambda p_i + \lambda q_i \tan\theta_i)$, the KKT condition equation for the active load demand (3.80) can be replaced by the following NCP function, and in addition the non-negativity constraint for *Pd* (3.62) will be introduced in the formulation. Such mathematical transformations facilitate reductions in the computational effort of the algorithm, since there will be no extra computations for slack and dual variables associated with the active

load demand, and possible ill-conditioning complications due to the complementarity expressions may be avoided. Therefore, since the complementarity conditions from (3.81) are valid, the NCP function for the ISO problem is:

$$\Psi_i(Pd_i, (-\gamma_i + \delta_i Pd_i + \lambda p_i + \lambda q_i \tan\theta_i)) =$$
$$Pd_i + (-\gamma_i + \delta_i Pd_i + \lambda p_i + \lambda q_i \tan\theta_i) - \sqrt{Pd_i^2 + (-\gamma_i + \delta_i Pd_i + \lambda p_i + \lambda q_i \tan\theta_i)^2} = 0 \quad (3.86).$$

This expression will replace (3.80) in the set of the ISO KKT condition equations that result from the Lagrange function $L_{1\mu}$.

3.9.3 Formulation of the combined optimisation problem for the SFE solution

In order to obtain a combined problem that represents the overall electricity market equilibrium problem, the following arguments are brought into attention. The active power Pg_{F_i} and the nodal prices λp_i present in the firms' optimisation problem (3.64)-(3.65) that can be expressed as implicit functions of all generating firms' strategies, are produced by the nonlinear optimisation programming problem of the ISO (3.54)-(3.62) [134]. Therefore, the values of Pg_{F_i} and λp_i should satisfy the ISO KKT conditions, which represent the original ISO optimisation problem. Hence, the ISO KKT conditions can be incorporated into the strategic firms' optimisation problem as equality constraints, to form a combined optimisation problem that can be solved to give the market SFE point.

By applying the above considerations, the resulting combined optimisation problem for the market solution is:

$$Maximise \left\{ \Pi_F(x) = \sum_{i=1}^{NG} (\lambda p_i Pg_{F_i} - \alpha_{F_i} Pg_{F_i} - \frac{1}{2}\beta_{F_i} Pg_{F_i}^2) \right\} \quad (3.87)$$

subject to:

$$k_{F_i}^{\min} \le k_{F_i} \le k_{F_i}^{\max} \quad (3.88)$$

KKT condition equations of the ISO problem (3.73)-(3.79), (3.86) (3.89).

By applying the Fiacco-McCormick Barrier method to the combined problem in order to eliminate the inequality constraints for the strategic bids, the maximisation problem in (3.87)-(3.89) is transformed into an equivalent minimisation problem with equality constraints only, such that:

$$\textit{Minimise} \left\{ -\Pi_F(x) - \mu \sum_{i=1}^{NG} \ln(sl_{k_{F_i}}) - \mu \sum_{i=1}^{NG} \ln(su_{k_{F_i}}) \right\} \tag{3.90}$$

subject to:

$$k_{F_i} - sl_{k_{F_i}} - k_{F_i}^{\min} = 0 \tag{3.91}$$

$$k_{F_i} + su_{k_{F_i}} - k_{F_i}^{\max} = 0 \tag{3.92}$$

KKT condition equations of the ISO problem (3.73)-(3.79), (3.86) (3.93).

Thus, by introducing Lagrange multipliers for each constraint in (3.90)-(3.93), considering each ISO KKT condition in (3.93) separately, the following Lagrange function for the combined problem yields:

$$\begin{aligned} L_{2\mu} = & -\Pi_F(x) - \mu \sum_{i=1}^{NG} \ln(sl_{k_{F_i}}) - \mu \sum_{i=1}^{NG} \ln(su_{k_{F_i}}) \\ & - \pi l_{k_{F_i}} [k_{F_i} - sl_{k_{F_i}} - k_{F_i}^{\min}] - \pi u_{k_{F_i}} [k_{F_i} + su_{k_{F_i}} - k_{F_i}^{\max}] \\ & + \omega_x [-\nabla_x \Pi_{ISO}(x) - \sum_{i=1}^{N} \nabla_x \Delta P_i \lambda p_i - \sum_{i=1}^{N} \nabla_x \Delta Q_i \lambda q_i - (\pi l_n + \pi u_n) \sum_n \nabla_x h_n] \\ & + \sum_{i=1}^{N} \omega_{\lambda p_i} [-\Delta P_i] + \sum_{i=1}^{N} \omega_{\lambda q_i} [-\Delta Q_i] \\ & + \sum_n \omega_{sl_n} [\mu - sl_n \pi l_n] + \sum_n \omega_{su_n} [\mu + su_n \pi u_n] \\ & + \sum_n \omega_{\pi l_n} [-(h_n - sl_n - h_n^{\min})] + \sum_n \omega_{\pi u_n} [-(h_n + su_n - h_n^{\max})] \\ & - \sum_{i=1}^{N} \omega_\Psi [\Psi(Pd_i, (-\gamma_i + \delta_i Pd_i \lambda p_i + \lambda q_i \tan\theta_i))] \end{aligned} \tag{3.94}$$

where ω_x, $\omega_{\lambda p_i}$, $\omega_{\lambda q_i}$, ω_{sl_n}, ω_{su_n}, $\omega_{\pi l_n}$, $\omega_{\pi u_n}$ and ω_Ψ are the Lagrange multipliers for the KKT condition equations (3.73)-(3.79) and (3.86), respectively, which were incorporated into the firms' optimisation problem as equality constraints, and $\pi l_{k_{F_i}} > 0$ and $\pi u_{k_{F_i}} < 0$ are the Lagrange multipliers associated with the strategic bids.

By differentiating the Lagrange function $L_{2\mu}$, the 1st order KKT condition equations for the combined optimisation problem are obtained as shown below:

$$\begin{aligned}\nabla_x L_{2\mu} = &-\nabla_x \Pi_F(x) + \sum \omega_x[-\nabla_x \nabla_x \Pi_{ISO}(x)] \\ &+ \sum \omega_x[-\sum \nabla_x(\nabla_x \Delta P_i)\lambda p_i - \sum \nabla_x(\nabla_x \Delta Q_i)\lambda q_i] \\ &+ \sum \omega_x[-\sum \nabla_x(\nabla_x h_n)\pi l_n - \sum \nabla_x(\nabla_x h_n)\pi u_n] \\ &- \sum \omega_{\lambda p_i} \nabla_x \Delta P_i - \sum \omega_{\lambda q_i} \nabla_x \Delta Q_i \\ &- \sum \omega_{\pi l_n} \nabla_x h_n - \sum \omega_{\pi u_n} \nabla_x h_n = 0 \end{aligned} \quad (3.95)$$

$$\nabla_{Pd} L_{2\mu} = -\sum \omega_{\lambda p_i} \nabla_{Pd} \Delta P_i - \sum \omega_{\lambda q_i} \nabla_{Pd} \Delta Q_i - \sum \omega_\Psi \nabla_{Pd} \Psi = 0 \quad (3.96)$$

$$\nabla_{\lambda p_i} L_{2\mu} = -\sum \nabla_{\lambda p_i} \Pi_F(x) - \sum \omega_x \nabla_x \Delta P_i - \omega_\Psi \nabla_{\lambda p_i} \Psi = 0 \quad (3.97)$$

$$\nabla_{\lambda q_i} L_{2\mu} = -\sum \omega_x \nabla_x \Delta Q_i - \omega_\Psi \nabla_{\lambda q_i} \Psi = 0 \quad (3.98)$$

$$\nabla_{\pi l_n} L_{2\mu} = -\sum \omega_x \nabla_x h_n - \omega_{sl_n} sl_n = 0 \quad (3.99)$$

$$\nabla_{\pi u_n} L_{2\mu} = -\sum \omega_x \nabla_x h_n + \omega_{su_n} su_n = 0 \quad (3.100)$$

$$\nabla_{sl_n} L_{2\mu} = -\omega_{sl_n} \pi l_n + \omega_{\pi l_n} = 0 \quad (3.101)$$

$$\nabla_{su_n} L_{2\mu} = \omega_{su_n} \pi u_n - \omega_{\pi u_n} = 0 \quad (3.102)$$

$$\begin{aligned}\nabla_{\omega_x} L_{2\mu} = &\sum [-\nabla_x \Pi_{ISO}(x) - \sum \nabla_x \Delta P_i \lambda p_i - \sum \nabla_x \Delta Q_i \lambda q_i \\ &- \sum \nabla_x h_n \pi l_n - \sum \nabla_x h_n \pi u_n] = 0 \end{aligned} \quad (3.103)$$

$$\nabla_{\omega_{\lambda p_i}} L_{2\mu} = -\Delta P_i = 0 \quad (3.104)$$

$$\nabla_{\omega_{\lambda q_i}} L_{2\mu} = -\Delta Q_i = 0 \quad (3.105)$$

$$\nabla_{\omega_{\pi l_n}} L_{2\mu} = -[h_n - sl_n - h_n^{\min}] = 0 \quad (3.106)$$

$$\nabla_{\omega_{\pi u_n}} L_{2\mu} = -[h_n + su_n - h_n^{\max}] = 0 \quad (3.107)$$

$$\nabla_{\omega_{sl_n}} L_{2\mu} = \mu - sl_n \pi l_n = 0 \quad (3.108)$$

$$\nabla_{\omega_{su_n}} L_{2\mu} = \mu + su_n \pi u_n = 0 \quad (3.109)$$

$$\nabla_{\omega_\Psi} L_{2\mu} = -\Psi = 0 \quad (3.110)$$

$$\nabla_{k_{F_i}} L_{2\mu} = -\sum \nabla_{k_{F_i}} \omega_x \nabla_x \Pi_{ISO}(x) - (\pi l_{k_{F_i}} + \pi u_{k_{F_i}}) \nabla_{k_{F_i}} k_{F_i} = 0 \quad (3.111)$$

$$\nabla_{sl_{kFi}} L_{2\mu} = \mu - sl_{k_{F_i}} \pi l_{k_{F_i}} = 0 \quad (3.112)$$

$$\nabla_{su_{k_{F_i}}} L_{2\mu} = \mu + su_{k_{F_i}} \pi u_{k_{F_i}} = 0 \quad (3.113)$$

$$\nabla_{\pi l_{k_{F_i}}} L_{2\mu} = -[h_{k_{F_i}} - sl_{k_{F_i}} - k_{F_i}^{\min}] = 0 \quad (3.114)$$

$$\nabla_{\pi u_{k_{F_i}}} L_{2\mu} = -[h_{k_{F_i}} + su_{k_{F_i}} - k_{F_i}^{\max}] = 0 \quad (3.115).$$

The KKT conditions (3.95)-(3.115) obtained from the Lagrange function $L_{2\mu}$ represent the overall market equilibrium problem. These are then linearized using Taylor series expansion with the application of the Newton's method, in order to proceed for the solution of the SFE problem.

3.9.4 Linearization of the market problem's KKT system

Recalling from equation (3.16) in Section 3.2, the linearization of the above KKT conditions can be achieved by computing the Jacobian J of each expression g from (3.95)-(3.115) with respect to all of its variables y, and then setting $J \cdot \Delta y = -g$. Hence the complete set of the linearized equations for the solution of the market equilibrium problem are obtained as follows:

$$
\begin{aligned}
-\nabla_x L_{2\mu} = & \Big\{ -\nabla_x^2 \Pi_F - \sum \omega_x [\sum \nabla_x^3 \Delta P_i \lambda p_i + \sum \nabla_x^3 \Delta Q_i \lambda q_i] \\
& \quad - \sum \omega_x [\sum \nabla_x^3 h_n \pi l_n + \sum \nabla_x^3 h_n \pi u_n] \\
& \quad - \sum \omega_{\lambda p_i} \nabla_x^2 \Delta P_i - \sum \omega_{\lambda q_i} \nabla_x^2 \Delta Q_i \\
& \quad - \sum \omega_{\pi l_n} \nabla_x^2 h_n - \sum \omega_{\pi u_n} \nabla_x^2 h_n \Big\} \cdot \Delta x \\
& + \Big\{ - \sum \omega_x [\sum \nabla_x^2 \Delta P_i] - \sum \nabla_{\lambda p_i} \nabla_x \Pi_F \Big\} \cdot \Delta \lambda p_i \\
& + \Big\{ - \sum \omega_x [\sum \nabla_x^2 \Delta Q_i] \Big\} \cdot \Delta \lambda q_i \\
& + \Big\{ - \sum \omega_x [\sum \nabla_x^2 h_n] \Big\} \cdot \Delta \pi l_n \\
& + \Big\{ - \sum \omega_x [\sum \nabla_x^2 h_n] \Big\} \cdot \Delta \pi u_n \\
& + \Big\{ - \sum \nabla_x^2 \Pi_{ISO} - \sum \nabla_x^2 \Delta P_i \lambda p_i - \sum \nabla_x^2 \Delta Q_i \lambda q_i \\
& \quad - \sum \nabla_x^2 h_n \pi l_n - \sum \nabla_x^2 h_n \pi u_n \Big\} \cdot \Delta \omega_x \\
& + \Big\{ - \sum \nabla_x \Delta P_i \Big\} \cdot \Delta \omega_{\lambda p_i} \\
& + \Big\{ - \sum \nabla_x \Delta Q_i \Big\} \cdot \Delta \omega_{\lambda q_i} \\
& + \Big\{ - \sum \nabla_x h_n \Big\} \cdot \Delta \omega_{\pi l_n} \\
& + \Big\{ - \sum \nabla_x h_n \Big\} \cdot \Delta \omega_{\pi u_n} \\
& + \Big\{ - \sum \nabla_{k_{F_i}} \nabla_x^2 \omega_x \Pi_{ISO} \Big\} \cdot \Delta k_{F_i}
\end{aligned}
\tag{3.116}
$$

$$
\begin{aligned}
-\nabla_{Pd} L_{2\mu} = & \Big\{ - \sum \omega_\Psi \nabla_{Pd}^2 \Psi \Big\} \cdot \Delta Pd \\
& + \Big\{ - \sum \omega_\Psi \nabla_{\lambda p_i} \nabla_{Pd} \Psi \Big\} \cdot \Delta \lambda p_i \\
& + \Big\{ - \sum \omega_\Psi \nabla_{\lambda q_i} \nabla_{Pd} \Psi \Big\} \cdot \Delta \lambda q_i \\
& + \Delta \omega_{\lambda p_i} \\
& + \{ \tan \theta_i \} \cdot \Delta \omega_{\lambda q_i} \\
& + \Big\{ - \sum \nabla_{Pd} \Psi \Big\} \cdot \Delta \omega_\Psi
\end{aligned}
\tag{3.117}
$$

$$
\begin{aligned}
-\nabla_{\lambda p_i} L_{2\mu} = & \left\{ -\sum \nabla_x \nabla_{\lambda p_i} \Pi_F - \sum \omega_x \nabla_x^2 \Delta P_i \right\} \cdot \Delta x \\
& + \left\{ -\omega_\Psi \nabla_{Pd} \nabla_{\lambda p_i} \Psi \right\} \cdot \Delta P d \\
& + \left\{ -\omega_\Psi \nabla_{\lambda p_i}^2 \Psi \right\} \cdot \Delta \lambda p_i \\
& + \left\{ -\omega_\Psi \nabla_{\lambda p_i} \nabla_{\lambda q_i} \Psi \right\} \cdot \Delta \lambda q_i \\
& + \left\{ -\sum \nabla_x \Delta P_i \right\} \cdot \Delta \omega_x \\
& + \left\{ -\sum \nabla_{\lambda p_i} \Psi \right\} \cdot \Delta \omega_\Psi
\end{aligned} \tag{3.118}
$$

$$
\begin{aligned}
-\nabla_{\lambda q_i} L_{2\mu} = & \left\{ -\sum \omega_x \nabla_x^2 \Delta Q_i \right\} \cdot \Delta x \\
& + \left\{ -\omega_\Psi \nabla_{Pd} \nabla_{\lambda q_i} \Psi \right\} \cdot \Delta P d \\
& + \left\{ -\omega_\Psi \nabla_{\lambda p_i} \nabla_{\lambda q_i} \Psi \right\} \cdot \Delta \lambda p_i \\
& + \left\{ -\omega_\Psi \nabla_{\lambda q_i}^2 \Psi \right\} \cdot \Delta \lambda q_i \\
& + \left\{ -\sum \nabla_x \Delta Q_i \right\} \cdot \Delta \omega_x \\
& + \left\{ -\sum \nabla_{\lambda q_i} \Psi \right\} \cdot \Delta \omega_\Psi
\end{aligned} \tag{3.119}
$$

$$
\begin{aligned}
-\nabla_{\pi l_n} L_{2\mu} = & \left\{ -\sum \omega_x \nabla_x^2 h_n \right\} \cdot \Delta x \\
& + \left\{ -\omega_{sl_n} \right\} \cdot \Delta s l_n \\
& + \left\{ -\sum \nabla_x h_n \right\} \cdot \Delta \omega_x \\
& + \left\{ -sl_n \right\} \cdot \Delta \omega_{sl_n}
\end{aligned} \tag{3.120}
$$

$$
\begin{aligned}
-\nabla_{\pi u_n} L_{2\mu} = & \left\{ -\sum \omega_x \nabla_x^2 h_n \right\} \cdot \Delta x \\
& + \left\{ \omega_{su_n} \right\} \cdot \Delta s u_n \\
& + \left\{ -\sum \nabla_x h_n \right\} \cdot \Delta \omega_x \\
& + \left\{ su_n \right\} \cdot \Delta \omega_{su_n}
\end{aligned} \tag{3.121}
$$

$$
\begin{aligned}
-\nabla_{sl_n} L_{2\mu} = & \left\{ -\omega_{sl_n} \right\} \cdot \Delta \pi l_n \\
& + \Delta \omega_{\pi l_n} \\
& + \left\{ -\pi l_n \right\} \cdot \Delta \omega_{sl_n}
\end{aligned} \tag{3.122}
$$

$$
\begin{aligned}
-\nabla_{su_n} L_{2\mu} = & \left\{ \omega_{su_n} \right\} \cdot \Delta \pi u_n \\
& - \Delta \omega_{\pi u_n} \\
& + \left\{ \pi u_n \right\} \cdot \Delta \omega_{su_n}
\end{aligned} \tag{3.123}
$$

$$
\begin{aligned}
-\nabla_{\omega_x} L_{2\mu} = & \left\{ -\sum \nabla_x^2 \Pi_{ISO} - \sum \nabla_x^2 \Delta P_i \lambda p_i - \sum \nabla_x^2 \Delta Q_i \lambda q_i \right. \\
& \left. - \sum \nabla_x^2 h_n \pi l_n - \sum \nabla_x^2 h_n \pi u_n \right\} \cdot \Delta x \\
& + \left\{ -\sum \nabla_x \Delta P_i \right\} \cdot \Delta \lambda p_i \\
& + \left\{ -\sum \nabla_x \Delta Q_i \right\} \cdot \Delta \lambda q_i \\
& + \left\{ -\sum \nabla_x h_n \right\} \cdot \Delta \pi l_n \\
& + \left\{ -\sum \nabla_x h_n \right\} \cdot \Delta \pi u_n \\
& + \left\{ -\sum \nabla_{k_{F_i}} \nabla_x \Pi_{ISO} \right\} \cdot \Delta k_{F_i}
\end{aligned} \tag{3.124}
$$

$$
\begin{aligned}
-\nabla_{\omega_\Psi} L_{2\mu} = & \left\{ -\sum \nabla_{Pd} \Psi \right\} \cdot \Delta Pd \\
& + \left\{ -\sum \nabla_{\lambda p_i} \Psi \right\} \cdot \Delta \lambda p_i \\
& + \left\{ -\sum \nabla_{\lambda q_i} \Psi \right\} \cdot \Delta \lambda q_i
\end{aligned} \tag{3.125}
$$

$$
\begin{aligned}
-\nabla_{\omega_{\lambda p_i}} L_{2\mu} = & \left\{ -\sum \nabla_x \Delta P_i \right\} \cdot \Delta x \\
& + \left\{ -\sum \nabla_{Pd} \Delta P_i \right\} \cdot \Delta Pd
\end{aligned} \tag{3.126}
$$

$$
\begin{aligned}
-\nabla_{\omega_{\lambda q_i}} L_{2\mu} = & \left\{ -\sum \nabla_x \Delta Q_i \right\} \cdot \Delta x \\
& + \left\{ -\sum \nabla_{Pd} \Delta Q_i \right\} \cdot \Delta Pd
\end{aligned} \tag{3.127}
$$

$$
\begin{aligned}
-\nabla_{\omega_{\pi l_n}} L_{2\mu} = & \left\{ -\sum \nabla_x h_n \right\} \cdot \Delta x \\
& + \Delta s l_n
\end{aligned} \tag{3.128}
$$

$$
\begin{aligned}
-\nabla_{\omega_{\pi u_n}} L_{2\mu} = & \left\{ -\sum \nabla_x h_n \right\} \cdot \Delta x \\
& - \Delta s u_n
\end{aligned} \tag{3.129}
$$

$$
\begin{aligned}
-\nabla_{\omega_{sl_n}} L_{2\mu} = & \left\{ -sl_n \right\} \cdot \Delta \pi l_n \\
& + \left\{ -\pi l_n \right\} \cdot \Delta s l_n
\end{aligned} \tag{3.130}
$$

$$
\begin{aligned}
-\nabla_{\omega_{su_n}} L_{2\mu} = & \left\{ su_n \right\} \cdot \Delta \pi u_n \\
& + \left\{ \pi u_n \right\} \cdot \Delta s u_n
\end{aligned} \tag{3.131}
$$

$$
\begin{aligned}
-\nabla_{k_{F_i}} L_{2\mu} = & \left\{ -\sum \nabla_{k_{F_i}} \nabla_x^2 \omega_x \Pi_{ISO} \right\} \cdot \Delta x \\
& + \left\{ -\sum \nabla_{k_{F_i}} \nabla_x \Pi_{ISO} \right\} \cdot \Delta \omega_x \\
& - \Delta \pi l_{k_{F_i}} \\
& - \Delta \pi u_{k_{F_i}}
\end{aligned} \tag{3.132}
$$

$$-\nabla_{\pi l_{k_{F_i}}} L_{2\mu} = -\Delta k_{F_i} + \Delta s l_{k_{F_i}} \tag{3.133}$$

$$-\nabla_{\pi u_{k_{F_i}}} L_{2\mu} = -\Delta k_{F_i} - \Delta s u_{k_{F_i}} \tag{3.134}$$

$$-\nabla_{s l_{k_{F_i}}} L_{2\mu} = \left\{-s l_{k_{F_i}}\right\} \cdot \Delta \pi l_{k_{F_i}} + \left\{-\pi l_{k_{F_i}}\right\} \cdot \Delta s l_{k_{F_i}} \tag{3.135}$$

$$-\nabla_{s u_{k_{F_i}}} L_{2\mu} = \left\{s u_{k_{F_i}}\right\} \cdot \Delta \pi u_{k_{F_i}} + \left\{\pi u_{k_{F_i}}\right\} \cdot \Delta s u_{k_{F_i}} \tag{3.136}.$$

The set of the above linearized equations can be solved simultaneously to give the electricity market equilibrium solution. In order to enhance the efficiency and robustness of the solution algorithm the linearized equations are rearranged into a Newton matrix equation by applying sparse matrix techniques. The mathematical formulation is as follows.

3.9.5 Formulation of the Newton matrix equation

The linearized equations (3.116)-(3.136) that represent the market equilibrium problem are rearranged into the following symmetrical Newton matrix equation:

$$\begin{bmatrix} W & U & H_{k_{F_i}1} \\ U^T & 0 & H_{k_{F_i}2} \\ H^T_{k_{F_i}1} & H^T_{k_{F_i}2} & H_{k_{F_i}3} \end{bmatrix} \begin{bmatrix} \Delta(x_p, x_d) \\ \Delta\omega \\ \Delta k_{F_i} \end{bmatrix} = \begin{bmatrix} -\nabla_{(x_p, x_d)} L_{2\mu} \\ -\nabla_{\omega} L_{2\mu} \\ -\nabla_{k_{F_i}} L_{2\mu} \end{bmatrix} \tag{3.137}$$

where

$$W = \begin{bmatrix} 0 & 0 & -\omega_{sl} & 0 & 0 \\ 0 & 0 & 0 & \omega_{su} & 0 \\ -\omega_{sl} & 0 & 0 & 0 & -\omega_x \nabla_x^2 h \\ 0 & \omega_{su} & 0 & 0 & -\omega_x \nabla_x^2 h \\ 0 & 0 & -\omega_x \nabla_x^2 h & -\omega_x \nabla_x^2 h & K \end{bmatrix},$$

$$K = \begin{bmatrix} K_{xx} & K_{\lambda x} & 0 \\ K^T_{\lambda x} & -\omega_\Psi \nabla^2_\lambda \Psi & -\omega_\Psi \nabla_{Pd} \nabla_\lambda \Psi \\ 0 & -\omega_\Psi \nabla_{Pd} \nabla_\lambda \Psi & -\omega_\Psi \nabla^2_{Pd} \Psi \end{bmatrix},$$

$$K_{xx} = -\nabla_x^2 \Pi_F - \omega_x \lambda \nabla_x^3 \Delta G - \omega_x (\pi l + \pi u) \nabla_x^3 h - \omega_\lambda \nabla_x^2 \Delta G - (\omega_{\pi l} + \omega_{\pi u}) \nabla_x^2 h,$$

$$K_{\lambda x} = -\omega_x \nabla_x^2 \Delta G - \nabla_\lambda \nabla_x \Pi_F,$$

$$U = \begin{bmatrix} -\pi l & 0 & I & 0 & 0 \\ 0 & \pi u & 0 & -I & 0 \\ -sl & 0 & 0 & 0 & -\nabla_x h \\ 0 & su & 0 & 0 & -\nabla_x h \\ 0 & 0 & -\nabla_x h & -\nabla_x h & H \end{bmatrix},$$

$$H = \begin{bmatrix} H_{xx} & H_{\lambda x} & 0 \\ H_{\lambda x}^T & 0 & -\nabla_\lambda \Psi \\ 0 & -\nabla_{Pd} \Delta G & -\nabla_{Pd} \Psi \end{bmatrix},$$

$$H_{xx} = -\nabla_x^2 \Pi_{ISO} - \lambda \nabla_x^2 \Delta G - (\pi l + \pi u) \nabla_x^2 h,$$

$$H_{\lambda x} = -\nabla_x \Delta G,$$

$$G = [P, Q]^T,$$

$$\lambda = [\lambda p, \lambda q]^T.$$

The primal and dual variables are represented by x_p and x_d respectively, and the $H_{k_{F_i}}$ terms are the contributions of the bidding factor k_{F_i}. In order to reduce the computational effort of the algorithm during the iterative procedure, the slack and dual variables associated with the bidding parameter k_{F_i}, which are contained into the $H_{k_{F_i}}$ sub-matrices, have been eliminated from the Newton step vector using Gaussian elimination, as proposed in [190] and applied in the formulation of the nonlinear primal-dual interior point OPF in [177] and [165].

For the elimination of the slack variables $\Delta sl_{k_{F_i}}$ and $\Delta su_{k_{F_i}}$ from the Newton step vector, equations (3.135) and (3.136) are rewritten with respect to their Δ-terms, such that:

$$\Delta sl_{k_{F_i}} = [\nabla_{sl_{k_{F_i}}} L_{2\mu} - sl_{k_{F_i}} \Delta \pi l_{k_{F_i}}] / \pi l_{k_{F_i}} \quad (3.138)$$

$$\Delta su_{k_{F_i}} = [-\nabla_{su_{k_{F_i}}} L_{2\mu} - su_{k_{F_i}} \Delta \pi u_{k_{F_i}}] / \pi u_{k_{F_i}} \quad (3.139).$$

These equations are then substituted into the linearized equations for the dual variables of the bidding parameter (3.133) and (3.134), such that:

$$-\nabla_{\pi l_{k_{F_i}}} L_{2\mu} = -\Delta k_{F_i} + [\nabla_{sl_{k_{F_i}}} L_{2\mu} - sl_{k_{F_i}} \Delta \pi l_{k_{F_i}}] / \pi l_{k_{F_i}} \tag{3.140}$$

$$-\nabla_{\pi u_{k_{F_i}}} L_{2\mu} = -\Delta k_{F_i} + [\nabla_{su_{k_{F_i}}} L_{2\mu} + su_{k_{F_i}} \Delta \pi u_{k_{F_i}}] / \pi u_{k_{F_i}} \tag{3.141}.$$

By rearranging these equations and defining new expressions for the $-\nabla_{\pi l_{k_{F_i}}} L_{2\mu}$ and $-\nabla_{\pi u_{k_{F_i}}} L_{2\mu}$ terms from the right-hand vector in the Newton matrix equation (3.137) denoted by '*':

$$[-\nabla_{\pi l_{k_{F_i}}} L_{2\mu}]^* = -\Delta k_{F_i} - sl_{k_{F_i}} \Delta \pi l_{k_{F_i}} / \pi l_{k_{F_i}} \tag{3.142}$$

$$[-\nabla_{\pi u_{k_{F_i}}} L_{2\mu}]^* = -\Delta k_{F_i} + su_{k_{F_i}} \Delta \pi u_{k_{F_i}} / \pi u_{k_{F_i}} \tag{3.143}$$

where the revised right-hand parts in (3.142)-(3.143) are equal to:

$$[-\nabla_{\pi l_{k_{F_i}}} L_{2\mu}]^* = -\nabla_{\pi l_{k_{F_i}}} L_{2\mu} - \nabla_{sl_{k_{F_i}}} L_{2\mu} / \pi l_{k_{F_i}} \tag{3.144}$$

$$[-\nabla_{\pi u_{k_{F_i}}} L_{2\mu}]^* = -\nabla_{\pi u_{k_{F_i}}} L_{2\mu} - \nabla_{su_{k_{F_i}}} L_{2\mu} / \pi u_{k_{F_i}} \tag{3.145}.$$

By this elimination of the right-hand parts that correspond to equations (3.135) and (3.136) from the Newton matrix equation, there will be less computational effort for each iteration. After the solution of the reduced Newton equation, the values for $\Delta sl_{k_{F_i}}$ and $\Delta su_{k_{F_i}}$ can be retrieved using (3.138) and (3.139).

The same procedure is applied to eliminate the Newton step terms $\Delta \pi l_{k_{F_i}}$ and $\Delta \pi u_{k_{F_i}}$ associated with the dual variables. To do so, rearrange equations (3.142) and (3.143), such that:

$$\Delta \pi l_{k_{F_i}} = \{-[-\nabla_{\pi l_{k_{F_i}}} L_{2\mu}]^* - \Delta k_{F_i}\} \pi l_{k_{F_i}} / sl_{k_{F_i}} \tag{3.146}$$

$$\Delta \pi u_{k_{F_i}} = \{-[-\nabla_{\pi u_{k_{F_i}}} L_{2\mu}]^* + \Delta k_{F_i}\} \pi u_{k_{F_i}} / su_{k_{F_i}} \tag{3.147}.$$

By substituting these equations into (3.132) and defining a revised right-hand term for the linearized equation of the bidding parameter k_{F_i}:

$$\begin{aligned}[-\nabla_{k_{F_i}} L_{2\mu}]^* = &\{-\sum \nabla_{k_{F_i}} \nabla_x^2 \omega_x \Pi_{ISO}\} \cdot \Delta x + \{-\sum \nabla_{k_{F_i}} \nabla_x \Pi_{ISO}\} \cdot \Delta \omega_x \\ &+ [(\pi l_{k_{F_i}} / sl_{k_{F_i}}) - (\pi u_{k_{F_i}} / su_{k_{F_i}})] \Delta k_{F_i}\end{aligned} \tag{3.148}$$

where the revised right-hand part for the k_{F_i} term is:

$$[-\nabla_{k_{F_i}} L_{2\mu}]^* = -\nabla_{k_{F_i}} L_{2\mu} - [-\nabla_{\pi l_{k_{F_i}}} L_{2\mu}]^* \pi l_{k_{F_i}} / sl_{k_{F_i}} + [-\nabla_{\pi u_{k_{F_i}}} L_{2\mu}]^* \pi u_{k_{F_i}} / su_{k_{F_i}} \tag{3.149}$$

which is the actual right-hand term for k_{F_i} that appears in the final form of the Newton equation in (3.137).

By observing equation (3.148) it can be seen that there are three elements, associated with the bidding parameter k_{F_i}, remaining in the Newton matrix after the elimination. These elements are the nonzero entries in the resulting $H_{k_{F_i}}$ sub-matrices that correspond to the rows of ΔPg, $\Delta\omega_{Pg}$ and Δk_{F_i} of the Newton step vector, such that:

$$H_{k_{F_i}1} = -\sum \nabla_{k_{F_i}} \nabla^2_{Pg} \omega_{Pg} \Pi_{ISO} = \beta_i \omega_{Pg_i} \tag{3.150}$$

$$H_{k_{F_i}2} = -\sum \nabla_{k_{F_i}} \nabla_{Pg} \Pi_{ISO} = \alpha_i + \beta_i Pg_i \tag{3.151}$$

$$H_{k_F 3} = (\pi l_{k_{F_i}} / sl_{k_{F_i}}) - (\pi u_{k_{F_i}} / su_{k_{F_i}}) \tag{3.152}.$$

In order to further improve the computational efficiency of the implemented algorithm, sparse matrix techniques are applied for the arrangement of the individual elements in the Newton matrix (3.137). The desirable configuration of the Newton matrix, expected to be very efficient, requires the majority of its elements to attain the same sparse matrix structure as that of the admittance matrix used in the conventional Newton power flow [190]. In order to preserve the sparsity of the structure, the matrix elements that correspond to the bus and branch variables are rearranged into a 4 by 4 block structure, with each block corresponding to a particular bus or branch. The typical arrangement of the elements in the symmetrical *K* matrix and the *H* matrix from (3.137) are as shown:

$$K = \left[\begin{array}{ccc|ccc|ccc|ccc}
Kt_it_i & Kt_ie_i & Kt_if_i & -\omega_x\nabla_{t_i}\nabla_x\Delta P_i & -\omega_x\nabla_{t_i}\nabla_x\Delta Q_i & Kt_ie_j & Kt_if_j & -\omega_x\nabla_{t_i}\nabla_x\Delta P_j & -\omega_x\nabla_{t_i}\nabla_x\Delta Q_j & 0 & 0 & 0 \\
 & Ke_ie_i & Ke_if_i & -\omega_x\nabla_{e_i}\nabla_x\Delta P_i & -\omega_x\nabla_{e_i}\nabla_x\Delta Q_i & Ke_ie_j & Ke_if_j & -\omega_x\nabla_{e_i}\nabla_x\Delta P_j & -\omega_x\nabla_{e_i}\nabla_x\Delta Q_j & 0 & 0 & 0 \\
 & & Kf_if_i & -\omega_x\nabla_{f_i}\nabla_x\Delta P_i & -\omega_x\nabla_{f_i}\nabla_x\Delta Q_i & Kf_ie_j & Kf_if_j & -\omega_x\nabla_{f_i}\nabla_x\Delta P_j & -\omega_x\nabla_{f_i}\nabla_x\Delta Q_j & 0 & 0 & 0 \\
 & & & -\omega_\phi\nabla^2_{\lambda p_i}\Psi & -\omega_\phi\nabla_{\lambda p_i}\nabla_{\lambda q_i}\Psi & -\omega_x\nabla_{e_j}\nabla_x\Delta P_i & -\omega_x\nabla_{f_j}\nabla_x\Delta P_i & 0 & 0 & -\nabla_{Pg}\nabla_{\lambda p}\Pi_F & 0 & -\omega_\phi\nabla_{\lambda p}\nabla_{Pd}\Psi \\
 & & & & -\omega_\phi\nabla^2_{\lambda q_i}\Psi & -\omega_x\nabla_{e_j}\nabla_x\Delta Q_i & -\omega_x\nabla_{f_j}\nabla_x\Delta Q_i & 0 & 0 & 0 & 0 & -\omega_\phi\nabla_{\lambda q}\nabla_{Pd}\Psi \\
\hline
 & & & & & Ke_je_j & Ke_jf_j & -\omega_x\nabla_{e_j}\nabla_x\Delta P_j & -\omega_x\nabla_{e_j}\nabla_x\Delta Q_j & 0 & 0 & 0 \\
 & & & & & & Kf_jf_j & -\omega_x\nabla_{f_j}\nabla_x\Delta P_j & -\omega_x\nabla_{f_j}\nabla_x\Delta Q_j & 0 & 0 & 0 \\
 & & & & & & & -\omega_\phi\nabla^2_{\lambda p_j}\Psi & -\omega_\phi\nabla_{\lambda p_j}\nabla_{\lambda q_j}\Psi & 0 & 0 & 0 \\
 & & & & & & & & -\omega_\phi\nabla^2_{\lambda p_j}\Psi & 0 & 0 & 0 \\
\hline
 & & & & & & & & & K_{PgPg} & 0 & 0 \\
 & & & & & & & & & & K_{QgQg} & 0 \\
 & & & & & & & & & & & -\omega_\phi\nabla^2_{Pd}\Psi
\end{array}\right] \tag{3.153}$$

$$
H = \left[\begin{array}{ccccc|ccccc|ccc}
Ht_it_i & Hte_i & Htf_i & -\nabla_t\Delta P_i & -\nabla_t\Delta Q_i & Ht_ie_j & Ht_if_j & -\nabla_{t_j}\Delta P_j & -\nabla_{t_j}\Delta Q_j & 0 & 0 & 0 \\
He_it_i & He_ie_i & He_if_i & -\nabla_{e_i}\Delta P_i & -\nabla_{e_i}\Delta Q_i & He_ie_j & He_if_j & -\nabla_{e_i}\Delta P_j & -\nabla_{e_i}\Delta Q_j & 0 & 0 & 0 \\
Hf_it_i & Hf_ie_i & Hf_if_i & -\nabla_{f_i}\Delta P_i & -\nabla_{f_i}\Delta Q_i & Hf_ie_j & Hf_if_j & -\nabla_{f_i}\Delta P_j & -\nabla_{f_i}\Delta Q_j & 0 & 0 & 0 \\
-\nabla_{t_i}\Delta P_i & -\nabla_{e_i}\Delta P_i & -\nabla_{f_i}\Delta P_i & 0 & 0 & -\nabla_{e_j}\Delta P_i & -\nabla_{f_j}\Delta P_i & 0 & 0 & -\nabla_{Pg}\Delta P & 0 & -\nabla_{\lambda p}\Psi \\
-\nabla_{t_i}\Delta Q_i & -\nabla_{e_i}\Delta Q_i & -\nabla_{f_i}\Delta Q_i & 0 & 0 & -\nabla_{e_j}\Delta Q_i & -\nabla_{f_j}\Delta Q_i & 0 & 0 & 0 & -\nabla_{Qg}\Delta Q & -\nabla_{\lambda q}\Psi \\
\hline
He_jt_i & He_je_i & He_jf_i & -\nabla_{e_j}\Delta P_i & -\nabla_{e_j}\Delta Q_i & He_je_j & He_jf_j & -\nabla_{e_j}\Delta P_j & -\nabla_{e_j}\Delta Q_j & 0 & 0 & 0 \\
Hf_jt_i & Hf_je_i & Hf_jf_i & -\nabla_{f_j}\Delta P_i & -\nabla_{f_j}\Delta Q_i & Hf_je_j & Hf_jf_j & -\nabla_{f_j}\Delta P_j & -\nabla_{f_j}\Delta Q_j & 0 & 0 & 0 \\
-\nabla_{t_i}\Delta P_j & -\nabla_{e_i}\Delta P_j & -\nabla_{f_i}\Delta P_j & 0 & 0 & -\nabla_{e_j}\Delta P_j & -\nabla_{f_j}\Delta P_j & 0 & 0 & 0 & 0 & 0 \\
-\nabla_{t_i}\Delta Q_j & -\nabla_{e_i}\Delta Q_j & -\nabla_{f_i}\Delta Q_j & 0 & 0 & -\nabla_{e_j}\Delta Q_j & -\nabla_{f_j}\Delta Q_j & 0 & 0 & 0 & 0 & 0 \\
\hline
0 & 0 & 0 & -\nabla_{Pg}\Delta P & 0 & 0 & 0 & 0 & 0 & H_{PgPg} & 0 & 0 \\
0 & 0 & 0 & 0 & -\nabla_{Qg}\Delta Q & 0 & 0 & 0 & 0 & 0 & H_{QgQg} & 0 \\
0 & 0 & 0 & -\nabla_{Pd}\Delta P & -\nabla_{Pd}\Delta Q & 0 & 0 & 0 & 0 & 0 & 0 & -\nabla_{Pd}\Psi
\end{array}\right]
\tag{3.154}
$$

The diagonal blocks in the *K* and *H* matrices correspond to the bus elements, and the off-diagonal blocks that contain the subscripts *i-j* to the branch elements. For each sub-matrix, the transformer elements were assigned positions adjacent to the group of these bus and branch blocks on the upper row and left column, while the generation and load elements were positioned on the lower row and right column, as shown. The rest of the elements in the *W* and *U* sub-matrices in (3.137) are diagonal matrices that contain the elements associated with the slack and dual variables of the inequality constraints. The three H_{k_F} vectors in (3.137) contain the three elements from (3.148) that result from the elimination of the slack and dual variables associated with k_{F_i}. The aforementioned sparse matrix techniques that are applied on the Newton matrix enhance the performance of the algorithm and thus reduce the computational effort needed to reach the solution of the problem.

3.10 Implementation issues for the primal-dual interior point algorithm

In order to obtain the solution for the SFE market problem, the Newton matrix (3.137) is solved iteratively by the primal-dual interior point algorithm. The flow chart for the solution procedure of the algorithm is presented in Figure 9.

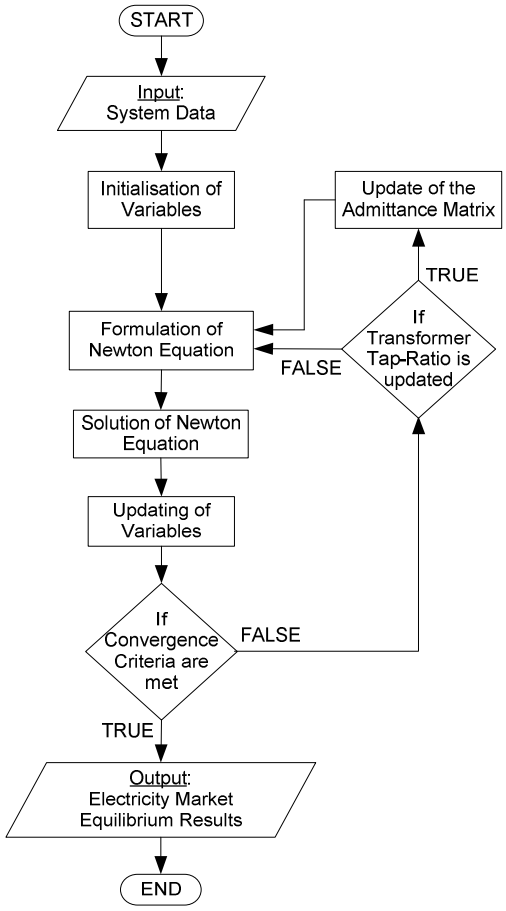

Figure 9: Flowchart of the solution procedure for the SFE algorithm.

The only requirement for the initialisation of the variables in order to initiate the iterative process is to assign values to the variables that are interior to the bound constraints. Hence, the initialisation values are chosen as follows:

- the voltage initial conditions are set for a flat start,
- the generation variables Pg_{F_i} and Qg_{F_i} are set to the average values between their maximum and minimum limits,
- the transformer tap-ratios t_i are set to 1,
- the bidding parameters k_{F_i} are set to 1,
- the slack variables sl_n and su_n are set to $(h_n - h_n^{\min})$ and $(h_n^{\max} - h_n)$ respectively,
- the dual variables πl_n and πu_n are set to μ / sl_n and $-\mu / su_n$ respectively,
- the dual variables λp_i and λq_i are set to $MC_{Pg_{F_i}}$ and zero respectively,
- all the auxiliary dual variables ω are set equal to zero.

After choosing initial values for the system variables, the algorithm obtains values for the Δ-terms in the Newton step vector from (3.137) for each iteration, and the primal and dual variables are updated by using modified versions of expression (3.17) that include step-length parameters. These parameters, also called step-sizes, are incorporated in the formulation in order to control the Newton step, and hence the speed and convergence capabilities of the algorithmic procedure, in order to avoid divergence problems or slow iterative processes. Furthermore, the step-lengths can be multiplied by a factor that is slightly less than 1, in order to prevent them from hitting their boundary. Therefore, the update of the primal and dual variables, x_p and x_d respectively, is based on the following expressions:

$$x_p^{(k+1)} = x_p^{(k)} + \sigma\alpha_p \Delta x_p \tag{3.155}$$

$$x_d^{(k+1)} = x_d^{(k)} + \sigma\alpha_d \Delta x_d \tag{3.156}$$

where α_p and α_d are the primal and dual step-lengths parameters respectively, the factor σ is in the domain [0.995 – 0.99995], and k is the iteration count. The step-lengths are determined based on the values of the slack and dual variables and their associated Newton step elements, as follows:

$$\alpha_p = \min[\ \min(-sl / \Delta sl), \min(-su / \Delta su), 1\ ] \tag{3.157}$$

$$\alpha_d = \min[\ \min(-\pi l / \Delta \pi l), \min(-\pi u / \Delta \pi u), 1\ ] \tag{3.158}$$

for those $\Delta sl < 0$, $\Delta su < 0$, $\Delta \pi l < 0$ and $\Delta \pi u > 0$.

The error function in the analysis of the primal-dual interior point method can be defined as the complementary gap *Cgap*, which represents the difference between the primal and dual objective functions [178]. This gap must be zero at the optimum solution and it can be determined for each iteration by:

$$Cgap = \sum_n (sl_n \pi l_n - su_n \pi u_n) \tag{3.159}.$$

The relationship between the complementary gap and the barrier parameter is implicit in the KKT condition equations associated with the slack and dual variables (3.99)-(3.102), (3.112)-(3.115). Hence, the barrier parameter μ that was introduced with the slack variables in the objective function of the original optimisation problem can be reduced based on a predicted decrease of the

complementary gap [165]. Therefore, for each iteration, the barrier parameter can be evaluated by:

$$\mu = \frac{\beta}{M} Cgap \tag{3.160}$$

where β is the centering parameter chosen from the domain [0.01 – 0.2], and M is the number of single-sided inequalities in the system constraints. The centering parameter β represents the expected cut in the complementary gap for the next iteration and it is used to manipulate the direction of the Newton step in order to improve the centrality of the solution within the interior of the constraints' boundaries.

The break point for the algorithm convergence is defined by specified tolerances imposed on the levels of the power mismatches (3.55)-(3.56) and the complementary gap (3.159), which in turn reduces the barrier parameter μ as in (3.160). The tolerances used for the work in this Thesis were set to 5×10^{-4} for the reduction of the complementary gap and to 1×10^{-4} p.u. for minimisation of the absolute bus active and reactive power mismatch equations. When the gap and the power mismatches become less than the specified tolerances as the iterative process progresses, the algorithm converges to the optimum solution for the market problem that is a Nash equilibrium point.

3.11 Conclusions for Chapter 3

This chapter has provided a layout of the work presented in this Thesis and has described in detail the methodology employed for the implementation of the electricity market SFE algorithm. The reasons for choosing the linear SFE model over the other oligopolistic equilibrium methods have been explained, while the advantages of employing the AC model for the power network over the linearized DC approach have been outlined. The electricity market algorithm has been implemented using the nonlinear primal-dual interior point method, which is able to accommodate the bi-level market problem and deal with the mathematical complexity involved, in order to enhance the computational efficiency of the model. The detailed mathematical formulation of the market problem, which incorporates the AC power flow representation for meshed

networks, has been presented along with the implementation issues of the interior point algorithm.

By incorporating several AC network features in the market model, the accuracy and realism of the acquired market predictions have been enhanced, enabling the investigation in the subsequent chapters of this Thesis of the impact of individual network constraints and system operational conditions on the electricity market equilibrium for non-trivial systems. The contributions of the work presented in this Thesis include, apart of investigations of several market conditions under AC modelling, aspects of research on the electricity market equilibrium that have not been addressed in the literature so far, such as the representation of on-load tap-changing transformers and grid-connected PV systems.

Chapter 4:
The impact of transformer tap-ratio control on the electricity market equilibrium

4.1 Introduction to transformer control

Transformer components serve as the link between generators and transmission lines in a power system, as well as between lines of different voltage levels. A transformer can regulate the voltage between the network buses and control the flow of active and reactive power in the system [202]. In the case where voltage adjustments are required under varying load conditions, on-load tap-changing transformer arrangements are applicable. The tapping arrangement of the transformer windings provides the necessary voltage regulation without interrupting the service by detecting voltage or reactive power variations across and through the transformer. An automatic tap-changing operation is initiated by small adjustments on the turns ratio to result in the desired voltage levels and facilitate the varying system conditions [203,204].

In the case of the electricity market operation, the system operator may utilise the function of such regulating transformer mechanisms to aid the social welfare maximisation process. Since the levels of the voltages across the system dictate whether there is transmission congestion present or not, and the firms' strategies and market prices are affected by network congestion, the application of on-load tap-changing transformers can regulate the voltages and power flows in such a way that the market clearing price is reduced to a value close to the marginal cost of generation and the social welfare is maximised. Hence, the importance of the application of transformer tap-ratio control is not only associated with assisting the operation of the power system, but also with the facilitation of a proper function of the electricity market.

The optimal power flow study in [205] shows that the incorporation of transformer tap-ratio control in the network model and the representation of the transformer branch have a noticeable effect on the voltage and power flow profiles of the system. If modelling of the electricity market is considered, the omission of representing the transformer, in terms of power flows through the transformer branch and tap-ratio control, may have undesirable effects on the resulting market predictions with deviations from the real solution due to false evaluation of the voltage and power flow levels in the network. The incorporation of transformer modelling into the market model will result in a more realistic market solution, as it will account for the voltage and power flow adjustments expected to take place in practice.

The remainder of this chapter provides an advanced review of the mathematical formulation associated with the transformer modelling in the electricity market equilibrium analysis and an extensive study of the impact of transformer tap-ratio control on the electricity market equilibrium based on numerical results. The expressions provided for the mathematical formulation are determined by following the mathematical derivation of the Newton matrix outlined in Chapter 3, focusing only on the terms associated with the transformer modelling. The numerical results investigate cases with and without transformer tap-ratio control, while the interrelation of tap-ratio control and network congestion is analysed.

4.2 Modelling of the transformer control in the electricity market equilibrium analysis

Before illustrating the impact of transformer tap-ratio control on the electricity market equilibrium by numerical results, the contribution of the transformer formulation to the electricity market equilibrium model is reviewed. From equations (3.137) and (3.153)-(3.154), the contribution of the incorporation of the transformer formulation in the primal-dual interior point algorithm to the Newton matrix, is twofold. Elements associated with the transformer component accruing from modelling the power transmission and losses of the transformer

branches, which incorporate the tap-ratio factor, appear in the bus and branch blocks K_{xx}, $K_{\lambda x}$, H_{xx}, $H_{\lambda x}$ in the K and H sub-matrices (see (3.137)). The transformer elements that result from inequality (3.61) for the modelling of the transformer tap-ratio control appear in the diagonal matrix elements associated with the slack and dual variables sl, su, πl, πu, ω_{sl}, ω_{su}, $\omega_{\pi l}$, $\omega_{\pi u}$ (the identity matrix elements for the latter two), and in the $[-\nabla_x h]$ blocks, in sub-matrices W and U in (3.137). These contributions can be clearly seen by isolating the transformer-related parts of the Lagrange function $L_{2\mu}$ for the combined market problem (3.94) and of the resulting linearized KKT condition equations that constitute the Newton matrix. The part of the Lagrange function for the transformer contribution is:

$$\begin{aligned} L_{2\mu}^{TR} = \omega_t[-\sum_{i=1}^{NT}\nabla_t \Delta P_i^{TR}\lambda p_i - \sum_{i=1}^{NT}\nabla_t \Delta Q_i^{TR}\lambda q_i - (\pi l_t + \pi u_t)\nabla_t h_t] \\ + \sum_{i=1}^{NT}\omega_{\lambda p_i}[-\Delta P_i^{TR}] + \sum_{i=1}^{NT}\omega_{\lambda q_i}[-\Delta Q_i^{TR}] \\ + \omega_{sl_t}[\mu - sl_t \pi l_t] + \omega_{su_t}[\mu + su_t \pi u_t] \\ - \omega_{\pi l_t}[h_t - sl_t - h_t^{\min}] - \omega_{\pi u_t}[h_t + su_t - h_t^{\max}] \end{aligned} \quad (4.1)$$

where NT is the number of transformers in the system, and ΔP_i^{TR} and ΔQ_i^{TR} are the parts of the active and reactive power mismatch equations (3.55)-(3.56) associated with the transformer branch power flows, given by $\Delta P_i^{TR} = -\sum_j P_{ij}^{TR}$ and $\Delta Q_i^{TR} = -\sum_j Q_{ij}^{TR}$, which can be derived using (3.38) and (3.41). Only these power flow terms are shown here, since the formulation presented corresponds only to the contribution from modelling the transformer component.

The parts of the linearized KKT equations (3.116)-(3.131) that result from the transformer branch modelling are:

- from (3.116): $$-\nabla_t L_{2\mu} = -[\sum \omega_x \lambda p_i \nabla_t \nabla_x^2 \Delta P_i^{TR} + \sum \omega_x \lambda q_i \nabla_t \nabla_x^2 \Delta Q_i^{TR} + \sum \omega_{\lambda p_i} \nabla_t \nabla_x \Delta P_i^{TR} + \sum \omega_{\lambda q_i} \nabla_t \nabla_x \Delta Q_i^{TR}]\Delta x - \sum \omega_x \nabla_t \nabla_x \Delta P_i^{TR} \Delta\lambda p_i - \sum \omega_x \nabla_t \nabla_x \Delta Q_i^{TR} \Delta\lambda q_i - [\sum \lambda p_i \nabla_t \nabla_x \Delta P_i^{TR} + \sum \lambda q_i \nabla_t \nabla_x \Delta Q_i^{TR}]\Delta\omega_x - \sum \nabla_t \Delta P_i^{TR} \Delta\omega_{\lambda p_i} - \sum \nabla_t \Delta Q_i^{TR} \Delta\omega_{\lambda q_i} - \nabla_t h_t \Delta\omega_{\pi l_t} - \nabla_t h_t \Delta\omega_{\pi u_t}$$ (4.2)

$$-\nabla_x L_{2\mu} = -[\sum \omega_t \lambda p_i \nabla_t \nabla_x^2 \Delta P_i^{TR} + \sum \omega_t \lambda q_i \nabla_t \nabla_x^2 \Delta Q_i^{TR}]\Delta x - \sum \omega_t \nabla_t \nabla_x \Delta P_i^{TR} \Delta\lambda p_i - \sum \omega_t \nabla_t \nabla_x \Delta Q_i^{TR} \Delta\lambda q_i$$ (4.3)

- from (3.118): $$-\nabla_{\lambda p_i} L_{2\mu} = -\sum \omega_t \nabla_t \nabla_x \Delta P_i^{TR} \Delta x - \sum \nabla_t \Delta P_i^{TR} \Delta\omega_t$$ (4.4)

- from (3.119): $$-\nabla_{\lambda q_i} L_{2\mu} = -\sum \omega_t \nabla_t \nabla_x \Delta Q_i^{TR} \Delta x - \sum \nabla_t \Delta Q_i^{TR} \Delta\omega_t$$ (4.5)

- from (3.124): $$-\nabla_{\omega_t} L_{2\mu} = -[\sum \lambda p_i \nabla_t \nabla_x \Delta P_i^{TR} + \sum \lambda q_i \nabla_t \nabla_x \Delta Q_i^{TR}]\Delta x - \sum \nabla_t \Delta P_i^{TR} \Delta\lambda p_i - \sum \nabla_t \Delta Q_i^{TR} \Delta\lambda q_i - \nabla_t h_t \Delta\pi l_t - \nabla_t h_t \Delta\pi u_t$$ (4.6)

- from (3.126): $$-\nabla_{\omega_{\lambda pi}} L_{2\mu} = -\sum \nabla_t \Delta P_i^{TR} \Delta t$$ (4.7)

- from (3.127): $$-\nabla_{\omega_{\lambda qi}} L_{2\mu} = -\sum \nabla_t \Delta Q_i^{TR} \Delta t$$ (4.8)

and those resulting from the modelling of the transformer tap-ratio control are:

- from (3.120): $$-\nabla_{\pi l_t} L_{2\mu} = -\omega_{sl_t} \Delta sl_t - \nabla_t h_t \Delta\omega_t - sl_t \Delta\omega_{sl_t}$$ (4.9)

- from (3.121): $$-\nabla_{\pi u_t} L_{2\mu} = \omega_{su_t} \Delta su_t - \nabla_t h_t \Delta\omega_t + su_t \Delta\omega_{su_t}$$ (4.10)

- from (3.122): $$-\nabla_{sl_t} L_{2\mu} = -\omega_{sl_t} \Delta\pi l_t + \Delta\omega_{\pi l_t} - \pi l_t \Delta\omega_{sl_t}$$ (4.11)

- from (3.123): $$-\nabla_{su_t} L_{2\mu} = \omega_{su_t} \Delta\pi u_t - \Delta\omega_{\pi u_t} + \pi u_t \Delta\omega_{su_t}$$ (4.12)

- from (3.128): $$-\nabla_{\omega_{\pi l_t}} L_{2\mu} = -\nabla_t h_t \Delta t + \Delta sl_t$$ (4.13)

- from (3.129): $$-\nabla_{\omega_{\pi u_t}} L_{2\mu} = -\nabla_t h_t \Delta t - \Delta su_t$$ (4.14)

- from (3.130): $$-\nabla_{\omega_{sl_t}} L_{2\mu} = -sl_t \Delta\pi l_t - \pi l_t \Delta sl_t$$ (4.15)

- from (3.131): $$-\nabla_{\omega_{su_t}} L_{2\mu} = su_t \Delta\pi u_t + \pi u_t \Delta su_t$$ (4.16).

Note that the transformer contribution extends to K_{xx} and $K_{\lambda x}$ elements other than the K_{xt} and $K_{\lambda t}$, i.e. outside the first row and column of the K matrix (3.153), as can be seen from (4.3)-(4.5). This is owing to the fact that all the bus variables (e, f, λp, λq) are associated with the transmission flows through the transformer branches. By observing the $-\nabla L_{2\mu}$ and Δ-terms of equations (4.2)-(4.16), the individual elements of the Newton matrix equation (3.137) that result from the transformer contribution can be derived. These elements are presented in Appendix I and the evaluation of their derivative terms is given in Appendix II.

The 3rd order derivative terms contained in the K matrix from expressions (4.2)-(4.3) stem from the bi-level nature of the market equilibrium problem. Such terms would have not been encountered in a primal-dual interior point OPF formulation that incorporates only a single objective function. This holds for the transmission line modelling as well. The appearance of the K matrix, which corresponds to the ISO KKT system that was incorporated into the firms' optimisation problem, results in twice as many Newton matrix elements for the model, which are also of higher complexity, compared to a typical OPF problem.

By similar considerations as for equations (4.2)-(4.8), the contribution from modelling the transmission line power flows and losses can be obtained using the linearized KKT equations (3.116)-(3.131). Furthermore, the Newton matrix elements that result from the other network inequality constraints (3.57)-(3.60) can be straightforwardly acquired in a similar manner as (4.9)-(4.16). The contribution for the MVA transmission constraint (3.57), which is a complex functional inequality, requires more computations than the other constraints in order to calculate the associated 2nd and 3rd order derivative terms.

4.3 Introduction to the analysis of the impact of transformer tap-ratio control on the electricity market equilibrium

Several test cases were performed for the investigation of the effects from optimising the transformer tap-ratio on the electricity market outcome, using the primal-dual interior point algorithm that utilises the k_F-parameterization for the

linear SFE formulation. The subsequent sections provide numerical tests on a 5-bus and the IEEE 30-bus systems. Each transformer in the test systems is assumed to be equipped with an on-load tap-changing mechanism that allows the tap-ratio setting to take values between specified limits. Cases that correspond to different operating aspects that involve binding limits on power generation and transmission power flows are examined for two different tap-ratio control modes. The first mode corresponds to a fixed tap-ratio at the value of 1.0 for all transformers in the system. For the second mode, the values of the tap-ratios are optimised within a ±10% interval from the value of 1.0. i.e. in the domain 0.9 to 1.1. The limits for the bidding parameter k_F were set to $k_F^{\min} = 0$ and $k_F^{\max} = 10$ as in [134]. The values for the tap-ratios presented correspond to κ, as defined in (3.30). The results for the social welfare correspond to the true social welfare as in (2.9) and not the quasi function from (3.54). All the power quantities are calculated using the per-unit (p.u.) measuring system. The results for the equilibrium market outcome with discussions for each case are given below.

4.4 Numerical results on the 5-bus test system

The 5-bus test system used for Cases 1 to 8 outlined in this section consists of 5 buses with load demand, which are interconnected together with a series of 3 transmission lines and 2 transformer branches TR1 and TR2, and 2 generating units, as shown in Figure 10. The transmission lines and the transformers have impedances equal to $z = 1/y_t = (0.01 + j0.1)$ p.u. The generating unit connected to bus 1 is owned by generating firm F_1 and that at bus 2 by generating firm F_2. The marginal cost of generation at buses 1 and 2 are taken to be $MC_{Pg_1} = 11.0 + 0.009Pg_1$ £/MWh and $MC_{Pg_2} = 10.8 + 0.010Pg_2$ £/MWh respectively. The linear inverse load demand functions are equal at all buses, being $D_{Pd_i} = 40 - 0.060Pd_i$ £/MWh. (Note that the linear inverse load demand function from this point onwards will be indicated by D_{Pd} rather than MD.) The load power factor of the system is set to 0.90 to simulate normal operating conditions. The results for test Cases 1 to 8 are presented in Tables 4.1 and 4.2. Table 4.1 shows the values of nodal prices, bidding parameters k_{F_i}, firms'

profits, and social welfare, while the network parameters are presented in Table 4.2.

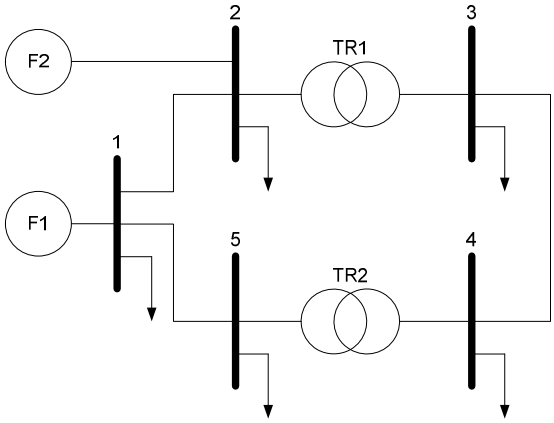

Figure 10: The 5-bus test system.

TABLE 4.1
CASES 1 TO 8 FOR THE 5-BUS TEST SYSTEM:
NODAL PRICES, BIDDING PARAMETERS, FIRMS' PROFITS AND SOCIAL WELFARE

Case No.	Active Constraint	Transformer Tap-Ratio Control Mode	Nodal Prices λp_i (£/MWh)					Bidding Strategies		Generating Firm's Profit (£/hour)		Social Welfare (£/hour)
			λp_1	λp_2	λp_3	λp_4	λp_5	k_{F1}	k_{F2}	F_1	F_2	
1	None	**Fixed**	**30.2**	**29.5**	**31.4**	**32.6**	**31.9**	**2.416**	**1.959**	**3085**	**7057**	**13640**
2		**±10%**	**31.0**	**30.2**	**31.7**	**32.7**	**32.4**	**2.481**	**1.923**	**3175**	**8357**	**14820**
3	$Pg_2^{\max} = 4.0$ p.u.	**Fixed**	**31.3**	**30.7**	**32.3**	**33.3**	**32.7**	**2.536**	**1.608**	**2948**	**7141**	**12940**
4		**±10%**	**33.3**	**32.6**	**33.7**	**34.3**	**34.2**	**2.751**	**1.788**	**2662**	**7924**	**12460**
5	$S_{12}^{\max} = S_{15}^{\max} = 0.5$ p.u.	**Fixed**	**27.4**	**28.6**	**32.3**	**35.4**	**37.6**	**2.106**	**2.014**	**3430**	**5470**	**12650**
6		**±10%**	**26.9**	**31.0**	**34.6**	**37.9**	**41.1**	**1.944**	**2.449**	**4573**	**3580**	**11480**
7	$S_{TR1}^{\max} = 0.25$ p.u.	**Fixed**	**29.6**	**25.8**	**41.8**	**38.1**	**34.1**	**2.246**	**1.928**	**4256**	**3548**	**11180**
8		**±10%**	**30.0**	**26.2**	**43.7**	**39.2**	**34.6**	**2.277**	**1.960**	**4369**	**3597**	**11230**

TABLE 4.2
CASES 1 TO 8 FOR THE 5-BUS TEST SYSTEM: SYSTEM PARAMETERS

Case No.	Active Constraint	Transformer Tap-Ratio Control Mode	Pg_1 (p.u.)	Pg_2 (p.u.)	Qg_1 (p.u.)	Qg_2 (p.u.)	$\sum Pd_i$ (p.u.)	$\sum Qd_i$ (p.u.)	Tap-Ratio	
									κ_1	κ_2
1	None	**Fixed**	**1.67**	**4.26**	**1.73**	**1.66**	**5.87**	**2.84**	**1.000**	**1.000**
2		**±10%**	**1.65**	**4.92**	**2.32**	**1.83**	**6.47**	**3.13**	**0.900**	**0.973**
3	$Pg_2^{\max} = 4.0$ p.u.	**Fixed**	**1.50**	**4.00**	**1.62**	**1.54**	**5.45**	**2.64**	**1.000**	**1.000**
4		**±10%**	**1.22**	**4.00**	**1.77**	**1.45**	**5.15**	**2.49**	**0.900**	**0.974**
5	$S_{12}^{\max} = S_{15}^{\max} = 0.5$ p.u.	**Fixed**	**2.23**	**3.40**	**0.85**	**2.11**	**5.60**	**2.71**	**1.000**	**1.000**
6		**±10%**	**3.16**	**1.86**	**1.17**	**1.45**	**4.99**	**2.42**	**0.900**	**1.020**
7	$S_{TR1}^{\max} = 0.25$ p.u.	**Fixed**	**2.43**	**2.59**	**1.53**	**0.98**	**5.01**	**2.42**	**1.000**	**1.000**
8		**±10%**	**2.44**	**2.55**	**1.40**	**1.11**	**4.98**	**2.41**	**1.100**	**1.030**

- ***Cases 1 and 2: No binding constraints*:**

The first two test cases have been examined in order to demonstrate the effect of transformer tap-ratio control on the electricity market equilibrium under normal operating conditions with no network congestion present. In Case 1 it is assumed that there is no tap-ratio control, in which the tap-ratio value is set to 1.0. In Case 2, the tap-ratio control is active and it can be seen in Table 4.2 that both tap-ratios are optimised to a value below 1.0, resulting in a large increase in production. Although the change in nodal prices between Cases 1 and 2 is small, the transformer tap-ratio control has produced a significant increase in the active and reactive power generation in Case 2. This resulted in larger profits for both firms, especially for firm F_2, even though it has decreased slightly its bidding parameter. Also, when the tap-ratio control is active, the load demand and the social welfare are increased.

- ***Cases 3 and 4: Generation capacity constraint*:**

This is another typical example which is considered in order to examine the effect of tap-ratio control in the presence of generation capacity constraints. Generation capacity limit has been imposed to the generating unit of firm F_2, such that $Pg_2^{\max} = 4.0\,\text{p.u.}$ and is binding for both Cases 3 and 4 as shown in Table 4.2. In Case 4, in which tap-ratio is optimised, higher bidding factors are observed for both firms when compared with Case 3 where tap-ratio control is inactive. This action results in higher nodal prices as can be seen in Table 4.1. Although firm F_2 has capacity availability limitation, the increase in nodal prices is sufficient in order to produce higher profits in Case 4. On the other hand, the increase in nodal prices is not sufficient to increase the profits of firm F_1, which withholds its capacity, thus there is lower profit for this firm at this time. From this example, it is concluded that the presence of tap-ratio control gives enough incentives to the strategic firms to exercise market power in a different way than in the uncontrolled case, resulting in a different market outcome.

- ***Cases 5 and 6: Transmission line capacity constraint*:**

Further cases were examined for investigating the impact of transformer tap-ratio control on the electricity market under stressed operating conditions in the power

network. In order to do so, the transmission capacity limits of the lines between buses 1-2 and 1-5 were set to $S_{12}^{\max} = S_{15}^{\max} = 0.5\,\text{p.u.}$ and are binding for both cases. When operating the system at these extreme conditions, the impact of transformer tap-ratio control on the electricity market is more intense. In Case 6, in which the tap-ratio control is optimised, the bidding factors k_{F_i} of both firms have been altered significantly resulting in a considerable variation in the nodal prices, if compared with Case 5 where the tap-ratio is fixed to 1.0. The nodal prices at buses 2, 3, 4 and 5 are significantly increased, whilst the nodal price at bus 1 is slightly decreased. This variation of nodal prices resulted in lower social welfare in Case 6 compared with Case 5.

In Case 6, the presence of transformer tap-ratio control has given enough incentives to the generating firms to change their bidding strategies. Firm F_1 has decreased its bidding factor whilst firm F_2 has significantly increased its own. The generating unit of firm F_1 situated at bus 1 has submitted a lower bid and managed to generate an increased amount of active power, despite the fact that this generating unit is isolated due to transmission congestion from both sides. In Case 5, a large proportion of the demand at bus 1 is supplied by the unit at bus 2. In Case 6, since firm F_1 has submitted a lower bid, all the demand at bus 1 is supplied by its unit that is situated at bus 1. Hence, there is increased production of power for firm F_1 and subsequently higher profits. Note that in Case 6 the power flows from bus 1 to bus 2, unlike Case 5 where power flows from bus 2 to bus 1. On the other hand, this resulted in much lower generation for firm F_2, thus lower profits. By considering this example it is concluded that, from the preliminary results, the impact of transformer tap-ratio control on the electricity market outcome in the presence of binding network constraints is crucial.

- ***Cases 7 and 8: Transformer capacity constraint*:**

These test cases have been performed in order to examine the effect of tap-ratio control when the transformer power capacity is congested. The power capacity limit of transformer TR1 has been set equal to $S_{TR1}^{\max} = 0.25\,\text{p.u.}$ For Cases 7 and 8 for which the two different tap-ratio control modes are applied, the total

generation is at the same level, but the bidding factors k_{F_i} of both firms have been increased slightly resulting in higher nodal prices. Consequently, there is slightly larger profit for both firms. In Case 8, the values of tap-ratio for both transformers have been increased above the value of 1.0, while if compared with Case 2 in which there is no active constraint, the tap-ratio values have been decreased below 1.0. Thus, using this example it is found that the transformer tap-ratio adjustment has a significant impact on the market outcome, even when the generation is at the same levels for both the controlled and the uncontrolled case.

4.5 Numerical results on the IEEE 30-bus system

Further test cases were examined using the IEEE 30-bus system to show the effects of transformer tap-ratio control on larger systems. The IEEE 30-bus system consists of 30 buses, 37 transmission lines, 6 generators, 21 load demand nodes and 4 on-load tap-changing transformers. Diagrams for the IEEE test systems can be found in [191]. The generating units at buses 1, 2, 5, 8, 11 and 13 are owned by firms F_1 to F_6 respectively. For this system, two cases were examined. Similarly to the previous examples, in Case 9, the tap-ratio control is considered to be inactive, hence it is set to the fixed value of 1.0 for all transformers, whereas in Case 10 the values of tap-ratios are optimised within ±10% interval from the value of 1.0. The results for the bidding parameters k_{F_i}, firms' profits, power distribution in the network and social welfare are presented in Table 4.3. The results for the nodal prices λp_i for both Cases 9 and 10 are presented in Table 4.4 in adjacent columns allowing direct comparison of the price outcome for each bus. The firms situated at the generation buses are indicated in the first column of Table 4.4 within parentheses.

TABLE 4.3
CASES 9 TO 10 FOR THE IEEE 30-BUS SYSTEM:
BIDDING PARAMETERS, FIRMS' PROFITS, POWER DISTRIBUTION AND SOCIAL WELFARE

Case No.	Tap-Ratio Control Mode	Bidding Strategies						Generating Firm's Profit (£/hour)						$\sum Pg_i$ (p.u.)	$\sum Qg_i$ (p.u.)	$\sum Pd_i$ (p.u.)	$\sum Qd_i$ (p.u.)	Social Welfare (£/hour)
		k_{F1}	k_{F2}	k_{F3}	k_{F4}	k_{F5}	k_{F6}	F_1	F_2	F_3	F_4	F_5	F_6					
9	**Fixed**	**2.805**	**3.424**	**2.009**	**1.922**	**1.678**	**1.690**	**797**	**448**	**4825**	**1835**	**845**	**834**	**5.62**	**2.53**	**5.55**	**2.50**	**11990**
10	**±10%**	**2.618**	**1.274**	**2.011**	**1.881**	**1.667**	**1.622**	**1141**	**2218**	**4278**	**1781**	**703**	**722**	**6.80**	**3.20**	**6.71**	**3.01**	**13830**

TABLE 4.4
CASES 9 TO 10 FOR THE IEEE 30-BUS SYSTEM: COMPARISON OF NODAL PRICES (£/MWHOUR)

Bus No. (firm)	Case 9: Nodal Prices without Tap-Ratio Control	Case 10: Nodal Prices with ±10% Tap-Ratio Control
1 (F_1)	**35.9**	**34.0**
2 (F_2)	**35.8**	**33.8**
3	**37.5**	**36.3**
4	**37.5**	**36.4**
5 (F_3)	**30.4**	**29.9**
6	**37.5**	**36.4**
7	**38.3**	**37.2**
8 (F_4)	**35.5**	**34.7**
9	**37.2**	**36.3**
10	**38.0**	**37.3**
11 (F_5)	**36.2**	**35.8**
12	**37.7**	**37.0**
13 (F_6)	**36.4**	**34.9**
14	**38.9**	**38.5**
15	**38.8**	**38.3**
16	**38.5**	**38.0**
17	**38.4**	**37.8**
18	**39.2**	**38.9**
19	**39.2**	**38.9**
20	**39.1**	**38.7**
21	**38.4**	**37.7**
22	**38.3**	**37.7**
23	**39.0**	**38.5**
24	**38.7**	**38.1**
25	**38.2**	**37.5**
26	**38.8**	**38.2**
27	**37.7**	**36.9**
28	**37.2**	**36.3**
29	**39.1**	**38.6**
30	**39.3**	**39.0**

- ***Cases 9 and 10: Results for the larger system*:**

By observing the results of Cases 9 and 10 in Table 4.3, it can be seen that the bidding strategies k_{F_i} were significantly affected by the introduction of transformer tap-ratio control. For example, the value of k_{F_i} for the unit at bus 2

was reduced from 3.424 to 1.274. The total production and load demand levels were also affected. The active and reactive power generations in the system are increased when the tap-ratio is optimised, and, as a result, the nodal prices λp_i are reduced at all buses, up to decrements of 2.0 £/MWh. This results in a variation in the distribution of profits among the generating firms, affecting also the social welfare, which is favoured by the operation of the tap-ratio control. By comparing Cases 9 and 10 it is found that the transformer tap-ratio control significantly affects the market outcome in larger scale systems, so that it cannot be neglected from the electricity market equilibrium models.

4.6 Discussion on the impact of transformer tap-ratio control based on the numerical results of Cases 1 to 10

The presence of transformer tap-ratio control gives enough incentives to the strategic generating firms to exercise market power in a different way than the uncontrolled case, resulting in a different market outcome. The existence of tap-ratio control that causes the different strategic actions by the firms, results in a different market outcome in terms of nodal prices, profits and social welfare. In the presence of binding network constraints the impact of transformer tap-ratio control is more intense on the electricity market. Hence, from the preliminary results presented above, it is concluded that the incorporation of transformer tap-ratio control in the electricity market equilibrium models is necessary for achieving more realistic results. In order to do so, the implementation of the AC power flow model for the formulation of the electricity network is required. Since the tests presented above have shown that the effects of the transformer tap-ratio control are more intense when transmission congestion is present in the electricity network, further cases, for which the congestion is gradually increased, are performed on the 5-bus test system.

4.7 Investigation of the impact of transformer tap-ratio control in congested transmission networks

This section aims to demonstrate the impact of the operation of tap-ratio control in conjunction with the presence of transmission congestion in the network, on the electricity market. In order to model the strategic interactions of the generating firms in the interesting situation of network transmission congestion further cases are performed on the 5-bus test system. The system description is the same as in Section 4.4 and Figure 10. Cases 11 to 16 are performed by gradually increasing the transmission congestion in the system, in order to show that the impact of tap-ratio control on the market outcome is dependent on the level of congestion. Furthermore, Cases 17 and 18 show that, apart of the dependency of the effects of tap-ratio control on the congestion, the presence of these two factors in the system may give the opportunity to the strategic firms to interfere with the decisions of the ISO for their benefit, in such a way that the ISO is forced to impose transmission congestion in the network. In Cases 11, 13, 15 and 17 the tap-ratio control is inactive, i.e. the tap-ratio value is fixed to 1.0, while in Cases 12, 14, 16 and 18 the tap-ratio setting of each transformer can be optimised within the limits of ±10% from the value of 1.0. Cases 11 and 12 are identical to Cases 1 and 2 in Section 4.4 and are used as a benchmark. The results for the market outcome, the system parameters and the power distribution in the network are presented in Tables 4.5 and 4.6 for Cases 11 to 16, and in Table 4.7 for Cases 17 and 18.

TABLE 4.5
CASES 11 TO 16 FOR THE 5-BUS TEST SYSTEM:
NODAL PRICES, BIDDING PARAMETERS, FIRMS' PROFITS AND SOCIAL WELFARE

Case No.	Active Constraint	Tap-Ratio Control Mode	Nodal Prices λp_i (£/MWh)					Bidding Strategies		Generating Firm's Profit (£/hour)		Social Welfare (£/hour)
			λp_1	λp_2	λp_3	λp_4	λp_5	k_{F1}	k_{F2}	F_1	F_2	
11	None	**Fixed**	**30.2**	**29.5**	**31.4**	**32.6**	**31.9**	**2.416**	**1.959**	**3085**	**7057**	**13640**
12		**±10%**	**31.0**	**30.2**	**31.7**	**32.7**	**32.4**	**2.481**	**1.923**	**3175**	**8357**	**14820**
13	$S_{15}^{\max} = 1.0$ p.u.	**Fixed**	**29.3**	**29.3**	**31.8**	**33.6**	**34.1**	**2.422**	**1.881**	**2150**	**7638**	**13440**
14		**±10%**	**31.8**	**31.1**	**32.8**	**34.1**	**34.4**	**2.746**	**1.243**	**1299**	**8913**	**12850**
15	$S_{12}^{\max} = S_{15}^{\max} = 0.4$ p.u.	**Fixed**	**27.5**	**28.7**	**32.7**	**36.1**	**38.8**	**2.125**	**2.051**	**3361**	**5203**	**12080**
16		**±10%**	**32.8**	**33.3**	**35.4**	**37.1**	**38.5**	**2.717**	**2.516**	**2547**	**5284**	**9258**

TABLE 4.6
CASES 11 TO 16 FOR THE 5-BUS TEST SYSTEM: SYSTEM PARAMETERS

Case No.	Active Constraint	Tap-Ratio Control Mode	Pg_1 (p.u.)	Pg_2 (p.u.)	Qg_1 (p.u.)	Qg_2 (p.u.)	$\sum Pd_i$ (p.u.)	$\sum Qd_i$ (p.u.)	Tap-Ratio	
									κ_1	κ_2
11	None	**Fixed**	**1.67**	**4.26**	**1.73**	**1.66**	**5.87**	**2.84**	**1.000**	**1.000**
12		**±10%**	**1.65**	**4.92**	**2.32**	**1.83**	**6.47**	**3.13**	**0.900**	**0.973**
13	$S_{15}^{\max} = 1.0$ p.u.	**Fixed**	**1.21**	**4.75**	**1.72**	**1.74**	**5.90**	**2.86**	**1.000**	**1.000**
14		**±10%**	**0.63**	**5.00**	**1.57**	**1.99**	**5.55**	**2.69**	**0.900**	**0.989**
15	$S_{12}^{\max} = S_{15}^{\max} = 0.4$ p.u.	**Fixed**	**2.16**	**3.19**	**0.89**	**1.87**	**5.34**	**2.58**	**1.000**	**1.000**
16		**±10%**	**1.20**	**2.49**	**0.59**	**1.37**	**3.66**	**1.77**	**0.900**	**1.000**

TABLE 4.7
CASES 17 TO 18 FOR THE 5-BUS TEST SYSTEM: MARKET OUTCOME AND SYSTEM PARAMETERS

Case No.	Tap-Ratio Control Mode	Nodal Prices λp_i (£/MWh)					Bidding Strategies		Firm's Profit (£/hour)		Social Welfare (£/hour)	$\sum Pg_i$ (p.u.)	$\sum Qg_i$ (p.u.)	$\sum Pd_i$ (p.u.)	$\sum Qd_i$ (p.u.)	Tap-Ratio	
		λp_1	λp_2	λp_3	λp_4	λp_5	k_{F1}	k_{F2}	F_1	F_2						κ_1	κ_2
17	**Fixed**	**30.2**	**29.5**	**31.4**	**32.6**	**31.9**	**2.416**	**1.959**	**3083**	**7058**	**13640**	**5.93**	**3.39**	**5.87**	**2.84**	**1.000**	**1.000**
18	**±10%**	**32.2**	**31.3**	**33.3**	**33.7**	**33.3**	**2.600**	**2.062**	**3118**	**8001**	**13700**	**5.89**	**3.66**	**5.81**	**2.81**	**0.900**	**0.957**

- ***Cases 11 and 12: No congestion*:**

In Cases 11 and 12 there is no transmission line congestion and their only difference is the applied tap-ratio control mode, which is optimised only in Case 12. The nodal prices in Case 12 show an increase when compared with those of Case 11, with a maximum price deviation of 0.8 £/MWh at bus 1. In Case 12, the profits of firm F_2 are significantly increased due to the increased active production that resulted from the submission of a smaller bidding parameter. Firm F_1, which has submitted a higher bidding parameter, shows a slight decrease in active production in Case 12, but manages to receive higher profit than in Case 11 due to the higher nodal price at its bus. However, by observing the bidding parameters of the two firms, it can be seen that the firms have not altered their strategic actions significantly. The social welfare and load demand are higher in Case 12 where the transformer tap-ratio control is in operation.

- ***Cases 13 and 14: Low level transmission congestion*:**

In Cases 13 and 14 a transmission line capacity limit has been imposed in the line between buses 1 and 5, such that $S_{15}^{\max} = 1.0$ p.u. Comparing the nodal prices

resulting from the operation with the two different tap-ratio control modes it can be observed that, once again, all prices have been increased for the case where the tap-ratio setting is allowed to vary within certain limits. The price deviation has a wider range than that of Cases 11 and 12, up to a maximum price difference of 2.5 £/MWh at bus 1. When observing the bidding parameters of the two firms, it can be seen that they have both significantly altered their bidding strategies. The production of firm F_1 in Case 14 has been decreased by a half due to the fact that the power flow from its generator bus to the load buses 5 and 4 is less than that of Case 13, thus, even though the bidding parameter of firm F_1 has been increased by about 13% and the nodal price at its bus has the highest increment, its profit has shown a reduction of 40%. Since firm F_2 is able in Case 14 to provide more power to bus 4 via transformer branch TR1, which has optimised its tap-ratio setting to the minimum value, avoiding the congested branch, it has decreased its bidding parameter by 34% compared to Case 13. This resulted in increased active production in Case 14 and, in conjunction with the higher nodal price at its bus, firm F_2 gains a much higher profit compared to Case 13. The lower active production as switching from Case 13 to Case 14 resulted in lower load demand and hence lower social welfare. The optimisation of the transformer tap-ratio has an adverse effect on the social welfare in the presence of transmission congestion in Cases 13 and 14, which is exactly the opposite of that observed in Cases 11 and 12 under normal operating network conditions.

- ***Cases 15 and 16: Heavily transmission congestion conditions*:**

In Cases 15 and 16, the transmission network is operated in highly stressed conditions by setting the maximum capacity limits for lines 1-2 and 1-5 equal to 0.4 p.u. When comparing the nodal prices for the different tap-ratio control modes in Cases 15 and 16, it can be seen that the price deviation for each bus differs from one another. The highest price deviation, observed at bus 1, is 5.3 £/MWh, which is much larger than the deviations in Cases 11 to 14. Both firms have significantly increased their bidding parameters in Case 16, while their active production has been reduced. In Case 15, the power produced by firm F_1 flows in the direction from bus 1 towards buses 5, 4 and 3. In Case 16, its active production is equal to the load demand of bus 1 and the power flows in and out

of bus 1 are equal. This resulted in a much lower profit for firm F_1 even though that its bidding parameter and the nodal price at its bus have considerably increased. Consequently, the optimisation of the transformer tap-ratio settings in Case 16 has given the opportunity to firm F_2 to supply power equal to that of the load demand at buses 2 to 5. Therefore, despite the fact that its active power production in Case 16 is much less than that of Case 15, firm F_2 attains a slightly higher profit due to the increased nodal prices. For these cases, where the transmission congestion is more intense, the optimisation of the transformer tap-ratio in Case 16 resulted in a much lower social welfare compared to Case 15, due to the enormous reduction in active load demand. This reduction in the price-responsive active load demand is caused by the drop of the active production, which is a result of the different equilibrium strategies chosen by the generating firms that correspond to the different tap-ratio control modes.

- ***Cases 17 and 18: Tap-ratio control imposes congestion*:**

One situation that can be of particular interest is investigated in test Cases 17 and 18. For these two cases the capacity limit of transformer branch TR1 has been set to $S_{TR1}^{\max} = 2.0\,\text{p.u.}$ In Case 17, where the tap-ratio control is inactive, the power S_{23} transmitted through branch TR1 is equal to 1.59p.u. Therefore, there is no congestion in the network branches and the results are identical to those of Case 11. In Case 18, in which the tap-ratio control is activated, it is observed that the capacity constraint of transformer branch TR1 is binding and hence congestion exists in the system. The power flow S_{23} has changed from 1.59p.u. (in Case 17) to 2.00p.u. (in Case 18). By observing the results for these two cases in Table 4.7, it can be seen that in Case 18 both firms have increased their bidding parameters resulting in increased nodal prices, with a maximum price difference of 2.0 £/MWh, and consequently higher profits, since the power generation is maintained basically at the same levels. The transformer tap-ratio control gives enough incentives to the strategic firms to alter their bidding strategies in such a way to interfere with the ISO decisions in order to cause transmission congestion in the network, and consequently to force the nodal prices to increase. This results in higher profits for the firms, but keeps the generation production at the same levels as in the case in which the tap-ratio control is inactive. The social

welfare in Case 18 is higher than in Case 17 (mainly due to the higher surplus for the producers since the active load demand is maintained at the same level with a minor decrement), but it is still lower than Case 12, which is comparable to Case 18 and there is no transmission congestion in the network.

4.8 Discussion on the impact of transformer tap-ratio control in congested transmission networks based on the numerical results of Cases 11 to 18

The results obtained from test Cases 11 to 16 have shown that the effect of the tap-ratio control on the electricity market outcome becomes more perceptible as the transmission congestion in the network is more intense. The operation of the transformer tap-ratio control is found to be in favour of the social welfare in the absence of congestion, while it has adverse effects when congestion is present. As seen from the analysis of the results in Cases 17 and 18, the introduction of transformer tap-ratio control in the modelling of the electricity market does not only have a direct effect on the individual market parameters but also the consequent alterations of the generating firms' strategies force the ISO to interfere with the electrical operation of the system. The equilibrium decisions of the ISO on the tap-ratio settings might impose congestion in the network giving a totally different market outcome. This leads to the need for reconsidering the primal system design parameters. The impact of the strategic behaviour of the market participants on the operation of the electricity network should be taken into consideration in the network design process in order to avoid causing operational problems such as transmission congestion, thus securing the smooth operation of the electricity network. A sophisticated market equilibrium simulation algorithm with AC network modelling, taking into account all operational aspects including variable control methods, such transformer tap-ratio control, is required for the efficient design of modern power systems. Such considerations will help to avoid undesired incidents, such as the occurrence of transmission congestion, and will allow the network control functions to fully exploit the system abilities.

4.9 Conclusions for Chapter 4

In this chapter, the modelling of transformer tap-ratio control has been successfully implemented in the primal-dual nonlinear interior point algorithm, for the calculation of the SFE point in the electricity market. The algorithm has been used to show the importance of considering the transformer tap-ratio control in the electricity market equilibrium analysis. Preliminary numerical results have indicated that the presence of transformer tap-ratio control gives enough incentives to the strategic generating firms to exercise market power in a different way than in the uncontrolled case. This action results in different market outcome and different power distribution in the network. The regulation provided by the tap-ratio control can significantly affect the outcome of the equilibrium analysis with a direct impact on the nodal prices, firms' profits and social welfare. In the light of the above, it is concluded that the transformer tap-ratio control has a significant impact on the electricity market outcome and should not be neglected from the electricity market equilibrium models.

The numerical results performed in congested transmission networks have shown that the effect of the transformer tap-ratio control on the market equilibrium is more significant as the congestion in the transmission lines becomes more intense. It was observed that the operation of the tap-ratio control results in higher social welfare in the absence of transmission congestion, while it has adverse effects when congestion exists in the system. The operation of the tap-ratio control in conjunction with the presence of transmission line congestion in the network encourages the generating firms to alter their strategic actions and exercise market power in a different manner. Furthermore, in certain cases, the optimisation of the tap-ratio gives the opportunity to the strategic firms to alter their bidding strategies in order to interfere with the ISO decisions on the tap-ratio control settings to favour their benefits, in such a way to impose transmission network congestion in the system with the consequence of higher nodal prices and withheld generation. Therefore, the resulting effects from the market power exercised by the strategic firms must be taken into account during the system design. This will prevent undesired operational problems such as the

induction of congestion in the network and the performance of the system can be enhanced with the aid of the available network control functions. The direct and evident impact of the interrelation between the operation of transformer tap-ratio control and transmission congestion on the prices, profits, social welfare and power distribution in the network, shows the dependency of the market equilibrium outcome on the modelling of the network constraints and controls.

Chapter 5:

The impact of reactive power and voltage control on the electricity market equilibrium

5.1 Introduction to the analysis of reactive power control in the electricity market equilibrium model

As it has already been shown that the MVA transmission limits that depend on the reactive power flows have a great effect on the equilibrium point [133,120], the modelling of transmission capacity constraints using the AC network representation in the market equilibrium algorithms should be regarded as a necessity. The implementation of the AC network model in the proposed market equilibrium algorithm in this Thesis provides the ability to investigate the effect of reactive power, in terms of control functions, on the electricity market. Following the discussions in Section 2.9 about the possible influence of reactive power on the interactions between the strategic firms and the electricity market outcome, the impact of reactive power control in power flow market analysis is examined in this chapter.

The reactive power in an electrical power system is directly related to the voltages across the network (e.g. see equations in Section 3.5.1), to the operation of the generating units (in terms of reactive power generation and absorption), and to the load power factor, which is directly dependent on the reactive load demand. By considering these three factors, the impact of the following aspects on the electricity market equilibrium, is examined:

- different voltage control modes for generator buses,
- variation of the reactive power generation and absorption limits of the generating units in the system,
- load power factor adjustments.

For each of these three investigations, test cases are performed on a 3-bus system to show the direct effects on small networks, and on the IEEE 14-bus and 118-

bus systems to show the market behaviour on larger and more realistic networks. The simulations are performed using the k_F-parameterization SFE algorithm as discussed in Chapter 3, with the limits of the bidding parameter k_F set to $k_F^{\min} = 0$ and $k_F^{\max} = 10$. For the test systems with transformers in this study, the tap-ratio control settings are optimised within a range of 0.9 to 1.1. The results for the social welfare correspond to the true social welfare and all the power quantities are calculated in p.u.

5.2 Investigation of the voltage control on generator buses

In order to examine the effects of the application of voltage control on the generation buses on the market equilibrium outcome, two different voltage regulation control modes are employed. Mode 1 corresponds to network operation with the voltages of all the buses across the system to be optimised within a range of ±5% or ±10% from the rated value of 1.0 p.u. Mode 2 applies voltage control to the generation buses, for which the voltages are controlled and held constant to the fixed value of 1 p.u.

5.2.1 Voltage control: 3-bus system results

The 3-bus test system used for this analysis consists of 3 buses connected to each other by 3 transmission lines, as shown in Figure 11. Generation exists at buses 1 and 2 and load demand at buses 1 and 3. The marginal cost function of the generating unit at bus 1, owned by firm F_1, is $MC_{Pg_1} = 18 + 0.008Pg_1$ £/MWh, and that of the unit at bus 2, owned by firm F_2, is $MC_{Pg_2} = 15 + 0.010Pg_2$ £/MWh. The linear inverse load demand functions for buses 1 and 3 are $D_{Pd_1} = 40 - 0.08Pd_1$ £/MWh and $D_{Pd_3} = 40 - 0.06Pd_3$ £/MWh respectively. The load power factor was set to 0.7 at all buses to simulate conditions with high reactive power demand. Four test cases are performed on this system. Cases 1 and 2 correspond to operation with no network congestion, while Cases 3 and 4 are performed by setting a tight transmission capacity limit on one of the transmission line branches in the network. Cases 1 and 3 correspond to voltage

regulation Mode 1 and are performed using voltage optimisation of ±5%, while Cases 2 and 4 correspond to Mode 2 and voltage control is applied on the generation buses. The numerical results for the nodal prices, firms' profits, bidding strategies, and social welfare are presented in Table 5.1, while The power distribution in the network is presented in Table 5.2, where a minus sign on the value of Qg_i indicates reactive power absorption from the generating unit at bus *i*.

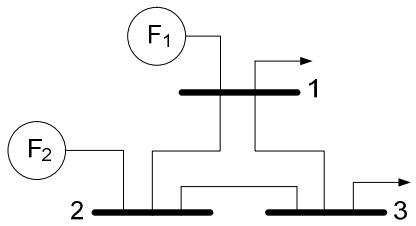

Figure 11: The 3-bus test system.

TABLE 5.1
CASES 1 TO 4 FOR THE 3-BUS TEST SYSTEM:
NODAL PRICES, BIDDING PARAMETERS, FIRMS' PROFITS AND SOCIAL WELFARE

Case No.	Transmission Line Capacity Limit	Voltage Regulation Mode	Nodal Prices λp_i (£/MWh)			Bidding Strategies		Generating Firm's Profit (£/hour)		Social Welfare (£/hour)
			λp_1	λp_2	λp_3	k_{F1}	k_{F2}	F_1	F_2	
1	None	**1**	**29.4**	**29.4**	**29.4**	**1.561**	**1.720**	**1117**	**2775**	**5539**
2		**2**	**33.1**	**33.1**	**33.1**	**1.772**	**2.070**	**1213**	**1702**	**3601**
3	$S_{23}^{\max} = 0.3$ p.u.	**1**	**33.1**	**28.9**	**37.3**	**1.768**	**1.869**	**1316**	**605**	**2667**
4		**2**	**31.6**	**28.8**	**34.4**	**1.672**	**1.878**	**1439**	**460**	**2714**

TABLE 5.2
CASES 1 TO 4 FOR THE 3-BUS TEST SYSTEM: POWER DISTRIBUTION IN THE NETWORK

Case No.	Transmission Line Capacity Limit	Voltage Regulation Mode	Pg_1	Pg_2	Qg_1	Qg_2	Pd_1	Pd_3	Qd_1	Qd_3
1	None	**1**	**1.02**	**2.08**	**2.45**	**1.16**	**1.33**	**1.77**	**1.36**	**1.81**
2		**2**	**0.82**	**0.97**	**1.40**	**0.54**	**0.87**	**0.93**	**0.88**	**0.94**
3	$S_{23}^{\max} = 0.3$ p.u.	**1**	**0.89**	**0.44**	**1.91**	**-0.48**	**0.86**	**0.47**	**0.88**	**0.48**
4		**2**	**1.10**	**0.34**	**1.31**	**0.17**	**1.06**	**0.38**	**1.08**	**0.39**

- ***Cases 1 and 2: No binding transmission limit*:**

Cases 1 and 2 are identical in terms of network parameters, with the only difference being the applied voltage control mode. In Case 1 the voltages at the generator buses are optimised within the limits of 0.95 and 1.05 p.u. (Mode 1),

while in Case 2, they are fixed to 1 p.u. (Mode 2). The adjustment of the voltage control mode has a significant effect on the equilibrium point, as shown in Tables 5.1 and 5.2. The results show that by controlling the generation voltages the generating firms withhold their active generation by submitting higher bidding parameters. This results in significantly larger nodal prices in Case 2 compared with Case 1, and the reduced active generation has the consequence of much lower active load demand. These effects cause the social welfare in Case 2 to be reduced by 35% compared to Case 1. Even though the active generation of firm F_1 is decreased by 20%, it manages to raise its profit due to the high increase of the nodal price at its bus. On the other hand, the increase in nodal prices in Case 2 was not adequate to cover the reduction in the production of firm F_2, which was decreased to less than half compared with Case 1, thus its profit is significantly reduced.

- ***Cases 3 and 4: Binding transmission limit*:**

Cases 3 and 4 are performed by setting the transmission line capacity limit of branch 2-3 to $S_{23}^{\max} = 0.3\,\text{p.u.}$ in order to impose transmission congestion in the network and investigate the impact of voltage control on the market equilibrium under stressed network conditions. With Case 1 being the benchmark, the introduction of the binding transmission limit in Case 3 seriously affects the production of firm F_2, which does not have load demand on its bus, resulting in an enormous decrease in its profit. By comparing Cases 3 and 4, it can be observed that there is a reduction in the nodal prices and a small increase in social welfare when controlling the generation voltages. This is in contrast with the comparison of Cases 1 and 2, for which there is no transmission congestion in the system and the introduction of regulation Mode 2 resulted in higher nodal prices and lower social welfare. The impact on the profits of the generating firms is similar as that between Cases 1 and 2, but the production of firm F_1 is increased and that of firm F_2 is significantly decreased in Case 4 compared with Case 3. The tests performed with the binding transmission limit have shown that the effect of the voltage control on the electricity market equilibrium depends on the network operating conditions.

5.2.2 Voltage control: IEEE 14-bus system results

The IEEE 14-bus system [191] used for this analysis consists of 14 buses of which 11 have load demand, 20 transmission lines and 5 generators owned by strategic generating firms entitled F_1 to F_5 respectively. Case 5 is performed using voltage optimisation of ±5% for Mode 1 and Case 6 using voltage control as in Mode 2. The results for the firms' profits, bidding strategies, power distribution in the network and social welfare are presented in Table 5.3, while the nodal prices are given in Table 5.4 allowing direct comparison for the two cases. In Table 5.4, the generation buses are indicated by the firms' title in the parentheses next to the bus number in the first column.

TABLE 5.3
CASES 5 TO 6 FOR THE IEEE 14-BUS SYSTEM:
BIDDING PARAMETERS, FIRMS' PROFITS, POWER DISTRIBUTION AND SOCIAL WELFARE

Case No.	Voltage Regulation Mode	Bidding Strategies					Generating Firm's Profit (£/hour)					$\sum Pg_i$	$\sum Qg_i$	$\sum Pd_i$	$\sum Qd_i$	Social Welfare (£/hour)
		k_{F1}	k_{F2}	k_{F3}	k_{F4}	k_{F5}	F_1	F_2	F_3	F_4	F_5					
5	**1**	**1.738**	**2.262**	**1.850**	**1.748**	**1.785**	**3704**	**~0**	**1730**	**4112**	**1907**	**6.83**	**0.14**	**6.63**	**4.48**	**14310**
6	**2**	**1.847**	**1.860**	**0.897**	**1.748**	**2.053**	**3613**	**467**	**1746**	**4212**	**1428**	**6.30**	**-0.11**	**6.13**	**2.37**	**13360**

TABLE 5.4
CASES 5 TO 6 FOR THE IEEE 14-BUS SYSTEM: COMPARISON OF NODAL PRICES (£/MWHOUR)

Bus No. (firm)	Case 5: Nodal Prices for Voltage Mode 1	Case 6: Nodal Prices for Voltage Mode 2
1 (F_1)	**30.6**	**31.9**
2 (F_2)	**32.5**	**33.9**
3 (F_3)	**32.8**	**33.0**
4	**33.5**	**34.6**
5	**33.3**	**34.4**
6 (F_4)	**32.4**	**32.9**
7	**33.9**	**35.3**
8 (F_5)	**33.9**	**38.1**
9	**34.4**	**35.2**
10	**35.6**	**36.9**
11	**35.7**	**36.7**
12	**36.6**	**37.4**
13	**35.5**	**36.3**
14	**37.1**	**38.0**

- ***Cases 5 and 6: Results for the IEEE 14-bus system*:**

When voltage control is applied for Case 6, the generating firms alter their strategic offers as can be seen in Table 5.3. A significant variation is observed in the bidding parameters of the firms, which are seriously affected at the equilibrium point that corresponds to the application of voltage control, such as for the unit at bus 3 for which the value of k_{F_3} is reduced from 1.850 to 0.897.

The change in strategies in Case 6 results in a small decrease in the level of power production compared to Case 5. However, the nodal prices at all buses are rising, up to increments of 4.2 £/MWh, and there is a significant variation in the distribution of the profits among the generating firms. Firms F_1 and F_5, which submitted higher bidding parameters in Case 6, face reductions in profit, while the profit of the other three firms rises. For example, firm F_2 receives a zero profit in Case 5, while by reducing its bidding parameter by about 20% when voltage control was introduced in Case 6, it receives a noticeable profit. The small reduction in active production, and hence active load demand, between Cases 5 and 6 resulted in a small reduction in the social welfare.

5.2.3 Voltage control: IEEE 118-bus system results

The IEEE 118-bus system [191] consists of 118 buses with load demand, 170 transmission lines, 9 on-load tap-changing transformers, and 54 generators owned by individual strategic firms. Case 7 is performed using voltage optimisation of ±10% for voltage Mode 1, i.e. in the domain of 0.9 to 1.1 p.u., and Case 8 corresponds to voltage control for Mode 2. Results summarising the range of the nodal prices, firms' profits and bidding strategies are provided in Table 5.5, while the results for the power distribution in the network and social welfare are shown in Table 5.6.

TABLE 5.5
CASES 7 TO 8 FOR THE IEEE 118-BUS SYSTEM: RESULTS FOR COMPARISON

Case No.	Voltage Regulation Mode	Average Nodal Price (£/MWh)	Profit (£/hour)			Bidding Strategies k_F		
			max	min	average	max	min	average
7	**1**	**32.76**	**14770**	**1037**	**3115**	**1.795**	**0.929**	**1.232**
8	**2**	**33.26**	**13750**	**~0**	**2831**	**5.047**	**0.100**	**1.414**

TABLE 5.6
CASES 7 TO 8 FOR THE IEEE 118-BUS SYSTEM: POWER DISTRIBUTION AND SOCIAL WELFARE

Case No.	Voltage Regulation Mode	$\sum Pg_i$	$\sum Qg_i$ generation	$\sum Qg_i$ absorption	$\sum Pd_i$	$\sum Qd_i$	Social Welfare (£/hour)
7	1	**137.70**	**35.08**	**-1.35**	**135.62**	**37.18**	**226600**
8	**2**	**117.46**	**27.18**	**-2.73**	**115.97**	**28.91**	**222000**

- ***Cases 7 and 8: Results for the IEEE 118-bus system*:**

The application of voltage control on the large IEEE 118-bus system has a considerable effect on the electricity market equilibrium. The results show significant differences on the average firms' profits and bidding parameters between Cases 7 and 8, indicating that the generating firms have incentives to perceptibly alter their strategic actions depending on the applied voltage regulation mode. The power distribution in the network exhibits large differences between the two cases, as the introduction of Mode 2 results in reduced active and reactive generation, and increased reactive power absorption, with the consequence of higher average nodal price and lower social welfare. The numerical results on this more realistic system have demonstrated the evident impact of voltage control on the electricity market outcome.

5.2.4 Discussion on the impact of voltage control based on the numerical results of Cases 1 to 8

The employment of different voltage regulation modes on the generation buses, which is directly related to the reactive power generation and hence to the overall power distribution in the network, has shown by examining a variety of test systems that the voltage control greatly affects the market equilibrium point. Depending on the allowable limits on the voltage at the generation buses, a significant variation on the bidding parameters of the strategic offers has been observed, showing that the generating firms alter their strategies in order to favour their profit. Apart from the consequent redistribution of the profits among the firms, these actions have an impact on the nodal prices, social welfare, and power distribution in the network, resulting in a different market equilibrium for both the small and the large systems tested. The voltage control of the generation

buses results in higher nodal prices and lower social welfare under normal operating conditions, while it reduces the high prices that exist in the presence of transmission congestion being in favour of the social welfare.

This investigation has shown that the strategic firms have the ability to exploit the network features, such as the voltages and reactive power in the system, in order to exercise market power and increase their profits in the presence or absence of network congestion. The impact of voltage control in the case where transmission congestion exists in the network is different of that for normal operating conditions. The incorporation of reactive power modelling and bus voltage constraints in the electricity market equilibrium model has given the opportunity to investigate the interactions between the strategic firms for different voltage regulation modes and obtain a more realistic prediction for the market outcome.

5.3 Investigation of the reactive power generation and absorption limits

The modelling of the generating units in the electricity market algorithm that takes place in Chapter 3 includes representation of the reactive power generation and the reactive power absorption limits. The following analysis examines the impact of limitations on the reactive power generation and absorption from the generating units on the electricity market outcome. It should be recalled that the market model considers that the reactive services from the generating units do not account for any profit but it is mandatory for the generating firms to provide the required reactive power generation or absorption as it is scheduled by the ISO in the market clearing process. The reactive generation of each generating unit in the mathematical formulation of the algorithm is taken as a positive quantity, while reactive absorption is indicated by a negative sign. Similarly, the inductive loads connected to the network, which absorb reactive power from the system, correspond to positive reactive load demand, while the capacitive loads, which generate reactive power, are represented by negative reactive load demand. In order to counterbalance the loads' effects, the generating units are required to

generate reactive power in the presence of inductive loads or to absorb reactive power in order to dispose the reactive power generated from capacitive loads.

5.3.1 Reactive power generation limits: 3-bus system results

The 3-bus system is of the same structure as in Figure 11, but load demand exists at all buses. The marginal cost function of the generating unit at bus 1, owned by firm F_1, is $MC_{Pg_1} = 11 + 0.009Pg_1$ £/MWh, and that of the unit at bus 2, owned by firm F_2, is $MC_{Pg_2} = 10.8 + 0.010Pg_2$ £/MWh. The linear inverse load demand function is the same for all buses and is equal to $D_{Pd_i} = 40 - 0.06Pd_i$ £/MWh. The voltages at the generation buses are controlled to 1 p.u. and the load power factor is set to 0.9 at all buses to simulate normal operating conditions. Case 9 is performed with no binding limits, while the reactive power generation limit of the unit at bus 2 is set to $Qg_2^{\max} = 0.8$ p.u. for Case 10. The results are shown in Tables 5.7 and 5.8.

TABLE 5.7
CASES 9 TO 10 FOR THE 3-BUS TEST SYSTEM:
NODAL PRICES, BIDDING PARAMETERS, FIRMS' PROFITS AND SOCIAL WELFARE

Case No.	Reactive Power Constraints	Nodal Prices λp_i (£/MWh)			Bidding Strategies		Generating Firm's Profit (£/hour)		Social Welfare (£/hour)
		λp_1	λp_2	λp_3	k_{F1}	k_{F2}	F_1	F_2	
9	None	**29.2**	**28.9**	**29.9**	**2.311**	**2.041**	**3201**	**5541**	**11667**
10	$Qg_1^{\max} = 0.8$ p.u.	**32.3**	**31.7**	**32.6**	**2.708**	**2.397**	**2169**	**4771**	**8495**

TABLE 5.8
CASES 9 TO 10 FOR THE 3-BUS TEST SYSTEM: POWER DISTRIBUTION IN THE NETWORK

Case No.	Reactive Power Constraints	Pg_1	Pg_2	Qg_1	Qg_2	Pd_1	Pd_2	Pd_3	Qd_1	Qd_2	Qd_3
9	None	**1.84**	**3.37**	**1.40**	**1.32**	**1.79**	**1.85**	**1.55**	**0.87**	**0.89**	**0.75**
10	$Qg_1^{\max} = 0.8$ p.u.	**1.04**	**2.42**	**0.80**	**0.97**	**1.00**	**1.38**	**1.07**	**0.48**	**0.67**	**0.52**

- ***Cases 9 and 10: Results for the 3-bus system*:**

By observing the results of Cases 9 and 10, it can be seen that restricting the reactive power generation has a perceptible impact on the market equilibrium

outcome. The strategic firms in Case 10 increase their bidding parameters and produce lower active power, resulting in higher nodal prices and reduced social welfare compared to Case 9. This comparison resembles that between Cases 1 and 2 for the introduction of voltage control, since for both situations the generating units are not allowed to fully utilise their reactive capabilities. However, in Cases 9 and 10 the increase in nodal prices was not enough to sustain the profits of the generating firms, which undergo high reductions due to the lower active production.

5.3.2 Reactive power generation and absorption limits: IEEE 14-bus system results

The IEEE 14-bus system [191] used in this section consists of 14 buses with load demand, 17 transmission lines, 3 on-load tap-changing transformers and 5 generators located at buses 1, 2, 3, 6, and 8, owned by strategic generating firms entitled F_1 to F_5 respectively. The voltages at all buses can be optimised by the ISO within the range of 0.9 to 1.1 p.u. Cases 11 to 13 examine the impact of reactive power generation and Cases 14 to 15 the impact of reactive power absorption. The numerical results for the generating firms and social welfare are presented in Table 5.9 and the power distribution in the network is shown in Table 5.10. The nodal prices are given in Table 5.11, where the location of each generating firm is indicated, to allow direct comparison between the cases.

- ***Cases 11 to 13: Reactive power generation limits*:**

The reactive load demand in Cases 11 to 13 is of inductive nature at all buses and therefore all the generating units generate reactive power. The reactive capabilities of the generating units in Case 11 are sufficient to satisfy the reactive load demand in the system without reaching the maximum operating limits for the reactive power generation. For Case 12, the maximum reactive power limit of the generating unit at bus 6 was reduced to $Qg_6^{\max} = 0.25\,\text{p.u.}$ confining its reactive power generation at that value. It can be observed from Table 5.11 that all the nodal prices have been increased compared with Case 11. The highest increment is 0.9£/MWh observed at buses 2 and 6, for which the generating units

TABLE 5.9
CASES 11 TO 15 FOR THE IEEE 14-BUS SYSTEM:
FIRMS' PROFITS, BIDDING PARAMETERS AND SOCIAL WELFARE

Case No.	Reactive Power Constraints	Generating Firms' Profit (£/hour)					Bidding Strategies					Social Welfare (£/hour)
		F_1	F_2	F_3	F_4	F_5	k_{F1}	k_{F2}	k_{F3}	k_{F4}	k_{F5}	
11	None (Inductive *Pd* only)	**1329**	**3651**	**2968**	**2215**	**1755**	**1.626**	**1.481**	**1.508**	**1.297**	**1.244**	**17030**
12	$Qg_6^{\max} = 0.25$ p.u.	**1342**	**3278**	**2925**	**1519**	**1619**	**1.668**	**1.561**	**1.563**	**1.394**	**1.284**	**14670**
13	$Qg_{1,8}^{\max} = 0.50$ p.u. $Qg_{2,3,6}^{\max} = 0.25$ p.u.	**1750**	**1447**	**2431**	**1206**	**563**	**1.819**	**1.883**	**1.801**	**1.528**	**1.446**	**8958**
14	None (Inductive and Capacitive *Pd*)	**1335**	**3727**	**2971**	**2203**	**1669**	**1.623**	**1.475**	**1.507**	**1.299**	**1.249**	**17010**
15	$Qg_2^{\min} = -0.10$ p.u.	**1355**	**3392**	**3197**	**1953**	**1549**	**1.655**	**1.519**	**1.502**	**1.338**	**1.284**	**15980**

TABLE 5.10
CASES 11 TO 15 FOR THE IEEE 14-BUS SYSTEM: POWER DISTRIBUTION IN THE NETWORK

Case No.	Reactive Power Constraints	Pg_1	Pg_2	Pg_3	Pg_6	Pg_8	Qg_1	Qg_2	Qg_3	Qg_6	Qg_8	$\sum Pd_i$	$\sum Qd_i$ inductive	$\sum Qd_i$ capacitive
11	None (Inductive *Pd* only)	**1.10**	**3.24**	**2.63**	**2.54**	**2.25**	**0.08**	**1.43**	**0.52**	**2.38**	**1.21**	**11.47**	**4.30**	**0**
12	$Qg_6^{\max} = 0.25$ p.u.	**1.05**	**2.65**	**2.41**	**1.49**	**1.89**	**0.26**	**1.76**	**0.58**	**0.25**	**1.47**	**9.29**	**3.36**	**0**
13	$Qg_{1,8}^{\max} = 0.50$ p.u. $Qg_{2,3,6}^{\max} = 0.25$ p.u.	**1.12**	**0.88**	**1.54**	**0.94**	**0.49**	**0.50**	**0.25**	**0.25**	**0.25**	**0.50**	**4.88**	**1.62**	**0**
14	None (Inductive and Capacitive *Pd*)	**1.11**	**3.32**	**2.64**	**2.52**	**2.13**	**~0**	**-1.64**	**0.04**	**2.45**	**1.33**	**11.42**	**3.38**	**-2.55**
15	$Qg_2^{\min} = -0.10$ p.u.	**1.08**	**2.89**	**2.82**	**2.09**	**1.82**	**~0**	**-0.10**	**~0**	**1.31**	**1.44**	**10.36**	**3.18**	**-1.98**

TABLE 5.11
CASES 11 TO 15 FOR THE IEEE 14-BUS SYSTEM: COMPARISON OF NODAL PRICES (£/MWHOUR)

Bus No. (firm)	Nodal Prices λp_i				
	Case 11	Case 12	Case 13	Case 14	Case 15
1 (F_1)	**30.1**	**30.8**	**33.7**	**30.0**	**30.6**
2 (F_2)	**30.2**	**31.1**	**34.4**	**30.2**	**30.5**
3 (F_3)	**30.0**	**30.7**	**34.0**	**29.9**	**30.1**
4	**33.5**	**34.1**	**36.4**	**33.5**	**34.0**
5	**33.2**	**33.8**	**36.1**	**33.2**	**33.7**
6 (F_4)	**32.5**	**33.4**	**35.8**	**32.5**	**32.9**
7	**34.1**	**34.8**	**37.0**	**34.1**	**34.5**
8 (F_5)	**33.9**	**34.5**	**36.9**	**33.9**	**34.4**
9	**34.6**	**35.3**	**37.2**	**34.6**	**34.9**
10	**35.6**	**36.0**	**37.4**	**35.6**	**36.0**
11	**35.5**	**36.0**	**37.2**	**35.5**	**35.9**
12	**36.0**	**36.6**	**37.6**	**36.0**	**36.5**
13	**35.3**	**35.9**	**37.2**	**35.3**	**35.8**
14	**36.8**	**37.2**	**37.9**	**36.8**	**37.2**

suffer higher active power reductions than the other units. The active production of the unit with the limited reactive generation at bus 6 is reduced by more than 40%. The other generating units in Case 12 have increased their reactive generation so that the system is compensated for the reactive limitations of the generator at bus 6, but the total reactive generation and demand are reduced by more than 20% compared with those of Case 11.

In Case 12 all units have submitted higher bidding parameters than those in Case 11, as an attempt to maintain their profits. None of the firms, except firm F_1, can achieve this due to the noticeable reduction in their active production. The profit of firm F_4 in Case 12 is reduced by more than 30% compared with Case 11. Firm F_1, which maintains a similar active production as that of Case 11, is favoured by the increase in nodal prices and gains a slightly higher profit. The social welfare has been decreased by about 14%, due to the lower active load demand.

In Case 13, strict reactive power generation limits have been imposed at all generators in the system, resulting in a limitation of the total reactive power generation. The limits for buses 1 and 8 were set to $Qg_{1,8}^{\max} = 0.50\,\text{p.u.}$ and for buses 2, 3 and 6 to $Qg_{2,3,6}^{\max} = 0.25\,\text{p.u.}$ and they are all binding. The observations

on the changes of the results for the market outcome and power distribution are similar to those of the comparison between Cases 11 and 12, but much more intense, with the exception that the active power generation at bus 1 is slightly increased. The nodal prices have been further increased, with incremental deviations between Cases 12 and 13 up to a range of 3.3£/MWh, and all the firms have submitted higher bidding parameters. In Case 13, all the firms, except firm F_1, receive much lower profits due to the high reductions in their active power generation. Firm F_1, which has increased its active production, is favoured by the higher nodal prices, and in conjunction with its higher submitted bid, it receives a much higher profit compared with Cases 11 and 12. Nevertheless, the total active and reactive generation and load demand in the system have been decreased by half compared with Case 12, resulting in a significant reduction in the social welfare (by about 40%).

- ***Cases 14 to 15: Reactive power absorption limits*:**

For the test Cases 14 and 15, capacitive reactive load demand has been assigned at buses 2 to 5. The results for Case 14 are similar to those of Case 11, with the exception that the generator at bus 2 is absorbing reactive power from the network and the consequent redistribution of reactive generation among the other units. The same unit is producing the highest active power generation, thus firm F_2 gains the highest profit as in Case 11. In Case 15, the generator at bus 2 is confined to operate with a limit on its reactive absorption capabilities, such that $Qg_2^{\min} = -0.10$ p.u. This has a consequence on the reactive load demand, on both the inductive and capacitive components, which are decreased compared with Case 14. The capacitive reactive demand is satisfied mainly by reactive power absorption from the inductive loads in the network since the generator at bus 2 can cover only 5% of it.

The nodal prices in Case 15 have shown a small increase compared with those of Case 14. The generating units that submitted higher bidding parameters than those of Case 14 produce lower active power, while the unit at bus 3 that submitted a slightly lower bidding parameter has achieved a higher active generation. The profit of firm F_1 was slightly increased due to the increased

bidding parameter in conjunction with the higher nodal price at bus 1, while the profits of firms F_2, F_4 and F_5 show a decrease of 7% to 11% as a consequence of the perceptible lower active productions. Firm F_3 receives a higher profit than that in Case 14 since its active production is increased, benefited by the reduction in the active power of the rival generating units. The active load demand in Case 15 has been decreased by about 9% compared with Case 14, resulting in a reduction of 6% in the social welfare.

5.3.3 Reactive power generation limits: IEEE 118-bus system results

The description of the IEEE 118-bus system [191] is similar to that in Section 5.2.3, with the bus voltages optimised within the range of ±10% from the value of 1 p.u. Case 16 is performed with no binding limits on the reactive power generation, while strict reactive power generation limits in the range of 0.05 to 2.0 p.u. are imposed on 26 out of the 54 generating units of the system, such that the availability of the system's reactive generation capacity is reduced by 38.6%, in Case 17. The availability for the reactive absorption capacity in the system is the same for both cases and the reactive load demand is of inductive nature at all buses. Results for the nodal prices, firms' profits and bidding strategies are provided in Table 5.12, while the results for the power distribution in the network and social welfare are given in Table 5.13.

TABLE 5.12
CASES 16 TO 17 FOR THE IEEE 118-BUS SYSTEM: RESULTS FOR COMPARISON

Case No.	*Qg* limits binding	Average Nodal Price (£/MWh)	Profit (£/hour)			Bidding Strategies k_F		
			max	min	average	max	min	average
16	No	**32.78**	**14700**	**1309**	**3193**	**1.764**	**0.824**	**1.148**
17	Yes	**32.84**	**14420**	**893**	**3072**	**1.824**	**0.015**	**1.229**

TABLE 5.13
CASES 16 TO 17 FOR THE IEEE 118-BUS SYSTEM: POWER DISTRIBUTION AND SOCIAL WELFARE

Case No.	*Qg* limits binding	$\sum Pg_i$	$\sum Qg_i$ generation	$\sum Qg_i$ absorption	$\sum Pd_i$	$\sum Qd_i$	Social Welfare (£/hour)
16	No	**141.76**	**40.16**	**-4.68**	**139.67**	**39.30**	**231300**
17	Yes	**133.95**	**32.99**	**-1.07**	**131.92**	**35.69**	**222200**

- ***Cases 16 and 17: Results for the IEEE 118-bus system*:**

From Table 5.13 it can be seen that when limitations on the reactive power generation are imposed on the generating units for Case 17, all the overall power quantities in the system are decreased compared to Case 16. Therefore, the average profit for the generating firms has been decreased, as a consequence of the reduced active production. The reactive power generation, which is the variable that has been deliberately confined, is reduced by 18%, while the reactive power absorption has been reduced by almost 80%.

The maximum profit for both cases corresponds to the same generating unit and is slightly decreased (by only 2%), supported by the nodal price increment at that bus, which partially counterbalances the reduction in its active power generation. The minimum profit has been reduced considerably (by 32%). The maximum and average values for the bidding parameters are higher in Case 17, as the generating firms attempt to compensate for their loss in profit due to the reduced active power generation. The average nodal price is higher in Case 17 than in Case 16, being in agreement with the observations in the smaller systems.

5.3.4 Discussion on the impact of limitations on the reactive power generation and absorption based on the numerical results of Cases 9 to 17

The numerical results in test Cases 9 to 17 have shown that the variation of the limits of the generating units' reactive capabilities have a significant impact on the electricity market outcome. The simulations on the 3-bus and the IEEE 14-bus systems have shown that when a limitation is imposed on either the reactive generation or absorption of the generating units, the active and reactive power generations and load demands are reduced, resulting in increased nodal prices across the system and lower social welfare, depending on the level of confinement of the reactive power limits. As anticipated, the generating firms alter their bidding strategies in order to favour their profits, which are in general reduced due to the reductions in active power generation. It has also been shown that the impact of limiting the reactive power generation is more intense than that of confining the reactive power absorption. The observations for the test cases

performed on the IEEE 118-bus system are in good agreement with those on the smaller systems.

5.4 Investigation of the load power factor adjustments

Variations of the load power factor, which is defined as $\text{p.f.} = \cos\theta = \cos[\tan^{-1}(Qd / Pd)]$, are expected to affect the market outcome, since they will result in different values for the equilibrium price-responsive active and reactive load demand. Test cases have been performed for a range of lagging load power factors, i.e. all loads are of inductive nature, with the benchmark corresponding to zero reactive load demand, i.e. to unity load power factor. The load power factor for the 3-bus and IEEE 14-bus systems is equal at all buses, for each case.

5.4.1 Load power factor adjustments: 3-bus system results

The 3-bus system used for Cases 18 to 21 is identical to that in Section 5.2.1. Case 18 corresponds to unity load power factor and Cases 19 to 21 are performed by successively reducing the power factor by steps of 0.1. The numerical results for the market outcome are provided in Table 5.14. Note that Case 21 with power factor of 0.7 is the same as Case 2.

TABLE 5.14
CASES 18 TO 21 FOR THE 3-BUS TEST SYSTEM: MARKET OUTCOME

Case No.	Load Power Factor	Nodal Prices λp_i (£/MWh)			Bidding Strategies		Generating Firm's Profit (£/hour)		$\sum Pg_i$	$\sum Qg_i$	$\sum Pd_i$	$\sum Qd_i$	Social Welfare (£/hour)
		λp_1	λp_2	λp_3	k_{F1}	k_{F2}	F_1	F_2					
18	**1.0**	**28.9**	**28.9**	**28.9**	**1.513**	**1.715**	**1430**	**2407**	**3.24**	**0.23**	**3.24**	**0**	**5634**
19	**0.9**	**29.2**	**29.2**	**29.2**	**1.545**	**1.718**	**1221**	**2656**	**3.14**	**1.83**	**3.14**	**1.52**	**5573**
20	**0.8**	**32.6**	**32.6**	**32.6**	**1.746**	**2.000**	**1209**	**2216**	**2.15**	**1.78**	**2.15**	**1.62**	**4222**
21	**0.7**	**33.1**	**33.1**	**33.1**	**1.772**	**2.070**	**1213**	**1702**	**1.79**	**1.94**	**1.79**	**1.83**	**3601**

- ***Cases 18 and 21: Results for the 3-bus system*:**

By comparing the four test cases on the 3-bus system, it can be seen that as the value of power factor decreases the nodal prices increase and the social welfare decreases, as a consequence of the higher bidding parameters submitted by the strategic firms. Lower load power factors entail higher reactive and lower active load demand, hence the reactive generation is increasing towards lower values of the power factor, but the active generation is decreasing. Thus, despite the higher nodal prices in Cases 20 and 21, the generating firms receive less profit than in Cases 18 and 19 due to the much lower active production.

5.4.2 Load power factor adjustments: IEEE 14-bus system results

The description of the IEEE 14-bus system is the same as in Section 5.3.2. The linear inverse load demand functions at the system buses were set to $D_{Pd_i} = 40 - 0.060Pd_i$ £/MWh for $i = 1 \text{ to } 5$, $D_{Pd_i} = 40 - 0.065Pd_i$ £/MWh for $i = 6 \text{ to } 9$, and $D_{Pd_i} = 40 - 0.080Pd_i$ £/MWh for $i = 10 \text{ to } 14$. Cases 22 to 24 correspond to load power factors of 1.0, 0.9 and 0.8 respectively. The results for the generating firms and the social welfare are provided in Table 5.15 and the power distribution is shown in Table 5.16. The nodal prices are graphically presented in Figure 12, allowing direct comparison between the test cases.

TABLE 5.15
CASES 22 TO 24 FOR THE IEEE 14-BUS SYSTEM:
FIRMS' PROFITS, BIDDING PARAMETERS AND SOCIAL WELFARE

Case No.	Load Power Factor	Generating Firms' Profit (£/hour)					Bidding Strategies					Social Welfare (£/hour)
		F_1	F_2	F_3	F_4	F_5	k_{F1}	k_{F2}	k_{F3}	k_{F4}	k_{F5}	
22	**1.0**	**3187**	**3750**	**3026**	**2197**	**1920**	**1.496**	**1.470**	**1.497**	**1.292**	**1.164**	**20210**
23	**0.9**	**3159**	**3401**	**2894**	**1786**	**1329**	**1.557**	**1.559**	**1.576**	**1.369**	**1.311**	**17210**
24	**0.8**	**3231**	**2713**	**2767**	**1575**	**915**	**1.611**	**1.673**	**1.651**	**1.409**	**1.361**	**14710**

TABLE 5.16
CASES 22 TO 24 FOR THE IEEE 14-BUS SYSTEM: POWER DISTRIBUTION IN THE NETWORK

Case No.	Load Power Factor	Pg_1	Pg_2	Pg_3	Pg_6	Pg_8	Qg_1	Qg_2	Qg_3	Qg_6	Qg_8	$\sum Pd_i$	$\sum Qd_i$ inductive	$\sum Qd_i$ capacitive
22	**1.0**	**2.84**	**3.36**	**2.72**	**2.56**	**2.50**	**-0.03**	**0.23**	**0.06**	**0.82**	**0.43**	**13.66**	**0**	**0**
23	**0.9**	**2.59**	**2.74**	**2.35**	**1.81**	**1.48**	**0.88**	**1.49**	**1.07**	**1.50**	**1.15**	**10.75**	**5.21**	**0**
24	**0.8**	**2.46**	**1.96**	**2.05**	**1.49**	**0.93**	**1.44**	**1.50**	**1.49**	**1.50**	**1.15**	**8.73**	**6.55**	**0**

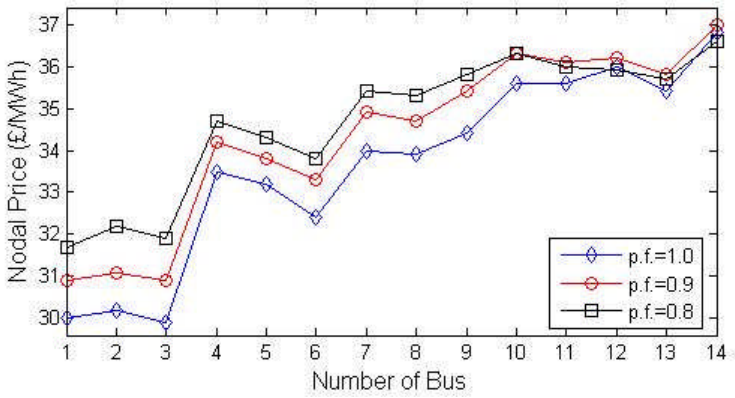

Figure 12: Nodal prices for Cases 22 to 24.

- ***Cases 22 and 24: Results for the IEEE 14-bus system*:**

As the power factor moves away from the value of 1.0 in Cases 22 to 24, the generators in the system are required to produce more reactive power to cover the increasing reactive load demand, and as a consequence the active production and total active load demand decrease. The nodal prices in the part of the system where the generators are situated (buses 1 to 9) show considerable increments as the active generation is reduced, as can be seen in Figure 12. On the contrary, the prices at buses 10 to 14, which are remote from the generating units, increase for the first step-down of the power factor, while they show a small decrease for the second step-down, despite the fact that these buses have higher demand functions than buses 1 to 9. The social welfare is successively reduced by equal shares of 15% as the power factor decreases by steps of 0.1, since the active load demand decreases accordingly to the power factor as the reactive demand is increasing.

For each subsequent decrement of the power factor all the generating firms are increasing their bidding parameters in order to maintain their profits, as a

reaction to the reduction in the active production requirements. None of the firms, except firm F_1, succeeds in this, since the higher bidding parameters and the increased nodal prices were not sufficient to compensate for the loss in profit due to the reduction in active power. Indeed, firm F_5, which suffers the largest active generation reduction (63%) between Cases 22 and 24, receives a profit reduced by 52%. Firm F_1 that suffers the lowest reduction in active production has only a small reduction in profit for the first step-down of the power factor, while for the second one it receives higher profit even compared with the unity power factor case. The low reduction in its active power production stems from the fact that, in Case 22, unlike the other units that were producing noticeable amounts of reactive power, the unit of firm F_1 was absorbing only a very small amount of reactive power from the network. Therefore, the increased reactive generation of that unit had only a small impact on the active production, and when it submitted a higher bidding parameter in Case 24, in conjunction with the higher nodal price at bus 1, it received a higher profit than in Cases 22 and 23.

5.4.3 Load power factor adjustments: IEEE 118-bus system results

The IEEE 118-bus system is investigated to show the impact of adjusting the load power factor at all the buses of a large system to the value of 1.0, when previously it was operated with different power factors at each bus. The system description is the same as in Section 5.3.3. In Case 25, the system buses have different values of lagging load power factors, ranging from 0.766 to 0.986, and four buses have unity power factors. The average load power factor for the system, calculated by considering the values of the individual power factors at each bus separately, is 0.906. In Case 26 the reactive load demand in the system is set to zero, for unity load power factor. The results for maximum, minimum and average values for nodal prices, firms' profits and bidding parameters are presented in Table 5.17, while the power distribution in the network and social welfare are shown in Table 5.18.

TABLE 5.17
CASES 25 TO 26 FOR THE IEEE 118-BUS SYSTEM: RESULTS FOR COMPARISON

Case No.	Unity Power Factor	Average Nodal Price (£/MWh)	Profit (£/hour)			Bidding Strategies k_F		
			max	min	average	max	min	average
25	No	**33.45**	**9441**	**495**	**2886**	**2.405**	**0.731**	**1.348**
26	Yes	**33.53**	**9758**	**1299**	**3024**	**2.411**	**0.084**	**1.127**

TABLE 5.18
CASES 25 TO 26 FOR THE IEEE 118-BUS SYSTEM: POWER DISTRIBUTION AND SOCIAL WELFARE

Case No.	Unity Power Factor	$\sum Pg_i$	$\sum Qg_i$ generation	$\sum Qg_i$ absorption	$\sum Pd_i$	$\sum Qd_i$	Social Welfare (£/hour)
25	No	**121.44**	**43.62**	**-0.22**	**120.19**	**53.00**	**202400**
26	Yes	**128.15**	**0.64**	**-11.38**	**127.01**	**0**	**210900**

- ***Cases 25 and 26: Results for the IEEE 118-bus system*:**

In Case 25 where the system load power factor is lagging, being less than 1.0, the reactive power absorption by the generating units is almost negligible compared with the reactive power generation, as shown in Table 5.18. In Case 26, where the reactive load demand is removed from all buses in the system, the reactive power generation has been reduced substantially (by 98.5%), since there is no reactive load demand to be satisfied. On the other hand, the reactive power absorption has been greatly increased. The overall active power generation has been increased by about 6% in the unity power factor case, since the active load demand has been increased as the reactive load demand was set to zero. Therefore, the social welfare is larger for the unity power factor case, being in agreement with the observations in the tests on the smaller systems.

The average bidding parameter submitted by the firms has been decreased by about 16% in Case 26, since the overall active power generation is increased. In addition, the shares of the active power and of the level of bidding parameters on the firms' profits were readjusted. Note that, in Case 26, the minimum bidding parameter appears to be about 10 times smaller than that of Case 25. The average profit in Case 26 has been increased by about 5% compared to Case 25, as the generating firms were benefited by the increased active production and the higher nodal prices. The maximum profit, which corresponds to the same

generating unit for both cases, has been slightly increased (by 3%), while the minimum profit has been substantially increased by 160%.

5.4.4 Discussion on the impact of load power factor adjustments based on the numerical results of Cases 18 to 26

The results obtained by performing load power factor adjustments show that as the power factor is decreasing, thus the reactive load demand is increasing, the active power generation and load demand in the system are considerably reduced, resulting in higher nodal prices and lower social welfare. As a reaction to the reduced active production requirements, the firms alter their strategies in order to maintain their profits. This cannot always be the case, due to the high reductions in active power that result in much lower profits for most firms.

The large changes observed on the minimum values of the profits and bidding parameters in the IEEE 118-bus system test cases, resulting from the power factor variations, show that vast alterations can occur at particular buses or areas in the system, which will result in an evident effect on certain firms' profits. The nodal prices have been found to be increased or decreased as the system load power factor varies, depending on the position of each bus and the reduction in active power generation in the surrounding area.

Comparing the cases for the examined systems, it can be observed that a larger system requires much more reactive power absorption by the generating units for unity power factor operation, than that required by smaller systems (absorption normalised to the corresponding active power generation). If strict reactive power absorption limits were required to be imposed on the generating units of a large system, as performed in Case 15 in Section 5.3.2, during the unity power factor operation, a definite effect is expected on the overall market outcome.

5.5 Conclusions for Chapter 5

Three different control methods related to the reactive power in the system have been examined in order to determine their impact on the strategic behaviour of the generating firms and the resulting effects on the electricity market equilibrium. Each of the investigations has provided evidence that the presence of reactive power in the network has a significant impact on the interactions between the strategic firms and on the electricity market outcome. The strategies of the firms are dependent on the variation of the system's reactive power and on the relative location of the individual generating units. The alterations in the strategic offers result in different nodal prices and therefore in different social welfare and redistribution of the profits among the generating firms.

Depending on the employed voltage regulation mode on the generation buses of the system, the firms change their strategies since the required generation levels, and hence the load demand, are directly affected. The application of voltage control on the generation buses results in higher nodal prices and lower social welfare under normal operating conditions compared to the uncontrolled case. On the contrary, in the presence of transmission congestion, the voltage control may reduce the high nodal prices caused by the congestion in the network being in favour of the social welfare.

The variations on the reactive power generation and absorption limits have a major impact on the power distribution in the network as a result of the reduced reactive capabilities of the generating units. Such limitations have the effect of considerable reductions in active and reactive generation, with the consequence of lower active and reactive load demand due to their price responsiveness, and the strategic firms anticipate this by submitting higher bids as an attempt to increase or maintain their profits. The impact on the market outcome in such circumstances is higher nodal prices and lower social welfare due to the considerable reductions in active production and load demand. These effects become greater as the limits grow tighter, with the impact of confining reactive generation being more severe than that of reactive absorption. In addition, it has

been shown that the change in the firms' profits is also dependable on the proximity of the generating units to the limited reactive capabilities areas.

As the load power factor is decreasing from the value of 1.0, the reactive load demand increases and the active load demand is expected to be reduced. Therefore, this has a direct impact on the active and reactive power generation, resulting in lower active production requirements for all the generating firms. The firms will then change their strategies in order to favour their profits by increasing their bids. The higher bidding parameters in conjunction with the lower active generation and load demand result in higher nodal prices and hence lower social welfare. However, the numerical results performed with load power factor step reductions of 0.1 and on the large system have shown that the increase in the market price is not sufficient to cover the loss due to the high reductions in active production, resulting in lower producers' surplus.

The aforementioned observations on the variation of the market outcome due to the reactive power control methods have proven the importance of representing the reactive power and voltage constraints in the electricity market equilibrium models. The reactive power modelling, in terms of power flows, generation and load demand, reveals the diverse manner in which the strategic firms exercise market power by exploiting the AC nonlinearities in realistic systems, which cannot be disclosed by examining models with DC linearized systems. The strategic behaviour of the generating firms is found to be dependent on the voltage regulation employed on the generation buses, the limitations on the reactive capabilities of the generating units and the allocated load power factors across the network. Hence, by considering these factors in the electricity market equilibrium model, a more realistic prediction for the electricity market outcome and a better interpretation of the interactions between the strategic firms can be obtained. The observations for the impact of the three different reactive power control methods on the electricity market are found to have several similarities, but the conclusions drawn are subject to the topology of the network, since reactive power is of zonal nature.

Chapter 6:
Choosing the location for the generating unit of a new entry in the electricity market

6.1 Introduction to the investigation of the locations of new entries in the electricity market

The liberalisation of the electricity sector has introduced competition at the generation level in order to give incentives to new generating firms to attempt to enter the electricity market. However, only a small number of independent generating firms have endeavoured to compete with the well-established state owned utility companies. This is the result of the distinctive characteristics and operational complexities of generating, transmitting and distributing the electrical power, which lead to economic implications that act as an entry barrier in the market for potential players, as already discussed in Chapter 1. The unique nature of the electricity market compels any potential generating firms to investigate several issues before attempting to enter the game. Most of these issues do not usually apply to markets of other commodities, but their consideration in the case of the electrical power pool trade will help the new generating firms to plan an efficient future strategy. Some features that the new firms may find essential to consider primarily are the ability of the existing firms to exercise market power for profit-maximisation, the available transmission capacities, the expected congestion conditions in the network, and the presence and levels of reactive power in the system. Furthermore, it may be important to obtain predictions for the capabilities and marginal costs of the generating units of the rival firms, and for the ISO obligations on maximising the social welfare, while an investigation on all the possible locations for situating their new generating units should be conducted.

The existing literature on the investigation of the new entries in the electricity market is mainly concerned with the entry barriers that exist due to the high

investment costs and predatory pricing, the facilitation of ease of entry, and the increase in capacity availability due to the additional generation investment after a new firm successfully enters the market. Such analyses and discussions can be found in [33,35,7,8,81,100,17,192]. However, to the best of my knowledge the choice of the best location for installing a new generating unit in the system, based on meshed AC network modelling, has not been examined in the existing literature. The following study raises the suspicion that by performing an investigation to obtain the optimum location for a new generating unit based on profit-maximising or other relevant criteria, the choice of the location may prevail over the existing entry barriers and a potential firm may overcome the hesitation of entering the market, motivated by the level of the expected future profits.

The research presented in this chapter shows that the choice of the location for a new firm to install new generating units is a crucial consideration. The investigation is concerned with how a potential generating firm can choose the best location to situate a new generating unit in order to achieve the highest profit possible. The analysis focuses on the effect of the location of the new unit on the profits of both the new firm and the existing companies, while the impact on the social welfare, nodal prices and bidding strategies is also discussed. Such analysis is made possible by the implementation of AC-network constrained market models, such as the one presented in this Thesis, which is able to handle large nonlinear systems with asymmetric firms and considers the operational aspects of the system.

6.2 Numerical results: the choice for the best location of a new entry's generating unit

The investigation for the choice of a new entry's location for new generating units takes place on the IEEE 14-bus system using the k_F-parameterization algorithm. The system structure is similar as in Section 5.3.2, but the version of the system used is presented in Figure 13 [191] for a more comprehensive interpretation of the numerical results. Each of the 5 generating units corresponds

to an existing firm, with a subscript corresponding to its bus number, e.g. F_8 for the firm that owns the unit at bus 8, for the ease of the market outcome comparison. The new entry will be represented by adding another generating unit in the system.

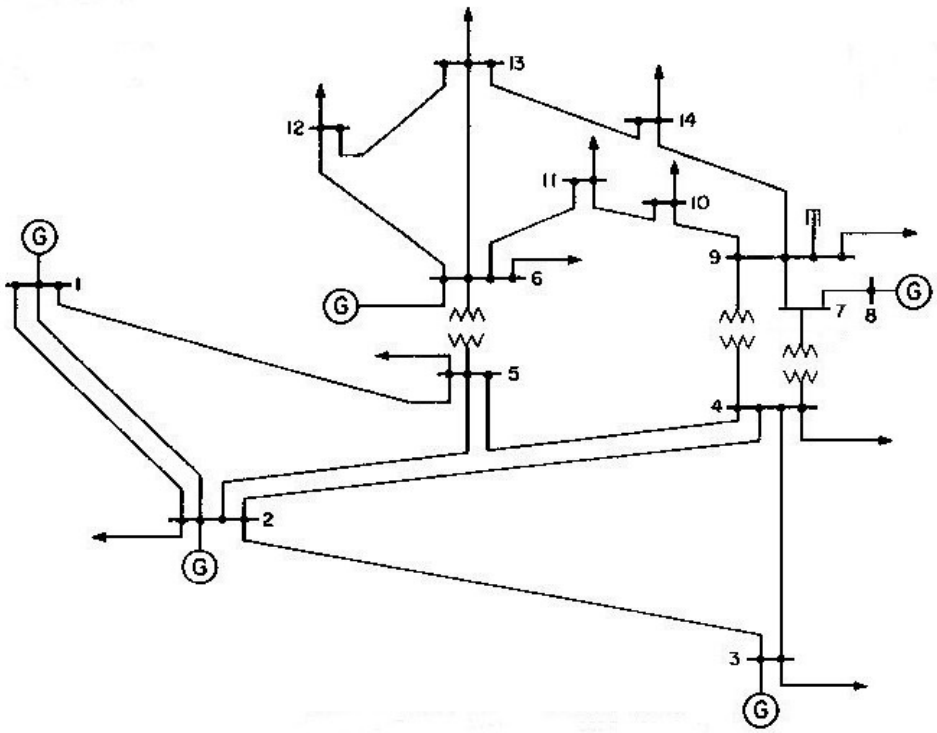

Figure 13: The modified IEEE 14-bus system.

The marginal cost functions of the generating units are:

$$MC_{Pg_i} = 17.5 + 0.009 Pg_i \text{ £/MWh} \quad \text{for } i = 1, 2, 3 \tag{6.1}$$

$$MC_{Pg_6} = 22.5 + 0.010 Pg_6 \text{ £/MWh} \tag{6.2}$$

$$MC_{Pg_8} = 25.0 + 0.010 Pg_8 \text{ £/MWh} \tag{6.3}$$

$$MC_{Pg_{new}} = 17.0 + 0.010 Pg_{new} \text{ £/MWh} \tag{6.4}.$$

The maximum active power generation capacities for the units in the system are set to:

$$Pg_{1,2,3}^{\max} = Pg_{new}^{\max} = 4.0 \text{ p.u.} \tag{6.5}$$

$$Pg_6^{\max} = 3.5 \text{ p.u.} \tag{6.6}$$

$$Pg_8^{\max} = 2.5 \text{ p.u.} \tag{6.7}.$$

The system is separated into two load demand zones. Zone 1 that includes buses 1 to 9 corresponds to lower quadratic load demand coefficient compared to Zone 2, which consists of buses 10 to 14. Hence, the load demand in Zone 1 has higher price responsiveness than Zone 2. Their linear inverse load demand functions are given by $D_{Pd_{Zone1}} = 40 - 0.06Pd_i$ £/MWh for $i = 1 \text{ to } 9$ (Zone 1), and $D_{Pd_{Zone2}} = 40 - 0.08Pd_j$ £/MWh for $j = 10 \text{ to } 14$ (Zone 2).

The test case performed for the initial electricity market structure before any potential player enters the game, where only the original five generators are connected on the system, is termed as the Base Case. Further tests, Cases 1 to 8, were performed by adding a new generator at different buses of the system successively, to simulate the effects of the new entry on the market. All the possible locations were examined but since, for some buses, the conclusions drawn were similar as those for adjacent buses, some cases have been omitted to avoid repeated discussions. The power distribution in the network is given in Table 6.1, where the results for the reactive power are also shown to emphasise the employment of the AC power network representation. The results for the firms' profits, bidding parameters and social welfare are presented in Table 6.2. Table 6.3 provides information about the nodal prices on selected buses (see Section 6.2.3). All the power terms are calculated in p.u.

TABLE 6.1
NUMERICAL RESULTS FOR THE POWER DISTRIBUTION IN THE NETWORK

Case	Location of new entry	Pg_1	Pg_2	Pg_3	Pg_6	Pg_8	Pg_{new}	Qg_1	Qg_2	Qg_3	Qg_6	Qg_8	Qg_{new}	$\sum Pd_i$	$\sum Qd_i$
Base	--	**2.76**	**3.22**	**2.63**	**2.55**	**2.26**	--	**1.09**	**1.43**	**0.52**	**2.38**	**1.21**	--	**13.13**	**5.31**
1	Bus 1	**1.20**	**3.30**	**2.64**	**2.55**	**2.26**	**1.58**	**0.24**	**1.45**	**0.53**	**2.40**	**1.22**	**0.86**	**13.24**	**5.35**
2	Bus 2	**2.88**	**1.75**	**2.39**	**2.44**	**2.15**	**2.07**	**1.17**	**0.63**	**0.61**	**2.44**	**1.21**	**0.82**	**13.36**	**5.42**
3	Bus 3	**2.77**	**3.03**	**1.35**	**2.52**	**2.21**	**1.72**	**1.10**	**1.52**	**0.26**	**2.41**	**1.21**	**0.21**	**13.28**	**5.34**
4	Bus 5	**2.71**	**2.31**	**2.44**	**1.08**	**1.79**	**3.99**	**0.77**	**1.15**	**0.43**	**1.98**	**1.22**	**2.24**	**14.06**	**5.66**
5	Bus 6	**2.76**	**2.88**	**2.52**	**0.01**	**2.19**	**4.00**	**1.07**	**1.45**	**0.52**	**1.67**	**1.22**	**0.97**	**14.03**	**5.67**
6	Bus 9	**2.76**	**3.18**	**2.62**	**2.67**	**~0**	**4.00**	**0.95**	**0.94**	**0.21**	**2.01**	**1.06**	**2.24**	**14.97**	**6.11**
7	Bus 10	**2.81**	**3.07**	**2.58**	**2.43**	**1.35**	**3.48**	**1.01**	**1.22**	**0.38**	**2.22**	**1.15**	**1.45**	**15.38**	**6.45**
8	Bus 12	**2.85**	**3.11**	**2.61**	**1.81**	**2.25**	**1.97**	**1.07**	**1.44**	**0.50**	**2.21**	**1.33**	**0.36**	**14.30**	**5.66**

TABLE 6.2
NUMERICAL RESULTS FOR THE FIRMS' PROFITS, BIDDING STRATEGIES AND SOCIAL WELFARE

Case	Location of new entry	Generating Firms' Profit (£/hour)						Bidding Strategies						Social Welfare (£/hour)
		F_1	F_2	F_3	F_6	F_8	F_{new}	k_{F1}	k_{F2}	k_{F3}	k_{F6}	k_{F8}	k_{Fnew}	
Base	--	**3125**	**3640**	**2968**	**2220**	**1758**	--	**1.505**	**1.482**	**1.508**	**1.297**	**1.244**	--	**19640**
1	Bus 1	**1431**	**3678**	**2956**	**2210**	**1750**	**1924**	**1.613**	**1.472**	**1.503**	**1.295**	**1.242**	**1.613**	**19980**
2	Bus 2	**3111**	**1996**	**2731**	**2130**	**1677**	**2419**	**1.474**	**1.558**	**1.526**	**1.301**	**1.247**	**1.558**	**20320**
3	Bus 3	**3123**	**3430**	**1520**	**2194**	**1718**	**1973**	**1.502**	**1.493**	**1.569**	**1.298**	**1.245**	**1.569**	**20100**
4	Bus 5	**3036**	**2738**	**2810**	**982**	**1323**	**5085**	**1.500**	**1.551**	**1.530**	**1.361**	**1.243**	**1.512**	**22370**
5	Bus 6	**3062**	**3266**	**2842**	**6**	**1701**	**4652**	**1.494**	**1.499**	**1.514**	**1.361**	**1.245**	**1.315**	**22180**
6	Bus 9	**3051**	**3504**	**2890**	**2336**	**~0**	**5500**	**1.491**	**1.472**	**1.495**	**1.294**	**3.350**	**1.102**	**24010**
7	Bus 10	**3106**	**3428**	**2870**	**2121**	**1009**	**3961**	**1.489**	**1.483**	**1.503**	**1.302**	**1.257**	**1.471**	**23810**
8	Bus 12	**3182**	**3516**	**2939**	**1573**	**1748**	**2255**	**1.493**	**1.488**	**1.509**	**1.320**	**1.244**	**1.551**	**21930**

TABLE 6.3
SELECTED NODAL PRICES (£/MWHOUR)

Case	Location of new entry	Examined bus	Base Case nodal price	Final nodal price	Price reduction
5	Bus 6	Bus 6	**32.5**	**30.6**	**1.9**
6	Bus 9	Bus 9	**34.6**	**32.7**	**1.9**
7	Bus 10	Bus 10	**35.6**	**30.1**	**5.5**
7	Bus 10	Bus 11	**35.5**	**33.3**	**2.2**
8	Bus 12	Bus 12	**36.0**	**29.4**	**6.6**

6.2.1 The interactions between the new firm and the existing firms

The entrance of the new firm in the market by installing a new generating unit on the network results in a significant change on the profits of the existing firms, while they alter their bidding strategies as an attempt to favour their benefits. By observing test Cases 1 to 8 in Table 6.2, it can be seen that, for all cases, the existing generator located at the bus where the new generating unit is connected submits higher bidding factor and generates lower active power than those of the other cases, and receives its lowest profit among all the test cases.

Firms F_6 in Case 5 and F_8 in Case 6 produce negligible amounts of active power and consequently receive almost zero profits. For both cases, the ISO has chosen to assign almost the entire active production needed to satisfy the active load

demand for the particular areas to the new firm's generating unit, which is reaching its maximum active generation limit. This decision of the ISO is based on the fact that the new generator's marginal cost is lower than those of the existing units at buses 6 and 8, as can be seen in (6.2)-(6.4), which are reflected on the submitted bids. Therefore, by preferring the new generator, the pool can assure the required active power and favour the social welfare at the same time, according to (3.54). Since the rival firms, F_6 in Case 5 and F_8 in Case 6, produce an approximately zero active production, their profits are not satisfactory, leading to economic failure. Compared with the Base Case, these firms have both increased their bidding parameter as an effort to raise the market clearing price and achieve acceptable profits, but this strategic action was not sufficient to confront the economic threat introduced by the generator of the new entrant with the lower marginal cost.

Comparing the marginal costs of the existing generating units at buses 1, 2 and 3 with that of the new generator, given in (6.1) and (6.4) respectively, it can be seen that one of the cost coefficients is slightly larger and the other is slightly lower. Therefore, in Cases 1, 2 and 3, the new unit does not supplant the existing unit situated at the same bus but the active production assigned to each generator is determined from the market equilibrium, in order to satisfy the optimisation conditions.

6.2.2 The choice for the best location for the new generating unit

By considering the above observations regarding the effects on the profits of the generating firms when the location of the new entry's generating unit is varied, the location that is the most beneficial for the new firm can be determined. If the only criterion considered is the maximisation of the new entrant's profit, then the best location is at bus 9, as in Case 6. If the fact that the presence of the new firm forces an existing company to economic failure raises political issues and the new entrant is concerned that it may be difficult to obtain a permit for building a power plant, Cases 5 and 6 should be rejected. Therefore, considering the existing results, the new company should choose to install the new generating unit at bus 5, as in Case 4, for facilitating a more convenient entry process.

The choice for the location of the new entry may also be affected by other factors, for instance, the price responsiveness of the load demand at particular areas of the system. If the new firm decides to install its generator in Zone 2, for which the load demand has lower price responsiveness, the choice for the best location will be at bus 10. This will result in the highest profit in Zone 2 compared with the other four locations and the new firm will not monopolise in the surrounding area. If the options are confined within Zone 1, then the selection for the location of the new unit should be either at bus 9, or bus 5 to avoid possible complications from political issues, as discussed above.

6.2.3 The effects of the new entry on the nodal prices and the social welfare

After the new entry connects its generating unit on the system, the market clearing price is changing compared with that of the Base Case and the nodal prices at several buses show substantial reductions. The largest reductions always occur at the vicinity of the new generator as expected. The nodal prices results for these cases are shown in Table 6.3, where the examined bus and the number of the case that is compared with that of the Base Case are indicated. For Cases 5 and 6 the nodal price reduction is 1.9 £/MWh, while for Cases 7 and 8 the reductions are 5.5 and 6.6 £/MWh respectively, at the buses where the new generator is located. Also in Case 7, the nodal price reduction of the bus adjacent to the new generator's bus is also high, being 2.2 £/MWh. In view of the above, it can be observed that the nodal price reductions in the adjacent area of the bus where the new generator is situated are more intense if the new entry is located at the buses with the lower price responsiveness load demand (Zone 2) rather than in Zone 1.

From the results for the social welfare in Table 6.2, it can be seen that after the new entry installs a new generator in the network the social welfare is always higher than that of the Base Case, independent of the location of the new unit. This is accompanied by the fact that after the new firm enters the market, the active load demand in the system is always higher than that of the Base Case, as shown in Table 6.1.

6.3 Conclusions for Chapter 6

A new entry in the electricity market seriously affects the profits and bidding strategies of the existing firms, while the social welfare increases independent of the new entry's location, as the active load demand rises, and substantial reductions on the nodal prices occur at the area where the new generating unit is installed. The increments for the social welfare observed on the examined system are as high as 22%, while nodal price reductions of the level of 18% have occurred. The highest nodal price reductions have been observed for the cases where the new unit is situated within the zone with the lower price-responsiveness load demand.

The location of the new generator dictates the alterations in the firms' profits, social welfare, nodal prices and power distribution in the network. It has been shown that the generators owned by existing firms in the system located at the vicinity of the new unit will undergo severe reductions in their active power production and profits, and under certain circumstances the effects of the new entry may lead an existing company to economic failure. The rescheduling of active production to different generating units from the ISO after the new entry is connected to the system, and hence the profits redistribution and after-effects on the existing firms, depend on the relative difference between the marginal cost functions of the various units.

The location of the generating unit owned by the new entrant is crucial for its profit, as well as for that of its rivals. It has been observed from the numerical results that the new entry receives different profits at different locations in the network. For example, at buses 1 and 3 it receives less than 2000 £/hour, while at buses 5 and 9 its profit exceeds the level of 5000 £/hour. This diversity in profits for the available locations in the system may be an adequate reason for the new entrant to overcome the possible entry barriers, as a particular location may be proved profitable enough to deal with them. Based on such thinking, the best location for the firm that enters the market to install its new generating unit has been successfully determined for the examined IEEE 14-bus system. The

decision for choosing the location to connect the new generating unit can be taken by finding the bus that leaves the highest profit for the new firm, while the choice may be confined by other factors such as political issues and the preference of connecting the new unit in different load demand zones in the system.

The investigation for choosing the best location for a new generating unit has been successfully conducted using the proposed AC market equilibrium model. This study has shown that the topology of the network is of critical importance in the case of electricity market analysis and the implemented market models should represent the meshed network features of the electric grid and the associated AC operational constraints. Such models must be versatile and robust, in order to provide the ability to adapt for the investigation of a wide range of power systems in terms of size and complexity.

Chapter 7:
Modelling of grid-connected photovoltaic systems in the electricity market equilibrium algorithm

7.1 Introduction to photovoltaic (PV) technology

It is widely accepted that the present levels of dependence on fossil fuels are unsustainable due to the natural resources depletion, the climate change related to CO_2 emissions and the predicted economic growth of emerging markets. The expected increase of the world population in accordance with the continuous economic development of many countries has as a direct consequence an increase in energy demand. At present, most of the energy supply is directly acquired using fossil fuel technologies, which are now reaching their limits in supply and source, while their usage has serious consequences on the environment. Steps for improvement have been undertaken, especially from the EU, for the development and large-scale deployment of a range of new and more sustainable technologies. A number of targets have been set for the integration of new energy technologies, with an important step being the commitment of the EU Member States to cover 20% of the total energy needs by utilising the available indigenous RES by 2020 commencing from the beginning of 2008 [28].

One of the most attractive and potential sources of energy considered to be able to meet the future energy needs is the sun. Installations of PV cells and modules around the world have seen a rapid growth in the past years at an average annual rate of more than 35%. The year-end worldwide cumulative installed capacity of solar PV systems has been increased from 1200 MW in 2000 to 9200 MW in 2007 [193]. According to the Greenpeace and European Photovoltaic Industry Association (EPIA) 2008 scenario [193], if adequate support mechanisms are adopted to make solar electricity competitive and serious commitment is made to

energy efficiency, the solar power produced globally will satisfy the electric needs of almost 14% of the world's population by 2030. Such figures correspond to a capacity of 281 GW, for which 60% of this would be in the grid-connected market. The associated grid-connected PV systems are expected to cover the energy needs of 1.28 billion people.

Even though the generation costs for PV systems are currently higher than other energy sources, the electricity prices from the impending large-scale PV energy production are expected to compete with the generation costs of fossil and nuclear sources, as economies of scale prevail. Such considerations stem from the fact that the PV generation costs have already been decreased in a trend expected to accelerate, while the general electricity prices from conventional sources are steadily rising [193]. As far as the EU electricity markets are concerned, solar electricity is expected to become cost competitive with residential electricity prices within the next few years, especially in Southern Europe; Central Europe is expected to gradually follow by 2020 (see [193], p. 41, Fig. 4.1). In the light of the above, the impact of grid-connected PV systems in the energy market needs to be investigated.

In addition to the attractive features in terms of future savings in electricity prices, supporting measures are employed for the promotion of solar electricity. The most effective market support mechanism for PV power generation has been the introduction of feed-in laws, which helps to diminish the present differences between the high PV installation costs and the operational costs of conventional generators. These laws oblige the system operator to purchase the power generated by the PV units at a predetermined feed-in tariff for a specified period of time (generally 20 years), giving motivation for PV investment and further expansion of the PV-based power markets. The feed-in tariffs for different countries vary depending on the resource conditions, such as the level of solar irradiance, and such support programmes are considered to be necessary until about 2020 [193].

The following study has been performed in order to examine the new environment that emerges as the power generation market is shifting from its

entirely conventional nature to a diverse market able to accommodate grid-connected PV plants in conjunction with the recent liberalisation of the electricity sector. The priority in scheduling the RES energy first in predetermined tariffs is expected to affect the electricity prices in bid-based markets, while the presence of PV generation, which is dependent on the level of solar irradiance and subject to the weather conditions, in the pool may further affect the market and network operational conditions. Furthermore, if the incumbent generating firms take into consideration the nature of PV generation and its presence in the electric grid while planning their bidding strategies, alterations may be observed on the interactions between them, with direct consequences on the overall market outcome.

7.2 Modelling the economic aspects of grid-connected PV systems in the electricity market model

The investigation of the integrated electricity market that considers conventional sources and grid-connected PV systems for power generation is initiated by modelling the economic aspects of PV generating units and the associated processes in the market equilibrium algorithm presented in Chapter 3. The market assumptions for the bid-based pool market, the ISO process and the behaviour of the strategic firms that own the conventional generating units in the system are the same as in Section 3.6. The additional considerations for integrating the PV generation in the model are outlined as follows.

The actual marginal cost of generation MC_{PV} of a PV generating unit is assumed to be constant, such that:

$$MC_{PV} = a_{PV} \tag{7.1}$$

since the PV generation cost does not change when producing different amounts of power. Note that a major advantage of PV technology is the low operational cost, which is negligible compared to its capital cost. However, the PV cost coefficient a_{PV} is much larger than the marginal cost of a conventional generating unit in operation due to the high capital cost for the PV installation. In the following market analysis the PV units are considered to have priority in the

market and they do not behave strategically. Instead, it is assumed that they bid their entire output to the pool at a predefined bidding function B_{PV}, being equal to the lowest linear cost coefficient α of the conventional generating units in the system, rather than revealing their true marginal cost. This is done in order to resemble competitive behaviour and at the same time avoid a higher market clearing price due to the extremely high true marginal cost MC_{PV}, as the ISO will schedule the PV unit's entire output first (since the B_{PV} function will always be lower than the marginal costs of the strategic generators in operation). Then, the PV units are paid the nodal prices at their bus and in addition they receive state subsidy for the quantity produced. Therefore, the feed-in tariff T_{PV} for the PV units is defined as:

$$T_{PV} = \lambda_{PV} + SS_{PV} \quad £/\text{MWh} \tag{7.2}$$

and therefore the profit acquired for the scheduled PV generation Pg_{PV} is:

$$\Pi_{PV} = (T_{PV} - MC_{PV})Pg_{PV} \quad £/\text{hour} \tag{7.3}$$

where λ_{PV} is the nodal price at the bus where the PV unit is located, and SS_{PV} is the state subsidy for the PV power produced. The state subsidy is not considered during the calculation of the social welfare in order to avoid deadweight gain complications as it is an exogenous factor, but it is considered for computing the profit of the PV units.

7.3 Numerical results using the PV systems economic model

In order to illustrate the effects of representing the economic aspects of grid-connected PV generating units in the electricity market algorithm before proceeding to the modelling of the PV operational aspects, numerical results on the IEEE 14-bus system that take into account the assumptions in Section 7.2 are presented below. The solar PV power generation units are assumed to generate active power at rated output value, which is entirely sold to the pool. The PV reactive power output in this section is considered to be negligible.

The description of the IEEE 14-bus system is the same as in Section 5.2.2. The 5 conventional generators, which are located at buses 1, 2, 3, 6 and 8 are owned by individual strategic firms, entitled F_1 to F_5 respectively. For the test cases that

incorporate PV power generation 5 solar PV generating units are connected to the system (located at buses 10 to 14), which are owned by a single firm F_{PV}. The marginal cost functions of the strategic generating units are:

$$MC_{Pg_1} = MC_{Pg_3} = 15 + 0.010Pg \quad (7.4)$$

$$MC_{Pg_2} = 15 + 0.008Pg \quad (7.5)$$

$$MC_{Pg_6} = 11 + 0.008Pg \quad (7.6)$$

$$MC_{Pg_8} = 18 + 0.008Pg \quad (7.7).$$

The actual marginal cost for each PV generating unit is:

$$MC_{PV} = 120 \text{ £/MWh} \quad (7.8).$$

The bidding function for each PV unit is set to be equal to the constant term of the cheapest conventional generating unit in the system, thus being:

$$B_{PV} = 11 \text{ £/MWh} \quad (7.9).$$

The state subsidy is assumed to be:

$$SS_{PV} = 150 \text{ £/MWh} \quad (7.10)$$

thus the feed-in tariff for each PV unit is:

$$T_{PV} = (\lambda_{PV} + 150) \text{ £/MWh} \quad (7.11)$$

and the profit for each PV unit is:

$$\Pi_{PV} = (\lambda_{PV} + 30)Pg_{PV} \text{ £/hour} \quad (7.12).$$

Test Cases 1 and 2 correspond to normal operating conditions with no network constraints binding, while tight limits have been set on two transmission lines in Cases 3 and 4 in order to impose congestion in the system. The 5 grid-connected PV generating units owned by firm F_{PV} are introduced in the system in Cases 2 and 4 and the market outcome is compared with Cases 1 and 3, for which the PV units are disconnected from the network and hence there is no PV generation present. The PV units in Cases 2 and 4 are assumed to cover 10% of the total available generation capacity in the system[5], while the other 90% corresponds to the capacity of the conventional generators. The results for the firms' profits, the power distribution in the network and the social welfare are provided in Table

[5] The 10% figure is used in accordance to the 13% target for share of RES energy in final consumption set for Cyprus by the EU directive [28]. Solar energy is the main renewable energy source available in Cyprus throughout the year.

7.1, the bidding strategies of the conventional generating units in Table 7.2, and the nodal prices in Table 7.3. The power quantities are calculated in p.u.

TABLE 7.1
CASES 1 TO 4 FOR PV SYSTEMS: FIRMS' PROFITS, POWER DISTRIBUTION AND SOCIAL WELFARE

Case No.	PV Generation	Network congestion	Generating Firm's Profit (£/hour)						$\sum Pg_i$	$\sum Qg_i$	$\sum Pd_i$	$\sum Qd_i$	Social Welfare (£/hour)
			F_1	F_2	F_3	F_4	F_5	F_{PV}					
1	No	No	**1074**	**3915**	**3239**	**4526**	**1375**	--	**8.94**	**0.52**	**8.77**	**3.11**	**18490**
2	Yes		**641**	**4073**	**3243**	**3215**	**819**	**12716**	**9.55**	**0.56**	**9.43**	**3.38**	**20870**
3	No	Yes	**1456**	**1938**	**1934**	**5324**	**1380**	--	**5.58**	**-0.81**	**5.49**	**1.93**	**12600**
4	Yes		**1336**	**1838**	**1852**	**4605**	**1591**	**13424**	**6.75**	**-0.26**	**6.68**	**2.36**	**15590**

TABLE 7.2
CASES 1 TO 4 FOR PV SYSTEMS: FIRMS' BIDDING STRATEGIES

Case No.	PV Generation	Network congestion	Generating Firm's Profit (£/hour)				
			k_{F1}	k_{F2}	k_{F3}	k_{F4}	k_{F5}
1	No	No	**1.949**	**1.789**	**1.767**	**2.410**	**1.767**
2	Yes		**2.017**	**1.798**	**1.780**	**2.560**	**1.798**
3	No	Yes	**2.175**	**2.170**	**1.413**	**1.738**	**1.895**
4	Yes		**2.107**	**1.297**	**1.404**	**1.217**	**1.347**

TABLE 7.3
CASES 1 TO 4 FOR PV SYSTEMS: NODAL PRICES

Bus No. (firm)	Nodal Prices λp_i			
	Case 1 (no PV)	Case 2 (with PV)	Case 3 (no PV)	Case 4 (with PV)
1 (F_1)	**30.6**	**31.1**	**34.3**	**33.2**
2 (F_2)	**30.7**	**30.9**	**34.8**	**33.8**
3 (F_3)	**30.5**	**30.7**	**34.8**	**34.0**
4	**32.6**	**32.7**	**34.7**	**34.3**
5	**32.6**	**32.8**	**35.2**	**34.4**
6 (F_4)	**31.1**	**31.5**	**38.4**	**34.8**
7	**33.2**	**33.2**	**31.6**	**33.2**
8 (F_5)	**33.1**	**33.1**	**35.4**	**34.3**
9	**33.8**	**33.6**	**42.9**	**38.1**
10 (F_{PV})	**34.8**	**33.7**	**42.7**	**37.9**
11 (F_{PV})	**34.6**	**33.2**	**41.3**	**36.9**
12 (F_{PV})	**35.6**	**33.8**	**40.0**	**36.7**
13 (F_{PV})	**34.3**	**32.9**	**40.1**	**36.4**
14 (F_{PV})	**36.3**	**34.3**	**41.9**	**37.7**

- ***Cases 1 to 2: No binding constraints*:**

Cases 1 and 2 have been studied in order to examine the effect of solar PV power generation on the electricity market under normal network operating conditions. From Table 7.2 it can be observed that in the presence of solar PV generation in Case 2, the generating firms have increased their bidding parameters affecting the market equilibrium and the market clearing price. In Case 2, the profits for firms F_1, F_4 and F_5 have been significantly reduced compared with Case 1, despite the higher submitted bids and the higher nodal prices. This is a result of the fact that a portion of the demand in Case 2 is satisfied from the PV power generation and the scheduled production of the aforementioned firms is reduced. From Table 7.3 it can be seen that the nodal prices at buses 10 to 14 where PV generation exists in Case 2 are significantly reduced compared with Case 1, whereas as moving away from the area of PV generation this is not the case. No change is observed for the nodal prices at intermediate buses between conventional and PV generation centres, while slight increments occur in the vicinity of the conventional generators due to the higher bid offers submitted from the strategic firms in Case 2. The total active power generation output, and hence the load demand in the system, have been increased in Case 2 thus the social welfare is higher compared to Case 1. The much higher profit of firm F_{PV} compared with the profits of the conventional generating firms in Case 2 occurs due to the support of the state subsidy.

- ***Cases 3 to 4: Binding network constraints*:**

The effect of PV generation on the electricity market when the network is operated in stressed conditions is examined in Cases 3 and 4. The nodal prices in Case 3 are much higher compared to Case 1 due to the network congestion. In Case 4 where the PV units produce electricity and therefore additional competitive supply exists, all the strategic firms have been forced to decrease their bidding parameters (especially the units at buses 2, 6 and 8), resulting in lower profits, except for firm F_5 which manages to increase its profit because of a small increase in its power generation. Reductions in nodal prices are observed in almost all buses, with the largest decrements, up to 4.8 £/MWh, at the buses where PV generation exists. In Case 4 the total active generation output has been increased compared to Case 3, due to the presence of PV generation. Thus the

social welfare has also been increased. The profit of firm F_{PV} in Case 4 is higher than that of Case 2 due to the higher nodal prices caused by the network congestion, which are incorporated in the feed-in tariff function (7.2).

7.4 Discussions on the PV economic model

It has been shown that the introduction of PV generation in the system reduces the market clearing price, since the firm that owns the PV generating units acts in a competitive manner. It has been observed that in the presence of network congestion the existence of PV generation forces the strategic conventional generating firms to decrease their bidding parameters in order to cope with the increased availability of supply. In either case, the social welfare is increased when PV generation is introduced, since the level of the price-responsive load demand in the system rises. It is important to note that, since the PV power generation output is entirely dependent on the solar irradiance, which in turn is dependent on the weather conditions that cannot be accurately forecast, it is understood that the strategic generating firms can take advantage of the lack of solar irradiance and hence competitive PV power generation, and act in an uncompetitive manner to attempt to force the nodal prices to rise at a particular bidding time interval in order to favour their profits.

Considering that the EU has set ambitious targets regarding the penetration of RES power generation in the system, it can be anticipated, based on the results presented above, that the introduction of RES generation, in the form of PV or other renewable weather-dependent energy sources, may cause problems in centralised markets as unpredictable price fluctuations may occur. In the case where the solar irradiance is inadequate for the PV units to generate power and there is lack of RES availability to satisfy the load demand, the market will be dependent entirely on conventional generation and with the exercise of market power from the strategic firms the prices would probably increase. This issue may be more intense if the network is not well designed for avoiding congestion that could be favourable for the strategic generating firms during peak demand intervals. Furthermore, this effect is likely to be more severe in small isolated

networks in which a large proportion of the generation capacity is expected to be satisfied by installing grid-connected PV systems in the forthcoming years. Such examples include the island of Cyprus and other Southern European isolated regions with no interconnection to the central European grid. A sudden change in the weather conditions can have a crucial impact on the outcome of the market, provided that the strategic firms are aware of the potential lack of availability in RES power supply.

In order to avoid undesired consequences on the market outcome, the weaknesses of the new diverse electricity market environment must be identified and the relevant authorities governing the market should take measures to keep the electricity prices at reasonable levels. Furthermore, the network system operators may be required to consider the possible strategic actions of the firms during the system design process, in order to avoid exploitation of a possible lack of availability in RES power generation that would result in higher nodal prices at the expense of social welfare. In order to investigate in depth the situation where the solar irradiance that produces the PV power output varies, the modelling of the operational aspects of grid-connected PV systems that explicitly represents the PV active and reactive power generation considering the relevant power quality issues takes place in the following section.

7.5 Modelling the operational aspects of grid-connected PV systems in the electricity market model, in terms of active and reactive PV power output

As more renewable energy systems are employed all over the world in order to provide alternative sources of electricity production and reduce CO_2 emissions from conventional power plants, certain issues that need to be addressed arise. In particular, for PV systems connected to the grid, one parameter of critical importance is the variation of the PV power output with respect to the intensity of solar irradiance. In order to examine the impact of the active and reactive power injected to the electric grid by PV generating units, as functions of the solar irradiance incident to the PV panel, on the electricity market, the following

model that is incorporated into the electricity market equilibrium algorithm is implemented based on real-life PV output performance data collected from an experimental PV park. The material and recorded data presented in Sections 7.5.1 and 7.5.2 have been provided by members of Academic Staff of the Department of Electrical and Computer Engineering, University of Cyprus, Nicosia, CY-1678, Cyprus. The information on the experimental PV units is provided only for reference. The investigation of the properties, specifications and function of the utilised experimental equipment is far beyond the scope of this analysis.

7.5.1 Experimental PV equipment

The University of Cyprus maintains an innovative experimental outdoor test facility for the performance evaluation of the latest PV technologies. The PV Park consists of 14 grid-connected PV systems of nominal power 1 kWp each, installed to provide the opportunity for direct performance comparisons under the climate conditions of Cyprus. For these, the annual irradiation measured by a pyranometer installed on the PV modules' plane has been 1997 kWh/m^2 with maximum contribution during the summer period. Twelve of the systems are mounted on mounting racks at the optimal inclination angle of 27.5° for annual yield in Cyprus and the other two are 2-axis tracking systems. The installed PV technologies involve a range from fixed system mono crystalline, multi crystalline silicon to amorphous thin film silicon, cadmium telluride (CdTe), $CuInGaSe_2$, HIT-cell and other solar cell technologies from various manufacturers. A detailed description of the PV technologies available on site can be found in [194]. The facility is equipped with meteorological instruments, which are connected to a central data acquisition system. Parameters that are measured at a resolution of a second include the solar global irradiation, wind direction and speed, and ambient and module temperature.

7.5.2 Processing the data collected from the experimental PV park

An experiment to record power measurements from the PV units has been performed according to the European standards EN50160: 1999 [195] and

EN61727: 1996 [196] in order to investigate the impact of the variation of solar irradiance on the output of the PV systems. The measurements for the electrical quantities were recorded using an analyser system, which comprises a central power quality analyser station, voltage clamps and current transformer sensors. The device can sample and record data when connected to the phases of a power system, taking measurements at desirable time intervals. In this evaluation the sample rate was 5 minutes for a time period of two weeks. The current and voltage sensors were connected to the three-phase output of the PV installation and measurements of the active and reactive power generation were taken. For the purpose of this investigation, the correlation between the power generation output and the level of solar irradiance was established.

The measurements of the active and reactive PV power generation were transformed into the per-unit system and normalised over each sampling interval. Statistical methods were used to construct graphical functions that relate the PV output to the applied normalised (%) solar irradiance *s*. The best fit representation for each power generation component was obtained by applying the least squares method on the power quality data collected. The model function used for the active power output p_{PV} is:

$$p_{PV} = m_1 + m_2 s \tag{7.13}$$

and for the reactive power output q_{PV} is:

$$q_{PV} = m_3 + m_4 \exp\{-0.5[\ln(s / m_5) / m_6]^2\} \tag{7.14}$$

where the *m* terms are the adjustable parameters to be determined. The active power delivered to the electricity network from the PV system has been found to vary linearly as the intensity of the applied solar irradiance increases, as shown in Figure 14, which is in good agreement with the work presented in [197-198]. In contrast, the reactive power produced by the PV system varies nonlinearly with the solar irradiance, as shown in Figure 15, having higher VAR values at low intensities.

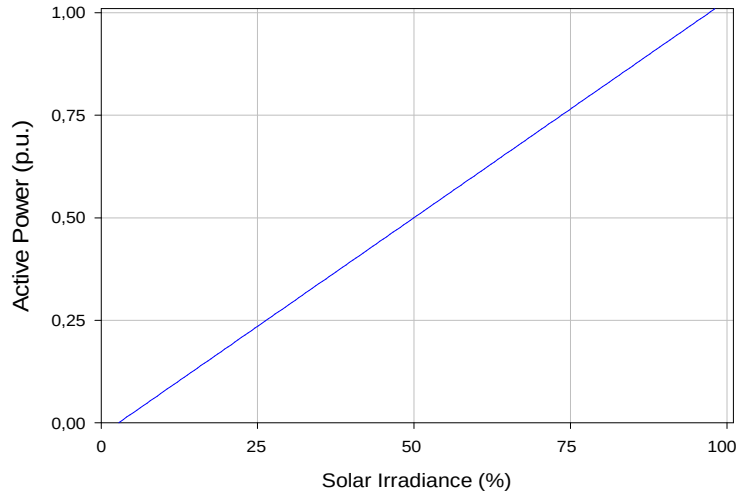

Figure 14: Best fit representation of the PV active power output vs. normalised solar irradiance.

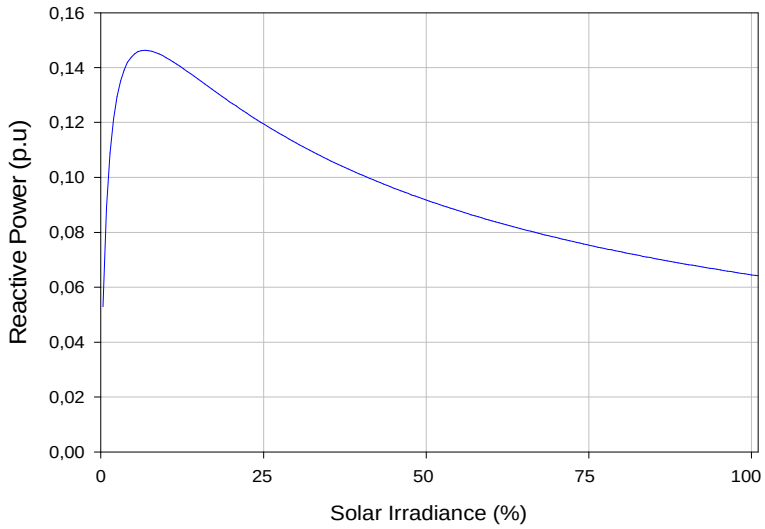

Figure 15: Best fit representation of the PV reactive power output vs. normalised solar irradiance.

7.5.3 Modelling the PV output performance in the electricity market algorithm

The economic aspects of the PV generating units have been modelled in the algorithm as in Section 7.2. The PV active and reactive power output is represented in the electricity market model according to the percentage intensity

of the solar irradiance chosen to be present for each case scenario. By specifying an input solar irradiance (%) incident to the PV panel, the level of the p.u. PV active power generation is determined from the experimental graph shown in Figure 14 and the corresponding p.u. PV reactive power generation is taken from the best-fit curve shown in Figure 15.

In order to investigate the effects of each component of the PV power generation on the electricity market outcome, the examined scenarios in the numerical results that follow are tested by two different models. The first model considers only the PV active power generation performance taken from Figure 14, referred to as "*Pg only*" model, while the second one considers both the PV active and reactive output components from Figures 14 and 15, referred to as "*Pg and Qg*" model. Note that in the following sections, for the cases where the *Qg* component of the PV generation is not modelled, all the other reactive power components of the system, including reactive power generation from the conventional generating units, are still present in the model. This is done in order to emphasise on the effects of the PV reactive generation.

7.6 Numerical results using the economic-operational PV systems model: the effect of the solar irradiance-dependent PV active and reactive power generation on the electricity market

Numerical tests were performed on a 5-bus test system in order to show the effects of the active and also reactive power generation from PV units on the market outcome, for different intensities of solar irradiance. In addition, test cases are performed on the larger IEEE 57-bus system, showing the effects of the PV units under more realistic scenarios. Cases for normal network operation, as well as under transmission congestion, are presented for both systems to show how the PV impact on the market is altered under dissimilar system operating conditions. The transformer tap-ratios for both systems can be optimised within the range of 0.9 to 1.1 and all the power quantities are calculated in p.u.

7.6.1 Numerical results on the 5-bus system

The 5-bus test system used for this investigation consists of 5 buses with load demand, 4 transmission lines, 2 transformer branches with on-load tap-changing transformers and 2 conventional generating units, as shown in Figure 16 (this system is different than the 5-bus system used in Chapter 4). The conventional generators are located at buses 1 and 5 and owned by the strategic firms F_1 and F_2 respectively, while the PV generation unit connected at bus 3 is owned by competitive firm F_{PV}. The bus voltages can be optimised within ±5% from the rated value of 1 p.u.

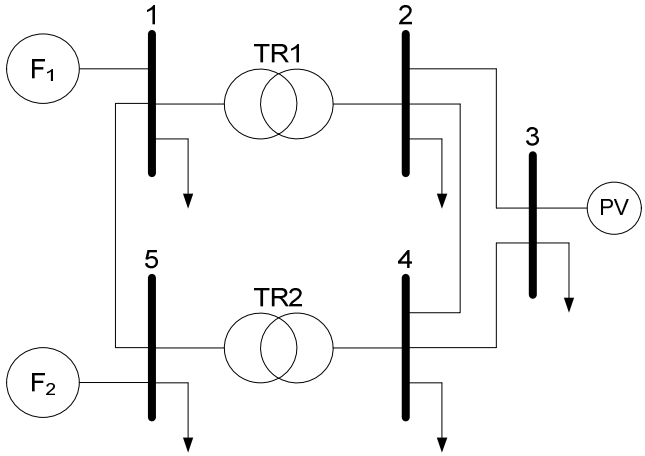

Figure 16: The 5-bus test system for the PV analysis.

The rated generation capacity of the PV unit (i.e. at 100% solar irradiance) is $Pg_{PV}^{\max} = 1\,\text{p.u.}$ and covers the 10% of the total generation capacity of the system[6]. The remaining 90% capacity corresponds to the two conventional generating units, such that $Pg_1^{\max} = 4\,\text{p.u.}$ and $Pg_5^{\max} = 5\,\text{p.u.}$ The marginal cost functions for the strategic generating firms F_1 and F_2 are:

$$MC_1 = 11 + 0.009Pg_1 \text{ £/MWh} \quad (7.15)$$

$$MC_5 = 10.8 + 0.010Pg_5 \text{ £/MWh} \quad (7.16).$$

Therefore, the predefined bidding function for the PV unit is:

$$B_{PV} = 10.8 \text{ £/MWh} \quad (7.17).$$

The actual marginal cost of the PV unit and the state subsidy are set to:

[6] See footnote 5, Section 7.3.

$$MC_{PV} = 125 \text{ £/MWh} \quad (7.18)$$

$$SS_{PV} = 150 \text{ £/MWh} \quad (7.19)$$

respectively. Hence the feed-in tariff is:

$$T_{PV} = (150 + \lambda_3) \text{ £/MWh} \quad (7.20).$$

- ***Cases 5 to 13: Normal operating conditions*:**

Test Cases 5 to 13 were performed with normal network operating conditions and no transmission congestion exists in the system. Case 5 is the reference case in which the solar irradiance is assumed to be zero. Cases 6 to 9 correspond to operations for different intensities of solar irradiance, while only the active power generation of the PV unit is considered in the model. Cases 10 to 13 show the results for the same intensities but with both the active and reactive PV power generation components modelled. The numerical results for Cases 5 to 13 are shown in Figure 17 and Tables 7.4 and 7.5.

From the results for Cases 5 to 9 it can be seen that when the PV unit is connected to the system the nodal prices at all buses are reduced gradually as the solar irradiance increases, with the higher decrement of 1.5 £/MWh being at the bus where the PV unit is situated. The active generation in the system, and hence the active load demand, become higher as the irradiance increases and, as a result, there is a significant rise in social welfare with a higher than 10% increment at full irradiance. Similar effects are observed for Cases 10 to 13 where the reactive generation of the PV unit is also considered, but with slightly

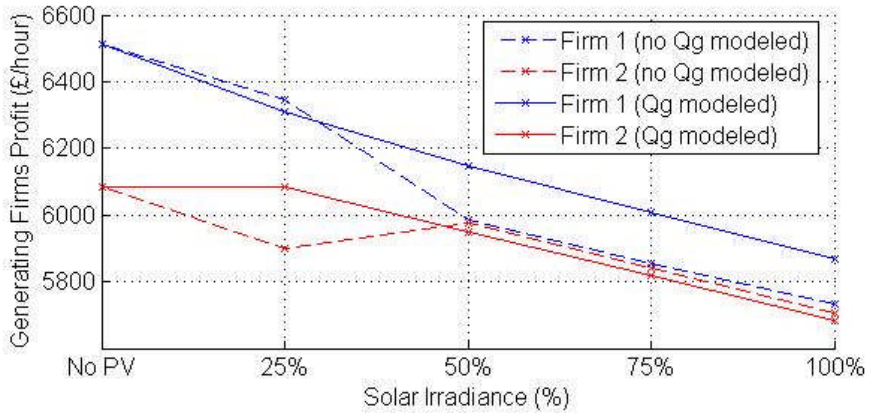

Figure 17: Cases 5 to 13 for PV systems: Strategic firms' profits (no congestion).

TABLE 7.4
CASES 5 TO 13 FOR PV SYSTEMS: NODAL PRICES (NO CONGESTION)

Case No.	Solar Irradiance	Nodal price (£/MWh)					PV model
		Bus 1	Bus 2	Bus 3	Bus 4	Bus 5	
5	No PV	**29.6**	**31.0**	**31.5**	**31.0**	**29.7**	--
6	25%	**28.7**	**30.1**	**30.8**	**30.2**	**28.7**	*Pg only*
7	50%	**28.5**	**29.9**	**30.5**	**30.0**	**28.5**	
8	75%	**28.5**	**29.8**	**30.2**	**29.9**	**28.5**	
9	100%	**28.4**	**29.7**	**30.0**	**29.8**	**28.5**	
10	25%	**28.7**	**30.1**	**30.7**	**30.2**	**28.7**	*Pg and Qg*
11	50%	**28.6**	**30.0**	**30.5**	**30.1**	**28.7**	
12	75%	**28.6**	**29.8**	**30.3**	**30.0**	**28.6**	
13	100%	**28.6**	**29.7**	**30.0**	**29.8**	**28.6**	

TABLE 7.5
CASES 5 TO 13 FOR PV SYSTEMS: POWER DISTRIBUTION AND SOCIAL WELFARE (NO CONGESTION)

Case No.	Solar Irradiance	$\sum Pg_i$	$\sum Qg_i$	$\sum Pd_i$	$\sum Qd_i$	Social Welfare (£/hour)	PV model
5	No PV	**7.41**	**4.69**	**7.30**	**3.53**	**16412**	--
6	25%	**7.93**	**4.90**	**7.81**	**3.78**	**17310**	*Pg only*
7	50%	**8.06**	**4.89**	**7.95**	**3.85**	**17618**	
8	75%	**8.14**	**4.86**	**8.04**	**3.89**	**17872**	
9	100%	**8.23**	**4.84**	**8.13**	**3.94**	**18121**	
10	25%	**8.00**	**4.97**	**7.88**	**3.82**	**17425**	*Pg and Qg*
11	50%	**8.08**	**4.92**	**7.98**	**3.86**	**17677**	
12	75%	**8.17**	**4.89**	**8.07**	**3.91**	**17927**	
13	100%	**8.25**	**4.86**	**8.16**	**3.95**	**18169**	

smaller decrements of the nodal prices at the buses of the two conventional generators. In addition, the increment of the social welfare for the first step increase of solar irradiance is lower between Cases 5 and 10 than that between Cases 5 and 6, since the PV reactive generation is at a high level.

The profits of the strategic firms for Cases 5 to 9 (shown by the dashed lines of the graph in Figure 17) show an irregular variation as the solar irradiance increases. The profit of firm F_1 (blue dashed line) decreases for all increments of the irradiance but with a higher change for the second step than for the others. The profit of firm F_2 (red dashed line) decreases for the first increment of the irradiance, increases for the second, and for the other two is decreasing by the

same amount. However, the pattern of the profits variation changes when the reactive power of the PV unit is considered in the model as in Cases 10 to 13 (solid lines in Figure 17). Both profits are decreasing by the same amounts for all increments of irradiance, except that of firm F_2 for the first step that stays the same. The profit of F_1 for Cases 9 and 13 (100% solar irradiance) is found to differ by more than 130 £/hour due to the modelling of the PV reactive generation.

- ***Cases 10 to 18: Network congestion*:**

The tests for Cases 14 to 22 were performed in the presence of network congestion. A maximum transmission limit was enforced on branch 1-2, such that $S_{12}^{\max} = 1.0$ p.u., in order to impose transmission congestion in the network. Case 14 is the reference case with no PV connected at the system. Cases 15 to 18 are performed using the "*Pg only*" PV model, while Cases 19 to 22 are performed using the "*Pg and Qg*" PV model. The market results are shown in Figure 18 and Tables 7.6 and 7.7.

Case 14 is the benchmark with zero solar irradiance, for which the nodal prices are much higher than those in Case 5 due to the congestion, except of the price at bus 1 that is supplied locally by the isolated firm F_1. As the solar irradiance increases, in both PV generation models, the nodal prices at the buses where the conventional generators are located increase slightly or remain the same as these firms increase their bids. Significant decrements are observed for the nodal prices of the other buses with a difference of up to 2.7 £/MWh due to the extra active

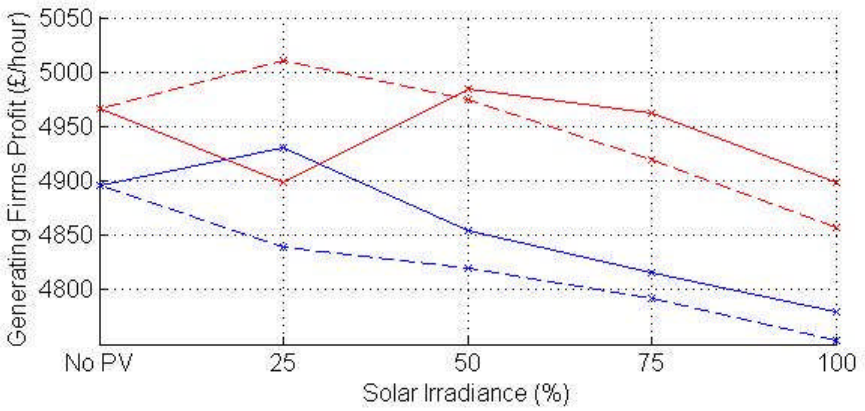

Figure 18: Cases 14 to 22 for PV systems: Strategic firms' profits (congestion).

TABLE 7.6
CASES 14 TO 22 FOR PV SYSTEMS: NODAL PRICES (CONGESTION)

Case No.	Solar Irradiance	Nodal price (£/MWh)					PV model
		Bus 1	Bus 2	Bus 3	Bus 4	Bus 5	
14	No PV	**29.2**	**35.8**	**35.2**	**34.0**	**30.2**	--
15	25%	**29.2**	**35.0**	**34.5**	**33.4**	**30.1**	*Pg only*
16	50%	**29.6**	**34.3**	**33.8**	**33.0**	**30.3**	
17	75%	**29.7**	**33.6**	**33.2**	**32.6**	**30.2**	
18	100%	**29.8**	**33.1**	**32.7**	**32.3**	**30.2**	
19	25%	**29.2**	**35.3**	**34.7**	**33.6**	**30.1**	*Pg and Qg*
20	50%	**29.2**	**34.4**	**33.9**	**33.1**	**30.0**	
21	75%	**29.7**	**33.7**	**33.3**	**32.7**	**30.2**	
22	100%	**29.8**	**33.1**	**32.7**	**32.3**	**30.2**	

TABLE 7.7
CASES 14 TO 22 FOR PV SYSTEMS: POWER DISTRIBUTION AND SOCIAL WELFARE (CONGESTION)

Case No.	Solar Irradiance	$\sum Pg_i$	$\sum Qg_i$	$\sum Pd_i$	$\sum Qd_i$	Social Welfare (£/hour)	PV model
14	No PV	**5.65**	**3.20**	**5.60**	**2.71**	**13198**	--
15	25%	**5.93**	**3.33**	**5.88**	**2.84**	**13842**	*Pg only*
16	50%	**6.04**	**3.37**	**5.99**	**2.90**	**14204**	
17	75%	**6.23**	**3.45**	**6.18**	**2.99**	**14672**	
18	100%	**6.40**	**3.53**	**6.36**	**3.08**	**15100**	
19	25%	**5.90**	**3.31**	**5.85**	**2.83**	**13803**	*Pg and Qg*
20	50%	**6.17**	**3.44**	**6.12**	**2.96**	**14421**	
21	75%	**6.26**	**3.48**	**6.21**	**3.01**	**14738**	
22	100%	**6.43**	**3.55**	**6.39**	**3.09**	**15166**	

power supplement by the PV unit. The social welfare in Cases 14 to 22, which is much lower than the corresponding in Cases 5 to 13 due to the congestion, shows higher increments for each step increase of the irradiance, with a final rise of almost 15% between Cases 14 and 18 or 22. Note that the social welfare increment for the "*Pg and Qg*" PV model is less than that of the model that disregards PV reactive generation, as the solar irradiance increases to 25% (where the PV reactive generation is at a high level), in contrast with the corresponding cases in the uncongested scenario.

The profits of the strategic firms in Cases 14 to 22 (Figure 18) are much lower than the corresponding for Cases 5 to 13 (Figure 17) due to the transmission

congestion restrictions that confine the active power generation. In contrast with the uncongested cases, firm F_1 receives lower profit than firm F_2 because the power transmission from its bus is limited. As the solar irradiance increases for the "*Pg only*" PV model, the profit of generator F_1 next to the congested branch is steadily decreasing (blue dashed line), while for F_2's profit (red dashed line) there is an increase as intensity increases to 25% but then it decreases linearly. When the PV reactive generation is considered in the model, the profits of the strategic firms (solid lines) increase or decrease irregularly when PV reactive generation is at high levels (i.e. at low irradiance), while they decrease smoothly for increments at solar intensities higher than 50%.

7.6.2 Numerical results on the IEEE 57-bus system

In order to illustrate further the effects of introducing PV modelling in the electricity market algorithm, test cases were performed under more realistic conditions on the larger IEEE 57-bus system [191]. This system consists of 57 buses of which 42 have load demand, 63 transmission lines, 17 transformer branches with on-load tap-changing transformers and 7 conventional generators, each forming an individual firm. Three PV generating units, each of rated capacity 1 p.u., with a total rated PV generation corresponding to 10% of the total generation capacity of the system, are connected at buses 21, 22 and 23 and owned by firm F_{PV}, which acts competitively. Again, $MC_{PV} = 125$ £/MWh and $SS_{PV} = 150$ £/MWh, and the bus voltages can be optimised within the range of ±10% from 1.0 p.u. Scenarios for two different operational conditions (with and without network congestion) have been performed. For each one, test cases are provided for zero, low (25%), and rated (100%) solar irradiance, examining both PV reactive generation models. For the transmission congestion scenario, the flow through two of the transmission lines of the system (8-9 and 12-13) is confined to 1.75 p.u. The results for normal operating conditions (Cases 23 to 27) are shown in Table 7.8 and those for the cases with transmission congestion (Cases 28 to 32) in Table 7.9.

TABLE 7.8
MARKET OUTCOME FOR CASES 23 TO 27 FOR PV SYSTEMS (NO CONGESTION)

Case No.	Solar Irradiance	$\sum Pg_i$	$\sum Qg_i$	$\sum Pd_i$	$\sum Qd_i$	Firms' surplus (£/hour)	PV profit (£/hour)	Social Welfare (£/hour)	PV model
23	No PV	**20.67**	**6.88**	**20.13**	**5.41**	**33470**	--	**42297**	--
24	25%	**20.20**	**6.78**	**19.70**	**5.46**	**33130**	**4630**	**42385**	*Pg only*
25	100%	**21.50**	**6.73**	**20.99**	**5.54**	**30980**	**16980**	**45690**	
26	25%	**21.39**	**7.19**	**20.87**	**5.73**	**33537**	**4633**	**44143**	*Pg and Qg*
27	100%	**21.75**	**6.90**	**21.24**	**5.66**	**31362**	**17100**	**46165**	

TABLE 7.9
MARKET OUTCOME FOR CASES 28 TO 32 FOR PV SYSTEMS (CONGESTION)

Case No.	Solar Irradiance	$\sum Pg_i$	$\sum Qg_i$	$\sum Pd_i$	$\sum Qd_i$	Firms' surplus (£/hour)	PV profit (£/hour)	Social Welfare (£/hour)	PV model
28	No PV	**19.92**	**6.65**	**19.45**	**5.50**	**32612**	--	**40279**	--
29	25%	**20.66**	**6.82**	**20.20**	**5.67**	**32426**	**4618**	**42114**	*Pg only*
30	100%	**20.81**	**6.67**	**20.32**	**5.59**	**30532**	**17150**	**44236**	
31	25%	**20.79**	**7.10**	**20.32**	**5.82**	**32869**	**4645**	**42506**	*Pg and Qg*
32	100%	**21.30**	**6.99**	**20.80**	**5.81**	**30974**	**17240**	**44980**	

- ***Cases 23 to 32: Results for the IEEE 57-bus system*:**

From the results on the larger system it can be seen that the introduction of the PV units eventuates in higher active load demand and favours the social welfare, especially for the cases with transmission congestion. Furthermore, as the solar irradiance increases from 25% to 100% between Cases 29-30 and 31-32, the power flow through the congested line 12-13 falls to a level lower than the limit relieving the congestion, and hence lowering the nodal prices contributing to the rise of social welfare. The introduction of PV reactive generation in the model further increases the social welfare, with the highest increment being 12% between Cases 28 and 32.

On the other hand, such changes have adverse effects on the strategic producers' surplus, which decreases in all cases, except those when the PV reactive generation is considered and the solar irradiance is at low levels (Cases 26 and 31). For these cases the PV units produce relatively high reactive power and the strategic firms change their strategies to benefit a small increase in their surplus.

However, at full irradiance there are high producers' surplus decrements for all cases and for both PV models, up to about 2500 £/hour, with the reductions for the "*Pg and Qg*" PV model being lower than the corresponding for the "*Pg only*" model. Once again it can be seen that the introduction of the PV reactive power generation in the model affects the profits of the strategic firms, resulting in increments at low solar irradiance rather than decrements (which is the case in the absence of PV reactive generation), and in smaller reductions than for the "*Pg only*" PV model at rated solar irradiance. The profit of firm F_{PV} increases with the solar irradiance as it is proportional to its active production. These results are in good agreement with those for the 5-bus system, showing that the model is applicable to a variety of power systems.

7.6.3 Discussion on the impact of solar irradiance on the electricity market equilibrium and the significance of PV reactive power modelling

In all scenarios where the PV reactive generation is not modelled, the strategic producers' surplus is reduced by the introduction of the PV unit on the system since alternative competitive active power becomes available. However, when PV reactive power is considered, small increments in producers' surplus are observed at low solar irradiance as a consequence of the alteration in the equilibrium strategies that results from the higher reactive power levels of the PV unit. By comparing the two PV reactive models, the producers' surplus for the cases with irradiance levels above 50% is always higher when the PV reactive generation is incorporated in the model, as the presence of the PV reactive generation enables different equilibrium strategies in both congested and uncongested scenarios.

The social welfare is raised when the PV generating unit is connected to the system for all test cases and is increasing with the intensity of solar irradiance. By comparing the two PV reactive models it can be seen that, for all cases, the social welfare at rated irradiance is higher when the PV reactive generation is considered due to the higher load demand. For low intensities of solar irradiance the social welfare is higher for the "*Pg and Qg*" model only under normal operating conditions. At the presence of network congestion, the extra PV

reactive power due to its nonlinear characteristic in the "*Pg and Qg*" model contributes to the congestion, since reactive power flows congest the system at the same extent as active transmission, and the resulting price-responsive load demand is lower than expected (since congestion raises the nodal prices; e.g. compare Cases 15 and 19 in Table 7.6). Hence, the social welfare at low solar irradiance is slightly less or at a similar level to that of the "*Pg only*" model.

The profit of the firm that owns the PV generating units is not directly dependent on the alterations of the strategic actions of the conventional generating firms, since PV generation is scheduled prior to the conventional active generation in the market clearing process, but it is affected by the nodal price at the PV unit's bus, which is incorporated into the feed-in tariff. Hence, the PV profit increases with the applied solar irradiance that dictates its active production and is expected to be higher in the presence of network congestion where the nodal prices are raised.

7.7 Conclusions for Chapter 7

The model of grid-connected PV systems, in terms of economic and operational considerations, has been successfully integrated into the electricity market equilibrium algorithm in order to investigate the effects of introducing PV generating units in the electric grid on the electricity market outcome. The PV power output that is directly dependent on the intensity of the applied solar irradiance has been explicitly represented based on statistical analysis on output performance data recorded in an outdoor experimental PV facility. The experimental data have shown that the PV active generation varies linearly with the intensity of solar irradiance, while the PV reactive generation follows a nonlinear relationship with higher VAR levels at low intensities. The PV economic model and two versions of the PV economic-operational model have been examined by obtaining numerical results on a variety of power systems. The two versions of the latter PV model correspond to different representations of the PV power output, in which either only the PV active generation is modelled, or both the active and reactive components of the PV output power are

modelled for a more realistic reflection of the PV unit operation. Comparisons of the different PV models are provided and the evident effects of introducing grid-connected PV generating units in the electricity market, considering the dependency of the PV output on the solar irradiance, have been demonstrated.

The numerical results obtained from the PV economic model have shown that when competitive PV active power is available at normal operating conditions, the strategic firms increase their bids as an attempt to raise the nodal prices and counterbalance the profit reductions due to the decreased scheduled conventional power production. In contrast, at the presence of network congestion, the strategic firms decrease their already high bids in order to increase their scheduled production and maintain their profits, with the consequence of lower nodal prices. The introduction of competitive PV generation results in higher social welfare for all cases.

The consideration of the intensity of the solar irradiance applied to the PV panel as an input to the electricity market model has shown that, if the strategic firms are aware of the operational aspects of the PV systems, the variations of the weather-dependent PV output will have significant effects on the electricity market outcome. Taking into account the expected growth in PV generation density in the electricity markets of the EU Member States, such variations of the PV output performance may be exploited by the strategic conventional generating firms in order to exercise market power as an attempt to increase their profits with the consequence of higher nodal prices and lower social welfare at low-level solar irradiance, especially in small isolated networks.

The comparison of the numerical results of the "*Pg only*" and "*Pg and Qg*" PV models has shown that the representation of the PV reactive generation in the market model is important. By disregarding the modelling of PV reactive generation, lower estimations for the producers' surplus and social welfare at rated irradiance may be obtained, while the social welfare may be overestimated at low irradiance in the presence of congestion. Furthermore, the variation pattern of the strategic firms' profits with respect to the solar irradiance changes significantly at low irradiance levels, if the PV reactive generation is considered

in the model. However, the social welfare is always higher when a PV unit is connected to the system independent of the consideration and the level of PV reactive power.

The impact of grid-connected PV systems on the electricity market equilibrium is found to be significant as the strategic conventional generating firms are able to take advantage of a possible shortage of the weather-dependent competitive PV generation and attempt to raise the market prices in order to favour their profits. The entities that will undertake the expected large-scale diffusion of the RES technologies required by the EU Member States should further investigate this issue by careful consideration of all the associated economic and operational aspects. In particular for the PV systems, the power quality characteristics of the PV output performance and their interrelation with the intensity of the applied solar irradiance should be explicitly addressed, while the equivalent concerns over the range of the available RES should also be examined.

Chapter 8:
Parameterization of supply functions in AC electricity market equilibrium models

8.1 Introduction to the comparison of the different SFE parameterization methods

The analysis that takes place in this chapter follows the discussions provided in Section 2.7 on the parameterization methods employed in the existing literature for the construction of the supply function bid. The numerical results that follow examine the relation between the equilibrium solutions resulting from the four different parameterization methods in the presence of AC network modelling. Since there has been no investigation of the impact of the parameterization chosen on the equilibrium solution, in applications with AC meshed networks or large systems, the proposed market equilibrium algorithm is used to examine several case studies that involve a variety of test systems under different network operational conditions, to further contribute to the subject.

The investigation follows the analysis of [113] and illustrates how the introduction of AC network constraints can affect the market results for the four parameterization methods and the relationships between them. The analysis of the numerical results emphasises the following: (a) comparison of the SFE market outcomes from the four different parameterization methods and investigation of their interrelation; (b) examination of the change of the parameterizations' impact on the solution when subject to different levels of network congestion; and (c) discrimination between the effects on small test systems and on larger more complex networks. Furthermore, comparison of the convergence characteristics of the SFE algorithm for the different parameterization methods is provided in the next chapter.

8.2 Description of the SFE electricity market algorithm for the different parameterization methods

The formulation of the proposed algorithm that takes place in Chapter 3 uses the k_F-parameterization method to construct the supply function bid offer. In order to have a clear picture on how the parameterization method employed affects the formulation of the proposed SFE market algorithm, and hence the resulting SFE solution, the mathematical derivation for the Newton matrix equation that is solved iteratively is briefly described here by considering all the different parameterization types.

The network modelling and the electricity market assumptions are as outlined in Sections 3.5 and 3.6 respectively, with the equation for the supply function bid (3.51) to be adjusted accordingly depending on the parameterization method chosen. Hence, the bid may take one of the following forms that correspond to the α-, β-, k_F- and (α, β)-parameterizations respectively:

$$SB_{F_i} = \hat{\alpha}_{F_i} + \beta_{F_i} Pg_{F_i} \tag{8.1}$$

$$SB_{F_i} = \alpha_{F_i} + \hat{\beta}_{F_i} Pg_{F_i} \tag{8.2}$$

$$SB_{F_i} = k_{F_i} (\alpha_{F_i} + \beta_{F_i} Pg_{F_i}) \tag{8.3}$$

$$SB_{F_i} = \hat{\alpha}_{F_i} + \hat{\beta}_{F_i} Pg_{F_i} \tag{8.4}$$

where $\hat{\alpha}_{F_i}$ and $\hat{\beta}_{F_i}$ are the parameterized terms that dictate the strategic behaviour of the generating firms for the α-, β-, and (α, β)-parameterizations, which correspond to the true cost coefficients α and β from the marginal cost function.

The quasi-social welfare function used for the optimisation problem of the ISO in Section 3.7, equation (3.54) that corresponds to the k_F-parameterization, may be substituted with:

$$\left\{ \Pi_{ISO}(x) = \sum_{i=1}^{NL} (\gamma_i Pd_i - \frac{1}{2}\delta_i Pd_i^2) - \sum_{i=1}^{NG} (\hat{\alpha}_{F_i} Pg_{F_i} + \frac{1}{2}\hat{\beta}_{F_i} Pg_{F_i}^2) \right\} \tag{8.5}$$

for the (α, β)-parameterization formulation, or the $\hat{\alpha}$ or $\hat{\beta}$ terms in (8.5) may be substituted by the true cost coefficients to represent the β- or α-parameterizations respectively.

The inequality for the restrictions on the strategic bids used in the optimisation problem of the generating firms in Section 3.8, equation (3.65) that corresponds to the k_F-parameterized supply function bid is replaced with:

$$b_{F_i}^{\min} \le b_{F_i} \le b_{F_i}^{\max} \tag{8.6}$$

where b_{F_i} is the set of strategic bidding variables depending on the parameterisation method, i.e. the set of all $\hat{\alpha}_{F_i}$, or all $\hat{\beta}_{F_i}$, or all k_{F_i}, or all $\hat{\alpha}_{F_i}$ and all $\hat{\beta}_{F_i}$ terms for all the generating units in the system. The $b_{F_i}^{\min}$ and $b_{F_i}^{\max}$ terms are the limits for the strategic variables present.

The formulation of the market algorithm follows the procedure described in Section 3.9. Depending on the parameterization method chosen, the Lagrange function (3.72) and the resulting KKT condition for the system variables (3.73) for the reformulation of the ISO problem will be different, since they include the quasi-social welfare term Π_{ISO} that depends on the bidding variables b_{F_i}. By proceeding to the formulation of the combined market problem for the equilibrium solution, the optimisation function (3.90) and the equality constraints resulting from the Fiacco-McCormick barrier method (3.91)-(3.92) may require modifications and additional slack variables depending on the bidding variables present. Hence, the Lagrange function (3.94) for the combined problem, which depends on the parameterization method, can be written, such that:

$$\begin{aligned} L_{2\mu} = & -\Pi_F - \mu \sum_{i=1}^{NG} [\ln(sl_{b_{F_i}}) + \ln(su_{b_{F_i}})] + \sum_i \omega_{\lambda_i} [-\Delta G_i] \\ & - \pi l_{b_{F_i}} [b_{F_i} - sl_{b_{F_i}} - b_{F_i}^{\min}] - \pi u_{b_{F_i}} [b_{F_i} + su_{b_{F_i}} - b_{F_i}^{\max}] \\ & + \omega_x [-\nabla_x \Pi_{ISO} - \sum_i \nabla_x \Delta G_i \lambda_i - \sum_n (\pi l_n + \pi u_n) \nabla_x h_n] \\ & + \sum_n \omega_{\pi_n} [-(h_n - s_n - h_n^m)] + \sum_n \omega_{s_n} [\mu - s_n \pi_n] - \sum_i \omega_\Psi \Psi_i \end{aligned} \tag{8.7}$$

where $\pi = [\pi l, \pi u]$, $s = [sl, -su]$, and $h^m = [h^{\min}, h^{\max}]$. The resulting KKT conditions of the combined market problem are provided below in a compact form for coherence:

$$\nabla_{(x,Pd_i)} L_{2\mu} = -\nabla_x \Pi_F + \sum_i \omega_x [-\nabla_x \nabla_x \Pi_{ISO} - \lambda_i \nabla_x \nabla_x \Delta G_i - \sum_n \pi_n \nabla_x \nabla_x h_n] - \sum_i \omega_{\lambda_i} \nabla_{(x,Pd_i)} \Delta G_i - \sum_n \omega_{\pi_n} \nabla_x h_n - \sum_i \omega_\Psi \nabla_{Pd_i} \Psi_i = 0 \quad (8.8)$$

$$\nabla_{\lambda_i} L_{2\mu} = -\sum_i \nabla_{\lambda_i} \Pi_F - \sum_i \omega_x \nabla_x \Delta G_i - \sum_i \omega_\Psi \nabla_{\lambda_i} \Psi_i = 0 \quad (8.9)$$

$$\nabla_{\pi_n} L_{2\mu} = -\sum_i \omega_x \sum_n \nabla_x h_n - \sum_n \omega_{s_n} s_n = 0 \quad (8.10)$$

$$\nabla_{s_n} L_{2\mu} = -\omega_{s_n} \pi_n + \omega_{\pi_n} = 0 \quad (8.11)$$

$$\nabla_{\omega_x} L_{2\mu} = \sum_i [-\nabla_x \Pi_{ISO} - \nabla_x \Delta G_i \lambda_i - \sum_n \nabla_x h_n \pi_n] = 0 \quad (8.12)$$

$$\nabla_{\omega_{\lambda_i}} L_{2\mu} = -\Delta G_i = 0 \quad (8.13)$$

$$\nabla_{\omega_{\pi_n}} L_{2\mu} = -[h_n - s_n - h_n^m] = 0 \quad (8.14)$$

$$\nabla_{\omega_{s_n}} L_{2\mu} = \mu - s_n \pi_n = 0 \quad (8.15)$$

$$\nabla_{\omega_\Psi} L_{2\mu} = -\Psi_i = 0 \quad (8.16)$$

$$\nabla_{b_{F_i}} L_{2\mu} = -\sum_i (\pi l_{b_{F_i}} + \pi u_{b_{F_i}}) \nabla_{b_{F_i}} b_{F_i} - \sum_i \nabla_{b_{F_i}} \omega_x \nabla_x \Pi_{ISO} = 0 \quad (8.17)$$

$$\nabla_{s_{bFi}} L_{2\mu} = \mu - s_{b_{F_i}} \pi_{b_{F_i}} = 0 \quad (8.18)$$

$$\nabla_{\pi_{bFi}} L_{2\mu} = -[b_{F_i} - s_{b_{F_i}} - b_{F_i}^m] = 0 \quad (8.19)$$

where $b^m = [b^{\min}, b^{\max}]$.

The expressions (8.8)-(8.19) represent the market equilibrium problem. It can be observed that equations (8.8), (8.12) and (8.17) include the term Π_{ISO} and equations (8.17)-(8.19) depend on the bidding variables b_{F_i}. Therefore, depending on the parameterization method chosen, the resulting market equilibrium solutions for the four methods are expected to differ from each other. By linearizing the above equations, the Newton matrix equation (3.137) can be re-written with respect to the bidding variables b_{F_i}, such that:

$$\left[\begin{array}{cc:cc:c} H_1 & H_2 & H_3 & H_4 & \\ H_2^T & X_1 & H_4^T & X_2 & B_1 \\ \hdashline H_3^T & H_4 & \multicolumn{2}{c:}{\multirow{2}{*}{0}} & B_2 \\ H_4^T & X_2^T & \multicolumn{2}{c:}{} & \\ \hdashline B_1^T & & B_2^T & & B_3 \end{array}\right] \left[\begin{array}{c} \Delta(x_p, x_d) \\ \hdashline \Delta\omega \\ \hdashline \Delta b_{F_i} \end{array}\right] = \left[\begin{array}{c} -\nabla_{(x_p, x_d)} L_{2\mu} \\ \hdashline -\nabla_{\omega} L_{2\mu} \\ \hdashline -\nabla_{b_{F_i}} L_{2\mu} \end{array}\right] \tag{8.20}$$

where the *H* terms correspond to the contribution of the slack variables and the Lagrange multipliers π and ω; the *X* terms to the contribution of the system variables *x* and the Lagrange multipliers λ; and the *B* terms to the contribution of the strategic variables b_{F_i} and their associated slack and dual variables. The detailed element structure for the *H* and *X* elements (depending on the type of parameterization if they contain the Π_{ISO} term) can be determined using the guidelines from Chapter 3. The slack and dual variables associated with the bidding variables b_{F_i}, which would be present in the *B* sub-matrices, are eliminated from the Newton step vector using Gaussian elimination following the same procedure as in Section 3.9.5 that was applied on the k_{F_i}-related terms. The nonzero entries in the resulting *B* sub-matrices for the (α, β)-parameterization (being analogous to equations (3.150)-(3.152) for the k_F-parameterization) that correspond to the rows of ΔPg, $\Delta\omega_{Pg}$ and $\Delta\alpha_{F_i} / \Delta\beta_{F_i}$ of the Newton step vector are:

$$B_1 = \Delta\beta_{F_i} - \Delta Pg_i = [\omega_{Pg_i}] \tag{8.21}$$

$$B_2 = [\Delta\alpha_{F_i} - \Delta\omega_{Pg_i}\,;\, \Delta\beta_{F_i} - \Delta\omega_{Pg_i}] = [1\,;\, Pg_i] \tag{8.22}$$

$$\begin{aligned} B_3 &= [\Delta\alpha_{F_i} - \Delta\alpha_{F_i}\,;\, \Delta\beta_{F_i} - \Delta\beta_{F_i}] \\ &= [(\pi l_{\alpha_{F_i}} / sl_{\alpha_{F_i}}) - (\pi u_{\alpha_{F_i}} / su_{\alpha_{F_i}})\,;\; (\pi l_{\beta_{F_i}} / sl_{\beta_{F_i}}) - (\pi u_{\beta_{F_i}} / su_{\beta_{F_i}})] \end{aligned} \tag{8.23}.$$

As the Newton matrix equation given in (8.20) depends on the type of parameterization chosen, two different algorithms were coded based on the above mathematical derivations. The first algorithm corresponds to the (α, β)-parameterization and the second one to the k_F-parameterization; the latter is the one used for the market analysis in Chapters 4 to 7. Using the (α, β)-algorithm, the α- and β-parameterization methods can be implemented by adjusting the

limits of the β or α parameters respectively, to force them to equal the true cost coefficient values from the marginal cost functions.

8.3 Introduction to the analysis of the market solution behaviour for the different SFE parameterization methods

In order to examine the behaviour of the market solution under the four different types of parameterization for the supply function bid, numerical results were performed in test systems ranging from 3 to 57 buses. The test systems involve cases with and without transmission congestion, as well as different bus voltage modes, in order to show the interrelations of the network operating conditions to the effects of the different parameterization methods on the market outcome.

The maximum and minimum limits for the parameterized terms in the strategic bids were set to $\alpha^{\min} = 0$, $\alpha^{\max} = 200$, $\beta^{\min} = 10^{-5}$, $\beta^{\max} = 6$, according to [116]. The limits for the bidding parameters k_F were set to $k_F^{\min} = 0$ and $k_F^{\max} = 10$ as in [134]. It has been checked that varying the limits within a reasonable domain does not affect the equilibrium solution. The nodal prices and α coefficients are measured in £/MWh; the profits, social welfare and β coefficients in £/hour; the k_F parameter is dimensionless; and all the power quantities are calculated in p.u. The transformer tap-ratio can be optimized by the ISO within the range of 0.9 and 1.1. The results for the firms' profits are indicated in the Tables by the firm's title, e.g. F_1. The results for the social welfare (S.W.) correspond to the true social welfare and not the quasi function from (3.54) or (8.5).

8.4 Numerical results on the 3-bus test system

The investigation begins with tests on the small 3-bus system shown in Figure 19, which consists of 3 buses with load demand, 3 transmission lines and 2 generators owned by firms F_1 and F_2. The inverse load demand functions are $D_1 = 40 - 0.06Pd_1$ £/MWh and $D_i = 40 - 0.065Pd_i$ £/MWh, for $i = 2, 3$ and the

marginal costs of generation are shown in the system diagram. Three different case scenarios have been simulated (Cases 1 to 3) using all the available parameterization methods and the numerical results for the market solution are shown in Table 8.1.

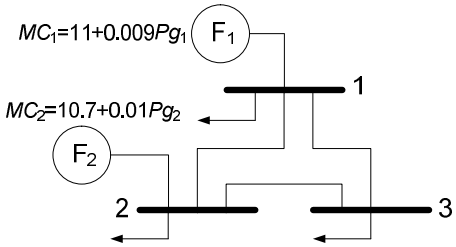

Figure 19: The 3-bus test system for the parameterization analysis.

TABLE 8.1
RESULTS FOR THE 3-BUS SYSTEM: MARKET SOLUTIONS FOR CASES 1 TO 3

Case 1: No Congestion and |V|±10%												
b	λp_1	λp_2	λp_3	F_1	F_2	ΣPg	ΣQg	ΣPd	ΣQd	S.W.	Bid_1	Bid_2
α,β	**26.9**	**26.6**	**27.2**	**3295**	**5442**	**6.10**	**3.19**	**6.08**	**2.94**	**12841**	α_1=0.735 β_1=0.119	α_2=0.063 β_2=0.069
α-	**27.1**	**26.9**	**27.5**	**3344**	**5525**	**6.10**	**3.19**	**6.07**	**2.94**	**12834**	α_1=25.15	α_2=22.96
β-	**27.1**	**26.8**	**27.5**	**3343**	**5526**	**6.10**	**3.19**	**6.08**	**2.94**	**12840**	β_1=0.073	β_2=0.041
k_F	**27.1**	**26.9**	**27.5**	**3344**	**5525**	**6.10**	**3.19**	**6.07**	**2.94**	**12834**	k_{F1}=2.089	k_{F2}=1.841
Case 2: max $S_{2\text{-}3}$ = 0.8 p.u. and |V|±10%												
b	λp_1	λp_2	λp_3	F_1	F_2	ΣPg	ΣQg	ΣPd	ΣQd	S.W.	Bid_1	Bid_2
α,β	**32.2**	**32.0**	**32.5**	**2747**	**4596**	**3.60**	**1.82**	**3.59**	**1.74**	**8790**	$\alpha_1=3\cdot10^{-15}$ β_1=0.241	$\alpha_2=9\cdot10^{-9}$ β_2=0.141
α-	**32.2**	**32.0**	**32.5**	**2780**	**4677**	**3.68**	**1.86**	**3.67**	**1.78**	**8927**	α_1=31.00	α_2=29.63
β-	**29.7**	**28.0**	**31.5**	**3349**	**4706**	**4.86**	**2.48**	**4.83**	**2.34**	**10974**	β_1=0.100	β_2=0.058
k_F	**32.2**	**32.0**	**32.5**	**2776**	**4679**	**3.67**	**1.86**	**3.67**	**1.77**	**8922**	k_{F1}=2.638	k_{F2}=2.453
Case 3: max $S_{2\text{-}3}$ = 0.8 p.u. and |V|±3%												
b	λp_1	λp_2	λp_3	F_1	F_2	ΣPg	ΣQg	ΣPd	ΣQd	S.W.	Bid_1	Bid_2
α,β	**29.1**	**27.0**	**31.3**	**3339**	**4546**	**5.02**	**2.57**	**5.01**	**2.42**	**11229**	α_1=29.21 $\beta_1=1\cdot10^{-4}$	α_2=27.31 $\beta_2=1\cdot10^{-5}$
α-	**29.9**	**28.4**	**31.5**	**3334**	**4709**	**4.74**	**2.44**	**4.73**	**2.29**	**10807**	α_1=28.21	α_2=25.53
β-	**29.7**	**28.0**	**31.5**	**3330**	**4704**	**4.84**	**2.48**	**4.82**	**2.33**	**10953**	β_1=0.100	β_2=0.058
k_F	**29.7**	**28.2**	**31.4**	**3355**	**4700**	**4.81**	**2.47**	**4.80**	**2.32**	**10923**	k_{F1}=2.342	k_{F2}=2.065

Case 1 corresponds to normal operating conditions and no congestion exists in the network, while the bus voltages can be optimized by the ISO within a wide domain of ±10% from the rated value of 1 p.u. The results for the α-, β-, and k_F-

parameterizations are identical, while those for the (α, β)-method show slight differences but still are very close to the others. For the α-, β-, and k_F-parameterizations the bids submitted from both firms are much higher than their marginal costs. On the other hand, the $\hat{a}$ bid coefficients for the (α, β)-parameterization are much smaller than the true values, hence the bids are much smaller than the marginal cost.

Case 2 has the same input data as Case 1, but the MVA transmission limit for line 2-3 is set to $S_{23}^{\max} = 0.8$ p.u., which is binding for all parameterizations. Therefore, Case 2 has higher nodal prices, reduced active and reactive generation, and lower social welfare compared with Case 1. However, the purpose of this investigation is not the comparison of the different network operations (as is the case for Chapters 4 to 7) but of the different parameterization types, for which the deviation of their corresponding solutions seems to be dependent on the network conditions. As can be seen in Table 8.1, the results for Case 2 are similar for the (α, β)-, α-, and k_F-parameterizations, while those for β-parameterization differ. Again, the results of the (α, β)-parameterization have small deviations from the others and the (α, β)-bids are much smaller than the corresponding marginal costs.

For Case 3, the bus voltage limits were lowered to ±3% from 1 p.u. while the line congestion was still present to show that the level of the restrictions on the bus voltages further affects the deviation between the solutions of the different parameterizations. (Note that a case for which the voltage limits were set to ±3% from 1 p.u. and no congestion was present was also performed, but apart from the effects of the voltage mode there were no appreciable differences between the solutions of the four parameterizations, as happened in Case 1.) From the results for Case 3 in Table 8.1 it can be seen that, unlike Case 2, the solution of the β-parameterization has become very similar with those of the α- and k_F-methods, while the results for the (α, β)-parameterization differ from those by a noticeable deviation.

The above results lead to the conclusion that the four parameterizations behave in a different manner in the presence of transmission line congestion and that this impact depends on the bus voltage limits. Under normal operating conditions all methods give similar or identical solutions. When transmission congestion is introduced the β-parameterization gives different market solution from the other three methods, while when the voltage limits are narrowed in the presence of congestion the α-, β- and k_F-solutions become similar, and differ from the (α, β)-solution. For all tests the (α, β)-parameterization has at least a slight deviation from the other methods. In order to back these illations and examine a possible pattern for the observations, further cases are carried out on a 5-bus system.

8.5 Numerical results on the 5-bus test system

The 5-bus system consists of 5 buses with load demand, 3 transmission lines, 2 on-load tap-changing transformer branches and 2 generators owned by firms F_1 and F_2, as shown in Figure 20. The inverse load demand functions are $D_i = 40 - 0.065Pd_i$ £/MWh for $i = 1, 2$ and $D_j = 40 - 0.06Pd_j$ £/MWh for $j = 3, 4, 5$. The numerical results for the 5-bus system are provided in Tables 8.2 and 8.3.

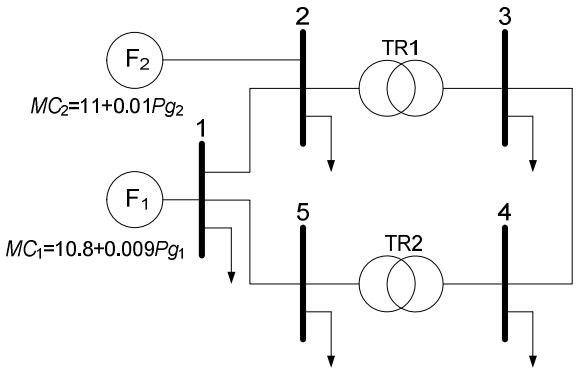

Figure 20: The 5-bus test system for the parameterization analysis.

The tests on the 5-bus system begin with the benchmark Case 4, for which there is no transmission congestion in the network and the bus voltage limits are set to ±5% from 1 p.u. Similarly to Case 1 of the smaller system, the market solutions from the α-, β- and k_F-parameterizations are very similar and there are small differences for the (α, β)-solution, as shown in Table 8.2.

TABLE 8.2
RESULTS FOR THE 5-BUS SYSTEM: MARKET SOLUTIONS FOR CASES 4 TO 6 (|V|±5%)

Case 4: No Congestion and |V|±5%										
b	λp_1	λp_2	λp_3	λp_4	λp_5	F_1	F_2	S.W.	Bid_1	Bid_2
α,β	**31.9**	**31.2**	**32.5**	**33.2**	**33.0**	**2749**	**8188**	**13552**	α_1=31.96 β_1=3·10^{-4}	α_2=31.27 β_2=1·10^{-5}
α-	**31.1**	**30.4**	**31.8**	**32.8**	**32.4**	**2920**	**8124**	**14134**	α_1=29.76	α_2=25.61
β-	**31.1**	**30.4**	**31.8**	**32.8**	**32.4**	**3032**	**8040**	**14157**	β_1=0.131	β_2=0.041
k_F	**31.1**	**30.4**	**31.8**	**32.8**	**32.4**	**2921**	**8124**	**14134**	k_{F1}=2.562	k_{F2}=1.926
Case 5: max $S = 2$ p.u. (branch 2-3 binding) and |V|±5%										
b	λp_1	λp_2	λp_3	λp_4	λp_5	F_1	F_2	S.W.	Bid_1	Bid_2
α,β	**29.1**	**27.7**	**32.4**	**32.6**	**31.4**	**3058**	**6941**	**14661**	α_1=29.50 β_1=4·10^{-5}	α_2=28.11 β_2=1·10^{-5}
α-	**29.7**	**28.3**	**32.7**	**32.9**	**31.8**	**3118**	**7204**	**14583**	α_1=28.11	α_2=23.47
β-	**32.7**	**32.0**	**33.2**	**33.8**	**33.6**	**2698**	**7949**	**12785**	β_1=0.173	β_2=0.050
k_F	**29.7**	**28.3**	**32.7**	**32.9**	**31.8**	**3119**	**7204**	**14584**	k_{F1}=2.402	k_{F2}=1.787
Case 6: max $S = 1$ p.u. (branches 1-5 and 2-3 binding) and |V|±5%										
b	λp_1	λp_2	λp_3	λp_4	λp_5	F_1	F_2	S.W.	Bid_1	Bid_2
α,β	**34.8**	**34.1**	**36.4**	**36.4**	**35.9**	**2369**	**5316**	**8783**	α_1=9·10^{-12} β_1=0.345	α_2=4·10^{-9} β_2=0.140
α-	**29.6**	**29.4**	**35.1**	**35.3**	**34.8**	**4205**	**4486**	**11846**	α_1=27.49	α_2=26.79
β-	**29.5**	**29.5**	**35.0**	**35.3**	**34.9**	**4390**	**4319**	**11863**	β_1=0.075	β_2=0.074
k_F	**29.6**	**29.4**	**35.1**	**35.3**	**34.8**	**4194**	**4495**	**11845**	k_{F1}=2.293	k_{F2}=2.157

TABLE 8.3
RESULTS FOR THE 5-BUS SYSTEM: MARKET SOLUTIONS FOR CASES 7 TO 8 (|V|±3%)

Case 7: No Congestion and |V|±3%										
b	λp_1	λp_2	λp_3	λp_4	λp_5	F_1	F_2	S.W.	Bid_1	Bid_2
α,β	**35.0**	**34.5**	**35.4**	**35.8**	**35.7**	**1881**	**6237**	**9122**	α_1=29.57 β_1=0.073	α_2=34.72 β_2=1·10^{-5}
α-	**35.1**	**34.5**	**35.4**	**35.8**	**35.7**	**1956**	**6339**	**9280**	α_1=34.32	α_2=31.67
β-	**29.6**	**29.1**	**30.9**	**32.2**	**31.7**	**2993**	**6547**	**13086**	β_1=0.113	β_2=0.045
k_F	**35.1**	**34.5**	**35.4**	**35.8**	**35.7**	**1956**	**6339**	**9280**	k_{F1}=3.038	k_{F2}=2.490
Case 8: max $S = 1$ p.u. (branch 2-3 binding) and |V|±3%										
b	λp_1	λp_2	λp_3	λp_4	λp_5	F_1	F_2	S.W.	Bid_1	Bid_2
α,β	**35.7**	**35.1**	**36.5**	**36.7**	**36.4**	**1799**	**5317**	**7884**	α_1=35.71 β_1=1·10^{-5}	α_2=35.13 β_2=1·10^{-5}
α-	**30.7**	**28.8**	**35.7**	**35.0**	**33.4**	**2846**	**5460**	**11435**	α_1=29.34	α_2=25.43
β-	**30.7**	**28.8**	**35.7**	**35.0**	**33.4**	**2888**	**5435**	**11449**	β_1=0.132	β_2=0.053
k_F	**30.7**	**28.8**	**35.7**	**35.0**	**33.4**	**2848**	**5459**	**11436**	k_{F1}=2.527	k_{F2}=2.003

For the next two Cases, the transmission capacity limits of the entire system are gradually reduced to 2 p.u. and 1 p.u. respectively, to examine low and more intense transmission congestion conditions. When the system transmission limits are reduced to 2 p.u. for Case 5, transmission congestion exists in the transformer branch TR1 between buses 2-3. Again, as in Case 2, the results from the β-parameterization are considerably different from those of the other methods, and the results for the α- and k_F-methods are identical, and differ by a small deviation from those of the (α, β)-parameterization. For Case 6 where the transmission limits are further reduced to 1 p.u., congestion exists in the transformer branch TR1 and in line branch 1-5. The results of the β-parameterization are now very close to those of the α- and k_F-methods, while the market outcome of the (α, β)-parameterization shows a significant deviation. This behaviour resembles Case 3 where the voltage limits are reduced in the presence of congestion.

In order to examine the interrelation between the similar observations for Case 3 that has reduced voltage limits and those for Case 6 that has intense transmission congestion, two more cases are examined on the 5-bus system for tighter bus voltage limits of ±3% from 1 p.u. These are Cases 7 and 8, which are performed with no congestion and under intense transmission congestion respectively, as shown in Table 8.3. By comparing Case 7 with Case 4, for which the voltage range has been reduced from ±5% to ±3% from 1 p.u., it can be seen that, unlike Case 4, the solution of the β-parameterization in Case 7 differs from the others, as in the cases where low transmission congestion was present (Cases 2 and 5). However, here there is no transmission congestion.

When the voltage range is reduced from Case 6 to Case 8 where the transmission limits in the network are set to 1 p.u., the overall power generation is reduced due to the voltage restrictions and, since less power is required to be transmitted in the network, one of the two congested lines is relieved. Therefore, there is only one transmission branch congested (TR1) in Case 8, but the deviation that existed in Case 6 between the solution of the (α, β)-parameterization and the other methods was sustained. The observations for Cases 6 and 8 are compatible with those for Case 3, where only the (α, β)-solutions show significant difference from those of the other parameterization methods.

8.6 Discussion on the different market solutions from the four parameterization methods based on the numerical results of Cases 1 to 8

The numerical results from the test cases on the 3-bus and the 5-bus systems are in good agreement and have shown that the market solutions from the different parameterization methods can be similar or have large deviations, depending on the presence and intensity of transmission congestion in conjunction with the level of the bus voltage limits. The α- and k_F-parameterization methods have been found to give very similar or identical solutions for all test cases independent of the operating network conditions. The solution of the β-parameterization is different from the other three when there is transmission congestion up to a certain level, or, in the absence of congestion, when there are tight limits for the bus voltages. The (α, β)-parameterization method gives solutions with significant differences from the other three methods if the transmission congestion is intense, or if there is congestion in the presence of tight bus voltage limits. Nonetheless, the market solution from the (α, β)-parameterization always has at least a small deviation from those of the other three methods.

According to the above observations it can be concluded that the presence and level of limitations associated with the power transmission and the bus voltages affect the market solution obtained from the four different supply function parameterization methods. Low level restrictions result in deviations on the solution of the β-parameterization and tighter restrictions affect the solution of the (α, β)-parameterization. It can also be seen that the effect of transmission congestion is more intense than that of voltage restrictions.

In contrast to the observations on the unconstrained and linearized systems in [113,104,114], the producers' surplus in all the (α, β)-test cases for the AC systems examined here is found to be lower than those of the other three parameterization methods. This may be explained as follows. Even though the outcome of any of the α-, β- and k_F-methods can be obtained using the (α, β)-

parameterization, it may not be an equilibrium point since a player may be able to implement another (α, β)-strategy that will result in higher profit (if the strategies of its rivals remain constant). The rivals will then anticipate this action and sequentially alter their strategies for their benefit, always subject to the network and market constraints present. Hence, the resulting equilibrium point, at which no firm will be able to further increase its profit, may correspond to a lower surplus for all the producers.

The investigations in [113] and [104] show that the (α, β)-profits in unconstrained systems equal those of the Cournot solution and quote the concept of focal equilibrium, which is mutually beneficial and preferred by all players. However, the introduction of the AC network modelling in the current study prevented such results, giving contradictory effects. Another observation is that an equilibrium (α, β)-strategy in the context of AC network modelling may require a bid that is much lower than the corresponding marginal cost function, as the particular player will gain profit due to the level of market price, which depends on several factors related to the nonlinear nature of the AC network and not only on the firms' strategies.

Furthermore, by observing the cases with moderate limitations on power transmission and bus voltages for which the β-parameterization gives different market solutions than the other three methods (Cases 2, 5 and 7), it can be seen that the producers' surplus for β-parameterization is always higher than that of the other methods. This is in agreement with the observations in [118], where market solutions for parameterizations of slopes and intercepts are compared for a 4-bus linearized DC system with transmission limits for active power. The authors of [118] postulate that by using the β-parameterization method the resulting equilibria resemble Cournot market outcomes, which might be the case under certain restrictions. This also holds for the results in [104], where the slope manipulation results in higher profits than the intercept-parameterization in an unconstrained system.

In addition to the cases provided above, several other tests not shown here were performed. These were examining the effect on the deviation between the

solutions from the four parameterization methods for power factor adjustments and for variation of other network constraints, such as the active and reactive generation limits. However, no significant difference was observed between the resulting market solutions from the different parameterization methods (as in Cases 1 and 4).

In order to examine if the above conclusions can be supported in the case of larger and more realistic systems, simulations on the IEEE 30-bus and 57-bus systems are described in the subsequent sections.

8.7 Numerical results on the IEEE 30-bus system

The IEEE 30-bus system [191] used here consists of 30 buses of which 22 have load demand, 37 transmission lines, 4 on-load tap-changing transformers, and 6 generators, each one forming an individual strategic firm (entitled F_1 to F_6). For this and for other larger systems the algorithm was unable to converge to an equilibrium solution when the (α, β)-parameterization was employed, possibly due to the complications discussed in Chapter 2, Section 2.7, but this will be further discussed in the next section. Convergence problems for the (α, β)-parameterization method have also been reported by [116]. Hence, only the solutions of the other three parameterization methods are provided for this system and the results are given in Table 8.4.

Based on the conclusions from the results on the 3-bus and 5-bus systems, it was investigated whether the β-parameterization method would have produced different results on the 30-bus system for a particular level of transmission congestion. The tests started from transmission limits of 2.0 p.u. for the entire network (Case 9), where there was no transmission congestion. The limits were gradually reduced and it was found that within the domain of 1.16 to 1.10 p.u., for which 3 transmission lines were congested, there was a deviation between the solution from the β-parameterization and the results from the α- and k_F-methods. Note that the range of transmission limits that resulted in different β-solutions for the 30-bus system is much smaller than those for the 3-bus and 5-bus systems.

TABLE 8.4
RESULTS FOR THE IEEE 30-BUS SYSTEM: MARKET SOLUTIONS FOR CASES 9 TO 11

Case 9: No Congestion and |V|±10%											
b	F_1	F_2	F_3	F_4	F_5	F_6	ΣPg	ΣQg	ΣPd	ΣQd	S.W.
α-	**3034**	**1709**	**5676**	**2815**	**731**	**1246**	**9.68**	**4.88**	**9.46**	**4.09**	**19559**
β-	**3033**	**1709**	**5679**	**2817**	**728**	**1246**	**9.68**	**4.88**	**9.46**	**4.09**	**19561**
k_F	**3034**	**1709**	**5676**	**2815**	**731**	**1246**	**9.68**	**4.88**	**9.46**	**4.09**	**19559**
Case 10: max $S = 1.13$ p.u. (3 lines binding) and |V|±10%											
b	F_1	F_2	F_3	F_4	F_5	F_6	ΣPg	ΣQg	ΣPd	ΣQd	S.W.
α-	**2840**	**1839**	**5212**	**3111**	**949**	**1258**	**9.25**	**4.74**	**9.06**	**4.02**	**18748**
β-	**2970**	**1845**	**5132**	**2980**	**950**	**1176**	**9.48**	**4.80**	**9.28**	**4.07**	**19103**
k_F	**2840**	**1838**	**5213**	**3112**	**947**	**1261**	**9.25**	**4.74**	**9.06**	**4.02**	**18744**
Case 11: max $S = 0.4$ p.u. (6 lines binding) and |V|±10%											
b	F_1	F_2	F_3	F_4	F_5	F_6	ΣPg	ΣQg	ΣPd	ΣQd	S.W.
α-	**2229**	**2339**	**3595**	**1988**	**356**	**514**	**7.01**	**2.87**	**6.97**	**2.96**	**14181**
β-	**2213**	**2338**	**3586**	**1987**	**358**	**519**	**7.01**	**2.85**	**6.96**	**2.95**	**14198**
k_F	**2230**	**2338**	**3595**	**1988**	**356**	**514**	**7.01**	**2.87**	**6.97**	**2.96**	**14182**

Case 10 presented in Table 8.4 corresponds to an intermediate case for a limit of 1.13 p.u. When the transmission limits were further reduced, the solutions of the α-, β- and k_F-parameterizations became very similar to each other. Case 11 shows the solutions for a limit of 0.4 p.u. For the latter case it can be presumed that, if an (α, β)-solution could be obtained, it would have been different from those of the other three methods, following the pattern observed for the smaller systems.

During the procedure of reducing the transmission limits, it was observed that for certain values the number of congested lines in the solutions from the different parameterizations was not the same, and hence their results were dissimilar since they corresponded to different network operations. Similar observations were also made when the bus voltage limits were varied. Further elaboration on this takes place in the next section on the IEEE 57-bus system. However, in all cases with the same number of congested lines, the parameterization solutions were following the pattern discussed above.

8.8 Numerical results on the IEEE 57-bus system

The larger IEEE 57-bus system [191] is tested to show the complications that arise in relation to the solutions provided from the different parameterization methods for more realistic situations. This system consists of 57 buses of which 42 have load demand, 63 transmission lines, 17 on-load tap-changing transformers, and 7 generators, each one forming an individual strategic firm (entitled F_1 to F_7). Again, results are presented for the α-, β-, and k_F-parameterizations, as shown in Table 8.5. The last column of the Table shows the number of congested lines cL for each equilibrium solution.

TABLE 8.5
RESULTS FOR THE IEEE 57-BUS SYSTEM: MARKET SOLUTIONS FOR CASES 12 TO 13

Case 12: No Congestion and |V|±10%													
b	F_1	F_2	F_3	F_4	F_5	F_6	F_7	S.W.	ΣPg	ΣQg	ΣPd	ΣQd	cL
α-	**6122**	**4866**	**1437**	**1803**	**9459**	**1768**	**7759**	**41229**	**19.86**	**6.58**	**19.36**	**5.33**	**0**
β-	**6279**	**4797**	**1250**	**1755**	**8962**	**2532**	**7527**	**41083**	**19.87**	**6.54**	**19.38**	**5.33**	**0**
k_F	**6130**	**4859**	**1425**	**1801**	**9462**	**1761**	**7760**	**41158**	**19.82**	**6.56**	**19.32**	**5.33**	**0**
Case 13: max $S = 1.7$ p.u. and |V|±10%													
b	F_1	F_2	F_3	F_4	F_5	F_6	F_7	S.W.	ΣPg	ΣQg	ΣPd	ΣQd	cL
α-	**6837**	**3889**	**1448**	**1602**	**8929**	**2016**	**7592**	**40043**	**19.14**	**6.15**	**18.69**	**5.15**	**2**
β-	**7343**	**3148**	**1257**	**1641**	**8955**	**2664**	**7240**	**40277**	**19.45**	**6.18**	**19.00**	**5.16**	**3**
k_F	**6852**	**4346**	**9**	**1321**	**9349**	**2727**	**7362**	**37889**	**17.69**	**5.89**	**17.25**	**4.96**	**5**

Case 12 corresponds to normal operating conditions and no congestion exists in the network. When the MVA transmission limits of the system are reduced to 1.7 p.u. in order to impose transmission congestion (Case 13), the number of congested transmission lines for each parameterization method is different as shown in the last column of Table 8.5. Hence, the three solutions for Case 13 correspond to different network operating conditions and they significantly differ from each other. Different cases with a variety of reduced limits for particular transmission lines and for the entire network were examined, but the three parameterization methods were resulting in dissimilar network operations in almost all cases. This also happens for other larger systems. Even though for the

smaller systems the four parameterization methods were giving solutions that correspond to the same operating conditions under network congestion and at least two solutions were in numerical agreement, for the larger systems this is not the case. Similar observations are made for variations of the bus voltage limits, since the voltages have a direct impact on the reactive transmission flows.

The occurrence that the parameterization methods give solutions that correspond to different network operations only for the larger systems may be owing to the fact that there is a wider combination of alternative routes for the power flows to follow. In larger and more complex networks the active and reactive power flows can be redistributed to suit a more appropriate scenario for the ISO objective, for only a small change in the supply function bids submitted from the strategic firms (in this case resulting from the different form of the parameterized bids). An observation for dissimilar congestion configurations for the different parameterization methods has also been reported in [116], for a linearized DC 39-bus system.

As far as the (α, β)-parameterization is concerned, as a congestion pattern is changing for an adjustment in a bid during the iterative process, a different (α, β)-strategy may become more profitable for some player, and the successive resulting situation can correspond to a different congestion pattern that may give rise to a more profitable (α, β)-strategy for a different player, and so on. This may be another possible reason for the convergence problems of the (α, β)-parameterization for large systems as pure strategy Nash equilibria may not exist[7].

Referring to the above observations, the impact of the parameterization method chosen on the equilibrium solution for more realistic systems is evident. The investigation on whether there is a correct choice on the parameterization method for each particular power system and network conditions or not, is a topic of future research.

[7] Convergence problems may also be attributed to the existence of multiple equilibria as discussed in Section 2.7, but it should be recalled that these should not be expected in large numbers for realistic situations under the restrictive conditions of the AC model, according to [128].

8.9 Conclusions for Chapter 8

This chapter has examined the impact of the choice of parameterization method for the linear SFE model, on the electricity market equilibrium solution. It has been shown that, under the AC network modelling assumptions the (α, β)-parameterization does not yield Cournot solutions as mentioned in the literature, but, instead, the resulting producers' surplus is lower than that of the other three methods. This is due to the fact that an equilibrium (α, β)-solution with Cournot profits cannot be sustained in the presence of AC network constraints as it is affected by the interactions between the equilibrium strategies of the individual market players (which depend on the nonlinearities of the AC network). In addition, it was shown that it is not profit incentive for the strategic firms in the AC model to reveal their true intercept from the marginal cost in the (α, β)-parameterization, as in the unconstrained multi-period linear SFE model [79], while a profitable (α, β)-equilibrium strategy may require a bid that is much lower than the corresponding marginal cost function. The profit for the latter case will be owing to the increased level of market price, which depends on several factors related to the AC modelling, and not only on the strategic bids.

A pattern was observed for the relation between the equilibrium solutions from the different parameterization methods. For systems up to 30 buses, the α- and k_F-parameterizations resulted in identical solutions for all tests, while the solutions for all the parameterization methods were very similar for no transmission congestion or strict voltage limits. When limiting bounds were introduced in the network, different solutions were observed for the β-parameterization when the stress in the network was low, and for the (α, β)-parameterization in the presence of tighter network limits. However, no pattern was observed for larger systems, because each parameterization method was resulting in different number of congested lines, due to the complexity of the transmission network, and hence to dissimilar network operational conditions. Thus, it has been shown that the relation between the equilibrium solutions from the four parameterization methods is directly dependent on the presence and

severity of the transmission congestion in conjunction with the level of the bus voltage limits.

The proposed interior point algorithm has been able to provide solutions for the α-, β- and k_F-parameterization methods for all systems. The employment of the (α, β)-parameterization has successfully solved the small 3-bus and 5-bus test systems, while it has difficulties in converging to equilibrium solutions for large systems. These convergence problems may arise due to oscillations in the convergence process caused by a continuum of equilibria as reported in the literature. However, multiple equilibria for the (α, β)-parameterization are not to be expected in large numbers for realistic networks, but only for small trivial systems (for which the proposed algorithm did not encountered any particular convergence problems). Another possibility for the convergence complications of the (α, β)-parameterization is the successive alterations of the transmission congestion patterns in the network, which are responses to any adjustments in the strategic bids, owing to the complicated meshed network structure of larger systems. A change in the congestion pattern may render a different (α, β)-strategy more profitable for some player and the successive market conditions may correspond to a different congestion pattern that gives rise to a more profitable (α, β)-strategy for a different player, and so on. This is not the case for the other three parameterization methods, because they are allowed fewer degrees of freedom for the choice of the strategic supply function bid than the (α, β)-parameterization, and hence less complicated interactions between the players' strategies are expected.

Chapter 9:
Convergence characteristics of the electricity market SFE algorithm

9.1 Introduction to the computational performance characteristics of linear SFE models

Even though the computational time required for obtaining optimal solutions for the analysis of theoretical electricity market scenarios is not of primal importance, the conditions for simulating real-time practical situations during the market clearing process require high efficiency for the iterative procedure in terms of computational performance and robustness. For example, the application of an algorithm for the simulation of an electricity bid-based market with bidding intervals of 15 minutes entails computational requirements in the order of seconds, independent of the network operational conditions being able to handle any variations in the system parameters for each time interval.

The computational performance of a market equilibrium algorithm is directly related to the numerical method and mathematical framework employed, while the particular network representation and modelling of the bidding strategies also interfere with the efficiency of the algorithmic procedure. Factors that correspond to binding inequality constraints for certain market conditions, such as the presence of network congestion and reduced limits on constrained system variables, and the complexity of the examined system further affect the computational performance. In addition, functional inequality constraints may have a greater effect than simple inequality constraints when binding, due to higher execution times. The studies in the existing literature on the linear SFE models (presented in Chapter 2) occasionally provide information about the computational performance of the implemented market algorithms. The required CPU times for convergence reported in the literature are summarised in Table 9.1, where information on the numerical framework is provided for reference.

The studies on the AC-network linear SFE models did not elaborate on the computational performance of the algorithm, except [89], which mentions a number of iterations between 200 to 600 for solving the IEEE 14-bus system with 2 strategic players.

TABLE 9.1
CPU TIMES FOR THE LINEAR SFE MODELS REPORTED IN THE LITERATURE

Reference	Numerical method	Network representation	CPU time	System	Parameterization
[126]	Golden section search method	Quantity limits	3 seconds	6-firm structure	β-parameterization
[134]	NCP formulation	DC model	5 minutes	30-bus system	k_F-parameterization
[104]	Coevolutionary computation	No constraints	1 second	5-firm structure	All parameterizations
[136]	Lagrange optimisation	DC model	3 minutes	30-bus system	k_F-parameterization
[116]	CP formulation	DC model	172.8 seconds	39-bus system	(α, β)-parameterization
[116]	Diagonalization method	DC model	3.6 seconds	39-bus system	(α, β)-parameterization
[116]	Regularization method	DC model	61.9 seconds	39-bus system	(α, β)-parameterization
[114]	Diagonalization method	DC model	5 seconds	6-bus system	(α, β)-parameterization
[138]	Mixed integer NLP	DC model	27.5 seconds[8]	6-bus system	k_F-parameterization

It can be seen that the introduction of DC representation requires higher CPU times than the unconstrained cases and that the numerical method employed for the solution of the problem significantly affects the computational performance (see the three models from [116] on the 39-bus system). Small systems (6 buses) can be solved within 5 to 28 seconds, while the required CPU times for larger systems (30 to 39 buses) are ranging from few seconds to 5 minutes depending on the numerical framework. The parameterization method chosen also affects the CPU time requirements, as observed in [116] (not shown here).

By reviewing the models in the existing literature, it can be seen that the proposed numerical algorithms solve relatively small linearized DC systems in the order of seconds or minutes. However, the application of such algorithms in practical systems preconditions superior efficiency and reduced execution times.

[8] The CPU time given in [138] is 11 minutes for a 24-interval market simulation. The figure presented in Table 9.1 is the average CPU time per interval.

The implemented electricity market algorithm in this Thesis, which considers the more realistic AC network representation, has exhibited high computational performance with exceptionally low execution times. The convergence characteristics of the proposed algorithm are examined in the next sections.

9.2 Analysis of the convergence characteristics of the proposed electricity market SFE algorithm

The proposed algorithm has successfully been used for simulating various network and market conditions for several test systems ranging from 3 to 118 buses in Chapters 4 to 8. Solutions for small systems (3 to 5 buses) have been obtained in extremely low execution times, being in the order of few milliseconds. For example, the test cases for the 5-bus system in Chapter 7, Section 7.6.1 that include transformer components and congested transmission lines required a CPU execution time between 62 and 203 milliseconds with a number of iterations between 10 and 28. Such figures are one or two orders lower than the corresponding for the DC or unconstrained systems from the existing literature, as shown in Table 9.1. In order to demonstrate the efficiency of the proposed algorithm on solving larger systems, the presentation of the convergence characteristics of the algorithmic procedure are based on the test cases performed on the IEEE 14-bus and 118-bus systems in Chapter 5, Sections 5.3 and 5.4 respectively. The analysis includes graphical presentations of the iterative process in terms of power mismatch and complementary gap minimisations. In addition, the convergence process for the different parameterization methods is elaborated in Section 9.3.

Concerning the terminology used in this chapter, a reference to simple constraints denotes the bus voltage and transformer tap-ratio control constraints and the active and reactive power generation and absorption capacity limits (even though the voltage constraint, which is formulated in rectangular coordinates, is actually a quadratic function of the real and imaginary bus voltage components; see (3.60)). A functional constraint refers to the MVA transmission inequality constraint (3.57), which is a complicated function of the rectangular voltage

components. The tolerances of the break point for the algorithm are as described in Section 3.10. The algorithm was implemented and run on a Pentium® 4 CPU 3.20GHz, 0.99GB of RAM.

9.2.1 Convergence for the IEEE 14-bus system

The number of iterations and the required CPU time in milliseconds for each case performed on the IEEE 14-bus system are provided in Table 9.2, indicating the number of binding constraints. The Case No. refers to that used in Chapter 5. For this system, the number of variables updated after each iteration is 2259, the dimensions of the Newton matrix is 527×527 and the number of the active inequality constraints is 94.

TABLE 9.2
CONVERGENCE CHARACTERISTICS FOR THE IEEE 14-BUS SYSTEM

Case No.	No. of iterations	CPU time (milliseconds)	No. of simple binding constraints
11	11	203	8
12	12	219	7
13	8	140	7
14	11	188	7
15	16	281	7
22	12	203	8
23	11	187	8
24	14	265	7

From Table 9.2 it can be seen that for all the tests on the 14-bus system, the algorithm converges within 8 to 16 iterations, requiring 140 to 281 milliseconds of CPU time. The algorithm demonstrates excellent computational performance, proving its efficiency with an average CPU time of 211 milliseconds for the examined test cases, which is much lower even from that for the small unconstrained market structures reported in the literature. The algorithm was tested on hundreds of different test cases for this system, with a broad range of different input parameters and constraint limits. It has demonstrated its robustness by providing consistent results for all tests and reaching feasible solutions for the Nash equilibrium in milliseconds, for a system that involves repeated updates of more than 2250 variables.

By comparing the performance of the algorithm with that of the AC model in [89], which solves the same system with a number of iterations between 200 to 600 for 2 strategic players considering constant reactive load demand and no transformers, it can be seen that the model in this Thesis is by 17 to 50 times more efficient. This proves that the primal-dual interior point formulation is more computationally efficient than the diagonalization schemes.

9.2.2 Convergence for the IEEE 118-bus system

The behaviour of the algorithm convergence for the larger IEEE 118-bus system is presented in Table 9.3 and Figures 21 and 22. Table 9.3 shows the number of iterations, the required CPU time in seconds, the number of functional inequality constraints, i.e. the MVA transmission branch constraints, that are binding and the number of simple binding constraints. The Case No. is as in Chapter 5. In Figures 21 and 22, the maximum absolute active or reactive power mismatch and the complementary gap, respectively, are plotted for each iteration. The number of the variables updated for each iteration in the iterative process for this system is 17350, the dimensions of the Newton matrix are 4064×4064 and the number of the associated active inequality constraints is 758.

TABLE 9.3
CONVERGENCE CHARACTERISTICS FOR THE IEEE 118-BUS SYSTEM

Case No.	No. of iterations	CPU time (seconds)	No. of MVA binding constraints	No. of simple binding constraints
16	44	7.563	0	80
17	43	7.343	0	91
25	43	7.562	7	77
26	46	8.500	7	78

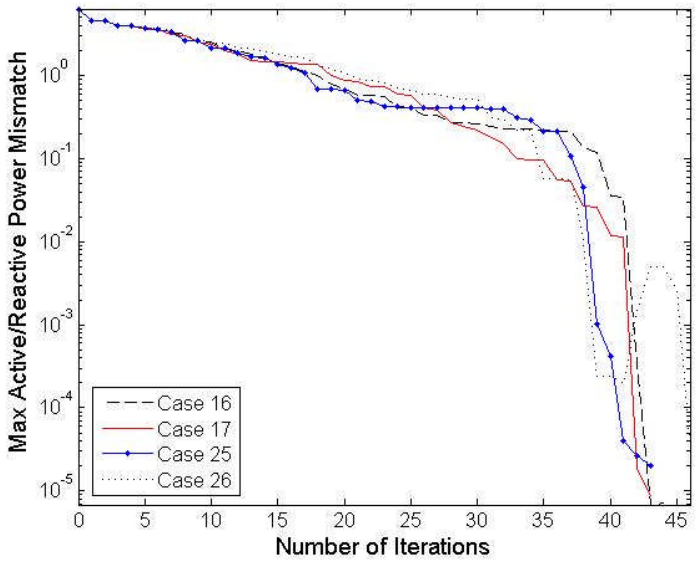

Figure 21: Maximum absolute active/reactive power mismatches for the convergence of the IEEE 118-bus system test cases.

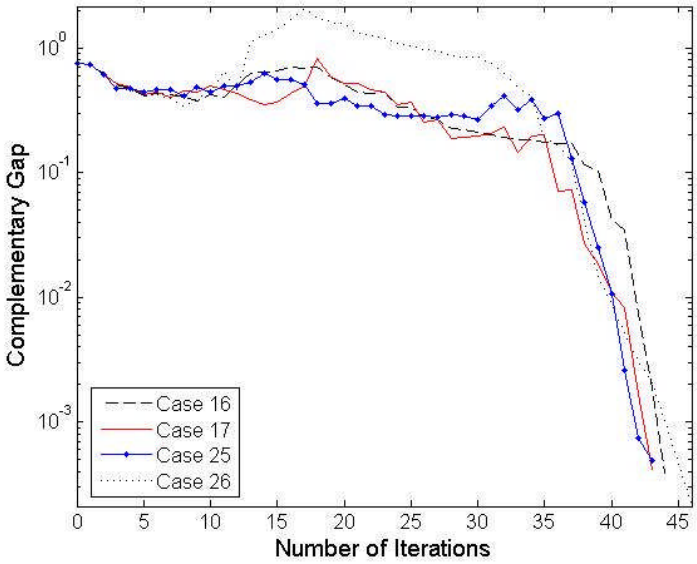

Figure 22: Complementary gap minimisation for the convergence of the IEEE 118-bus system test cases.

By observing the information provided for the 118-bus system, it can be seen that for most of the cases the convergence characteristics are very similar, with CPU times between 7.3 to 8.5 seconds. However, it should be mentioned that the binding functional inequality constraints in Cases 25 and 26, and the additional simple binding constraints in Case 17 do not reduce the efficiency of the

algorithm in terms of convergence. By comparing the characteristics for Cases 26 and 16, which have about the same number of simple binding constraints but differ by 7 binding functional constraints, the increment in the required CPU time is inexpensive, being less than 1 second with only 2 extra iterations. The graphical presentation of the iterative process shows that the algorithm demonstrates quadratic convergence characteristics near the final solution.

To further test the ability of the implemented algorithm to converge in very small CPU times, Case 26 was performed again, with strict MVA limits of 1 p.u. at all transmission branches in the system. The output results have indicated that 20 of the MVA functional inequality constraints were binding at that limit, imposing heavy transmission congestion in the network. However, the algorithm converged within 48 iterations in 9.843 seconds. The extra 13 binding functional inequality constraints have increased the required CPU time by less than 1.35 seconds, compared with the original Case 26. This shows that the implemented algorithm is extremely efficient and robust, being able to provide SFE results for large power systems, such as the IEEE 118-bus system, subject to several binding functional and simple inequality constraints, dealing with tens of thousands variables being updated after each iteration. These advantageous features stem from the fundamental principles of the interior point method.

9.2.3 Discussions on the convergence of the algorithm

The algorithm has proven its efficiency and robustness on solving large scale nonlinear systems, such as the examined IEEE 118-bus system. It has been shown that the proposed electricity market model is able to handle larger power systems than those involved in the existing literature, since it can provide SFE results under various network operational conditions independent of the system complexity, while it has improved realism and accuracy of the resulting market outcome. The exceptional computational performance and the small required processing time of the algorithm, along with its ability to provide robust market solutions, give the opportunity to employ the proposed model for simulations of electricity markets of large systems under on-line environments. Markets with small bidding time intervals, such as half hour or 15 minutes, can be investigated,

by modifying the algorithm accordingly to take into consideration the transition between successive time intervals and accommodate the power generation and load demand fluctuations.

9.3 Investigation of the computational performance of the different parameterization methods

In order to check if the convergence characteristics of the primal-dual interior point algorithm are different and examine any dissimilarities in its efficiency for each parameterization method under the AC network representation, the average required CPU time and average number of iterations for the test systems investigated in Chapter 8 are presented in Table 9.4. The minimization of the absolute power mismatches and complementary gap, for each parameterization method in Case 5 from Chapter 8, are illustrated graphically in Figures 23 and 24 respectively.

TABLE 9.4
CONVERGENCE CHARACTERISTICS FOR THE DIFFERENT PARAMETERIZATION METHODS

Parameterization method	System	Average CPU time (milliseconds)	Average No. of iterations
(α, β)-	3-bus	**57**	**18**
	5-bus	**190**	**25**
α-	3-bus	**26**	**9**
	5-bus	**87**	**13**
	30-bus	**698**	**22**
	57-bus	**2078**	**26**
β-	3-bus	**16**	**8**
	5-bus	**119**	**15**
	30-bus	**697**	**22**
	57-bus	**2219**	**26**
k_F-	3-bus	**26**	**9**
	5-bus	**88**	**13**
	30-bus	**713**	**23**
	57-bus	**4594**	**34**

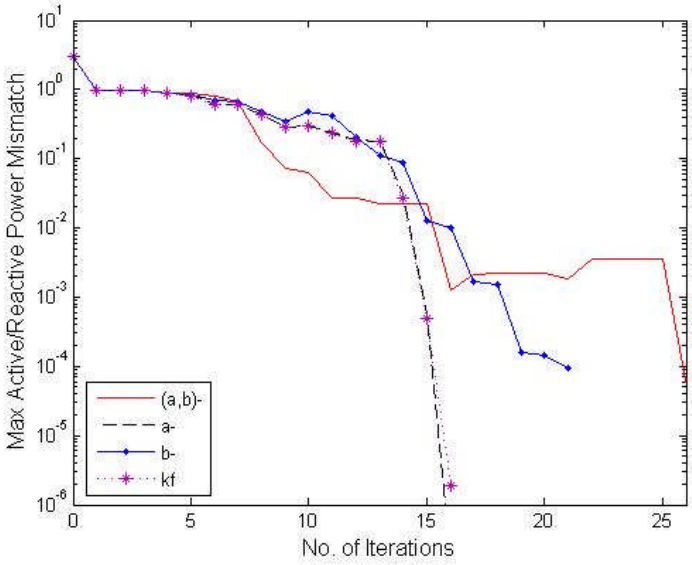

Figure 23: Maximum absolute active/reactive power mismatches for the convergence of the different parameterization methods.

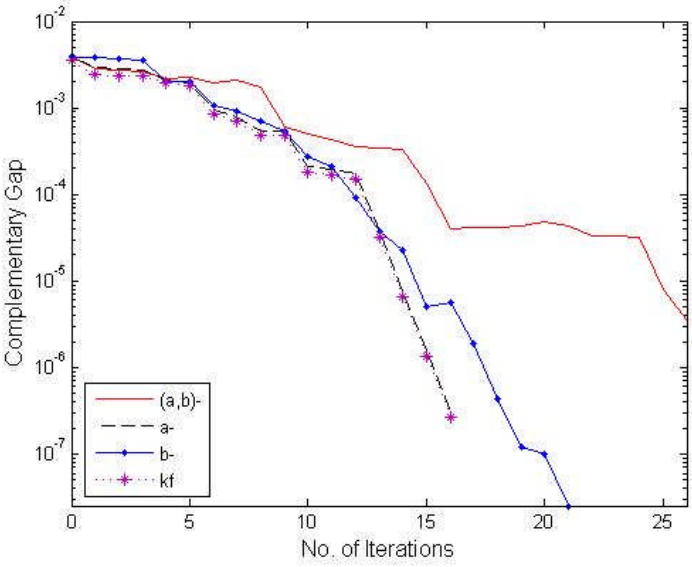

Figure 24: Complementary gap minimisation for the convergence of the different parameterization methods.

From Table 9.4 it can be seen that the CPU times and number of iterations for the α-, β- and k_F-methods are similar, while the (α, β)-parameterization requires a CPU time and number of iterations about twice those for the other three methods, when converging. However, all the CPU times are comparable and relatively small, since there are of the order of milliseconds to a few seconds. By

comparing the different parameterization cases for the IEEE 57-bus system, it can be seen that the k_F- parameterization that resulted in more congested lines than the others (see Case 13, Chapter 8) requires higher CPU time, but the 3 extra functional binding constraints involve an additional execution time of only 2.5 seconds. The figures presented show that the computational performance of the algorithm is equally superior for all the parameterizations. The only weakness of the proposed model is the convergence problems for solving large systems using the (α, β)-parameterization.

Case 5 from Chapter 8 was chosen for the graphical representation of the convergence characteristics for the four parameterization methods in Figures 23 and 24, because all parameterizations provide solutions and involve strict limits with two functional inequality and other simple constraints binding (see Chapter 8). From the graphs it can be seen that the α- and k_F-methods show exactly the same quadratic converging behaviour, while the behaviour of β-parameterization deviates from those two after about 15 iterations. The β- and (α, β)-parameterization algorithms demonstrate quadratic convergence characteristics as well, near the final solution.

9.4 Factors that enhance the computational performance of the algorithm

The presentation of the convergence characteristics of the proposed electricity market algorithm in the previous sections and the comparison with the models in the existing literature, have proven its superior computational performance. The factors that contribute to the enhancement of the algorithm's efficiency and made possible the application of AC network modelling on large systems with reduced execution times are summarised below:

- ***Application of the primal-dual interior point method*:**

The mathematical formulation of the bi-level market problem using this method exhibits improved convergence for solving large systems. This is owing to the fact that the convergence process of the interior point algorithm is very

insensitive to the size and complexity of the problem as the number of iterations increases with the logarithm of the number of variables involved.

- ***Rectangular coordinates representation*:**

By representing the system variables and power flows in rectangular coordinates complex form, the computational efficiency of the algorithm is enhanced due to the advantages of the resulting quadratic objective functions and constraints (see Section 3.1).

- ***Introduction of complementarity function*:**

The complementarity formulation for the ISO KKT condition and the non-negativity constraint of the active load demand variable enhances the computational performance of the algorithm since there are no extra slack and dual variables involved in the computations. In addition, the robustness of the algorithm is improved, since any possible ill-conditioning complications due to the complementarity expressions are eliminated.

- ***Sparse matrix techniques*:**

By arranging the elements in the Newton matrix in a 4 by 4 structure in order to resemble the sparse configuration of the admittance matrix in the conventional Newton power flow, the processing of individual sub-matrices for the system variables and the slack/dual variables can be accomplished. This reduces the matrix storage requirements and the computational effort in the algorithmic procedure.

- ***Elimination of slack and dual variables*:**

The elimination of the slack and dual variables associated with the bidding variables from the Newton matrix equation using Gaussian elimination, which is made possible by the application of the aforementioned sparse matrix techniques, reduces the computational effort during the iterative process. This is so because they are retrieved after the solution of the Newton matrix equation and are not involved during the calculation of the Newton step vector.

9.5 Conclusions for Chapter 9

The convergence characteristics of the proposed interior point algorithm were investigated, demonstrating the superior computational performance and robustness of the implemented electricity market model in providing Nash SFE solutions. The application of the algorithm on large nonlinear power systems with CPU times of the order of few seconds has been successful, dealing with tens of thousands of variables and constraints. These features have been compared with the computational performances of the models in the existing literature, showing that the formulation of the bi-level market problem by employing the primal-dual interior point method is superior over the diagonalization and the other methods proposed. It has been shown that even when several functional or simple constraints are binding the computational performance of the algorithm does not deteriorate, proving the functionality of the interior point method. The distinct characteristics of this method have made possible the realisation of the AC network representation that adds realism to the electricity market model and improves the accuracy of the market predictions, giving the opportunity for the proposed model to be applied for market simulations of practical power systems.

The convergence to SFE market solutions for the different parameterization methods has been examined to show that the algorithm can perform equally well independent of the modelling of the strategic bid. It has been found that, if the algorithm converges, the execution times are similar for all the parameterization methods, being in the order of milliseconds or few seconds. The α-, β-and k_F-parameterizations did not exhibit any problems in providing robust equilibrium solutions, while the employment of the (α, β)-parameterization method is accompanied by convergence problems for large systems.

Chapter 10:
Epilogue

10.1 Concluding remarks

The work presented in this Thesis has focused on the analysis of the strategic behaviour of the profit-maximising market participants in bid-based electricity pool markets and the role of the network characteristics and constraints in providing incentives for the exercise of market power. A nonlinear primal-dual interior point algorithm based on linear SFE theory has been implemented using the AC network representation to simulate several case scenarios on small and large power systems for the investigation of different aspects related to the system and market operation. The strategic behaviour of the individual generating firms that own generating units with linear marginal costs of generation is modelled by supply function bid offers that are constructed by parameterizing their linear marginal cost functions. The market clearing price for each time interval of the bidding process is determined in terms of nodal prices in order to represent the energy price and the short-term transmission costs.

The mathematical formulation for the market problem involves a number of features that enhance the computational performance of the algorithm, which is able to provide equilibrium solutions for realistic AC systems with CPU times in the order of a few seconds, with the potential for applications on practical power systems and markets with small bidding time intervals. The proposed model can be utilised to serve the interests of (a) the ISO for determining the required system parameters for social welfare maximisation and preventing anti-competitive behaviour from the strategic players, (b) the generating firms for building optimum strategies according to the equilibrium bid predictions for profit maximisation, and (c) the system designer for identifying the areas of the system that are most prone to the exercise of market power due to the

weaknesses in the network structure with the prospect for improvements to assist the social welfare maximisation process.

The contributions of this Thesis can be separated into three parts. The first one depicts the effects of the network features in general and of different controls in particular on the strategic actions of the generating firms and on the electricity market outcome. The second contribution is the examination of case studies involving the introduction of new generating units on the electricity market in terms of conventional sources and photovoltaic grid-connected systems. The last part of the analysis addresses the issue of modelling the strategic behaviour of the generating firms by implementing different forms of linear supply function bids. Investigations on these three topics have been performed under normal and stressed network operational conditions to show the interrelation of network congestion with the resulting effects on the electricity market outcome.

10.2 Evaluation of the presented work

The analysis described in the preceding chapters has proven the importance of employing the AC network representation for the implementation of electricity market models, as the presence of reactive power and control methods in the system have a major impact on the strategic behaviour of the generating firms that considerably affect the market outcome. The impact of control methods on the electricity market outcome has been examined by investigating various test cases with transformer tap-ratio control, voltage control on the generation buses, limitations on the reactive power capabilities of the generating units, and load power factor adjustments. It has been shown that each of the aforementioned control methods has a distinct effect on the nodal prices, firms' strategies and profits, social welfare and power distribution in the network. The implementation of each of these control functions in the electricity market algorithm contributes to the realism and accuracy of the market solution, providing the opportunity for practical applications. Furthermore, it has been shown that the operation of the control functions is affected by the degree of congestion present in the network and the market operators should take such considerations into account during the

system design process in order to avoid associated inefficiencies due to market power complications.

By implementing the more realistic AC meshed network model to represent the electric power system, the investigation of a variety of topics related to the interactions between the strategic firms and the topology of the network became possible. Two different studies that involve the introduction of new generating units in the system have taken place. The first one examines how the location of new conventional generators affects the interactions between the existing and new firms in the market and the effects on the market outcome. The numerical results have shown that the profits of the new firm and the existing companies are directly related to the location of the new generators and the topology of the network, while the overall market outcome is affected accordingly. The second investigation is concerned with the introduction of grid-connected solar energy production in the electricity market and the economic and operational aspects of grid-connected photovoltaic systems are explicitly represented in the electricity market model based on data collected from an outdoor PV park. The numerical analysis shows that the strategic generating firms are given incentives from the characteristics of the PV units to change their strategies and affect the market outcome for their benefit, while it is demonstrated that modelling of the nonlinear PV reactive generation and of the dependency of PV power production on the intensity of the applied solar irradiance is required for a more accurate market solution.

Following the employment of linear SFE theory based on supply functions constructed by parameterizing the linear marginal cost of generation for the investigation of the strategic interactions in the electricity market, analysis takes place to illustrate the effect of modelling the supply function bid using different parameterization methods on the resulting equilibrium solution. The four parameterization methods that vary the slope and/or intercept of the marginal cost functions have been implemented in the electricity market model and several test cases have been performed on a variety of power systems. The numerical analysis has shown that the market solutions obtained from the four different parameterization methods may be very similar or differ substantially, depending

on the level of network congestion present and the size of the system. The observations on the interrelation between the market solutions from the different parameterizations have been compared with those in the existing literature and noteworthy conclusions related to the AC meshed network modelling have been drawn.

10.3 The major contributions of this Thesis

The major contributions of this Thesis are summarised as follows:

1) Implementation of a nonlinear primal-dual interior point algorithm based on linear SFE theory and AC network modelling for equilibrium analysis of the electricity market, applicable to large systems with superior computational performance.
2) Modelling of the transformer power flows, losses and tap-ratio control in the equilibrium market algorithm.
3) Investigation of the impact of transformer tap-ratio, reactive power and voltage control on the electricity market equilibrium.
4) Investigation of the effects of a new generating unit's location on the electricity market outcome
5) Modelling of grid-connected PV generating units in the electricity market algorithm, with representation of the economic and technical aspects, and analysis of the effects of solar irradiance levels and PV reactive power generation on the electricity market.
6) Implementation of the four different parameterization methods for the linear SFE model and investigation of the interrelation between the resulting market equilibrium solutions.

The main factors that enabled the research in this Thesis to take place are the employment of the AC network model and the high efficiency of the algorithm, which is owing to the valuable features of the interior point method. The general observations of the work presented suggest that the representation of the AC network nonlinearities should be included in the analysis of electricity markets in order to provide a better understanding for the strategic behaviour of the market

participants and obtain more realistic market predictions. In addition, it has been shown that the topology of the network under investigation affects the market outcome and therefore the implemented market model must be flexible and able to adapt to the particularities of each study.

10.4 Suggestions for further research

The versatile nature of the primal-dual interior point method provides the opportunity for further expansion of the electricity market algorithm by incorporating extra equality or inequality constraints in the formulation to represent other network components and controls. For example, the capability curve constraint for a synchronous generator characterised by the field, armature and absorption limits of the machine can be incorporated in the model by defining additional inequalities in the ISO problem and appropriate system variables and elements in the Newton matrix equation, to represent the trade-off between the active and reactive power generation. In a similar manner, other network components, such as reactive sources (e.g. shunt reactors and capacitor banks), and control functions, such as phase-shifting transformers, can be added in the formulation of the AC market algorithm. The integration of these and other components in the market model will provide the ability for further analysis of the issue of market power in practical systems and result in more realistic market outcome predictions.

Apart from the representation of additional network components, inequality constraints can be incorporated in the interior point formulation to model a market with price caps, while the existing constraints for the bidding variables can be utilised to represent bid caps on the strategic offers. As there has been no investigation of the SFE model that applies price and bid caps on AC systems in the literature, useful observations related to the nonlinearities of practical systems may be obtained. Another topic that can be examined using the implemented market model is the effect of demand elasticity on the strategic behaviour of the market participants by considering simultaneously price-responsive and constant components for both active and reactive load demand.

An interesting subject can be examined by modelling a joint market for active and reactive power. Reactive nodal pricing can be accomplished for synchronous generators and reactors by incorporating bid offers and profit components for the reactive generation in the market algorithm. Using this model, analysis that can shed light on how strategic firms would compete in a joint active and reactive power generation market with supply function bidding can be undertaken. Other possible investigations may include the comparison of synchronous generators with other reactive sources in terms of economic efficiency, the trade-off between the profits from the active and the reactive power sales, and the extent to which the AC network components interfere with the ability of the strategic players to exercise market power in the case of active and reactive nodal pricing.

Other more challenging relevant research topics include the modelling of multi-period bid-based pool markets and the implementation of piece-wise supply function bid offers using the AC meshed network structure. A multi-period market model requires the consideration of intertemporal network constraints for the generating units, such as initial conditions and start-up costs, ramp up and down rate limits, minimum up and down times, and maximum start-ups and shut-downs, which can be represented accordingly in the interior point formulation. A model that uses piece-wise supply function bids can be obtained by iterating in the bid offers function space and can be refined by reducing the length of the successive segments of the optimal supply function trace in order to provide market solutions that correspond to the general SFE format. Both of these advanced models can be implemented in conjunction with any of the ideas mentioned in the beginning of this section with the prospect that such research studies on AC market structures may lead to the establishment of new conceptual ideas about the function of practical bid-based energy pool markets.

References:

[1] S. Stoft, "Power system economics: designing markets for electricity", *IEEE Press, Wiley-Interscience*, 2002.

[2] International Energy Agency, "Electricity market reform: an IEA handbook", *OECD/IEA*, 1999.

[3] G. Rothwell and T. Gómez, "Electricity economics: Regulation and deregulation", *IEEE Press, Wiley-Interscience*, 2003.

[4] E. O. Taylor and G. A. Boal, "Power system economics", *Edward Arnold (Publishers) Ltd*, London, 1969.

[5] H. Averch and L. L. Johnson, "Behavior of the firm under regulatory constraint", *The American Economic Review*, vol. 52, issue 5, pp. 1052-1069, Dec. 1962.

[6] International Energy Agency, "Competition in electricity markets", *OECD/IEA*, 2001.

[7] R. Green, "Reshaping the CEGB: electricity privatization in the UK", *Utilities Policy*, vol. 1, issue 3, pp. 245-254, Apr. 1991.

[8] R. Green and D. M. Newbery, "Competition in the British electricity spot market", *The Journal of Political Economy*, vol. 100, no. 5, pp. 929-953, Oct. 1992.

[9] http://www.nordpool.com/en/

[10] The European Commission, "Opening up to choice: the single electricity market", 1999.

[11] International Energy Agency, "Electricity reform: power generation costs and investment", *OECD/IEA*, 1999.

[12] http://www.edf.com

[13] http://www.vattenfall.com

[14] M. Shahidehpour, H. Yamin and Z. Li, "Market operations in electric power systems: forecasting, scheduling, and risk management", *IEEE Press, Wiley-Interscience*, 2002.

[15] Y.-H. Song and X.-F. Wang, "Operation of market-oriented power systems", *Springer: Power Systems*, 2003.

[16] D. S. Kirschen and G. Strbac, "Fundamentals of power system economics", *John Wiley & Sons Ltd*, 2004.

[17] A. K. David and F. Wen, "Market power in electricity supply", *IEEE Transactions on Energy Conversion*, vol. 16, no. 4, pp. 352-360, Dec. 2001.

[18] S. Hunt and G. Shuttleworth, "Competition and choice in electricity", *John Wiley & Sons*, 1996.

[19] K. Bhattacharya, M. H. J. Bollen and J. E. Daalder, "Operation of restructured power systems", *Kluwer Academic Publishers*, 2001.

[20] F. C. Schweppe, M. C. Caramanis, R. D. Tabors and R. E. Bohn, "Spot pricing of electricity", *Kluwer Academic Publishers*, 1988.

[21] R. Ethier, R. Zimmerman, T. Mount, W. Schulze and R. Thomas, "A uniform price auction with locational price adjustments for competitive electricity markets", *Electrical Power and Energy Systems*, vol. 21, pp. 103-110, 1999.

[22] N. Fabra, "Tacit collusion in repeated auctions: uniform versus discriminatory", *The Journal of Industrial Economics*, vol. 51, no. 3, pp. 271-293, Sept. 2003.

[23] G. Federico and D. Rahman, "Bidding in an electricity pay-as-bid auction", *Journal of Regulatory Economics*, vol. 24, no. 2, pp. 175-211, 2003.

[24] H. Haghighat, H. Seifi, A. R. Kian, "The role of market pricing mechanism under imperfect competition", *Decision Support Systems*, vol. 45, pp. 267-277, 2008.

[25] Y. S. Son, R. Baldick, K.-H. Lee and S. Siddiqi, "Short-term electricity market auction game analysis: uiniform and pay-as-bid pricing", *IEEE Transactions on Power Systems*, vol. 19, no. 4, pp. 1990-1998, Nov. 2004.

[26] R. E. Bohn, M. C. Caramanis and F. C. Schweppe, "Optimal pricing in electrical networks over space and time", *Rand Journal of Economics*, vol. 15, no. 3, pp. 360-376, Autumn 1984.

[27] W. W. Hogan, "Contract networks for electric power transmission", *Journal of Regulatory Economics*, vol. 4, pp. 211-242, 1992.

[28] Commission of the European communities, “Directive of the European Parliament and of the Council on the promotion of the use of energy from renewable sources”, Brussels, 23 Jan. 2008.
[29] T. J. Overbye, J. D. Weber and K. J. Patten, “Analysis and visualization of market power in electric power systems”, *Decision Support Systems*, vol. 30, pp. 229-241, 2001.
[30] B. F. Hobbs and R. E. Schuler, “An assessment of the deregulation of electric power generation using network models of imperfect spatial markets”, *Papers of the Regional Science Association*, vol. 57, pp. 75-89, 1985.
[31] W. W. Hogan, “A market power model with strategic interaction in electricity networks”, *Energy Journal*, vol. 18, issue 4, pp. 107-141, 1997.
[32] S. Borenstein, J. Bushnell and S. Stoft, “The competitive effects of transmission capacity in a deregulated electricity industry”, *Rand Journal of Economics*, vol. 31, no. 2,pp. 294-325, Summer 2000.
[33] S. Borenstein and J. Bushnell, “Market power in California electricity markets”, *Utilities Policy*, vol. 5, no. 3/4, pp. 219-236, 1995.
[34] R. E. Schuler, “Analytic and experimentally derived estimates of market power in deregulated electricity systems: policy implications for the management and institutional evolution of the industry”, *Decision Support Systems*, vol. 30, pp. 341-355, 2001.
[35] C. D. Wolfram, “Measuring duopoly power in the British electricity spot market”, *The American Economic Review*, vol. 89, no. 4, pp. 805-826, Sept. 1999.
[36] D. Gautam and N. Mithulananthan, “Optimal DG placement in deregulated electricity market”, *Electric Power Systems Research*, vol. 77, pp. 1627-1636, 2007.
[37] S. Borenstein and J. Bushnell, “An empirical analysis of the potential for market power in California’s electricity industry”, *The Journal of Industrial Economics*, vol. 47, no. 3, pp. 285-323, Sept. 1999.
[38] J. Nash, “Non-cooperative games”, *Annals of Mathematics*, vol. 54, no. 2, pp. 286-295, Sept. 1951.
[39] D. Fudenberg and J. Tirole, “Game theory”, *The MIT Press*, 1991.
[40] T. C. Schelling, “The strategy of conflict”, *Harvard University Press*, 1960.
[41] J. Tirole, “The theory of industrial organization”, *The MIT Press*, 1988.
[42] A. Cournot, “Recherches sur les principes mathématiques de la théorie des richesses”, *Paris: L. Hachette*, 1838.
[43] S. Borenstein, J. Bushnell and C. Knittel, “Market power in electricity markets: beyond concentration measures”, *The Energy Journal*, vol. 20, no. 4, pp. 65-88, 1999.
[44] W. W. Hogan, “Market power analysis and transmission constraints: an exploration”, *Harvard Electricity Policy Group Special Seminar*, Washington DC, 7 Dec. 1995.
[45] J. B. Cardell, C. C. Hitt and W. W. Hogan, “Market power and strategic interaction in electricity networks”, *Resource and Energy Economics*, vol. 19, pp. 109-137, 1997.
[46] W. W. Hogan, “A market power model with strategic interaction in electricity networks”, *Harvard Institute for International Development*, 15 July 1997.
[47] L. B. Cunningham, R. Baldick and M. L. Baughman, “An empirical study of applied game theory: transmission constrained Cournot behavior”, *IEEE Transactions on Power Systems*, vol. 17, no. 1, pp. 166-172, Feb. 2002.
[48] J. Contreras, M. Klusch and J. B. Krawczyk, “Numerical solutions to Nash-Cournot equilibria in coupled constraint electricity markets”, *IEEE Transactions on Power Systems*, vol. 19, no. 1, pp. 195-206, Feb. 2004.
[49] S. S. Oren, “Economic inefficiency of passive transmission rights in congested electricity systems with competitive generation”, *Energy Journal*, vol. 18, issue 1, pp. 63-83, 1997.
[50] S. S. Oren, “Passive transmission rights will not do the job”, *The Electricity Journal*, pp. 22-33, June 1997.
[51] S. Stoft, “How financial transmission rights curb market power”, *Working Paper PWP-049*, University of California Energy Institute, June 1997.
[52] S. Stoft, “Financial transmission rights meet Cournot: how TCCs curb market power”, *The Energy Journal*, vol. 20, issue 1, pp. 1-23, 1999.
[53] A. Ehrenmann and K. Neuhoff, “A comparison of electricity market designs in networks”, *CMI Working Paper 31*, University of Cambridge, revised Oct. 2004.
[54] J.-Y. Wei and Y. Smeers, “Spatial oligopolistic electricity models with Cournot generators and regulated transmission prices”, *Operations Research*, vol. 47, no. 1, pp. 102-112, Jan.-Feb. 1999.

[55] B. F. Hobbs, “Linear complementarity models of Nash-Cournot competition in bilateral and POOLCO power markets”, *IEEE Transactions on Power Systems*, vol. 16, no. 2, pp. 194-202, May 2001.
[56] Y. Chen, and B. F. Hobbs, “An oligopolistic power market model with tradable NO_x permits”, *IEEE Transactions on Power Systems*, vol. 20, no. 1, pp.119-129, Feb. 2005.
[57] B. F. Hobbs, E. Bartholomew, Y. Chen, G. Drayton and W. Lise, “Improved transmission representations in oligopolistic market models”, *PSCE 2006 IEEE PES Conference*, Atlanta USA, pp. 81-86, 29 Oct.-01 Nov. 2006.
[58] B. F. Hobbs and J. S. Pang, “Nash-Cournot equilibria in electric power markets with piecewise linear demand functions and joint constraints”, *Operations Research*, vol. 55, no. 1, pp. 113-127, Jan.-Feb. 2007.
[59] J. Yao, S. S. Oren and I. Adler, “Computing Cournot equilibria in two settlement electricity markets with transmission constraints”, *IEEE Proceedings of the 37th Hawaii International Conference on System Sciences*, 5-8 Jan. 2004.
[60] J. Yao, B. Willems, S. S. Oren and I. Adler, “Cournot equilibrium in price-capped two-settlement electricity markets”, *IEEE Proceedings of the 38th Hawaii International Conference on System Sciences*, 3-6 Jan. 2005.
[61] S. S. Oren , J. Yao and I. Adler, “Computiing two-settlement equilibrium in a transmission-constrained oligopolistic electricity market”, *PSCE 2006 IEEE PES Conference*, Atlanta USA, pp. 87-89, 29 Oct.-01 Nov. 2006.
[62] J. Yao, S. S. Oren, and I. Adler, “Cournot equilibria in two-settlement electricity markets with system contingencies”, *International Journal of Critical Infrastructures*, vol. 3, no. 1/2, pp. 142-160, 2007.
[63] J. Yao, I. Adler and S. S. Oren, “Modeling and computing two-settlement oligopolistic equilibrium in a congested electricity network”, *Operations Research*, vol. 56, no. 1, pp. 34-47, Jan.-Feb. 2008.
[64] K. Neuhoff, J. Barquin, M. G. Boots, A. Ehrenmann, B. F. Hobbs, F. A. M. Rijkers and M. Vázquez, “Network-constrained Cournot models of liberalized electricity markets: the devil is in the details”, *Energy Economics*, vol. 27, pp. 495-525, 2005.
[65] F. S. Wen and A. K. David, “Oligopolistic electricity market production under incomplete information”, *IEEE Power Engineering Review*, pp. 58-61, Apr. 2001.
[66] V. P. Gountis and A. G. Bakirtzis, “Efficient determination of Cournot equilibria in electricity markets”, *IEEE Transactions on Power Systems*, vol. 19, no. 4, pp. 1837-1844, Nov. 2004.
[67] G. Bautista, M. F. Anjos and A. Vannelli, “Modeling market power in electricity markets: is the devil only in the details?”, *The Electricity Journal*, vol. 20, issue 1, pp. 82-92, Jan./Feb. 2007.
[68] G. Bautista, M. F. Anjos and A. Vannelli, “Analysis of market power using an AC transmission system”, *PSCE 2006 IEEE PES Conference*, Atlanta USA, pp. 677-682, 29 Oct.-01 Nov. 2006.
[69] G. Bautista, M. F. Anjos and A. Vannelli, “Formulation of oligopolistic competition in AC power networks: an NLP approach”, *IEEE Transactions on Power Systems*, vol. 22, no. 1, pp. 105-115, Feb. 2007.
[70] G. Bautista, M. F. Anjos and A. Vannelli, “Beyond the use of linear approximations for modelling Nash-Cournot equilibria”, *IEEE PES Power Tech 2007 Conference*, pp. 831-836, 1-5 July 2007.
[71] J. Bertrand, “Théorie mathématique de la richesse sociale”, *Journal des Savants*, pp. 499-508, 1883.
[72] B. F. Hobbs, U. Helman and J.-S. Pang, “Equilibrium market power modeling for large scale power systems”, *IEEE PES Summer Meeting 2001*, vol. 1, pp. 558-563, 15-19 July 2001.
[73] Z. Younes and M. Ilic, “Generation strategies for gaming transmission constraints: will the deregulated electric power market be an oligopoly?”, *Decision Support Systems*, vol. 24, pp. 207-222, 1999.
[74] B. F. Hobbs, “Network models of spatial oligopoly with an application to deregulation of electricity generation”, *Operations Research*, vol. 34, no. 3, pp. 395-409, May-June 1986.
[75] B. F. Hobbs, “Mill pricing versus spatial price discrimination under Bertrand and Cournot spatial competition”, *The Journal of Industrial Economics*, vol. 35, no. 2, pp. 173-191, Dec. 1986.

[76] K.-H. Lee and R. Baldick, "Solving three-player games by the matrix approach with application to an electric power market", *IEEE Transactions on Power Systems*, vol. 18, no. 4, pp. 1573-1580, Nov. 2003.
[77] C. M. Ruibal and M. Mazumbar, "Forecasting the mean and the variance of electricity prices in deregulated markets", *IEEE Transactions on Power Systems*, vol. 23, no. 1, pp. 25-32, Feb. 2008.
[78] P. D. Klemperer and M. A. Meyer, "Supply function equilibria in oligopoly under uncertainty", *Econometrica*, vol. 57, no. 6, pp. 1243-1277, Nov. 1989.
[79] R. Baldick, R. Grant and E. Kahn, "Theory and application of linear supply function equilibrium in electricity markets", *Journal of Regulatory Economics*, vol. 25, no. 2, pp. 143-167, 2004.
[80] F. Bolle, "Supply function equilibria and the danger of tacit collusion: the case of spot markets for electricity", *Energy Economics*, vol. 14, no. 2, pp. 94-102, Apr. 1992.
[81] R. Green, "Increasing competition in the British electricity spot market", *The Journal of Industrial Economics*, vol. 44, no. 2, pp. 205-216, June 1996.
[82] H. von Stackelberg, "The theory of the market economy", translated from the German by A. Peacock, 1952, *William Hodge and Company Ltd*, original title: Grundlagen der theoretischen volkswirtschaftslehre.
[83] S. Leyffer and T. Munson, "Solving multi-leader-follower games", *Argonne National Laboratory Preprint ANL/MCS-P1243-0405*, 22 Apr. 2005.
[84] B. F. Hobbs and K. A. Kelly, "Using game theory to analyze electric transmission pricing policies in the United States", *European Journal of Operational Research*, vol. 56, pp. 154-171, 1992.
[85] M. de L. Latorre and S. Granville, "The Stackelberg equilibrium applied to AC power systems–a non-interior point algorithm", *IEEE Transactions on Power Systems*, vol. 18, no. 2, pp. 611-618, May 2003.
[86] Y. Chen, B. F. Hobbs, S. Leyffer and T. Munson, "Leader-follower equilibria for electric power and NO_x allowances markets", *Computational Management Science*, vol. 3, pp. 307-330, 2006.
[87] B. F. Hobbs, C. B. Metzler and J.-S. Pang, "Strategic gaming analysis for electric power systems: an MPEC approach", *IEEE Transactions on Power Systems*, vol. 15, no. 2, pp. 638-645, May 2000.
[88] J.-S. Pang and M. Fukushima, "Quasi-variational inequalities, generalized Nash equilibria, and multi-leader-follower games", *Computational Management Science*, vol. 2, pp. 21-56, 2005.
[89] G. Bautista, M. F. Anjos and A. Vannelli, "Numerical study of affine supply function equilibrium in AC network-constrained markets", *IEEE Transactions on Power Systems*, vol. 22, no. 3, pp. 1174-1184, Aug. 2007.
[90] A. L. Bowley, "The mathematical groundwork of economics", *Oxford Clarendon Press*, 1924.
[91] A. García-Alcalde, M. Ventosa, M. Rivier, A. Ramos and G. Relaño, "Fitting electricity market models. A conjectural variations approach", *14th Power Systems Computation Conference (PSCC)*, Sevilla, 24-28 June 2002.
[92] Y. Song, Y. Ni, F. Wen, Z. Hou and F. F. Wu, "Conjectural variation based bidding strategy in spot markets: fundamentals and comparison with classical game theoretical bidding strategies", *Electric Power Systems Research*, vol. 67, pp. 45-51, 2003.
[93] Y. Song, Y. Ni, F. Wen and F. F. Wu, "Conjectural variation based learning model of strategic bidding in spot market", *Electrical Power & Energy Systems*, vol. 26, pp. 797-804, 2004.
[94] C. J. Day, B. F. Hobbs and J.-S. Pang "Oligopolistic competition in power networks: a conjectured supply function approach", *IEEE Transactions on Power Systems*, vol. 17, no. 3, pp. 597-607, Aug. 2002.
[95] T. Peng and K. Tomsovic, "Optimal bidding strategies: an empirical conjectural approach", *School of EECS*, Washington State University, 2003.
[96] G. Bautista, V. H. Quintana and J. A. Aguado, "An oligopolistic model of an integrated market for energy and spinning reserve", *IEEE Transactions on Power Systems*, vol. 21, no. 1, pp. 132-142, Feb. 2006.
[97] E. Bompard, Y. Ma, R. Napoli, G. Abrate and E. Ragazzi, "The impact of price responsiveness on strategic equilibrium in competitive electricity markets", *Electrical Power & Energy Systems*, vol. 29, pp. 397-407, 2007.

[98] J. Delgado and D. Moreno, "Coalition-proof supply function equilibria in oligopoly", *Journal of Economic Theory*, vol. 114, pp. 231-254, 2007.
[99] J. Evans and R. Green, "Why did British electricity prices fall after 1998?", *CMI Working Paper 26*, University of Surrey and University of Birmingham, revised July 2005.
[100] D. M. Newbery, "Competition, contracts, and entry in the electricity spot market", *Rand Journal of Economics*, vol. 29, no. 4, pp. 726-749, Winter 1998.
[101] E. J. Anderson and H. Xu, "Supply function equilibrium in electricity spot markets with contracts and price caps", *Journal of Optimization Theory and Applications*, vol. 124, no. 2, pp. 257-283, Feb. 2005.
[102] R. Baldick and W. Hogan, "Capacity constrained supply function equilibrium models of electricity markets: Stability, non-decreasing constraints, and function space iterations", *Working Paper PWP-089*, University of California Energy Institute, revised Aug. 2002.
[103] R. Baldick and W. Hogan, "Stability of supply function equilibria implications for daily versus hourly bids in a poolco market", *Journal of Regulatory Economics*, vol. 30, no. 2, pp. 119-139, 2006.
[104] H. Chen, K. P. Wong, C. Y. Chung and D. H. M. Nguyen, "A coevolutionary approach to analyzing supply function equilibrium model", *IEEE Transactions on Power Systems*, vol. 21, no. 3, pp. 1019-1028, Aug. 2006.
[105] A. Rudkevich, M. Duckworth and R. Rosen, "Modeling electricity pricing in a deregulated generation industry: the potential for oligopoly pricing in a poolco", *The Energy Journal*, vol. 19, no. 3, pp. 19-48, 1998.
[106] A. Rudkevich, "Supply function equilibrium: theory and applications", *IEEE Proceedings of the 36th Hawaii International Conference on System Sciences*, 6-9 Jan. 2003.
[107] A. Rudkevich, "On the supply function equilibrium and its applications in electricity markets", *Decision Support Systems*, vol. 40, pp. 409-425, 2005.
[108] E. J. Anderson and A. B. Philpott, "Using supply functions for offering generation into an electricity market", *Operations Research*, vol. 50, no. 3, pp. 477-489, May-June 2002.
[109] F. Bolle, "Competition with supply and demand functions", *Energy Economics*, vol. 23, pp. 253-277, 2001.
[110] E. J. Anderson and H. Xu, "Nash equilibria in electricity markets with discrete prices", *Mathematical Methods of Operational Research*, vol. 60, pp. 215-238, 2004.
[111] Y. Liu and F. F. Wu, "Existence, uniqueness, stability of linear supply function equilibrium in electricity markets", *IEEE PES General Meeting 2004*, vol. 1, pp. 249-254, 6-10 June 2004.
[112] R. Baldick, R. Grant and E. Kahn, "Linear supply function equilibrium: generalizations, application, and limitations", *Working Paper PWP-078*, University of California Energy Institute, revised Aug. 2000.
[113] R. Baldick, "Electricity market equilibrium models: the effect of parametrization", *IEEE Transactions on Power Systems*, vol. 17, no. 4, pp. 1170-1176, Nov. 2002.
[114] H. Haghighat, H. Seifi, A. R. Kian "Gaming analysis in joint energy and spinning reserve markets", *IEEE Transactions on Power Systems*, vol. 22, no. 4, pp. 2074-2085, Nov. 2007.
[115] X. Hu, D. Ralph, E. K. Ralph, P. Bardsley and M. C. Ferris, "Electricity generation with looped transmission networks: bidding to an ISO", *CMI Working Paper 65*, University of Cambridge, revised 12 Dec. 2004.
[116] X. Hu and D. Ralph, "Using EPECs to model bilevel games in restructured electricity markets with locational prices", *Operations Research*, vol. 55, no. 5, pp. 809-827, Sept.-Oct. 2007.
[117] R. Green, "The electricity contract market in England and Wales", *The Journal of Industrial Economics*, vol. 47, no. 1, pp. 107-124, Mar. 1999.
[118] C. A. Berry, B. F. Hobbs, W. A. Meroney, R. P. O'Neil and W. R. Stewart Jr, "Understanding how market power can arise in network competition: a game theoretic approach", *Utilities Policy*, vol. 8, pp. 139-158, 1999.
[119] H. Niu, R. Baldick and G. Zhu, "Supply function equilibrium bidding strategies with fixed forward contracts", *IEEE Transactions on Power Systems*, vol. 20, no. 4, pp. 1859-1867, Nov. 2005.
[120] J. D. Weber and T. J. Overbye, "An individual welfare maximisation algorithm for electricity markets", *IEEE Transactions on Power Systems*, vol. 17, no. 3, pp. 590-596, Aug. 2002.

[121] A. Halseth, "Market power in the Nordic electricity market", *Utilities Policy*, vol. 7, pp. 259-268, 1998.
[122] E. Bompard, W. Lu and R. Napoli, "Network constraint impacts on the competitive electricity markets under supply-side strategic bidding", *IEEE Transactions on Power Systems*, vol. 21, no. 1, pp. 160-170, Feb. 2006.
[123] E. Bompard, Y. C. Ma, R. Napoli and C. W. Jiang, "Assessing the market power due to network constraints in competitive electricity markets", *Electric Power Systems Research*, vol. 76, pp. 953-961, 2006.
[124] R. W. Ferrero, J. F. Rivera and S. M. Shahidehpour, "Application of games with incomplete information for pricing electricity in deregulated power pools", *IEEE Transactions on Power Systems*, vol. 13, no. 1, pp. 184-189, Feb. 1998.
[125] E. Elia, A. Maiorano, Y. H. Song and M. Trovato, "Novel methodology for simulation studies of strategic behavior of electricity producers", *IEEE PES Summer Meeting 2000*, vol. 4, pp. 2235-2241, 16-20 July 2000.
[126] F. Wen and A. K. David, "Optimal bidding strategies and modeling of imperfect information among competitive generators", *IEEE Transactions on Power Systems*, vol. 16, no. 1, pp. 15-21, Feb. 2001.
[127] F. Wen and A. K. David, "Optimal bidding strategies for competitive generators and large consumers", *Electrical Power & Energy Systems*, vol. 23, pp. 37-43, 2001.
[128] P. F. Correia, T. J. Overbye and I. A. Hiskens, "Searching for noncooperative equilibria in centralized electricity markets", *IEEE Transactions on Power Systems*, vol. 18, no. 4, pp. 1417-1424, Nov. 2003.
[129] Y. F. Liu and F. F. Wu, "Impact of suppliers' learning behaviour on the market equilibrium under repeated linear supply-function bidding", *IEE Proceedings-Generation, Transmission, Distribution*, vol. 153, no. 1, pp. 44-50, Jan. 2006.
[130] A. Minoia, D. Ernst, M. Dicorato, M. Trovato and M. Ilic, "Reference transmission network: a game theory approach", *IEEE Transactions on Power Systems*, vol. 21, no. 1, pp. 249-259, Feb. 2006.
[131] Y. Liu and F. F. Wu, "Impacts of network constraints on electricity market equilibrium", *IEEE Transactions on Power Systems*, vol. 22, no. 1, pp. 126-135, Feb. 2007.
[132] A. Badri, S. Jadid, M. Rashidinejad and M. P. Moghaddam, "Optimal bidding strategies in oligopoly markets considering bilateral contracts and transmission constraints", *Electric Power Systems Research*, vol. 78, pp. 1089-1098, 2008.
[133] J. D. Weber and T. J. Overbye, "A two-level optimization problem for analysis of market bidding strategies", *IEEE PES Summer Meeting 1999*, vol. 2, pp. 682-687, 18-22 July 1999.
[134] X. Wang, Y. Li and S. Zhang, "Oligopolistic equilibrium analysis for electricity markets: a nonlinear complementarity approach", *IEEE Transactions on Power Systems*, vol. 19, no. 3, pp. 1348-1355, Aug. 2004.
[135] T. Li and M. Shahidehpour, "Strategic bidding of transmission-constrained GENCOs with incomplete information", *IEEE Transactions on Power Systems*, vol. 20, no. 1, pp. 437-447, Feb. 2005.
[136] E. Bompard, Y. Ma, R. Napoli and G. Abrate, "The demand elasticity impacts on the strategic bidding behavior of the electricity producers", *IEEE Transactions on Power Systems*, vol. 22, no. 1, pp. 188-197, Feb. 2007.
[137] S. G. Petoussis, X. P. Zhang and K. R. Godfrey, "Electricity market equilibrium analysis based on nonlinear interior point algorithm with complementarity constraints", *IET Generation, Transmission, Distribution*, vol. 1, no. 4, pp. 603-612, July 2007.
[138] S. Soleymani, A. M. Ranjbar and A. R. Shirani, "Strategic bidding of generating units in competitive electricity market with considering their reliability", *Electrical Power & Energy Systems*, vol. 30, pp. 193-201, 2008.
[139] G. Facchini, P. J. Hammond and H. Nakata, "Spurious deadweight gains", *Economic Letters*, vol. 72, pp. 33-37, 2001.
[140] R. W. Ferrero, S. M. Shahidehpour and V. C. Ramesh, "Transaction analysis in deregulated power systems using game theory", *IEEE Transactions on Power Systems*, vol. 12, no. 3, pp. 1340-1347, Aug. 1997.
[141] F. L. Alvarado, T. Overbye and P. Sauer, "Measuring reactive market power", *IEEE PES Winter Meeting 1991*, vol. 1, pp. 294-296, 31 Jan.-04 Feb. 1999.
[142] P. F. Correia, "Games with incomplete and asymmetric information in poolco markets", *IEEE Transactions on Power Systems*, vol. 20, no. 1, pp. 83-89, Feb. 2005.

[143] J.C. Harsanyi, "Games with incomplete information played by "Bayesian" players, I-III", *Management Science*, vol. 14, no. 3, pp. 159-182, 320-334, 486-502, Nov. 1967.
[144] G. S. Fishman, "Monte Carlo: concepts, algorithms, and applications", *Springer*, 1996.
[145] F. Wen and A. K. David, "Strategic bidding in reserve market", *Proceedings of the 5th APSCOM 2000 Conference*, pp. 80-85, Hong Kong, Oct. 2000.
[146] F. S. Wen and A. K. David, "Optimally co-ordinated bidding strategies in energy and ancillary service markets", *IEE Proceedings-Generation, Transmission, Distribution*, vol. 149, no. 3, pp. 331-339, May 2002.
[147] F. Wen and A. K. David, "Coordination of bidding strategies in day-ahead energy and spinning reserve markets", *Electrical Power & Energy Systems*, vol. 24, pp. 251-261, 2002.
[148] V. P. Gountis and A. G. Bakirtzis, "Bidding strategies for electricity producers in a competitive electricity marketplace", *IEEE Transactions on Power Systems*, vol. 19, no. 1, pp. 356-365, Feb. 2004.
[149] Y. Ma, C. Jiang, Z. Hou and C. Wang, "The formulation of the optimal strategies for the electricity producers based on the particle swarm optimization algorithm", *IEEE Transactions on Power Systems*, vol. 21, no. 4, pp. 1663-1671, Nov. 2006.
[150] P. Bajpai, S. K. Punna and S. N. Singh, "Swarm intelligence-based strategic bidding in competitive electricity markets", *IET Generation, Transmission, Distribution*, vol. 2, no. 2, pp. 175-184, Mar. 2008.
[151] J. Carpentier, "Contribution a l'étude du dispatching économique", *Bulletin de la Société Française des Electriciens*, ser. 8, vol. 3, pp. 431-447, Aug. 1962.
[152] H. W. Dommel and W. F. Tinney, "Optimal power flow solutions", *IEEE Transactions on Apparatus and Systems*, vol. 87, no. 10, pp. 1866-1876, Oct. 1968.
[153] A. J. Wood and B. F. Wollenberg, "Power generation operation and control", *John Wiley & Sons Inc.*, 2nd edition, 1996.
[154] J. A. Momoh, "Electric power system applications of optimization", *Marcel Dekker Inc.*, 2001.
[155] J. A. Momoh, M. E. El-Hawary and R. Adapa, "A review on selected optimal power flow literature to 1993 Part I: nonlinear and quadratic programming approaches", *IEEE Transactions on Power Systems*, vol. 14, no. 1, pp. 96-104, Feb. 1999.
[156] J. A. Momoh, M. E. El-Hawary and R. Adapa, "A review on selected optimal power flow literature to 1993 Part II: Newton, linear programming and interior point methods", *IEEE Transactions on Power Systems*, vol. 14, no. 1, pp. 105-111, Feb. 1999.
[157] M. Huneault and F. D. Galiana, "A survey of the optimal power flow literature", *IEEE Transactions on Power Systems*, vol. 6, no. 2, pp. 762-770, May 1991.
[158] H. W. Kuhn and A. W. Tucker, "Nonlinear programming", *Proceedings of 2nd Berkeley Symposium on Mathematica, Statistics and Probability, University of California Press*, pp. 481-492, 1951.
[159] R. W. Cottle, F. Giannessi and J-L. Lions, "Variational inequalities and complementarity problems", *John Wiley & Sons*, 1980.
[160] A. Fischer, "A special Newton-type optimization method", *Optimization*, vol. 24, pp. 269-284, 1992.
[161] S. Dirkse, and M. C. Ferris, "The PATH solver: a non-monotone stabilization scheme for mixed complementarity problems", *Optimization Methods and Software*, vol. 5, pp. 123–156, 1995.
[162] D. Ralph and Y. Smeers, "EPECs as models for electricity markets", *PSCE 2006 IEEE PES Conference*, Atlanta USA, pp. 74-80, 29 Oct.-01 Nov. 2006.
[163] P. Skantze and J. Chapman, "Price dynamics in the deregulated California energy market", *Proceedings of IEEE PES 1999 Winter Meeting*, New York, 31 Jan. - 04 Feb. 1999.
[164] G. Strbac and D. Kirschen, "Assessing the competitiveness of demand-side bidding", *IEEE Transactions on Power Systems*, vol. 14, no. 1, pp. 120-125, Feb. 1999.
[165] G. L. Torres and V. H. Quintana, "An interior-point method for nonlinear optimal power flow using voltage rectangular coordinates", *IEEE Transactions on Power Systems*, vol. 13, no. 4, pp. 1211-1218, Nov. 1998.
[166] A. V. Fiacco and G. P. McCormick, "Nonlinear programming: sequential unconstrained minimization techniques", *John Wiley and Sons Inc.*, 1968.
[167] N. Karmarkar, "A new polynomial-time algorithm for linear programming", *Combinatorica*, vol. 4, no. 4, pp. 373-395, 1984.

[168] P. E. Gill, W. Murray, M. A. Saunders, J. A. Tomlin and M. H. Wright, "On projected Newton barrier methods for linear programming and an equivalence to Karmarkar's projective method", *Mathematical Programming*, vol. 36, pp. 186-209, 1986.
[169] R. Marsten, R. Subramanian, M. Saltzman, I. Lustig and D. Shanno, "Interior point methods for linear programming: just call Newton, Lagrange, and Fiacco and McCormick!", *Interfaces*, vol. 20, no. 4, pp. 105-116, July-Aug. 1990.
[170] J. L. Lagrange, "Mécanique Analytique", Paris, France, 1788.
[171] I. Newton, "Philosophiæ naturalis principia mathematica", London, England, 1687.
[172] N. Megiddon, "Progress in mathematical programming, Chapter 3: Pathways to the optimal set in linear programming" *Springer-Verlag*, New York, USA.
[173] D. C. Monteiro and I. Adler, "Interior path following primal-dual algorithms. Part I: linear programming", *Mathematical Programming*, vol. 44, pp. 27-41, 1989.
[174] S. Mehrotra, "On the implementation of a primal-dual interior point method", *SIAM Journal of Optimization*, vol. 2, no. 4, pp. 575-601, Nov. 1992.
[175] I. J. Lustig, R. E. Marsten and D. F. Shanno, " On implementing Mehrotra's predictor-corrector interior-point method for linear programming", *SIAM Journal of Optimization*, vol. 2, no. 3, pp. 435-449, Aug. 1992.
[176] J. D. Glover and M. S. Sarma, "Power system analysis and design", *Brooks/Cole*, 3rd edition, 2002.
[177] S. Granville, "Optimal reactive dispatch through interior point methods", *IEEE Transactions on Power Systems*, vol. 9, no. 1, pp. 136-146, Feb. 1994.
[178] Y.-C. Wu, A. S. Debs and R. E. Marsten, "A direct nonlinear predictor-corrector primal-dual interior point algorithm for optimal power flows", *IEEE Transactions on Power Systems*, vol. 9, no. 2, pp. 876-883, May 1994.
[179] X. Yan and V. H. Quintana, "An efficient predictor-corrector interior point algorithm for security-constrained economic dispatch", *IEEE Transactions on Power Systems*, vol. 12, no. 2, pp. 803-810, May 1997.
[180] H. Wei, H. Sasaki, J. Kubokawa and R. Yokoyama, "An interior point nonlinear programming for optimal power flow problems with a novel data structure", *IEEE Transactions on Power Systems*, vol. 13, no. 3, pp. 870-877, Aug. 1998.
[181] V. H. Quintana, G. L. Torres and J. Medina-Palomo, "Interior-point methods and their applications to power systems: a classification of publications and software codes", *IEEE Transactions on Power Systems*, vol. 15, no. 1, pp. 170-176, Feb. 2000.
[182] K. Xie, Y.-H. Song, J. Stonham, E. Yu and G. Liu, "Decomposition model and interior point methods for optimal spot pricing of electricity in deregulation environments", *IEEE Transactions on Power Systems*, vol. 15, no. 1, pp. 39-50, Feb. 2000.
[183] K. Xie and Y. H. Song, "Power market oriented optimal power flow via an interior point method", *IEE Proceedings on Generation, Transmission, Distribution*, vol. 148, no. 6, pp. 549-556, Nov. 2001.
[184] R. A. Jabr, A. H. Coonick and B. J. Cory, "A primal-dual interior point method for optimal power flow dispatching", *IEEE Transactions on Power Systems*, vol. 17, no. 3, pp. 654-662, Aug. 2002.
[185] R. A. Jabr, "A primal-dual interior-point method to solve the optimal power flow dispatching problem", *Optimization and Engineering*, vol. 4, pp. 309-336, 2003.
[186] H. Wang, C. E. Murillo-Sanchez, R. D. Zimmerman and R. J. Thomas, "On computational issues of market-based optimal power flow", *IEEE Transactions on Power Systems*, vol. 22, no. 3, pp. 1185-1193, Aug. 2007.
[187] Z.-Q. Luo, J.-S. Pang and D. Ralph, "Mathematical programs with equilibrium constraints", *Cambridge University Press*, Cambridge, United Kingdom, 1996.
[188] T. Gönen, "Modern power system analysis", *John Wiley & Sons*, USA, 1988.
[189] F. Facchinei and C Kanzow, "A nonsmooth inexact Newton method for the solution of large-scale nonlinear complementarity problems", *Mathematical Programming*, vol. 76, pp. 493-512, 1997.
[190] D. I. Sun, B. Ashley, B. Brewer, A. Hughes and W. F. Tinney, "Optimal power flow by Newton approach", *IEEE Transactions on Power Apparatus and Systems*, vol. PAS-103, no. 10, pp. 2864-2880, Oct. 1984.
[191] http://www.ee.washington.edu/research/pstca/
[192] B. F. Hobbs, J. Inon and S. E. Stoft, "Installed capacity requirements and price caps: oil on the water, or fuel on the fire?", *The Electricity Journal*, vol. 14, issue 6, pp. 23-34, July 2001.

[193] Greenpeace and EPIA, "Solar generation V - 2008: solar electricity for over one billion people and two million jobs by 2020", *EPIA a.i.s.b.l./Greenpeace International*, Sept. 2008.
[194] B. Zinsser, G. Makrides, W. Schmitt, G. Georghiou and J. Werner, "Annual energy yield of 13 photovoltaic technologies in Germany and in Cyprus", *Proceedings of European Photovoltaic Solar Energy Conference (EUPVSEC) 2007*, pp.3114-3117, Sept. 2007.
[195] EN 50160: 1999. Voltage characteristics of electricity supplied by public distribution systems.
[196] EN 61727: 1996. Photovoltaic (PV) systems. Characteristics of the utility interface.
[197] G. J. Yu, J. H. So, Y. S. Jung and G. H. Kang, "Performance results of 15KW BIPV sunshade system", *31st IEEE Photovoltaic Specialists Conference*, pp. 1722-1725, Jan. 2005.
[198] D. Chenvidhya, J. Thongporn, U. Sangpanich, N. Wongyao, K. Kirtikara and C. Jivacate, "A Thai national demonstration project on PV grid-interactive systems: power quality observation", *Proceedings of 3rd World Conference on Photovoltaic Energy Conversion*, vol. 3, pp. 2152-2154, May 2003.
[199] X.-P. Zhang, E. Handschin and M. M. Yao, "Modeling of the generalized unified power flow controller (GUPFC) in a nonlinear interior point OPF", *IEEE Transactions on Power Systems*, vol. 16, no. 3, pp. 367-373, Aug. 2001.
[200] X.-P. Zhang and E. Handschin, "Advanced implementation of UPFC in a nonlinear interior-point OPF", *IEE Proceedings-Generation, Transmission, Distribution*, vol. 148, no. 5, pp. 489-496, Sept. 2001.
[201] X. P. Zhang, S. G. Petoussis and K. R. Godfrey, "Novel nonlinear interior point optimal power flow (OPF) method based on current mismatch formulation", *IEE Proceedings-Generation, Transmission, Distribution*, vol. 125, no. 6, pp. 795-805, Nov. 2005.
[202] J. J. Grainger and W. D. Stevenson Jr., "Power system analysis", *McGraw-Hill Inc.*, International Editions 1994.
[203] A. C. Franklin and J. S. C. Franklin, "The J&P transformer book", *Butterworth Heinmann*, 11th edition, 1983.
[204] M. S. Carlovic, "Modelling and analysis of under-load tap-changing transformer control systems", *IEEE Transactions on Apparatus and Systems*, vol. PAS-103, no. 7, pp. 1909-1915, July 1984.
[205] E. Acha, H. Ambriz-Perez and C. R. Fuerte-Esquivel, "Advanced transformer modeling in an optimal power flow using Newton's method", *IEEE Transactions on Power Systems*, vol. 15, no. 1, pp. 290-298, Feb. 2000.

APPENDIX I

Contribution of the transformer formulation in the electricity market equilibrium algorithm

Appendix I:

List of the elements of the Newton matrix equation that result from the modelling of transformer

Appendix I presents the expanded terms for the individual contributions to the elements of the Newton matrix and right-hand vector of (3.137) from the modelling of transformer power flows and losses, and tap-ratio control, as derived from the linearized versions of the KKT condition equations for the market problem (4.2)-(4.16). Each linearized equation precedes the elements for which it is responsible for, and the right-hand vector element, which is calculated from the KKT system (3.95)-(3.110) is presented last. Note that the *x* terms in equations (4.2)-(4.16) correspond to $x = [e_i, f_i, e_j, f_j, t]$, since they represent only the transformer contribution. The inequality term h_t is equal to the tap-ratio *t*, as defined in Section 3.5.2. The element of the Newton matrix that corresponds to the row of $-\nabla_a L_{2\mu}$ in the right-hand vector and the column of Δb from the associated linearized equation is represented by Δa - Δb. Since the Newton matrix is symmetric, the element Δa - Δb is identical to Δb - Δa. The evaluated expressions for the derivative terms in the following elements can be found in Appendix II. Note that the following elements may not be the actual elements of the Newton matrix equation in the formulation of the interior point algorithm but only a part of them, since they correspond only to the transformer contribution. The modelling of other network components may also contribute to the following elements of the Newton matrix equation.

Analysis of equation (4.2):

$$
\begin{aligned}
-\nabla_t L_{2\mu} = -[&\sum \omega_x \lambda p_i \nabla_t \nabla_x^2 \Delta P_i^{TR} + \sum \omega_x \lambda q_i \nabla_t \nabla_x^2 \Delta Q_i^{TR} + \sum \omega_{\lambda p_i} \nabla_t \nabla_x \Delta P_i^{TR} + \sum \omega_{\lambda q_i} \nabla_t \nabla_x \Delta Q_i^{TR}] \Delta x \\
&- \sum \omega_x \nabla_t \nabla_x \Delta P_i^{TR} \Delta \lambda p_i - \sum \omega_x \nabla_t \nabla_x \Delta Q_i^{TR} \Delta \lambda q_i \\
&- [\sum \lambda p_i \nabla_t \nabla_x \Delta P_i^{TR} + \sum \lambda q_i \nabla_t \nabla_x \Delta Q_i^{TR}] \Delta \omega_x \\
&- \sum \nabla_t \Delta P_i^{TR} \Delta \omega_{\lambda p_i} - \sum \nabla_t \Delta Q_i^{TR} \Delta \omega_{\lambda q_i} - \nabla_t h_t \Delta \omega_{\pi l_t} - \nabla_t h_t \Delta \omega_{\pi u_t}
\end{aligned}
$$

Elements of Newton matrix:

$$\begin{aligned}\Delta t\text{-}\Delta e_i &= -\sum \omega_x \lambda p_i \nabla_t \nabla_{e_i} \nabla_x \Delta P_i^{TR} - \sum \omega_x \lambda q_i \nabla_t \nabla_{e_i} \nabla_x \Delta Q_i^{TR} - \sum \omega_{\lambda p_i} \nabla_t \nabla_{e_i} \Delta P_i^{TR} - \sum \omega_{\lambda q_i} \nabla_t \nabla_{e_i} \Delta Q_i^{TR} \\ &= -\lambda p_i (\omega_{e_i} \nabla_t \nabla_{e_i} \nabla_{e_i} \Delta P_i^{TR} + \omega_{f_i} \nabla_t \nabla_{e_i} \nabla_{f_i} \Delta P_i^{TR} + \omega_{e_j} \nabla_t \nabla_{e_i} \nabla_{e_j} \Delta P_i^{TR} + \omega_{f_j} \nabla_t \nabla_{e_i} \nabla_{f_j} \Delta P_i^{TR} + \omega_t \nabla_t \nabla_{e_i} \nabla_t \Delta P_i^{TR}) \\ &\quad - \lambda p_j (\omega_{e_i} \nabla_t \nabla_{e_i} \nabla_{e_i} \Delta P_j^{TR} + \omega_{f_i} \nabla_t \nabla_{e_i} \nabla_{f_i} \Delta P_j^{TR} + \omega_{e_j} \nabla_t \nabla_{e_i} \nabla_{e_j} \Delta P_j^{TR} + \omega_{f_j} \nabla_t \nabla_{e_i} \nabla_{f_j} \Delta P_j^{TR} + \omega_t \nabla_t \nabla_{e_i} \nabla_t \Delta P_j^{TR}) \\ &\quad - \lambda q_i (\omega_{e_i} \nabla_t \nabla_{e_i} \nabla_{e_i} \Delta Q_i^{TR} + \omega_{f_i} \nabla_t \nabla_{e_i} \nabla_{f_i} \Delta Q_i^{TR} + \omega_{e_j} \nabla_t \nabla_{e_i} \nabla_{e_j} \Delta Q_i^{TR} + \omega_{f_j} \nabla_t \nabla_{e_i} \nabla_{f_j} \Delta Q_i^{TR} + \omega_t \nabla_t \nabla_{e_i} \nabla_t \Delta Q_i^{TR}) \\ &\quad - \lambda q_j (\omega_{e_i} \nabla_t \nabla_{e_i} \nabla_{e_i} \Delta Q_j^{TR} + \omega_{f_i} \nabla_t \nabla_{e_i} \nabla_{f_i} \Delta Q_j^{TR} + \omega_{e_j} \nabla_t \nabla_{e_i} \nabla_{e_j} \Delta Q_j^{TR} + \omega_{f_j} \nabla_t \nabla_{e_i} \nabla_{f_j} \Delta Q_j^{TR} + \omega_t \nabla_t \nabla_{e_i} \nabla_t \Delta Q_j^{TR}) \\ &\quad - \omega_{\lambda p_i} \nabla_t \nabla_{e_i} \Delta P_i^{TR} - \omega_{\lambda p_j} \nabla_t \nabla_{e_i} \Delta P_j^{TR} - \omega_{\lambda q_i} \nabla_t \nabla_{e_i} \Delta Q_i^{TR} - \omega_{\lambda q_j} \nabla_t \nabla_{e_i} \Delta Q_j^{TR}\end{aligned}$$

$$\begin{aligned}\Delta t\text{-}\Delta f_i &= -\sum \omega_x \lambda p_i \nabla_t \nabla_{f_i} \nabla_x \Delta P_i^{TR} - \sum \omega_x \lambda q_i \nabla_t \nabla_{f_i} \nabla_x \Delta Q_i^{TR} - \sum \omega_{\lambda p_i} \nabla_t \nabla_{f_i} \Delta P_i^{TR} - \sum \omega_{\lambda q_i} \nabla_t \nabla_{f_i} \Delta Q_i^{TR} \\ &= -\lambda p_i (\omega_{e_i} \nabla_t \nabla_{f_i} \nabla_{e_i} \Delta P_i^{TR} + \omega_{f_i} \nabla_t \nabla_{f_i} \nabla_{f_i} \Delta P_i^{TR} + \omega_{e_j} \nabla_t \nabla_{f_i} \nabla_{e_j} \Delta P_i^{TR} + \omega_{f_j} \nabla_t \nabla_{f_i} \nabla_{f_j} \Delta P_i^{TR} + \omega_t \nabla_t \nabla_{f_i} \nabla_t \Delta P_i^{TR}) \\ &\quad - \lambda p_j (\omega_{e_i} \nabla_t \nabla_{f_i} \nabla_{e_i} \Delta P_j^{TR} + \omega_{f_i} \nabla_t \nabla_{f_i} \nabla_{f_i} \Delta P_j^{TR} + \omega_{e_j} \nabla_t \nabla_{f_i} \nabla_{e_j} \Delta P_j^{TR} + \omega_{f_j} \nabla_t \nabla_{f_i} \nabla_{f_j} \Delta P_j^{TR} + \omega_t \nabla_t \nabla_{f_i} \nabla_t \Delta P_j^{TR}) \\ &\quad - \lambda q_i (\omega_{e_i} \nabla_t \nabla_{f_i} \nabla_{e_i} \Delta Q_i^{TR} + \omega_{f_i} \nabla_t \nabla_{f_i} \nabla_{f_i} \Delta Q_i^{TR} + \omega_{e_j} \nabla_t \nabla_{f_i} \nabla_{e_j} \Delta Q_i^{TR} + \omega_{f_j} \nabla_t \nabla_{f_i} \nabla_{f_j} \Delta Q_i^{TR} + \omega_t \nabla_t \nabla_{f_i} \nabla_t \Delta Q_i^{TR}) \\ &\quad - \lambda q_j (\omega_{e_i} \nabla_t \nabla_{f_i} \nabla_{e_i} \Delta Q_j^{TR} + \omega_{f_i} \nabla_t \nabla_{f_i} \nabla_{f_i} \Delta Q_j^{TR} + \omega_{e_j} \nabla_t \nabla_{f_i} \nabla_{e_j} \Delta Q_j^{TR} + \omega_{f_j} \nabla_t \nabla_{f_i} \nabla_{f_j} \Delta Q_j^{TR} + \omega_t \nabla_t \nabla_{f_i} \nabla_t \Delta Q_j^{TR}) \\ &\quad - \omega_{\lambda p_i} \nabla_t \nabla_{f_i} \Delta P_i^{TR} - \omega_{\lambda p_j} \nabla_t \nabla_{f_i} \Delta P_j^{TR} - \omega_{\lambda q_i} \nabla_t \nabla_{f_i} \Delta Q_i^{TR} - \omega_{\lambda q_j} \nabla_t \nabla_{f_i} \Delta Q_j^{TR}\end{aligned}$$

$$\begin{aligned}\Delta t\text{-}\Delta e_j &= -\sum \omega_x \lambda p_i \nabla_t \nabla_{e_j} \nabla_x \Delta P_i^{TR} - \sum \omega_x \lambda q_i \nabla_t \nabla_{e_j} \nabla_x \Delta Q_i^{TR} - \sum \omega_{\lambda p_i} \nabla_t \nabla_{e_j} \Delta P_i^{TR} - \sum \omega_{\lambda q_i} \nabla_t \nabla_{e_j} \Delta Q_i^{TR} \\ &= -\lambda p_i (\omega_{e_i} \nabla_t \nabla_{e_j} \nabla_{e_i} \Delta P_i^{TR} + \omega_{f_i} \nabla_t \nabla_{e_j} \nabla_{f_i} \Delta P_i^{TR} + \omega_{e_j} \nabla_t \nabla_{e_j} \nabla_{e_j} \Delta P_i^{TR} + \omega_{f_j} \nabla_t \nabla_{e_j} \nabla_{f_j} \Delta P_i^{TR} + \omega_t \nabla_t \nabla_{e_j} \nabla_t \Delta P_i^{TR}) \\ &\quad - \lambda p_j (\omega_{e_i} \nabla_t \nabla_{e_j} \nabla_{e_i} \Delta P_j^{TR} + \omega_{f_i} \nabla_t \nabla_{e_j} \nabla_{f_i} \Delta P_j^{TR} + \omega_{e_j} \nabla_t \nabla_{e_j} \nabla_{e_j} \Delta P_j^{TR} + \omega_{f_j} \nabla_t \nabla_{e_j} \nabla_{f_j} \Delta P_j^{TR} + \omega_t \nabla_t \nabla_{e_j} \nabla_t \Delta P_j^{TR}) \\ &\quad - \lambda q_i (\omega_{e_i} \nabla_t \nabla_{e_j} \nabla_{e_i} \Delta Q_i^{TR} + \omega_{f_i} \nabla_t \nabla_{e_j} \nabla_{f_i} \Delta Q_i^{TR} + \omega_{e_j} \nabla_t \nabla_{e_j} \nabla_{e_j} \Delta Q_i^{TR} + \omega_{f_j} \nabla_t \nabla_{e_j} \nabla_{f_j} \Delta Q_i^{TR} + \omega_t \nabla_t \nabla_{e_j} \nabla_t \Delta Q_i^{TR}) \\ &\quad - \lambda q_j (\omega_{e_i} \nabla_t \nabla_{e_j} \nabla_{e_i} \Delta Q_j^{TR} + \omega_{f_i} \nabla_t \nabla_{e_j} \nabla_{f_i} \Delta Q_j^{TR} + \omega_{e_j} \nabla_t \nabla_{e_j} \nabla_{e_j} \Delta Q_j^{TR} + \omega_{f_j} \nabla_t \nabla_{e_j} \nabla_{f_j} \Delta Q_j^{TR} + \omega_t \nabla_t \nabla_{e_j} \nabla_t \Delta Q_j^{TR}) \\ &\quad - \omega_{\lambda p_i} \nabla_t \nabla_{e_j} \Delta P_i^{TR} - \omega_{\lambda p_j} \nabla_t \nabla_{e_j} \Delta P_j^{TR} - \omega_{\lambda q_i} \nabla_t \nabla_{e_j} \Delta Q_i^{TR} - \omega_{\lambda q_j} \nabla_t \nabla_{e_j} \Delta Q_j^{TR}\end{aligned}$$

$$\begin{aligned}\Delta t\text{-}\Delta f_j &= -\sum \omega_x \lambda p_i \nabla_t \nabla_{f_j} \nabla_x \Delta P_i^{TR} - \sum \omega_x \lambda q_i \nabla_t \nabla_{f_j} \nabla_x \Delta Q_i^{TR} - \sum \omega_{\lambda p_i} \nabla_t \nabla_{f_j} \Delta P_i^{TR} - \sum \omega_{\lambda q_i} \nabla_t \nabla_{f_j} \Delta Q_i^{TR} \\ &= -\lambda p_i (\omega_{e_i} \nabla_t \nabla_{f_j} \nabla_{e_i} \Delta P_i^{TR} + \omega_{f_i} \nabla_t \nabla_{f_j} \nabla_{f_i} \Delta P_i^{TR} + \omega_{e_j} \nabla_t \nabla_{f_j} \nabla_{e_j} \Delta P_i^{TR} + \omega_{f_j} \nabla_t \nabla_{f_j} \nabla_{f_j} \Delta P_i^{TR} + \omega_t \nabla_t \nabla_{f_j} \nabla_t \Delta P_i^{TR}) \\ &\quad - \lambda p_j (\omega_{e_i} \nabla_t \nabla_{f_j} \nabla_{e_i} \Delta P_j^{TR} + \omega_{f_i} \nabla_t \nabla_{f_j} \nabla_{f_i} \Delta P_j^{TR} + \omega_{e_j} \nabla_t \nabla_{f_j} \nabla_{e_j} \Delta P_j^{TR} + \omega_{f_j} \nabla_t \nabla_{f_j} \nabla_{f_j} \Delta P_j^{TR} + \omega_t \nabla_t \nabla_{f_j} \nabla_t \Delta P_j^{TR}) \\ &\quad - \lambda q_i (\omega_{e_i} \nabla_t \nabla_{f_j} \nabla_{e_i} \Delta Q_i^{TR} + \omega_{f_i} \nabla_t \nabla_{f_j} \nabla_{f_i} \Delta Q_i^{TR} + \omega_{e_j} \nabla_t \nabla_{f_j} \nabla_{e_j} \Delta Q_i^{TR} + \omega_{f_j} \nabla_t \nabla_{f_j} \nabla_{f_j} \Delta Q_i^{TR} + \omega_t \nabla_t \nabla_{f_j} \nabla_t \Delta Q_i^{TR}) \\ &\quad - \lambda q_j (\omega_{e_i} \nabla_t \nabla_{f_j} \nabla_{e_i} \Delta Q_j^{TR} + \omega_{f_i} \nabla_t \nabla_{f_j} \nabla_{f_i} \Delta Q_j^{TR} + \omega_{e_j} \nabla_t \nabla_{f_j} \nabla_{e_j} \Delta Q_j^{TR} + \omega_{f_j} \nabla_t \nabla_{f_j} \nabla_{f_j} \Delta Q_j^{TR} + \omega_t \nabla_t \nabla_{f_j} \nabla_t \Delta Q_j^{TR}) \\ &\quad - \omega_{\lambda p_i} \nabla_t \nabla_{f_j} \Delta P_i^{TR} - \omega_{\lambda p_j} \nabla_t \nabla_{f_j} \Delta P_j^{TR} - \omega_{\lambda q_i} \nabla_t \nabla_{f_j} \Delta Q_i^{TR} - \omega_{\lambda q_j} \nabla_t \nabla_{f_j} \Delta Q_j^{TR}\end{aligned}$$

$$\begin{aligned}\Delta t\text{-}\Delta t &= -\sum \omega_x \lambda p_i \nabla_t \nabla_t \nabla_x \Delta P_i^{TR} - \sum \omega_x \lambda q_i \nabla_t \nabla_t \nabla_x \Delta Q_i^{TR} - \sum \omega_{\lambda p_i} \nabla_t \nabla_t \Delta P_i^{TR} - \sum \omega_{\lambda q_i} \nabla_t \nabla_t \Delta Q_i^{TR} \\ &= -\lambda p_i (\omega_{e_i} \nabla_t \nabla_t \nabla_{e_i} \Delta P_i^{TR} + \omega_{f_i} \nabla_t \nabla_t \nabla_{f_i} \Delta P_i^{TR} + \omega_{e_j} \nabla_t \nabla_t \nabla_{e_j} \Delta P_i^{TR} + \omega_{f_j} \nabla_t \nabla_t \nabla_{f_j} \Delta P_i^{TR} + \omega_t \nabla_t \nabla_t \nabla_t \Delta P_i^{TR}) \\ &\quad - \lambda p_j (\omega_{e_i} \nabla_t \nabla_t \nabla_{e_i} \Delta P_j^{TR} + \omega_{f_i} \nabla_t \nabla_t \nabla_{f_i} \Delta P_j^{TR} + \omega_{e_j} \nabla_t \nabla_t \nabla_{e_j} \Delta P_j^{TR} + \omega_{f_j} \nabla_t \nabla_t \nabla_{f_j} \Delta P_j^{TR} + \omega_t \nabla_t \nabla_t \nabla_t \Delta P_j^{TR}) \\ &\quad - \lambda q_i (\omega_{e_i} \nabla_t \nabla_t \nabla_{e_i} \Delta Q_i^{TR} + \omega_{f_i} \nabla_t \nabla_t \nabla_{f_i} \Delta Q_i^{TR} + \omega_{e_j} \nabla_t \nabla_t \nabla_{e_j} \Delta Q_i^{TR} + \omega_{f_j} \nabla_t \nabla_t \nabla_{f_j} \Delta Q_i^{TR} + \omega_t \nabla_t \nabla_t \nabla_t \Delta Q_i^{TR}) \\ &\quad - \lambda q_j (\omega_{e_i} \nabla_t \nabla_t \nabla_{e_i} \Delta Q_j^{TR} + \omega_{f_i} \nabla_t \nabla_t \nabla_{f_i} \Delta Q_j^{TR} + \omega_{e_j} \nabla_t \nabla_t \nabla_{e_j} \Delta Q_j^{TR} + \omega_{f_j} \nabla_t \nabla_t \nabla_{f_j} \Delta Q_j^{TR} + \omega_t \nabla_t \nabla_t \nabla_t \Delta Q_j^{TR}) \\ &\quad - \omega_{\lambda p_i} \nabla_t \nabla_t \Delta P_i^{TR} - \omega_{\lambda p_j} \nabla_t \nabla_t \Delta P_j^{TR} - \omega_{\lambda q_i} \nabla_t \nabla_t \Delta Q_i^{TR} - \omega_{\lambda q_j} \nabla_t \nabla_t \Delta Q_j^{TR}\end{aligned}$$

$$\Delta t\text{-}\Delta\lambda p_i = -\sum \omega_x \nabla_t \nabla_x \Delta P_i^{TR}$$
$$= -(\omega_{e_i} \nabla_t \nabla_{e_i} \Delta P_i^{TR} + \omega_{f_i} \nabla_t \nabla_{f_i} \Delta P_i^{TR} + \omega_{e_j} \nabla_t \nabla_{e_j} \Delta P_i^{TR} + \omega_{f_j} \nabla_t \nabla_{f_j} \Delta P_i^{TR} + \omega_t \nabla_t \nabla_t \Delta P_i^{TR})$$

$$\Delta t\text{-}\Delta\lambda p_j = -\sum \omega_x \nabla_t \nabla_x \Delta P_j^{TR}$$
$$= -(\omega_{e_i} \nabla_t \nabla_{e_i} \Delta P_j^{TR} + \omega_{f_i} \nabla_t \nabla_{f_i} \Delta P_j^{TR} + \omega_{e_j} \nabla_t \nabla_{e_j} \Delta P_j^{TR} + \omega_{f_j} \nabla_t \nabla_{f_j} \Delta P_j^{TR} + \omega_t \nabla_t \nabla_t \Delta P_j^{TR})$$

$$\Delta t\text{-}\Delta\lambda q_i = -\sum \omega_x \nabla_t \nabla_x \Delta Q_i^{TR}$$
$$= -(\omega_{e_i} \nabla_t \nabla_{e_i} \Delta Q_i^{TR} + \omega_{f_i} \nabla_t \nabla_{f_i} \Delta Q_i^{TR} + \omega_{e_j} \nabla_t \nabla_{e_j} \Delta Q_i^{TR} + \omega_{f_j} \nabla_t \nabla_{f_j} \Delta Q_i^{TR} + \omega_t \nabla_t \nabla_t \Delta Q_i^{TR})$$

$$\Delta t\text{-}\Delta\lambda q_j = -\sum \omega_x \nabla_t \nabla_x \Delta Q_j^{TR}$$
$$= -(\omega_{e_i} \nabla_t \nabla_{e_i} \Delta Q_j^{TR} + \omega_{f_i} \nabla_t \nabla_{f_i} \Delta Q_j^{TR} + \omega_{e_j} \nabla_t \nabla_{e_j} \Delta Q_j^{TR} + \omega_{f_j} \nabla_t \nabla_{f_j} \Delta Q_j^{TR} + \omega_t \nabla_t \nabla_t \Delta Q_j^{TR})$$

$$\Delta t\text{-}\Delta\omega_{e_i} = -\sum \lambda p_i \nabla_t \nabla_{e_i} \Delta P_i^{TR} - \sum \lambda q_i \nabla_t \nabla_{e_i} \Delta Q_i^{TR}$$
$$= -\lambda p_i \nabla_t \nabla_{e_i} \Delta P_i^{TR} - \lambda p_j \nabla_t \nabla_{e_i} \Delta P_j^{TR} - \lambda q_i \nabla_t \nabla_{e_i} \Delta Q_i^{TR} - \lambda q_j \nabla_t \nabla_{e_i} \Delta Q_j^{TR}$$

$$\Delta t\text{-}\Delta\omega_{f_i} = -\sum \lambda p_i \nabla_t \nabla_{f_i} \Delta P_i^{TR} - \sum \lambda q_i \nabla_t \nabla_{f_i} \Delta Q_i^{TR}$$
$$= -\lambda p_i \nabla_t \nabla_{f_i} \Delta P_i^{TR} - \lambda p_j \nabla_t \nabla_{f_i} \Delta P_j^{TR} - \lambda q_i \nabla_t \nabla_{f_i} \Delta Q_i^{TR} - \lambda q_j \nabla_t \nabla_{f_i} \Delta Q_j^{TR}$$

$$\Delta t\text{-}\Delta\omega_{e_j} = -\sum \lambda p_i \nabla_t \nabla_{e_j} \Delta P_i^{TR} - \sum \lambda q_i \nabla_t \nabla_{e_j} \Delta Q_i^{TR}$$
$$= -\lambda p_i \nabla_t \nabla_{e_j} \Delta P_i^{TR} - \lambda p_j \nabla_t \nabla_{e_j} \Delta P_j^{TR} - \lambda q_i \nabla_t \nabla_{e_j} \Delta Q_i^{TR} - \lambda q_j \nabla_t \nabla_{e_j} \Delta Q_j^{TR}$$

$$\Delta t\text{-}\Delta\omega_{f_j} = -\sum \lambda p_i \nabla_t \nabla_{f_j} \Delta P_i^{TR} - \sum \lambda q_i \nabla_t \nabla_{f_j} \Delta Q_i^{TR}$$
$$= -\lambda p_i \nabla_t \nabla_{f_j} \Delta P_i^{TR} - \lambda p_j \nabla_t \nabla_{f_j} \Delta P_j^{TR} - \lambda q_i \nabla_t \nabla_{f_j} \Delta Q_i^{TR} - \lambda q_j \nabla_t \nabla_{f_j} \Delta Q_j^{TR}$$

$$\Delta t\text{-}\Delta\omega_t = -\sum \lambda p_i \nabla_t \nabla_t \Delta P_i^{TR} - \sum \lambda q_i \nabla_t \nabla_t \Delta Q_i^{TR}$$
$$= -\lambda p_i \nabla_t \nabla_t \Delta P_i^{TR} - \lambda p_j \nabla_t \nabla_t \Delta P_j^{TR} - \lambda q_i \nabla_t \nabla_t \Delta Q_i^{TR} - \lambda q_j \nabla_t \nabla_t \Delta Q_j^{TR}$$

$$\Delta t\text{-}\Delta\omega_{\lambda p_i} = -\nabla_t \Delta P_i^{TR}$$

$$\Delta t\text{-}\Delta\omega_{\lambda p_j} = -\nabla_t \Delta P_j^{TR}$$

$$\Delta t\text{-}\Delta\omega_{\lambda q_i} = -\nabla_t \Delta Q_i^{TR}$$

$$\Delta t \text{ - } \Delta\omega_{\lambda q_j} = -\nabla_t \Delta Q_j^{TR}$$

$$\Delta t \text{ - } \Delta\omega_{\pi l_t} = -\nabla_t h_t = -1$$

$$\Delta t \text{ - } \Delta\omega_{\pi u_t} = -\nabla_t h_t = -1$$

Element of right-hand vector:

$$\begin{aligned}
-\nabla_t L_{2\mu} &= -[-\sum \omega_x \lambda p_i \nabla_t \nabla_x \Delta P_i^{TR} - \sum \omega_x \lambda q_i \nabla_t \nabla_x \Delta Q_i^{TR} - \sum \omega_{\lambda p_i} \nabla_t \Delta P_i^{TR} - \sum \omega_{\lambda q_i} \nabla_t \Delta Q_i^{TR} - \omega_{\pi l_t} \nabla_t \nabla_x h_t - \omega_{\pi u_t} \nabla_t \nabla_x h_t] \\
&= -[-\omega_{e_i} \lambda p_i \nabla_t \nabla_{e_i} \Delta P_i^{TR} - \omega_{f_i} \lambda p_i \nabla_t \nabla_{f_i} \Delta P_i^{TR} - \omega_{e_j} \lambda p_i \nabla_t \nabla_{e_j} \Delta P_i^{TR} - \omega_{f_j} \lambda p_i \nabla_t \nabla_{f_j} \Delta P_i^{TR} - \omega_t \lambda p_i \nabla_t \nabla_t \Delta P_i^{TR}] \\
&\quad -[-\omega_{e_i} \lambda p_j \nabla_t \nabla_{e_i} \Delta P_j^{TR} - \omega_{f_i} \lambda p_j \nabla_t \nabla_{f_i} \Delta P_j^{TR} - \omega_{e_j} \lambda p_j \nabla_t \nabla_{e_j} \Delta P_j^{TR} - \omega_{f_j} \lambda p_j \nabla_t \nabla_{f_j} \Delta P_j^{TR} - \omega_t \lambda p_j \nabla_t \nabla_t \Delta P_j^{TR}] \\
&\quad -[-\omega_{e_i} \lambda q_i \nabla_t \nabla_{e_i} \Delta Q_i^{TR} - \omega_{f_i} \lambda q_i \nabla_t \nabla_{f_i} \Delta Q_i^{TR} - \omega_{e_j} \lambda q_i \nabla_t \nabla_{e_j} \Delta Q_i^{TR} - \omega_{f_j} \lambda q_i \nabla_t \nabla_{f_j} \Delta Q_i^{TR} - \omega_t \lambda q_i \nabla_t \nabla_t \Delta Q_i^{TR}] \\
&\quad -[-\omega_{e_i} \lambda q_j \nabla_t \nabla_{e_i} \Delta Q_j^{TR} - \omega_{f_i} \lambda q_j \nabla_t \nabla_{f_i} \Delta Q_j^{TR} - \omega_{e_j} \lambda q_j \nabla_t \nabla_{e_j} \Delta Q_j^{TR} - \omega_{f_j} \lambda q_j \nabla_t \nabla_{f_j} \Delta Q_j^{TR} - \omega_t \lambda q_j \nabla_t \nabla_t \Delta Q_j^{TR}] \\
&\quad -[-\omega_{\lambda p_i} \nabla_t \Delta P_i^{TR} - \omega_{\lambda p_j} \nabla_t \Delta P_j^{TR} - \omega_{\lambda q_i} \nabla_t \Delta Q_i^{TR} - \omega_{\lambda q_j} \nabla_t \Delta Q_j^{TR} - \omega_{\pi l_t} - \omega_{\pi u_t}]
\end{aligned}$$

Analysis of equation (4.3):

$$\begin{aligned}
-\nabla_x L_{2\mu} &= -[\sum \omega_t \lambda p_i \nabla_t \nabla_x^2 \Delta P_i^{TR} + \sum \omega_t \lambda q_l \nabla_t \nabla_x^2 \Delta Q_i^{TR}] \Delta x \\
&\quad - \sum \omega_t \nabla_t \nabla_x \Delta P_i^{TR} \Delta \lambda p_i - \sum \omega_t \nabla_t \nabla_x \Delta Q_i^{TR} \Delta \lambda q_i
\end{aligned}$$

Elements of Newton matrix:

$$\begin{aligned}
\Delta e_i \text{ - } \Delta e_i &= -\sum \omega_t \lambda p_i \nabla_t \nabla_{e_i} \nabla_{e_i} \Delta P_i^{TR} - \sum \omega_t \lambda q_i \nabla_t \nabla_{e_i} \nabla_{e_i} \Delta Q_i^{TR} \\
&= -\omega_t \lambda p_i \nabla_t \nabla_{e_i} \nabla_{e_i} \Delta P_i^{TR} - \omega_t \lambda p_j \nabla_t \nabla_{e_i} \nabla_{e_i} \Delta P_j^{TR} - \omega_t \lambda q_i \nabla_t \nabla_{e_i} \nabla_{e_i} \Delta Q_i^{TR} - \omega_t \lambda q_j \nabla_t \nabla_{e_i} \nabla_{e_i} \Delta Q_j^{TR}
\end{aligned}$$

$$\begin{aligned}
\Delta e_i \text{ - } \Delta f_i &= -\sum \omega_t \lambda p_i \nabla_t \nabla_{e_i} \nabla_{f_i} \Delta P_i^{TR} - \sum \omega_t \lambda q_i \nabla_t \nabla_{e_i} \nabla_{f_i} \Delta Q_i^{TR} \\
&= -\omega_t \lambda p_i \nabla_t \nabla_{e_i} \nabla_{f_i} \Delta P_i^{TR} - \omega_t \lambda p_j \nabla_t \nabla_{e_i} \nabla_{f_i} \Delta P_j^{TR} - \omega_t \lambda q_i \nabla_t \nabla_{e_i} \nabla_{f_i} \Delta Q_i^{TR} - \omega_t \lambda q_j \nabla_t \nabla_{e_i} \nabla_{f_i} \Delta Q_j^{TR}
\end{aligned}$$

$$\begin{aligned}
\Delta e_i \text{ - } \Delta e_j &= -\sum \omega_t \lambda p_i \nabla_t \nabla_{e_i} \nabla_{e_j} \Delta P_i^{TR} - \sum \omega_t \lambda q_i \nabla_t \nabla_{e_i} \nabla_{e_j} \Delta Q_i^{TR} \\
&= -\omega_t \lambda p_i \nabla_t \nabla_{e_i} \nabla_{e_j} \Delta P_i^{TR} - \omega_t \lambda p_j \nabla_t \nabla_{e_i} \nabla_{e_j} \Delta P_j^{TR} - \omega_t \lambda q_i \nabla_t \nabla_{e_i} \nabla_{e_j} \Delta Q_i^{TR} - \omega_t \lambda q_j \nabla_t \nabla_{e_i} \nabla_{e_j} \Delta Q_j^{TR}
\end{aligned}$$

$$\begin{aligned}
\Delta e_i \text{ - } \Delta f_j &= -\sum \omega_t \lambda p_i \nabla_t \nabla_{e_i} \nabla_{f_j} \Delta P_i^{TR} - \sum \omega_t \lambda q_i \nabla_t \nabla_{e_i} \nabla_{f_j} \Delta Q_i^{TR} \\
&= -\omega_t \lambda p_i \nabla_t \nabla_{e_i} \nabla_{f_j} \Delta P_i^{TR} - \omega_t \lambda p_j \nabla_t \nabla_{e_i} \nabla_{f_j} \Delta P_j^{TR} - \omega_t \lambda q_i \nabla_t \nabla_{e_i} \nabla_{f_j} \Delta Q_i^{TR} - \omega_t \lambda q_j \nabla_t \nabla_{e_i} \nabla_{f_j} \Delta Q_j^{TR}
\end{aligned}$$

$$\Delta e_i \text{ - } \Delta t = \Delta t \text{ - } \Delta e_i$$

$$\Delta f_i \text{ - } \Delta e_i = \Delta e_i \text{ - } \Delta f_i$$

$$\Delta f_i - \Delta f_i = -\sum \omega_t \lambda p_i \nabla_t \nabla_{f_i} \nabla_{f_i} \Delta P_i^{TR} - \sum \omega_t \lambda q_i \nabla_t \nabla_{f_i} \nabla_{f_i} \Delta Q_i^{TR}$$

$$= -\omega_t \lambda p_i \nabla_t \nabla_{f_i} \nabla_{f_i} \Delta P_i^{TR} - \omega_t \lambda p_j \nabla_t \nabla_{f_i} \nabla_{f_i} \Delta P_j^{TR} - \omega_t \lambda q_i \nabla_t \nabla_{f_i} \nabla_{f_i} \Delta Q_i^{TR} - \omega_t \lambda q_j \nabla_t \nabla_{f_i} \nabla_{f_i} \Delta Q_j^{TR}$$

$$\Delta f_i - \Delta e_j = -\sum \omega_t \lambda p_i \nabla_t \nabla_{f_i} \nabla_{e_j} \Delta P_i^{TR} - \sum \omega_t \lambda q_i \nabla_t \nabla_{f_i} \nabla_{e_j} \Delta Q_i^{TR}$$

$$= -\omega_t \lambda p_i \nabla_t \nabla_{f_i} \nabla_{e_j} \Delta P_i^{TR} - \omega_t \lambda p_j \nabla_t \nabla_{f_i} \nabla_{e_j} \Delta P_j^{TR} - \omega_t \lambda q_i \nabla_t \nabla_{f_i} \nabla_{e_j} \Delta Q_i^{TR} - \omega_t \lambda q_j \nabla_t \nabla_{f_i} \nabla_{e_j} \Delta Q_j^{TR}$$

$$\Delta f_i - \Delta f_j = -\sum \omega_t \lambda p_i \nabla_t \nabla_{f_i} \nabla_{f_j} \Delta P_i^{TR} - \sum \omega_t \lambda q_i \nabla_t \nabla_{f_i} \nabla_{f_j} \Delta Q_i^{TR}$$

$$= -\omega_t \lambda p_i \nabla_t \nabla_{f_i} \nabla_{f_j} \Delta P_i^{TR} - \omega_t \lambda p_j \nabla_t \nabla_{f_i} \nabla_{f_j} \Delta P_j^{TR} - \omega_t \lambda q_i \nabla_t \nabla_{f_i} \nabla_{f_j} \Delta Q_i^{TR} - \omega_t \lambda q_j \nabla_t \nabla_{f_i} \nabla_{f_j} \Delta Q_j^{TR}$$

$$\Delta f_i - \Delta t = \Delta t - \Delta f_i$$

$$\Delta e_j - \Delta e_i = \Delta e_i - \Delta e_j$$

$$\Delta e_j - \Delta f_i = \Delta f_i - \Delta e_j$$

$$\Delta e_j - \Delta e_j = -\sum \omega_t \lambda p_i \nabla_t \nabla_{e_j} \nabla_{e_j} \Delta P_i^{TR} - \sum \omega_t \lambda q_i \nabla_t \nabla_{e_j} \nabla_{e_j} \Delta Q_i^{TR}$$

$$= -\omega_t \lambda p_i \nabla_t \nabla_{e_j} \nabla_{e_j} \Delta P_i^{TR} - \omega_t \lambda p_j \nabla_t \nabla_{e_j} \nabla_{e_j} \Delta P_j^{TR} - \omega_t \lambda q_i \nabla_t \nabla_{e_j} \nabla_{e_j} \Delta Q_i^{TR} - \omega_t \lambda q_j \nabla_t \nabla_{e_j} \nabla_{e_j} \Delta Q_j^{TR}$$

$$\Delta e_j - \Delta f_j = -\sum \omega_t \lambda p_i \nabla_t \nabla_{e_j} \nabla_{f_j} \Delta P_i^{TR} - \sum \omega_t \lambda q_i \nabla_t \nabla_{e_j} \nabla_{f_j} \Delta Q_i^{TR}$$

$$= -\omega_t \lambda p_i \nabla_t \nabla_{e_j} \nabla_{f_j} \Delta P_i^{TR} - \omega_t \lambda p_j \nabla_t \nabla_{e_j} \nabla_{f_j} \Delta P_j^{TR} - \omega_t \lambda q_i \nabla_t \nabla_{e_j} \nabla_{f_j} \Delta Q_i^{TR} - \omega_t \lambda q_j \nabla_t \nabla_{e_j} \nabla_{f_j} \Delta Q_j^{TR}$$

$$\Delta e_j - \Delta t = \Delta t - \Delta e_j$$

$$\Delta f_j - \Delta e_i = \Delta e_i - \Delta f_j$$

$$\Delta f_j - \Delta f_i = \Delta f_i - \Delta f_j$$

$$\Delta f_j - \Delta e_j = \Delta e_j - \Delta f_j$$

$$\Delta f_j - \Delta f_j = -\sum \omega_t \lambda p_i \nabla_t \nabla_{f_j} \nabla_{f_j} \Delta P_i^{TR} - \sum \omega_t \lambda q_i \nabla_t \nabla_{f_j} \nabla_{f_j} \Delta Q_i^{TR}$$

$$= -\omega_t \lambda p_i \nabla_t \nabla_{f_j} \nabla_{f_j} \Delta P_i^{TR} - \omega_t \lambda p_j \nabla_t \nabla_{f_j} \nabla_{f_j} \Delta P_j^{TR} - \omega_t \lambda q_i \nabla_t \nabla_{f_j} \nabla_{f_j} \Delta Q_i^{TR} - \omega_t \lambda q_j \nabla_t \nabla_{f_j} \nabla_{f_j} \Delta Q_j^{TR}$$

$$\Delta f_j - \Delta t = \Delta t - \Delta f_j$$

$$\Delta e_i - \Delta \lambda p_i = -\omega_t \nabla_t \nabla_{e_i} \Delta P_i^{TR}$$

$$\Delta e_i \text{ - } \Delta\lambda p_j = -\omega_t \nabla_t \nabla_{e_i} \Delta P_j^{TR}$$

$$\Delta f_i \text{ - } \Delta\lambda p_i = -\omega_t \nabla_t \nabla_{f_i} \Delta P_i^{TR}$$

$$\Delta f_i \text{ - } \Delta\lambda p_j = -\omega_t \nabla_t \nabla_{f_i} \Delta P_j^{TR}$$

$$\Delta e_j \text{ - } \Delta\lambda p_i = -\omega_t \nabla_t \nabla_{e_j} \Delta P_i^{TR}$$

$$\Delta e_j \text{ - } \Delta\lambda p_j = -\omega_t \nabla_t \nabla_{e_j} \Delta P_j^{TR}$$

$$\Delta f_j \text{ - } \Delta\lambda p_i = -\omega_t \nabla_t \nabla_{f_j} \Delta P_i^{TR}$$

$$\Delta f_j \text{ - } \Delta\lambda p_j = -\omega_t \nabla_t \nabla_{f_j} \Delta P_j^{TR}$$

$$\Delta e_i \text{ - } \Delta\lambda q_i = -\omega_t \nabla_t \nabla_{e_i} \Delta Q_i^{TR}$$

$$\Delta e_i \text{ - } \Delta\lambda q_j = -\omega_t \nabla_t \nabla_{e_i} \Delta Q_j^{TR}$$

$$\Delta f_i \text{ - } \Delta\lambda q_i = -\omega_t \nabla_t \nabla_{f_i} \Delta Q_i^{TR}$$

$$\Delta f_i \text{ - } \Delta\lambda q_j = -\omega_t \nabla_t \nabla_{f_i} \Delta Q_j^{TR}$$

$$\Delta e_j \text{ - } \Delta\lambda q_i = -\omega_t \nabla_t \nabla_{e_j} \Delta Q_i^{TR}$$

$$\Delta e_j \text{ - } \Delta\lambda q_j = -\omega_t \nabla_t \nabla_{e_j} \Delta Q_j^{TR}$$

$$\Delta f_j \text{ - } \Delta\lambda q_i = -\omega_t \nabla_t \nabla_{f_j} \Delta Q_i^{TR}$$

$$\Delta f_j \text{ - } \Delta\lambda q_j = -\omega_t \nabla_t \nabla_{f_j} \Delta Q_j^{TR}$$

Element of right-hand vector:

$$-\nabla_x L_{2\mu} = -[-\sum \omega_t \lambda p_i \nabla_t \nabla_x \Delta P_i^{TR} - \sum \omega_t \lambda q_i \nabla_t \nabla_x \Delta Q_i^{TR}]$$

decomposes to:

$$-\nabla_{e_i} L_{2\mu} = -[-\omega_t \lambda p_i \nabla_t \nabla_{e_i} \Delta P_i^{TR} - \omega_t \lambda p_j \nabla_t \nabla_{e_i} \Delta P_j^{TR} - \omega_t \lambda q_i \nabla_t \nabla_{e_i} \Delta Q_i^{TR} - \omega_t \lambda q_j \nabla_t \nabla_{e_i} \Delta Q_j^{TR}]$$

$$-\nabla_{f_i} L_{2\mu} = -[-\omega_t \lambda p_i \nabla_t \nabla_{f_i} \Delta P_i^{TR} - \omega_t \lambda p_j \nabla_t \nabla_{f_i} \Delta P_j^{TR} - \omega_t \lambda q_i \nabla_t \nabla_{f_i} \Delta Q_i^{TR} - \omega_t \lambda q_j \nabla_t \nabla_{f_i} \Delta Q_j^{TR}]$$

$$-\nabla_{e_j} L_{2\mu} = -[-\omega_t \lambda p_i \nabla_t \nabla_{e_j} \Delta P_i^{TR} - \omega_t \lambda p_j \nabla_t \nabla_{e_j} \Delta P_j^{TR} - \omega_t \lambda q_i \nabla_t \nabla_{e_j} \Delta Q_i^{TR} - \omega_t \lambda q_j \nabla_t \nabla_{e_j} \Delta Q_j^{TR}]$$

$$-\nabla_{f_j} L_{2\mu} = -[-\omega_t \lambda p_i \nabla_t \nabla_{f_j} \Delta P_i^{TR} - \omega_t \lambda p_j \nabla_t \nabla_{f_j} \Delta P_j^{TR} - \omega_t \lambda q_i \nabla_t \nabla_{f_j} \Delta Q_i^{TR} - \omega_t \lambda q_j \nabla_t \nabla_{f_j} \Delta Q_j^{TR}]$$

Analysis of equation (4.4):

$$-\nabla_{\lambda p_i} L_{2\mu} = -\sum \omega_t \nabla_t \nabla_x \Delta P_i^{TR} \Delta x - \sum \nabla_t \Delta P_i^{TR} \Delta \omega_t$$

Elements of Newton matrix:

$$\Delta\lambda p_i - \Delta e_i = \Delta e_i - \Delta\lambda p_i$$

$$\Delta\lambda p_j - \Delta e_i = \Delta e_i - \Delta\lambda p_j$$

$$\Delta\lambda p_i - \Delta f_i = \Delta f_i - \Delta\lambda p_i$$

$$\Delta\lambda p_j - \Delta f_i = \Delta f_i - \Delta\lambda p_j$$

$$\Delta\lambda p_i - \Delta e_j = \Delta e_j - \Delta\lambda p_i$$

$$\Delta\lambda p_j - \Delta e_j = \Delta e_j - \Delta\lambda p_j$$

$$\Delta\lambda p_i - \Delta f_j = \Delta f_j - \Delta\lambda p_i$$

$$\Delta\lambda p_j - \Delta f_j = \Delta f_j - \Delta\lambda p_j$$

$$\Delta\lambda p_i - \Delta\omega_t = -\nabla_t \Delta P_i^{TR}$$

$$\Delta\lambda p_j - \Delta\omega_t = -\nabla_t \Delta P_j^{TR}$$

Element of right-hand vector:

$$-\nabla_{\lambda p_i} L_{2\mu} = -[-\sum \omega_t \nabla_t \Delta P_i^{TR}]$$

decomposes to:

$$-\nabla_{\lambda p_i} L_{2\mu} = -[-\omega_t \nabla_t \Delta P_i^{TR}]$$

$$-\nabla_{\lambda p_j} L_{2\mu} = -[-\omega_t \nabla_t \Delta P_j^{TR}]$$

Analysis of equation (4.5):

$$-\nabla_{\lambda q_i} L_{2\mu} = -\sum \omega_t \nabla_t \nabla_x \Delta Q_i^{TR} \Delta x - \sum \nabla_t \Delta Q_i^{TR} \Delta \omega_t$$

Elements of Newton matrix:

$$\Delta\lambda q_i - \Delta e_i = \Delta e_i - \Delta\lambda q_i$$

$$\Delta\lambda q_j - \Delta e_i = \Delta e_i - \Delta\lambda q_j$$

$$\Delta\lambda q_i - \Delta f_i = \Delta f_i - \Delta\lambda q_i$$

$$\Delta\lambda q_j - \Delta f_i = \Delta f_i - \Delta\lambda q_j$$

$$\Delta\lambda q_i - \Delta e_j = \Delta e_j - \Delta\lambda q_i$$

$$\Delta\lambda q_j - \Delta e_j = \Delta e_j - \Delta\lambda q_j$$

$$\Delta\lambda q_i - \Delta f_j = \Delta f_j - \Delta\lambda q_i$$

$$\Delta\lambda q_j - \Delta f_j = \Delta f_j - \Delta\lambda q_j$$

$$\Delta\lambda q_i - \Delta\omega_t = -\nabla_t \Delta Q_i^{TR}$$

$$\Delta\lambda q_j - \Delta\omega_t = -\nabla_t \Delta Q_j^{TR}$$

Element of right-hand vector:

$$-\nabla_{\lambda q_i} L_{2\mu} = -[-\sum \omega_t \nabla_t \Delta Q_i^{TR}]$$

decomposes to:

$$-\nabla_{\lambda q_i} L_{2\mu} = -[-\omega_t \nabla_t \Delta Q_i^{TR}]$$

$$-\nabla_{\lambda q_j} L_{2\mu} = -[-\omega_t \nabla_t \Delta Q_j^{TR}]$$

Analysis of equation (4.6):

$$-\nabla_{\omega_t} L_{2\mu} = -[\sum \lambda p_i \nabla_t \nabla_x \Delta P_i^{TR} + \sum \lambda q_i \nabla_t \nabla_x \Delta Q_i^{TR}]\Delta x$$
$$-\sum \nabla_t \Delta P_i^{TR} \Delta\lambda p_i - \sum \nabla_t \Delta Q_i^{TR} \Delta\lambda q_i - \nabla_t h_t \Delta\pi l_t - \nabla_t h_t \Delta\pi u_t$$

Elements of Newton matrix:

$$\Delta\omega_t - \Delta e_i = -\sum \lambda p_i \nabla_t \nabla_{e_i} \Delta P_i^{TR} - \sum \lambda q_i \nabla_t \nabla_{e_i} \Delta Q_i^{TR}$$
$$= -\lambda p_i \nabla_t \nabla_{e_i} \Delta P_i^{TR} - \lambda p_j \nabla_t \nabla_{e_i} \Delta P_j^{TR} - \lambda q_i \nabla_t \nabla_{e_i} \Delta Q_i^{TR} - \lambda q_j \nabla_t \nabla_{e_i} \Delta Q_j^{TR}$$

$$\Delta\omega_t - \Delta f_i = -\sum \lambda p_i \nabla_t \nabla_{f_i} \Delta P_i^{TR} - \sum \lambda q_i \nabla_t \nabla_{f_i} \Delta Q_i^{TR}$$
$$= -\lambda p_i \nabla_t \nabla_{f_i} \Delta P_i^{TR} - \lambda p_j \nabla_t \nabla_{f_i} \Delta P_j^{TR} - \lambda q_i \nabla_t \nabla_{f_i} \Delta Q_i^{TR} - \lambda q_j \nabla_t \nabla_{f_i} \Delta Q_j^{TR}$$

$$\Delta\omega_t - \Delta e_j = -\sum \lambda p_i \nabla_t \nabla_{e_j} \Delta P_i^{TR} - \sum \lambda q_i \nabla_t \nabla_{e_j} \Delta Q_i^{TR}$$
$$= -\lambda p_i \nabla_t \nabla_{e_j} \Delta P_i^{TR} - \lambda p_j \nabla_t \nabla_{e_j} \Delta P_j^{TR} - \lambda q_i \nabla_t \nabla_{e_j} \Delta Q_i^{TR} - \lambda q_j \nabla_t \nabla_{e_j} \Delta Q_j^{TR}$$

$$\Delta\omega_t - \Delta f_j = -\sum \lambda p_i \nabla_t \nabla_{f_j} \Delta P_i^{TR} - \sum \lambda q_i \nabla_t \nabla_{f_j} \Delta Q_i^{TR}$$
$$= -\lambda p_i \nabla_t \nabla_{f_j} \Delta P_i^{TR} - \lambda p_j \nabla_t \nabla_{f_j} \Delta P_j^{TR} - \lambda q_i \nabla_t \nabla_{f_j} \Delta Q_i^{TR} - \lambda q_j \nabla_t \nabla_{f_j} \Delta Q_j^{TR}$$

$$\Delta\omega_t - \Delta t = \Delta t - \Delta\omega_t$$

$$\Delta\omega_t - \Delta\lambda p_i = \Delta\lambda p_i - \Delta\omega_t$$

$$\Delta\omega_t - \Delta\lambda p_j = \Delta\lambda p_j - \Delta\omega_t$$

$$\Delta\omega_t - \Delta\lambda q_i = \Delta\lambda q_i - \Delta\omega_t$$

$$\Delta\omega_t - \Delta\lambda q_j = \Delta\lambda q_j - \Delta\omega_t$$

$$\Delta\omega_t - \Delta\pi l_t = -\nabla_t h_t = -1$$

$$\Delta\omega_t - \Delta\pi u_t = -\nabla_t h_t = -1$$

Element of right-hand vector:

$$-\nabla_{\omega_t} L_{2\mu} = -[-\sum \lambda p_i \nabla_t \Delta P_i^{TR} - \sum \lambda q_i \nabla_t \Delta Q_i^{TR} - \nabla_t h_t \pi l_t - \nabla_t h_t \pi u_t]$$
$$= -[-\lambda p_i \nabla_t \Delta P_i^{TR} - \lambda p_j \nabla_t \Delta P_j^{TR} - \lambda q_i \nabla_t \Delta Q_i^{TR} - \lambda q_j \nabla_t \Delta Q_j^{TR} - \pi l_t - \pi u_t]$$

Analysis of equation (4.7):

$$-\nabla_{\omega_{\lambda pi}} L_{2\mu} = -\sum \nabla_t \Delta P_i^{TR} \Delta t$$

Elements of Newton matrix:

$$\Delta\omega_{\lambda p_i} - \Delta t = \Delta t - \Delta\omega_{\lambda p_i}$$

$$\Delta\omega_{\lambda p_j} - \Delta t = \Delta t - \Delta\omega_{\lambda p_j}$$

Element of right-hand vector:

$$-\nabla_{\omega_{\lambda p_i}} L_{2\mu} = -[-\sum \Delta P_i^{TR}]$$

decomposes to:

$$-\nabla_{\omega_{\lambda pi}} L_{2\mu} = -[-\Delta P_i^{TR}]$$

$$-\nabla_{\omega_{\lambda p_j}} L_{2\mu} = -[-\Delta P_j^{TR}]$$

Analysis of equation (4.8):

$$-\nabla_{\omega_{\lambda qi}} L_{2\mu} = -\sum \nabla_t \Delta Q_i^{TR} \Delta t$$

Elements of Newton matrix:

$$\Delta\omega_{\lambda q_i} - \Delta t = \Delta t - \Delta\omega_{\lambda q_i}$$

$$\Delta\omega_{\lambda q_j} - \Delta t = \Delta t - \Delta\omega_{\lambda q_j}$$

Element of right-hand vector:

$$-\nabla_{\omega_{\lambda q_i}} L_{2\mu} = -[-\sum \Delta Q_i^{TR}]$$

decomposes to:

$$-\nabla_{\omega_{\lambda q_i}} L_{2\mu} = -[-\Delta Q_i^{TR}]$$

$$-\nabla_{\omega_{\lambda q_j}} L_{2\mu} = -[-\Delta Q_j^{TR}]$$

Analysis of equation (4.9):

$$-\nabla_{\pi l_t} L_{2\mu} = -\omega_{sl_t} \Delta sl_t - \nabla_t h_t \Delta\omega_t - sl_t \Delta\omega_{sl_t}$$

Elements of Newton matrix:

$$\Delta\pi l_t - \Delta sl_t = -\omega_{sl_t}$$

$$\Delta\pi l_t - \Delta\omega_t = -\nabla_t h_t = -1$$

$$\Delta\pi l_t - \Delta\omega_{sl_t} = -sl_t$$

Element of right-hand vector:

$$-\nabla_{\pi l_t} L_{2\mu} = -[-\omega_t \nabla_t h_t - \omega_{sl_t} sl_t] = -[-\omega_t - \omega_{sl_t} sl_t]$$

Analysis of equation (4.10):

$$-\nabla_{\pi u_t} L_{2\mu} = \omega_{su_t} \Delta su_t - \nabla_t h_t \Delta\omega_t + su_t \Delta\omega_{su_t}$$

Elements of Newton matrix:

$$\Delta\pi u_t - \Delta su_t = \omega_{su_t}$$

$$\Delta\pi u_t - \Delta\omega_t = -\nabla_t h_t = -1$$

$$\Delta\pi u_t - \Delta\omega_{su_t} = su_t$$

Element of right-hand vector:

$$-\nabla_{\pi u_t} L_{2\mu} = -[-\omega_t \nabla_t h_t + \omega_{su_t} su_t] = -[-\omega_t - \omega_{su_t} su_t]$$

Analysis of equation (4.11):

$$-\nabla_{sl_t} L_{2\mu} = -\omega_{sl_t} \Delta\pi l_t + \Delta\omega_{\pi l_t} - \pi l_t \Delta\omega_{sl_t}$$

Elements of Newton matrix:

$$\Delta sl_t - \Delta\pi l_t = -\omega_{sl_t}$$

$$\Delta sl_t - \Delta\omega_{\pi l_t} = 1$$

$$\Delta sl_t - \Delta\omega_{sl_t} = -\pi l_t$$

Element of right-hand vector:

$$-\nabla_{sl_t} L_{2\mu} = -[-\omega_{sl_t} \pi l_t + \omega_{\pi l_t}]$$

Analysis of equation (4.12):

$$-\nabla_{su_t} L_{2\mu} = \omega_{su_t} \Delta\pi u_t - \Delta\omega_{\pi u_t} + \pi u_t \Delta\omega_{su_t}$$

Elements of Newton matrix:

$$\Delta su_t - \Delta \pi u_t = \omega_{su_t}$$

$$\Delta su_t - \Delta \omega_{\pi u_t} = -1$$

$$\Delta su_t - \Delta \omega_{su_t} = \pi u_t$$

Element of right-hand vector:

$$-\nabla_{su_t} L_{2\mu} = -[\omega_{su_t} \pi u_t - \omega_{\pi u_t}]$$

Analysis of equation (4.13):

$$-\nabla_{\omega_{\pi l_t}} L_{2\mu} = -\nabla_t h_t \Delta t + \Delta sl_t$$

Elements of Newton matrix:

$$\Delta \omega_{\pi l_t} - \Delta t = -\nabla_t h_t = -1$$

$$\Delta \omega_{\pi l_t} - \Delta sl_t = 1$$

Element of right-hand vector:

$$-\nabla_{\omega_{\pi l_t}} L_{2\mu} = +[h_t - sl_t - h_t^{\min}] = t - sl_t - t^{\min}$$

Analysis of equation (4.14):

$$-\nabla_{\omega_{\pi u_t}} L_{2\mu} = -\nabla_t h_t \Delta t - \Delta su_t$$

Elements of Newton matrix:

$$\Delta \omega_{\pi u_t} - \Delta t = -\nabla_t h_t = -1$$

$$\Delta \omega_{\pi u_t} - \Delta su_t = -1$$

Element of right-hand vector:

$$-\nabla_{\omega_{\pi u_t}} L_{2\mu} = +[h_t + su_t - h_t^{\max}] = t + su_t - t^{\max}$$

Analysis of equation (4.15):

$$-\nabla_{\omega_{sl_t}} L_{2\mu} = -sl_t \Delta \pi l_t - \pi l_t \Delta sl_t$$

Elements of Newton matrix:

$$\Delta\omega_{sl_t} - \Delta\pi l_t = -sl_t$$

$$\Delta\omega_{sl_t} - \Delta sl_t = -\pi l_t$$

Element of right-hand vector:

$$-\nabla_{\omega_{sl_t}} L_{2\mu} = -[\mu - sl_t \pi l_t]$$

Analysis of equation (4.16):

$$-\nabla_{\omega_{su_t}} L_{2\mu} = su_t \Delta\pi u_t + \pi u_t \Delta su_t$$

Elements of Newton matrix:

$$\Delta\omega_{su_t} - \Delta\pi u_t = su_t$$

$$\Delta\omega_{su_t} - \Delta su_t = \pi u_t$$

Element of right-hand vector:

$$-\nabla_{\omega_{su_t}} L_{2\mu} = -[\mu + su_t \pi u_t]$$

APPENDIX II

Derivative terms for the elements of the transformer contribution presented in Appendix I

Appendix II:

List of derivative terms included in the elements of the Newton matrix equation associated with the modelling of transformer

The derivatives terms presented here correspond to the transformer terms ΔP_i^{TR} and ΔQ_i^{TR} contained in the active and reactive power mismatch equations (3.55)-(3.56). For the examination of a transformer branch *i-j*, the corresponding terms for buses *i* and *j* can be determined from equations (3.38) and (3.41), subject to the location of the tap-ratio control mechanism. If the transformer tap-ratio control is located at bus *i*, the primary bus, the transformer contributions to the mismatch equations are:

$$\Delta P_i^{TR} = -P_{ij}^{TR} = -\left\{e_i[t^2(g_{ii}e_i - b_{ii}f_i) - t(g_{ij}e_j - b_{ij}f_j)] + f_i[t^2(b_{ii}e_i + g_{ii}f_i) - t(b_{ij}e_j + g_{ij}f_j)]\right\}$$

$$\Delta Q_i^{TR} = -Q_{ij}^{TR} = -\left\{-e_i[t^2(b_{ii}e_i + g_{ii}f_i) - t(b_{ij}e_j + g_{ij}f_j)] + f_i[t^2(g_{ii}e_i - b_{ii}f_i) - t(g_{ij}e_j - b_{ij}f_j)]\right\}$$

$$\Delta P_j^{TR} = -P_{ji}^{TR} = -\left\{e_j[-t(g_{ij}e_i - b_{ij}f_i) + (g_{jj}e_j - b_{jj}f_j)] + f_j[-t(g_{ij}f_i + b_{ij}e_i) + (b_{jj}e_j + g_{jj}f_j)]\right\}$$

$$\Delta Q_j^{TR} = -Q_{ji}^{TR} = -\left\{-e_j[-t(g_{ij}f_i + b_{ij}e_i) + (b_{jj}e_j + g_{jj}f_j)] + f_j[-t(g_{ij}e_i - b_{ij}f_i) + (g_{jj}e_j - b_{jj}f_j)]\right\}$$

If the transformer tap-ratio control is located at bus *j*, the secondary bus, the transformer contributions to the power mismatch equations are calculated by switching the indices from *i* to *j* and vice versa in the above equations, such that:

$$\Delta P_i^{TR} = -\left\{e_i[-t(g_{ij}e_j - b_{ij}f_j) + (g_{ii}e_i - b_{ii}f_i)] + f_i[-t(g_{ij}f_j + b_{ij}e_j) + (b_{ii}e_i + g_{ii}f_i)]\right\}$$

$$\Delta Q_i^{TR} = -\left\{-e_i[-t(g_{ij}f_j + b_{ij}e_j) + (b_{ii}e_i + g_{ii}f_i)] + f_i[-t(g_{ij}e_j - b_{ij}f_j) + (g_{ii}e_i - b_{ii}f_i)]\right\}$$

$$\Delta P_j^{TR} = -\left\{e_j[t^2(g_{jj}e_j - b_{jj}f_j) - t(g_{ij}e_i - b_{ij}f_i)] + f_j[t^2(b_{jj}e_j + g_{jj}f_j) - t(b_{ij}e_i + g_{ij}f_i)]\right\}$$

$$\Delta Q_j^{TR} = -\left\{-e_j[t^2(b_{jj}e_j + g_{jj}f_j) - t(b_{ij}e_i + g_{ij}f_i)] + f_j[t^2(g_{jj}e_j - b_{jj}f_j) - t(g_{ij}e_i - b_{ij}f_i)]\right\}$$

The *x* terms associated with the following formulations are those associated with the above equations, i.e. $x = [e_i, f_i, e_j, f_j, t]$. The derivative terms that correspond to the situation where the transformer tap-ratio control is located at bus *i* are given first and those at bus *j* follow next.

*Transformer tap-ratio control located at **bus i***:

1st derivatives:

$$\nabla_t \Delta P_i^{TR} = -\left\{e_i[2tg_{ii}e_i - (g_{ij}e_j - b_{ij}f_j)] + f_i[2tg_{ii}f_i - (b_{ij}e_j + g_{ij}f_j)]\right\}$$

$$\nabla_t \Delta Q_i^{TR} = -\left\{-e_i[2tb_{ii}e_i - (b_{ij}e_j + g_{ij}f_j)] + f_i[-2tb_{ii}f_i - (g_{ij}e_j - b_{ij}f_j)]\right\}$$

$$\nabla_t \Delta P_j^{TR} = -\left\{e_j[-(g_{ij}e_i - b_{ij}f_i)] + f_j[-(g_{ij}f_i + b_{ij}e_i)]\right\}$$

$$\nabla_t \Delta Q_j^{TR} = -\left\{-e_j[-(g_{ij}f_i + b_{ij}e_i)] + f_j[-(g_{ij}e_i - b_{ij}f_i)]\right\}$$

2nd derivatives:

$$\nabla_t \nabla_{e_i} \Delta P_i^{TR} = -\left\{4tg_{ii}e_i - (g_{ij}e_j - b_{ij}f_j)\right\}$$

$$\nabla_t \nabla_{f_i} \Delta P_i^{TR} = -\left\{4tg_{ii}f_i - (b_{ij}e_j + g_{ij}f_j)\right\}$$

$$\nabla_t \nabla_{e_j} \Delta P_i^{TR} = -\left\{-g_{ij}e_i - b_{ij}f_i\right\}$$

$$\nabla_t \nabla_{f_j} \Delta P_i^{TR} = -\left\{b_{ij}e_i - g_{ij}f_i\right\}$$

$$\nabla_t \nabla_t \Delta P_i^{TR} = -\left\{2g_{ii}e_i^2 + 2g_{ii}f_i^2\right\}$$

$$\nabla_t \nabla_{e_i} \Delta Q_i^{TR} = -\left\{-4tb_{ii}e_i + (b_{ij}e_j + g_{ij}f_j)\right\}$$

$$\nabla_t \nabla_{f_i} \Delta Q_i^{TR} = -\left\{-4tb_{ii}f_i - (g_{ij}e_j - b_{ij}f_j)\right\}$$

$$\nabla_t \nabla_{e_j} \Delta Q_i^{TR} = -\left\{b_{ij}e_i - g_{ij}f_i\right\}$$

$$\nabla_t \nabla_{f_j} \Delta Q_i^{TR} = -\left\{g_{ij}e_i + b_{ij}f_i\right\}$$

$$\nabla_t \nabla_t \Delta Q_i^{TR} = -\left\{-2b_{ii}e_i^2 - 2b_{ii}f_i^2\right\}$$

$$\nabla_t \nabla_{e_i} \Delta P_j^{TR} = -\left\{-g_{ij}e_j - b_{ij}f_j\right\}$$

$$\nabla_t \nabla_{f_i} \Delta P_j^{TR} = -\left\{b_{ij}e_j - g_{ij}f_j\right\}$$

$$\nabla_t \nabla_{e_j} \Delta P_j^{TR} = -\left\{-g_{ij}e_i + b_{ij}f_i\right\}$$

$$\nabla_t \nabla_{f_j} \Delta P_j^{TR} = -\left\{-g_{ij}f_i - b_{ij}e_i\right\}$$

$$\nabla_t \nabla_t \Delta P_j^{TR} = 0$$

$$\nabla_t \nabla_{e_i} \Delta Q_j^{TR} = -\{b_{ij} e_j - g_{ij} f_j\}$$

$$\nabla_t \nabla_{f_i} \Delta Q_j^{TR} = -\{g_{ij} e_j + b_{ij} f_j\}$$

$$\nabla_t \nabla_{e_j} \Delta Q_j^{TR} = -\{g_{ij} f_i + b_{ij} e_i\}$$

$$\nabla_t \nabla_{f_j} \Delta Q_j^{TR} = -\{-g_{ij} e_i + b_{ij} f_i\}$$

$$\nabla_t \nabla_t \Delta Q_j^{TR} = 0$$

3rd derivatives:

$$\nabla_t \nabla_{e_i} \nabla_{e_i} \Delta P_i^{TR} = -\{4tg_{ii}\}$$

$$\nabla_t \nabla_{e_i} \nabla_{f_i} \Delta P_i^{TR} = 0$$

$$\nabla_t \nabla_{e_i} \nabla_{e_j} \Delta P_i^{TR} = -\{-g_{ij}\}$$

$$\nabla_t \nabla_{e_i} \nabla_{f_j} \Delta P_i^{TR} = -\{b_{ij}\}$$

$$\nabla_t \nabla_{e_i} \nabla_t \Delta P_i^{TR} = -\{4g_{ii} e_i\}$$

$$\nabla_t \nabla_{f_i} \nabla_{e_i} \Delta P_i^{TR} = 0$$

$$\nabla_t \nabla_{f_i} \nabla_{f_i} \Delta P_i^{TR} = -\{4tg_{ii}\}$$

$$\nabla_t \nabla_{f_i} \nabla_{e_j} \Delta P_i^{TR} = -\{-b_{ij}\}$$

$$\nabla_t \nabla_{f_i} \nabla_{f_j} \Delta P_i^{TR} = -\{-g_{ij}\}$$

$$\nabla_t \nabla_{f_i} \nabla_t \Delta P_i^{TR} = -\{4g_{ii} f_i\}$$

$$\nabla_t \nabla_{e_j} \nabla_{e_i} \Delta P_i^{TR} = -\{-g_{ij}\}$$

$$\nabla_t \nabla_{e_j} \nabla_{f_i} \Delta P_i^{TR} = -\{-b_{ij}\}$$

$$\nabla_t \nabla_{e_j} \nabla_{e_j} \Delta P_i^{TR} = 0$$

$$\nabla_t \nabla_{e_j} \nabla_{f_j} \Delta P_i^{TR} = 0$$

$$\nabla_t \nabla_{e_j} \nabla_t \Delta P_i^{TR} = 0$$

$$\nabla_t \nabla_{f_j} \nabla_{e_i} \Delta P_i^{TR} = -\{b_{ij}\}$$

$$\nabla_t \nabla_{f_j} \nabla_{f_i} \Delta P_i^{TR} = -\{-g_{ij}\}$$

$$\nabla_t \nabla_{f_j} \nabla_{e_j} \Delta P_i^{TR} = 0$$

$$\nabla_t \nabla_{f_j} \nabla_{f_j} \Delta P_i^{TR} = 0$$

$$\nabla_t \nabla_{f_j} \nabla_t \Delta P_i^{TR} = 0$$

$$\nabla_t \nabla_t \nabla_{e_i} \Delta P_i^{TR} = -\{4 g_{ii} e_i\}$$

$$\nabla_t \nabla_t \nabla_{f_i} \Delta P_i^{TR} = -\{4 g_{ii} f_i\}$$

$$\nabla_t \nabla_t \nabla_{e_j} \Delta P_i^{TR} = 0$$

$$\nabla_t \nabla_t \nabla_{f_j} \Delta P_i^{TR} = 0$$

$$\nabla_t \nabla_t \nabla_t \Delta P_i^{TR} = 0$$

$$\nabla_t \nabla_{e_i} \nabla_{e_i} \Delta Q_i^{TR} = -\{-4tb_{ii}\}$$

$$\nabla_t \nabla_{e_i} \nabla_{f_i} \Delta Q_i^{TR} = 0$$

$$\nabla_t \nabla_{e_i} \nabla_{e_j} \Delta Q_i^{TR} = -\{b_{ij}\}$$

$$\nabla_t \nabla_{e_i} \nabla_{f_j} \Delta Q_i^{TR} = -\{g_{ij}\}$$

$$\nabla_t \nabla_{e_i} \nabla_t \Delta Q_i^{TR} = -\{-4b_{ii} e_i\}$$

$$\nabla_t \nabla_{f_i} \nabla_{e_i} \Delta Q_i^{TR} = 0$$

$$\nabla_t \nabla_{f_i} \nabla_{f_i} \Delta Q_i^{TR} = -\{-4tb_{ii}\}$$

$$\nabla_t \nabla_{f_i} \nabla_{e_j} \Delta Q_i^{TR} = -\{-g_{ij}\}$$

$$\nabla_t \nabla_{f_i} \nabla_{f_j} \Delta Q_i^{TR} = -\{b_{ij}\}$$

$$\nabla_t \nabla_{f_i} \nabla_t \Delta Q_i^{TR} = -\{-4b_{ii} f_i\}$$

$$\nabla_t \nabla_{e_j} \nabla_{e_i} \Delta Q_i^{TR} = -\{b_{ij}\}$$

$$\nabla_t \nabla_{e_j} \nabla_{f_i} \Delta Q_i^{TR} = -\{-g_{ij}\}$$

$$\nabla_t \nabla_{e_j} \nabla_{e_j} \Delta Q_i^{TR} = 0$$

$$\nabla_t \nabla_{e_j} \nabla_{f_j} \Delta Q_i^{TR} = 0$$

$$\nabla_t \nabla_{e_j} \nabla_t \Delta Q_i^{TR} = 0$$

$$\nabla_t \nabla_{f_j} \nabla_{e_i} \Delta Q_i^{TR} = -\{g_{ij}\}$$

$$\nabla_t \nabla_{f_j} \nabla_{f_i} \Delta Q_i^{TR} = -\{b_{ij}\}$$

$$\nabla_t \nabla_{f_j} \nabla_{e_j} \Delta Q_i^{TR} = 0$$

$$\nabla_t \nabla_{f_j} \nabla_{f_j} \Delta Q_i^{TR} = 0$$

$$\nabla_t \nabla_{f_j} \nabla_t \Delta Q_i^{TR} = 0$$

$$\nabla_t \nabla_t \nabla_{e_i} \Delta Q_i^{TR} = -\{-4 b_{ii} e_i\}$$

$$\nabla_t \nabla_t \nabla_{f_i} \Delta Q_i^{TR} = -\{-4 b_{ii} f_i\}$$

$$\nabla_t \nabla_t \nabla_{e_j} \Delta Q_i^{TR} = 0$$

$$\nabla_t \nabla_t \nabla_{f_j} \Delta Q_i^{TR} = 0$$

$$\nabla_t \nabla_t \nabla_t \Delta Q_i^{TR} = 0$$

$$\nabla_t \nabla_{e_i} \nabla_{e_i} \Delta P_j^{TR} = 0$$

$$\nabla_t \nabla_{e_i} \nabla_{f_i} \Delta P_j^{TR} = 0$$

$$\nabla_t \nabla_{e_i} \nabla_{e_j} \Delta P_j^{TR} = -\{-g_{ij}\}$$

$$\nabla_t \nabla_{e_i} \nabla_{f_j} \Delta P_j^{TR} = -\{-b_{ij}\}$$

$$\nabla_t \nabla_{e_i} \nabla_t \Delta P_j^{TR} = 0$$

$$\nabla_t \nabla_{f_i} \nabla_{e_i} \Delta P_j^{TR} = 0$$

$$\nabla_t \nabla_{f_i} \nabla_{f_i} \Delta P_j^{TR} = 0$$

$$\nabla_t \nabla_{f_i} \nabla_{e_j} \Delta P_j^{TR} = -\{b_{ij}\}$$

$$\nabla_t \nabla_{f_i} \nabla_{f_j} \Delta P_j^{TR} = -\{-g_{ij}\}$$

$$\nabla_t \nabla_{f_i} \nabla_t \Delta P_j^{TR} = 0$$

$$\nabla_t \nabla_{e_j} \nabla_{e_i} \Delta P_j^{TR} = -\{-g_{ij}\}$$

$$\nabla_t \nabla_{e_j} \nabla_{f_i} \Delta P_j^{TR} = -\{b_{ij}\}$$

$$\nabla_t \nabla_{e_j} \nabla_{e_j} \Delta P_j^{TR} = 0$$

$$\nabla_t \nabla_{e_j} \nabla_{f_j} \Delta P_j^{TR} = 0$$

$$\nabla_t \nabla_{e_j} \nabla_t \Delta P_j^{TR} = 0$$

$$\nabla_t \nabla_{f_j} \nabla_{e_i} \Delta P_j^{TR} = -\{-b_{ij}\}$$

$$\nabla_t \nabla_{f_j} \nabla_{f_i} \Delta P_j^{TR} = -\{-g_{ij}\}$$

$$\nabla_t \nabla_{f_j} \nabla_{e_j} \Delta P_j^{TR} = 0$$

$$\nabla_t \nabla_{f_j} \nabla_{f_j} \Delta P_j^{TR} = 0$$

$$\nabla_t \nabla_{f_j} \nabla_t \Delta P_j^{TR} = 0$$

$$\nabla_t \nabla_t \nabla_{e_i} \Delta P_j^{TR} = \nabla_t \nabla_t \nabla_{f_i} \Delta P_j^{TR} = \nabla_t \nabla_t \nabla_{e_j} \Delta P_j^{TR} = \nabla_t \nabla_t \nabla_{f_j} \Delta P_j^{TR} = \nabla_t \nabla_t \nabla_t \Delta P_j^{TR} = 0$$

$$\nabla_t \nabla_{e_i} \nabla_{e_i} \Delta Q_j^{TR} = 0$$

$$\nabla_t \nabla_{e_i} \nabla_{f_i} \Delta Q_j^{TR} = 0$$

$$\nabla_t \nabla_{e_i} \nabla_{e_j} \Delta Q_j^{TR} = -\{b_{ij}\}$$

$$\nabla_t \nabla_{e_i} \nabla_{f_j} \Delta Q_j^{TR} = -\{-g_{ij}\}$$

$$\nabla_t \nabla_{e_i} \nabla_t \Delta Q_j^{TR} = 0$$

$$\nabla_t \nabla_{f_i} \nabla_{e_i} \Delta Q_j^{TR} = 0$$

$$\nabla_t \nabla_{f_i} \nabla_{f_i} \Delta Q_j^{TR} = 0$$

$$\nabla_t \nabla_{f_i} \nabla_{e_j} \Delta Q_j^{TR} = -\{g_{ij}\}$$

$$\nabla_t \nabla_{f_i} \nabla_{f_j} \Delta Q_j^{TR} = -\{b_{ij}\}$$

$$\nabla_t \nabla_{f_i} \nabla_t \Delta Q_j^{TR} = 0$$

$$\nabla_t \nabla_{e_j} \nabla_{e_i} \Delta Q_j^{TR} = -\{b_{ij}\}$$

$$\nabla_t \nabla_{e_j} \nabla_{f_i} \Delta Q_j^{TR} = -\{g_{ij}\}$$

$$\nabla_t \nabla_{e_j} \nabla_{e_j} \Delta Q_j^{TR} = 0$$

$$\nabla_t \nabla_{e_j} \nabla_{f_j} \Delta Q_j^{TR} = 0$$

$$\nabla_t \nabla_{e_j} \nabla_t \Delta Q_j^{TR} = 0$$

$$\nabla_t \nabla_{f_j} \nabla_{e_i} \Delta Q_j^{TR} = -\{-g_{ij}\}$$

$$\nabla_t \nabla_{f_j} \nabla_{f_i} \Delta Q_j^{TR} = -\{b_{ij}\}$$

$$\nabla_t \nabla_{f_j} \nabla_{e_j} \Delta Q_j^{TR} = 0$$

$$\nabla_t \nabla_{f_j} \nabla_{f_j} \Delta Q_j^{TR} = 0$$

$$\nabla_t \nabla_{f_j} \nabla_t \Delta Q_j^{TR} = 0$$

$$\nabla_t \nabla_t \nabla_{e_i} \Delta Q_j^{TR} = \nabla_t \nabla_t \nabla_{f_i} \Delta Q_j^{TR} = \nabla_t \nabla_t \nabla_{e_j} \Delta Q_j^{TR} = \nabla_t \nabla_t \nabla_{f_j} \Delta Q_j^{TR} = \nabla_t \nabla_t \nabla_t \Delta Q_j^{TR} = 0$$

*Transformer tap-ratio control located at **bus j***:

1st derivatives:

$$\nabla_t \Delta P_i^{TR} = -\{e_i[-(g_{ij} e_j - b_{ij} f_j)] + f_i[-(g_{ij} f_j + b_{ij} e_j)]\}$$

$$\nabla_t \Delta Q_i^{TR} = -\{-e_i[-(g_{ij} f_j + b_{ij} e_j)] + f_i[-(g_{ij} e_j - b_{ij} f_j)]\}$$

$$\nabla_t \Delta P_j^{TR} = -\{e_j[2tg_{jj} e_j - (g_{ij} e_i - b_{ij} f_i)] + f_j[2tg_{jj} f_j - (b_{ij} e_i + g_{ij} f_i)]\}$$

$$\nabla_t \Delta Q_j^{TR} = -\{-e_j[2tb_{jj} e_j - (b_{ij} e_i + g_{ij} f_i)] + f_j[-2tb_{jj} f_j - (g_{ij} e_i - b_{ij} f_i)]\}$$

2nd derivatives:

$$\nabla_t \nabla_{e_i} \Delta P_i^{TR} = -\{-g_{ij} e_j + b_{ij} f_j\}$$

$$\nabla_t \nabla_{f_i} \Delta P_i^{TR} = -\{-g_{ij} f_j - b_{ij} e_j\}$$

$$\nabla_t \nabla_{e_j} \Delta P_i^{TR} = -\{-g_{ij} e_i - b_{ij} f_i\}$$

$$\nabla_t \nabla_{f_j} \Delta P_i^{TR} = -\{b_{ij} e_i - g_{ij} f_i\}$$

$$\nabla_t \nabla_t \Delta P_i^{TR} = 0$$

$$\nabla_t \nabla_{e_i} \Delta Q_i^{TR} = -\{g_{ij} f_j + b_{ij} e_j\}$$

$$\nabla_t \nabla_{f_i} \Delta Q_i^{TR} = -\{-g_{ij} e_j + b_{ij} f_j\}$$

$$\nabla_t \nabla_{e_j} \Delta Q_i^{TR} = -\{b_{ij} e_i - g_{ij} f_i\}$$

$$\nabla_t \nabla_{f_j} \Delta Q_i^{TR} = -\{g_{ij} e_i + b_{ij} f_i\}$$

$$\nabla_t \nabla_t \Delta Q_i^{TR} = 0$$

$$\nabla_t \nabla_{e_i} \Delta P_j^{TR} = -\{-g_{ij} e_j - b_{ij} f_j\}$$

$$\nabla_t \nabla_{f_i} \Delta P_j^{TR} = -\{b_{ij} e_j - g_{ij} f_j\}$$

$$\nabla_t \nabla_{e_j} \Delta P_j^{TR} = -\{4tg_{jj} e_j - (g_{ij} e_i - b_{ij} f_i)\}$$

$$\nabla_t \nabla_{f_j} \Delta P_j^{TR} = -\{4tg_{jj} f_j - (b_{ij} e_i + g_{ij} f_i)\}$$

$$\nabla_t \nabla_t \Delta P_j^{TR} = -\{2g_{jj} e_j^2 + 2g_{jj} f_j^2\}$$

$$\nabla_t \nabla_{e_i} \Delta Q_j^{TR} = -\{b_{ij} e_j - g_{ij} f_j\}$$

$$\nabla_t \nabla_{f_i} \Delta Q_j^{TR} = -\{g_{ij} e_j + b_{ij} f_j\}$$

$$\nabla_t \nabla_{e_j} \Delta Q_j^{TR} = -\{-4tb_{jj} e_j + (b_{ij} e_i + g_{ij} f_i)\}$$

$$\nabla_t \nabla_{f_j} \Delta Q_j^{TR} = -\{-4tb_{jj} f_j - (g_{ij} e_i - b_{ij} f_i)\}$$

$$\nabla_t \nabla_t \Delta Q_j^{TR} = -\{-2b_{jj} e_j^2 - 2b_{jj} f_j^2\}$$

3rd derivatives:

$$\nabla_t \nabla_{e_i} \nabla_{e_i} \Delta P_i^{TR} = 0$$

$$\nabla_t \nabla_{e_i} \nabla_{f_i} \Delta P_i^{TR} = 0$$

$$\nabla_t \nabla_{e_i} \nabla_{e_j} \Delta P_i^{TR} = -\{-g_{ij}\}$$

$$\nabla_t \nabla_{e_i} \nabla_{f_j} \Delta P_i^{TR} = -\{b_{ij}\}$$

$$\nabla_t \nabla_{e_i} \nabla_t \Delta P_i^{TR} = 0$$

$$\nabla_t \nabla_{f_i} \nabla_{e_i} \Delta P_i^{TR} = 0$$

$$\nabla_t \nabla_{f_i} \nabla_{f_i} \Delta P_i^{TR} = 0$$

$$\nabla_t \nabla_{f_i} \nabla_{e_j} \Delta P_i^{TR} = -\{-b_{ij}\}$$

$$\nabla_t \nabla_{f_i} \nabla_{f_j} \Delta P_i^{TR} = -\{-g_{ij}\}$$

$$\nabla_t \nabla_{f_i} \nabla_t \Delta P_i^{TR} = 0$$

$$\nabla_t \nabla_{e_j} \nabla_{e_i} \Delta P_i^{TR} = -\{-g_{ij}\}$$

$$\nabla_t \nabla_{e_j} \nabla_{f_i} \Delta P_i^{TR} = -\{-b_{ij}\}$$

$$\nabla_t \nabla_{e_j} \nabla_{e_j} \Delta P_i^{TR} = 0$$

$$\nabla_t \nabla_{e_j} \nabla_{f_j} \Delta P_i^{TR} = 0$$

$$\nabla_t \nabla_{e_j} \nabla_t \Delta P_i^{TR} = 0$$

$$\nabla_t \nabla_{f_j} \nabla_{e_i} \Delta P_i^{TR} = -\{b_{ij}\}$$

$$\nabla_t \nabla_{f_j} \nabla_{f_i} \Delta P_i^{TR} = -\{-g_{ij}\}$$

$$\nabla_t \nabla_{f_j} \nabla_{e_j} \Delta P_i^{TR} = 0$$

$$\nabla_t \nabla_{f_j} \nabla_{f_j} \Delta P_i^{TR} = 0$$

$$\nabla_t \nabla_{f_j} \nabla_t \Delta P_i^{TR} = 0$$

$$\nabla_t \nabla_t \nabla_{e_i} \Delta P_i^{TR} = \nabla_t \nabla_t \nabla_{f_i} \Delta P_i^{TR} = \nabla_t \nabla_t \nabla_{e_j} \Delta P_i^{TR} = \nabla_t \nabla_t \nabla_{f_j} \Delta P_i^{TR} = \nabla_t \nabla_t \nabla_t \Delta P_i^{TR} = 0$$

$$\nabla_t \nabla_{e_i} \nabla_{e_i} \Delta Q_i^{TR} = 0$$

$$\nabla_t \nabla_{e_i} \nabla_{f_i} \Delta Q_i^{TR} = 0$$

$$\nabla_t \nabla_{e_i} \nabla_{e_j} \Delta Q_i^{TR} = -\{b_{ij}\}$$

$$\nabla_t \nabla_{e_i} \nabla_{f_j} \Delta Q_i^{TR} = -\{g_{ij}\}$$

$$\nabla_t \nabla_{e_i} \nabla_t \Delta Q_i^{TR} = 0$$

$$\nabla_t \nabla_{f_i} \nabla_{e_i} \Delta Q_i^{TR} = 0$$

$$\nabla_t \nabla_{f_i} \nabla_{f_i} \Delta Q_i^{TR} = 0$$

$$\nabla_t \nabla_{f_i} \nabla_{e_j} \Delta Q_i^{TR} = -\{-g_{ij}\}$$

$$\nabla_t \nabla_{f_i} \nabla_{f_j} \Delta Q_i^{TR} = -\{b_{ij}\}$$

$$\nabla_t \nabla_{f_i} \nabla_t \Delta Q_i^{TR} = 0$$

$$\nabla_t \nabla_{e_j} \nabla_{e_i} \Delta Q_i^{TR} = -\{b_{ij}\}$$

$$\nabla_t \nabla_{e_j} \nabla_{f_i} \Delta Q_i^{TR} = -\{-g_{ij}\}$$

$$\nabla_t \nabla_{e_j} \nabla_{e_j} \Delta Q_i^{TR} = 0$$

$$\nabla_t \nabla_{e_j} \nabla_{f_j} \Delta Q_i^{TR} = 0$$

$$\nabla_t \nabla_{e_j} \nabla_t \Delta Q_i^{TR} = 0$$

$$\nabla_t \nabla_{f_j} \nabla_{e_i} \Delta Q_i^{TR} = -\{g_{ij}\}$$

$$\nabla_t \nabla_{f_j} \nabla_{f_i} \Delta Q_i^{TR} = -\{b_{ij}\}$$

$$\nabla_t \nabla_{f_j} \nabla_{e_j} \Delta Q_i^{TR} = 0$$

$$\nabla_t \nabla_{f_j} \nabla_{f_j} \Delta Q_i^{TR} = 0$$

$$\nabla_t \nabla_{f_j} \nabla_t \Delta Q_i^{TR} = 0$$

$$\nabla_t \nabla_t \nabla_{e_i} \Delta Q_i^{TR} = \nabla_t \nabla_t \nabla_{f_i} \Delta Q_i^{TR} = \nabla_t \nabla_t \nabla_{e_j} \Delta Q_i^{TR} = \nabla_t \nabla_t \nabla_{f_j} \Delta Q_i^{TR} = \nabla_t \nabla_t \nabla_t \Delta Q_i^{TR} = 0$$

$$\nabla_t \nabla_{e_i} \nabla_{e_i} \Delta P_j^{TR} = 0$$

$$\nabla_t \nabla_{e_i} \nabla_{f_i} \Delta P_j^{TR} = 0$$

$$\nabla_t \nabla_{e_i} \nabla_{e_j} \Delta P_j^{TR} = -\{-g_{ij}\}$$

$$\nabla_t \nabla_{e_i} \nabla_{f_j} \Delta P_j^{TR} = -\{-b_{ij}\}$$

$$\nabla_t \nabla_{e_i} \nabla_t \Delta P_j^{TR} = 0$$

$$\nabla_t \nabla_{f_i} \nabla_{e_i} \Delta P_j^{TR} = 0$$

$$\nabla_t \nabla_{f_i} \nabla_{f_i} \Delta P_j^{TR} = 0$$

$$\nabla_t \nabla_{f_i} \nabla_{e_j} \Delta P_j^{TR} = -\{b_{ij}\}$$

$$\nabla_t \nabla_{f_i} \nabla_{f_j} \Delta P_j^{TR} = -\{-g_{ij}\}$$

$$\nabla_t \nabla_{f_i} \nabla_t \Delta P_j^{TR} = 0$$

$$\nabla_t \nabla_{e_j} \nabla_{e_i} \Delta P_j^{TR} = -\{-g_{ij}\}$$

$$\nabla_t \nabla_{e_j} \nabla_{f_i} \Delta P_j^{TR} = -\{b_{ij}\}$$

$$\nabla_t \nabla_{e_j} \nabla_{e_j} \Delta P_j^{TR} = -\{4tg_{jj}\}$$

$$\nabla_t \nabla_{e_j} \nabla_{f_j} \Delta P_j^{TR} = 0$$

$$\nabla_t \nabla_{e_j} \nabla_t \Delta P_j^{TR} = -\{4 g_{jj} e_j\}$$

$$\nabla_t \nabla_{f_j} \nabla_{e_i} \Delta P_j^{TR} = -\{-b_{ij}\}$$

$$\nabla_t \nabla_{f_j} \nabla_{f_i} \Delta P_j^{TR} = -\{-g_{ij}\}$$

$$\nabla_t \nabla_{f_j} \nabla_{e_j} \Delta P_j^{TR} = 0$$

$$\nabla_t \nabla_{f_j} \nabla_{f_j} \Delta P_j^{TR} = -\{4 t g_{jj}\}$$

$$\nabla_t \nabla_{f_j} \nabla_t \Delta P_j^{TR} = -\{4 g_{jj} f_j\}$$

$$\nabla_t \nabla_t \nabla_{e_i} \Delta P_j^{TR} = 0$$

$$\nabla_t \nabla_t \nabla_{f_i} \Delta P_j^{TR} = 0$$

$$\nabla_t \nabla_t \nabla_{e_j} \Delta P_j^{TR} = -\{4 g_{jj} e_j\}$$

$$\nabla_t \nabla_t \nabla_{f_j} \Delta P_j^{TR} = -\{4 g_{jj} f_j\}$$

$$\nabla_t \nabla_t \nabla_t \Delta P_j^{TR} = 0$$

$$\nabla_t \nabla_{e_i} \nabla_{e_i} \Delta Q_j^{TR} = 0$$

$$\nabla_t \nabla_{e_i} \nabla_{f_i} \Delta Q_j^{TR} = 0$$

$$\nabla_t \nabla_{e_i} \nabla_{e_j} \Delta Q_j^{TR} = -\{b_{ij}\}$$

$$\nabla_t \nabla_{e_i} \nabla_{f_j} \Delta Q_j^{TR} = -\{-g_{ij}\}$$

$$\nabla_t \nabla_{e_i} \nabla_t \Delta Q_j^{TR} = 0$$

$$\nabla_t \nabla_{f_i} \nabla_{e_i} \Delta Q_j^{TR} = 0$$

$$\nabla_t \nabla_{f_i} \nabla_{f_i} \Delta Q_j^{TR} = 0$$

$$\nabla_t \nabla_{f_i} \nabla_{e_j} \Delta Q_j^{TR} = -\{g_{ij}\}$$

$$\nabla_t \nabla_{f_i} \nabla_{f_j} \Delta Q_j^{TR} = -\{b_{ij}\}$$

$$\nabla_t \nabla_{f_i} \nabla_t \Delta Q_j^{TR} = 0$$

$$\nabla_t \nabla_{e_j} \nabla_{e_i} \Delta Q_j^{TR} = -\{b_{ij}\}$$

$$\nabla_t \nabla_{e_j} \nabla_{f_i} \Delta Q_j^{TR} = -\{g_{ij}\}$$

$$\nabla_t \nabla_{e_j} \nabla_{e_j} \Delta Q_j^{TR} = -\{-4tb_{jj}\}$$

$$\nabla_t \nabla_{e_j} \nabla_{f_j} \Delta Q_j^{TR} = 0$$

$$\nabla_t \nabla_{e_j} \nabla_t \Delta Q_j^{TR} = -\{-4b_{jj} e_j\}$$

$$\nabla_t \nabla_{f_j} \nabla_{e_i} \Delta Q_j^{TR} = -\{-g_{ij}\}$$

$$\nabla_t \nabla_{f_j} \nabla_{f_i} \Delta Q_j^{TR} = -\{b_{ij}\}$$

$$\nabla_t \nabla_{f_j} \nabla_{e_j} \Delta Q_j^{TR} = 0$$

$$\nabla_t \nabla_{f_j} \nabla_{f_j} \Delta Q_j^{TR} = -\{-4tb_{jj}\}$$

$$\nabla_t \nabla_{f_j} \nabla_t \Delta Q_j^{TR} = -\{-4b_{jj} f_j\}$$

$$\nabla_t \nabla_t \nabla_{e_i} \Delta Q_j^{TR} = 0$$

$$\nabla_t \nabla_t \nabla_{f_i} \Delta Q_j^{TR} = 0$$

$$\nabla_t \nabla_t \nabla_{e_j} \Delta Q_j^{TR} = -\{-4b_{jj} e_j\}$$

$$\nabla_t \nabla_t \nabla_{f_j} \Delta Q_j^{TR} = -\{-4b_{jj} f_j\}$$

$$\nabla_t \nabla_t \nabla_t \Delta Q_j^{TR} = 0$$